AMPHIBOLES AND THEIR HOST ROCKS IN THE HIGH-GRADE METAMORPHIC PRECAMBRIAN OF ROGALAND/VEST-AGDER, SW. NORWAY

A.G.C.DEKKER

STELLINGEN

I

De door Saxena geponeerde charnockietgeotherm is gebaseerd op een niet juiste toepassing van de pyroxeenthermometer van Ross en Huebner.

S.K.Saxena (1977)
Science, 198, 614-617.
M.Ross & J.S.Huebner (1976)
Int. Symposium in Geothermometry and Geobarometry, Pennsylvania State University.

II

Het aantal petrografisch te bewerken monsters bij absolute ouderdomsbepalingen dient minimaal gelijk te zijn aan het aantal punten op het isochron.

A.Versteeve (1975)
Norges geol. Unders., 318, 1-50.

III

De grotere abundantie van ^{18}O wordt door Hoefs ten onrechte genoemd als voornaamste reden dat ^{17}O slechts zelden gemeten wordt.

J.Hoefs (1973)
Stable Isotope Geochemistry.

IV

De fossiele dinoflagellaten cyste-soort *Cleistosphaeridium mojsisovicsii* dient in een ander genus te worden ondergebracht.

S.J.Morbey (1975)
Palaeontographica, B, 152 (1-3), 1-75.

V

De eigenschappen in gepolariseerd licht van de wand van perforate, kalkschalige foraminiferen, geven een onvolledig beeld van de wandstructuur en hebben slechts een beperkte taxonomische waarde.

VI

Reconstructie van de eerste-fase plooiing in gebieden met twee gesuperponeerde plooiingen, volgens de methode gehanteerd door o.a. Ragan and Whitten is slechts in uitzonderingsgevallen bruikbaar.

D.H.Ragan (1973)
Structural Geology
E.H.T.Whitten (1966)
Structural Geology of Folded Rocks.

VII

Een groot gedeelte van de vloeistofinsluitsel-onderzoekingen berust volgens Gary, McAfee en Wolf nergens op.

M.Gary, R.McAfee Jr & C.L.Wolf (1973)
Glossary of Geology.

VIII

De mogelijkheid dat de Sirdalen ogengneiss-formatie met bovenliggende graniet en Espetveit ogengneiss een intrusiefcomplex vertegenwoordigt, vergelijkbaar met de lopoliet van Bjerkreim-Sokndal, dient niet onderschat te worden.

M.M.Kehlenbeck (1974)
Can.J.Earth Sci., 11, 1689-1703.

IX

De definitie van *free* volgens Gary, McAfee en Wolf is niet toepasbaar op elk *native element*.

M.Gary, R.McAfee Jr & C.L.Wolf (1973)
Glossary of Geology.

X

De druiven van Grapes zijn zuur.

R.H.Grapes, S.Hashimoto & S.Miyashita (1977)
J.Petrol., 18, 285-318.

XI

Het beperken van financiële steun aan wetenschappelijk onderzoek dat *te weinig resultaat* oplevert is vaak een completering van de vicieuze cirkel.

XII

Een opmerkelijk verschil tussen het werk van Sir Walter Scott en van ondergetekende is het magnifieke schrijftalent dat wel geëxposeerd wordt in de Waverley Novels.

XIII

Veel ambtenaren van sociale diensten schijnen niet te beseffen dat de uitkeringtrekkers hun indirecte werkgevers zijn.

Utrecht, 24 mei 1978
A.G.C.Dekker

Stellingen behorende bij het proefschrift "Amphiboles and their host rocks in the high-grade metamorphic Precambrian of Rogaland/Vest-Agder, SW.Norway.".

AMPHIBOLES AND THEIR HOST ROCKS IN THE HIGH-GRADE METAMORPHIC PRECAMBRIAN OF ROGALAND/VEST-AGDER, SW.NORWAY

A.G.C.Dekker

Abstract

In the high-grade metamorphic Precambrian of the Sirdal-Ørsdal area, Rogaland/Vest-Agder, south-west Norway, the Ca-amphiboles show a change in pleochroic colours, not only with changes in metamorphic grade, but also to some extend in bulk composition. A regional study was performed on the amphiboles to study their response to changes in metamorphic grade, the influence of the host rock chemistry, and the relation between chemical and physical parameters of the amphiboles, with an emphasis on colour. Analyses have been performed on amphiboles and their host rocks, and calculation methods and analysis technics are discussed.

Potassium-argon ages on 17 hornblendes indicate their cooling below 550°C about 950 Ma ago, after a high temperature, low pressure metamorphism (Abukuma-type). About the same time the Lopolith of Bjerkreim-Sokndal intruded. During the main metamorphic event, the pressure in the area was 3-5 kb, while water pressure and temperature varied, resulting in a metamorphic zoning from granulite facies to amphibolite facies. This metamorphic gradation formed a regional pattern of amphibole colours, which change from bluishgreen in the amphibolite facies terrain to brown in the granulite facies area.

Titanium, and to a lesser degree ferric and ferrous iron, are the most important chemical determinants of the Ca-amphibole colours. The rock composition is less important for the colour, but very important (especially the An-content of the coexisting plagioclase) for some other chemical characteristics of the Ca-amphiboles. Ca-amphiboles in the granulite facies are richer in titanium and potassium (and possibly

fluorine), and poorer in magnesia and aluminia (octahedral-site and total) than the Ca-amphiboles in the amphibolite facies, if host rocks of similar composition are compared.

After the main metamorphic event the pressure increased while the temperature decreased, and secondary amphiboles formed (mainly actinolite, but also hornblende and ferro-magnesian amphiboles). The oxidation-ratio of the Ca-amphiboles of the main phase forms a clear regional pattern which is independent of the metamorphic zoning; it may be related to a later tectonic event. No important formation of amphiboles has taken place after 950 Ma ago. The area was lifted to its present position; the cooling rate in the amphibolite facies terrain during, at least, the period between 1000 and 870 Ma ago was about $3^{o}C/Ma$, with an original geothermal gradient between 50 and $100^{o}C/km$. The cooling rate in the granulite facies area and in the lopolith has been much higher.

GEOLOGICA ULTRAIECTINA

Mededelingen van het Geologisch Instituut der Rijksuniversiteit te Utrecht

No 17

AMPHIBOLES AND THEIR HOST ROCKS IN THE HIGH-GRADE METAMORPHIC PRECAMBRIAN OF ROGALAND/VEST-AGDER, SW.NORWAY.

1978

Department of Petrology, Rijksuniversiteit Utrecht, Oude Gracht 320, Utrecht, The Netherlands.

AMPHIBOLES AND THEIR HOST ROCKS IN THE HIGH-GRADE METAMORPHIC PRECAMBRIAN OF ROGALAND/ VEST-AGDER, SW. NORWAY

PROEFSCHRIFT

ter verkrijging van de graad van doctor in de wiskunde en natuurwetenschappen aan de Rijksuniversiteit te Utrecht, op gezag van de Rector Magnificus Prof. Dr. A. Verhoeff, volgens besluit van het College van Decanen in het openbaar te verdedigen op woensdag 24 mei 1978 des namiddags te 4.15 uur

door

ALFONSUS GERARDUS CORNELIS DEKKER
geboren op 24 juli 1949 te Obdam

Promotoren : Dr. A. C. Tobi
Prof. Dr. R. D. Schuiling

Aan allen die mij de afgelopen jaren
begeleid en gevormd hebben,
wetenschappelijk en sociaal, in het
bijzonder aan Tony, Frans en
het jaar '66.

Met dank aan allen die hebben meegewerkt aan het tot stand komen van dit proefschrift.

Financiële steun werd ontvangen van de Nederlandse Organisatie voor Zuiver Wetenschappelijk Onderzoek (Z.W.O.) in de vorm van beurs 75-115.

Analyse faciliteiten werden beschikbaar gesteld door het:
--Petrochemisch laboratorium van het Geologisch en Mineralogisch Instituut te Leiden (WACOM),
--Z.W.O. Laboratorium voor Isotopen Geologie te Amsterdam, en het
--Instituut voor Aardwetenschappen der Vrije Universiteit te Amsterdam (WACOM).

But there it was, the whole history of science, a clear story of continuously new and changing explanations of old facts. The time spans of permanence seemed completely random, he could see no order in them. Some scientific truths seemed to last for centuries, others for less than a year. Scientific truth was not dogma, good for eternity, but a temporal quantitative entity that could be studied like anything else.

He studied scientific truths, then became upset even more by the apparent cause of their temporal condition. It looked as though the time spans of scientific truths are an inverse function of the intensity of scientific effort. Thus the scientific truths of the twentieth century seem to have a much shorter life-span than those of the last century because scientific activity is now much greater. If, in the next century, scientific activity increase tenfold, then the life expectancy of any scientific truth can be expected to drop to perhaps one-tenth as long as now. What shortens the life-span of the existing truth is the volume of hypotheses offered to replace it; the more the hypotheses, the shorter the time span of the truth. And what seems to be causing the number of hypotheses to grow in recent decades seems to be nothing other than scientific method itself. The more you look, the more you see. Instead of selecting one truth from a multitude you are increasing the multitude. What this means logically is that as you try to move towards unchanging truth through the application of scientific method, you actually do not move towards it at all. You move away from it! It is your application of scientific method that is causing it to change!

from : Zen and the art of motorcycle maintenance. (An inquiry into values): Robert M. Pirsig. Bantam Book B8880, 1975. Toronto/New York/London. William Morrow and Co., New York 1974.

INDEX

Introduction

In the high-grade metamorphic Precambrian of the Sirdal-Ørsdal area, Rogaland/Vest-Agder, south-west Norway (Hermans et al, 1975), the Ca-amphiboles show a change in pleochroic colours, not only with changes in metamorphic grade, but also with differences in petrologic environment.

Because this area is exposed very well and of appreciable size (50 X 60 km), it seemed to be a good area for a regional study of amphiboles, their response to metamorphic changes, the influence of the host rock chemistry, and the relation between amphibole colour, chemistry and other physical parameters. To what extent is it possible to use amphiboles, and especially hornblendes, as indicators of metamorphic grade?

This study consists of three parts:

--Part I (Chapter I and II): Amphibology of Rogaland/Vest-Agder. The regional aspects of amphiboles in a metamorphic environment of different grades, the relation with several igneous complexes, and the petrological implications.

--Part II (Chapter III-VII) : Methods and Data. Chemical and optical information of the amphiboles, and the chemistry and mineralogy of their host rocks, together with information on analytical methods and calculation procedures.

--Part III : Appendix. This part contains extensive sample descriptions with field-, macroscopic- and microscopic information, and notes on chemical and optical peculiarities.

Part I gives a general review of the results; parts II and III contain the data.

Explanation of the sample numbers

See Table I.1

Normal form : A 168 Complex form : E1232 F

The sample numbers are divided in three parts :

1: the normal form : a letter and a group of three figures. This is the original sample number, given in the field by the various geologists. The letter and figures are separated by a space.

2: the prefix, a figure directly behind the first letter. If it is present, it means that there is more then one amphibole in the same sample, and shows which of the amphiboles is under discussion The maximum value of the prefix number in this thesis is 4, as in N4528 B. If rocks are under discussion, no prefix is used. The main amphibole normally carries the number 1, less frequent amphiboles in the same sample the numbers 2-4. If only one amphibole is present, no prefix is used.

3: the tail; a letter or figure separated from the normal form by a space. A letter tells something about the handspecimen if the following letters are used:

B: banded, several bands are taken together

D: banded, only the dark band is taken into consideration

L: banded, only the light band is taken into consideration

F: "filon", dike or vein cutting through the hostrock

N: the hostrock through which a vein is cutting

A letter tells something about the amphibole if the following letters are used:

R: border zone of the amphibole

K: core of the amphibole

M: mean of several differing analyses of the same amphibole

A figure at the end means that several analyses of optically identical amphibole grains are presented, because they differ enough to justify their separate publication. If the amphibole is homogeneous, the

Sample	Coordinates	Formation	Rock name	Amphibole name
A 037 B	3411-65052	GG	Banded spinel-bearing amphibole gabbro	Ferroan pargasite
A 128	3411-65052	GG	Plagioclase-bearing 2-pyroxene hornblendite	Ferroan pargasite, border ferroan pargasitic hornblende
A 168	3337-65078	F	Alkalifeldspar granite	Magnesioriebeckite 62/riebeckite 38
B1016	3489-64761	LA	Biotite amphibole diorite	Ferro-hornblende (rim)
B2016	3489-64761	LA	Biotite amphibole diorite	Grunerite 59/cummingtonite 41 (core)
B 118 L	3560-64719	HM	Banded amphibole bearing 2-pyroxene charnockite	Edenitic hornblende near cross
B 254	3473-64824	HR	Olivine amphibolite	Titaniferous ferroan pargasite, border titaniferous magnesian hastingsite
B 322	3483-64765	LA	Apatite amphibole ilmenite hyperschenite	Ferroan pargasitic hornblende
D 172 D	3650-64975	MB	Amphibole biotite quartz gabbronorite gneiss	Edenitic hornblende border ferro-edenitic hornblende
D 307	3552-64941	MB	Amphibole gabbronorite	Titaniferous ferroan pargasitic hornblende, border titaniferous edenitic hornblende
D 442	3700-65053	MB	Biotite amphibolite	Edenitic hornblende near cross
D 444	3700-65053	MB	Biotite amphibolite	Magnesian hastingsitic hornblende near cross
E 067	3434-64824	LQ	Amphibole 2-pyroxene quartzmonzonite	Ferro-edenitic hornblende near cross
E 125	3375-64909	LA	Ore-rich amphibole gabbronorite	Titaniferous ferroan pargasite, border titaniferous magnesian hastingsite
E 128	3376-64921	LC	Amphibole mela-troctolite	Titaniferous pargasite
E 131	3364-64910	LA	Ore-rich amphibole-bearing norite	Ferroan pargasite, border pargasite
E1167	3423-64897	LQ	Clinopyroxene-olivine-bearing amphibole granite	Ferro-edenitic hornblende border hastingsitic hornblende
E2167	3423-64897	LQ	Clinopyroxene-olivine-bearing amphibole granite	Ferro-actinolite (late)
E 170	3413-64899	LQ	Clinopyroxene amphibolite	Ferroan pargasitic hornblende, border magnesian hastingsitic hornblende
E1232 F	3408-64826	AH	Biotite amphibole quartzmonzonite	Ferro-hornblende border ferro-tschermackitic hornblende
E2232 N	3408-64826	AH	Amphibole biotite mela-enorthosite	Actinolite (core)
E3232 N	3408-64826	AH	Amphibole biotite mela-anorthosite	Ferro-hornblende, near cross (rim)
F 005	3683-65114	MM	Biotite amphibole quartzmonzonite	Edenitic hornblende
F1043	3630-65084	MB	Biotite-bearing amphibole gneiss	Edenitic hornblende near cross
F2043	3630-65084	MB	Biotite-bearing amphibole gneiss	Actinolite (Late)
F1052 D	3604-65050	MM	Amphibole mela-syenite	Edenitic hornblende
F2052 D	3605-65050	MM	Amphibole mela-syenite	Actinolitic hornblende?, not analysed (late)
F3052 L	3604-65050	MM	Amphibole mela-alkalifeldspar quartzsyenite	Edenitic hornblende
F4052 L	3604-65050	MM	Amphibole mela-alkalifeldspar quartzsyenite	Actinolitic hornblende (late)
F 070 D	3618-65052	OE	Biotite amphibole angengneiss	Edenitic hornblende near cross
F 074	3631-65051	OE	Retrograde ortho-amphibolite	Edenitic hornblende
F1107 D	3606-65052	B	Apatite amphibole 2-pyroxene quartzmonzonorite	Edenitic hornblende, near cross
F2107 D	3606-65052	B	Apatite amphibole 2-pyroxene quartzmonzonorite	Edenitic hornblende, near cross
F1126	3637-65039	B	Retrograde amphibole biotite enderbite	Edenitic hornblende, near cross
F2126	3637-65039	B	Retrograde amphibole biotite enderbite	Variety of F1126, not analysed
F1252	3645-65132	O	Biotite-bearing amphibole augengneiss	Edenitic hornblende
F2252	3645-65132	O	Biotite-bearing amphibole augengneiss	Magnesio-hornblende/actinolite (complete series) (late)
F1433	3489-64775	LG	Amphibole pegmatite, not analysed	Ferro-edenitic hornblende, border hastingsitic hornblende
F2433	3489-64775	LC	Amphibole pegmatite, not analysed	Ferro-edenitic hornblende, border hastingsitic hornblende(late)
F 501	3408-64826	AH	Biotite amphibole quartzmonzodiorite	See E1232 F, not analysed
F1502 F	3408-64829	AH	Amphibole quartzmonzonite	See E3232 N, not analysed (rim)
F2502 F	3408-64829	AH	Amphibole quartzmonzonite	See E2232 N, not analysed (core)
F1502 N	3408-64829	AH	Amphibole biotite mela-anorthosite	See E3232 N, not analysed (rim)
F2502 N	3408-64829	AH	Amphibole biotite mela-anorthosite	See E2232 N, not analysed (core)
F1503	3408-64829	AH	Amphibole biotite mela-anorthosite	See E3232 N, not analysed (rim)
F2503	3408-64829	AH	Amphibole biotite mela-anorthosite	See E2232 N, not analysed (core)
H1047 B	3640-64912	O	Biotite-bearing amphibole gneiss	Edenitic hornblende, border edenite
H2047 B	3640-64912	O	Biotite-bearing amphibole gneiss	Actinolite ?, not analysed (late)
H1050	3639-64825	O	Amphibole gneiss	Edenitic hornblende
H2050	3639-64825	O	Amphibole gneiss	Actinolite ?, not analysed (late)
H 307	3657-64772	BB	Clinopyroxene biotite amphibolite	Ferroan pargasitic hornblende, near cross
H 325	3639-64734	HM	Orthopyroxene amphibolite	Titaniferous ferroan pargasitic hornblende, border ritaniferous ferroan pargasite
H 415	3609-64881	HR	Biotite-bearing amphibolite	Titaniferous edenitic hornblende, near cross

Table I.1.: List of analyzed samples. Rock names according to Hermans et al (1975). Ca-amphibole names according to Leake (1968), based on 23(O), microprobe information only (table IV.8 and fig.IV.8). Other amphiboles according to Ernst (1968), based on 23(O), Z+Y = 13, Fe^{3+} calculated (table IV.9), see section IV.2.

Special remarks: (Late): adaption to lower temperatures; younger than the other amphibole;
(Series): several analyses on a row;
border: within .05 - .15 ions from a name transition line (see section IV.2.5);
near cross: within .05 - .15 ions from more than one name transition lines.

Grid references are from the Universal Grid NGO, see fig. I.1.

J 119	3512-65065	UM	Amphibole gabbronorite	Titaniferous ferroan hastingsitic hornblende
L1143	3250-65068	AE	Amphibole-bearing anorthosite	Magnesio-hornblende/actinolitic hornblende (series) (rim)
L2143	3250-63008	AE	Amphibole-bearing anorthosite	Cummingtonite 69 / grunerite 31 (core)
N 103	3441-65016	MB	Apatite amphibole quartzmonzonorite	Edenitic hornblende
N1041 B	3690-65050	MB	Hypersthene biotite amphibole vein	Magnesio-hornblende
N2041 D	3690-65050	MB	Hypersthene biotite amphibole vein	Magnesio-hornblende/actinolitic hornblende (series)
N1266	3673-65007	MM	Biotite amphibole quartzsyenite	Edenitic hornblende
N2266	3673-65007	MM	Biotite amphibole quartzsyenite	Actinolite (late)
N 317	3535-64740	HR	2-Pyroxene amphibolite	Titaniferous ferroan pargasite, near cross
N 337	3491-64845	HB	Amphibole gabbronorite	Edenitic hornblende, border ferroan pargasitic hornblende
N1402 F	3437-64831	LQ	Amphibole granite	Titaniferous ferro-edenitic hornblende near cross
N2402 F	3437-64831	LQ	Amphibole granite	Ferro-hornblende
N1528 B	3423-64741	LC	Olivine-bearing mangerite + pyroxenite	Titaniferous hastingsitic hornblende, border titaniferous magnesian hastingsitic hornblende
N2528 B	3423-64741	LC	Olivine-bearing mangerite + pyroxenite	Not analysed
N3528 D	3423-64741	LC	Olivine-bearing mangerite + pyroxenite	Magnesian hastingsitic hornblende near cross
N4528 B	3423-64741	LC	Olivine-bearing mangerite + pyroxenite	Not analysed
N1572 L	3474-64822	HR	Olivine amphibole mela-norite	Pargasite, border ferroan pargasite
N2572 D	3474-64822	HR	Amphibole olivine hypersthenite	Pargasite*, not analysed
N 809	3552-64783	HM	Plagioclase-bearing 2-pyroxene hornblendite	Titaniferous ferroan pargasitic hornblende
N1827 F	3408-64825	MH	Biotite amphibole quartzmonzonite	Magnesian hastingsitic hornblende/ferro-hornblende (series) (rim)
N2827 F	3408-64825	MH	Biotite amphibole quartzmonzonite	Actinolite (core)
O 100	3364-65007	B	Amphibole norite	Titaniferous edenitic hornblende, border titaniferous ferroan pargasitic hornblende
P1097	3497-64951	SB	Amphibole m-granite	Ferro-edenitic hornblende
P2097	3497-64951	SB	Amphibole m-granite	Ferro-edenitic hornblende, border ferro-edenite
P 248	3469-64908	LA	Amphibole-bearing granite	Edenitic hornblende, border ferroan pargasitic hornblende
P 303	3405-64942	HR	Biotite amphibolite	Edenitic hornblende near cross
P1580 D	3476-64855	HB	Biotite amphibole norite	Ferroan pargasitic hornblende
P2580 L	3476-64855	HB	Diorite	Ferroan pargasitic hornblende
R 227	3489-64775	LC	Amphibole 2-pyroxene monzonorite	Ferro-edenitic hornblende, border ferro-hornblende
R1229	3490-64776	LC	2-Pyroxene monzonite	Ferro-edenitic hornblende near cross (rim)
R2229	3490-64776	LC	2-Pyroxene monzonite	Ferro-hornblende (series) (between rim and core)
R3229	3490-64776	LC	2-Pyroxene monzonite	Grunerite 75/cummingtonite 25 (core)
R1269	3487-64763	LB	Biotite amphibole monzonorite	Ferro-hornblende near cross (rim)
R2269	3487-64763	LB	Biotite amphibole monzonorite	Ferro-actinolite (core)
R 356	3482-64791	LQ	Olivine-clinopyroxene-hearing m-granite	Ferro-edenitic hornblende/ferro-hornblende (series)
R1668	3421-65155	SG	Amphibole monzonite	Ferro-edenitic hornblende near cross
R2668	3421-65155	SG	Amphibole monzonite	Ferro-edenitic hornblende near cross
S 147	3393-65138	HM	Charnockite (granite)	Magnesian hastingsitic hornblende, near cross
T1187	3396-65103	HM	Amphibole norite	Magnesian hastingsitic hornblende, near cross
T2187	3396-65103	HM	Amphibole norite	Magnesio-hornblende/actinolite
V 276	3409-65121	SG	Leucogranite	Hastingsitic hornblende
X 227	3409-65123	SG	Amphibole-bearing leuco-quartzmonzonite	Ferro-edenitic hornblende border magnesian hastingsitic hornblende
Y 363	3480-65178	MM	Biotite-amphibole-bearing granite	Edenite hornblende, border ferro-edenitic hornblende
W 012 D	3692-65053	MB	Biotite quartz amphibolite	Magnesio-hornblende, near cross
W 017 B	3718-65051	MB	Schistose biotite amphibole enderbite	Magnesio-hornblende, near cross
W 162 D	3725-65070	O	Biotite quartzmonzodiorite gneiss	Edenitic hornblende, near cross
W 196 B	3737-65095	MB	Schistose amphibole enderbite	Ferro-hornblende, near cross
W 217	3756-65102	MM	Amphibole-bearing biotite granite	Magnesian hastingsitic hornblende, near cross
W322a D	3744-65113	MB	Plagioclase-bearing hornblendite	Magnesio-hornblende
W222a L	3744-65113	MB	Amphibole mela-diorite	Edenitic hornblende near cross
Y1055	3362-65168	HM	Enderbite	Ferroan pargasitic hornblende, border magnesian hastingsitic hornblende
Y2055	3362-65168	HM	Enderbite	Ferro-hornblende, border magnesio-hornblende
Y1128	3346-65159	SG	Retrograde 2-pyroxene quartzsyenite	Hastingsitic hornblende/ferro-ed-nitic hornblende
Y2128	3346-65159	SG	Retrograde 2-pyroxene quartzsyenite	Ferro-actinolite
Y3131 B	3388-65162	SG	Garnet-bearing clinopyroxene quartzmonzonite	Hastingsite
Y2131 B	3388-65162	SG	Garnet-bearing clinopyroxene quartzmonzonite	Hastingsite
Y3131 K	3388-65162	SG	Garnet-bearing clinopyroxene quartzmonzonite	Ferro-tschermakite
Y3131 R	3388-65162	SG	Garnet-bearing clinopyroxene quartzmonzonite	Hastingsite

Table I.1.: continued.

Formations, explanation of symbols. AH : Haaland Helleren anorthosite; AE : Egersund anorthosite; B : folded basic intrusions; F : Faurefjell metasediments; GG : Gyadal garnetiferous migmatites. Granitic migmatites : MM : mainly massive; MB : mainly banded. Charnockitic migmatites: HM : mainly massive; HB : mainly banded; HR : border zone of lopolith. Bjerkreim-Sokndal lopolith : LA : phase A, leuconorites; LB : phase B, monzonorites; LC : phase C, pyroxene syenites and monzonites; LQ : phase C, pyroxene-quartz syenites and -monzonites. OE : Espetveit augen gneisses; O : Sirdalen augen gneisses; SB : Pyroxene syenite massif of Botnavatnet; SG : Pyroxene syenite massif of Gloppurdi.

For a general description of the formations, see Hermans et al (1975).

analyses will be similar and then the mean is given here. If not, a spread of analyses may be found, which sometimes indicates the start of the retrograde reaction: common hornblende ⟶ actinolite. If the change is optically recognisable, the amphiboles will get prefixes, and each of the two amphiboles may have a set of tail figures (e.g.: N1827 1-4 and N2827 1-3, table IV.7). The tail figure may then change into an M if the mean of several slightly differing analyses is used, as is the case when groups of analyses are plotted or when statistical calculations are done. If all the slightly differing analyses of a certain amphibole were then taken into consideration, they would influence the result too much. Sometimes one of the measurements is taken as the most representatieve for these plots and calculations (depending on the microprobe results).

It should be clear by now, that the sample number can give a lot of information about the rock or amphibole under discussion.

AMPHIBOLES AND THEIR HOST ROCKS IN THE HIGH-GRADE METAMORPHIC PRECAMBRIAN OF ROGALAND/VEST-AGDER, SW. NORWAY.

PART I

Amphibology

I : Optical and chemical amphibole parameters as indicators of a metamorphic zoning in Rogaland/Vest-Agder.

I.1. : Introduction

The high-grade metamorphic Precambrian of Rogaland/Vest-Agder (Hermans et al. 1975) is characterized by a granulite facies area in the west and an amphibolite facies area in the east (fig. I.1). The Caledonian front lies to the north-west of the investigated area. Several intrusive massifs were emplaced in the area before the end of the last main metamorphic event (Versteeve, 1975). The most south-western part contains various anorthosite massifs.

Samples of amphibole-carrying rocks were selected from the collections of the Department of Petrology, State University of Utrecht, and some additional sampling was performed. In this way all formations and amphibole-carrying rock types mentioned in Hermans et al (op.cit.) were represented in the amphibole collection. The selected amphiboles give an impression of the average amphibole content of every formation, and also of the most remarkable local features (see : Explanation of sample numbers, and table I.1).

The composition of the rock samples varies from ultramafic to leucogranitic (see Chapter III). The samples are divided in rocks from the large igneous complexes (= Igneous in table I.2 and Chapter VI), and from the metamorphic environment (= Migmatitic). The igneous complexes consist of the lopolith of Bjerkreim-Sokndal, the Gloppurdi- and Botnavatnet Massifs (Rietmeijer, 1978), and the anorthosites. Inside the metamorphic environment no further division was made.

All main amphibole groups are represented in the area : Ca-amphiboles are most common, Na-amphiboles are found in the Faurefjell metasediments, and Fe-Mg-amphiboles in some of the igneous rocks.

Chemistry, densities, magnetic properties, pleochroic colours and crystallographic parameters are described in Chapter IV. A general view of the variance in composition can be seen in fig. IV.8 and IV.10.

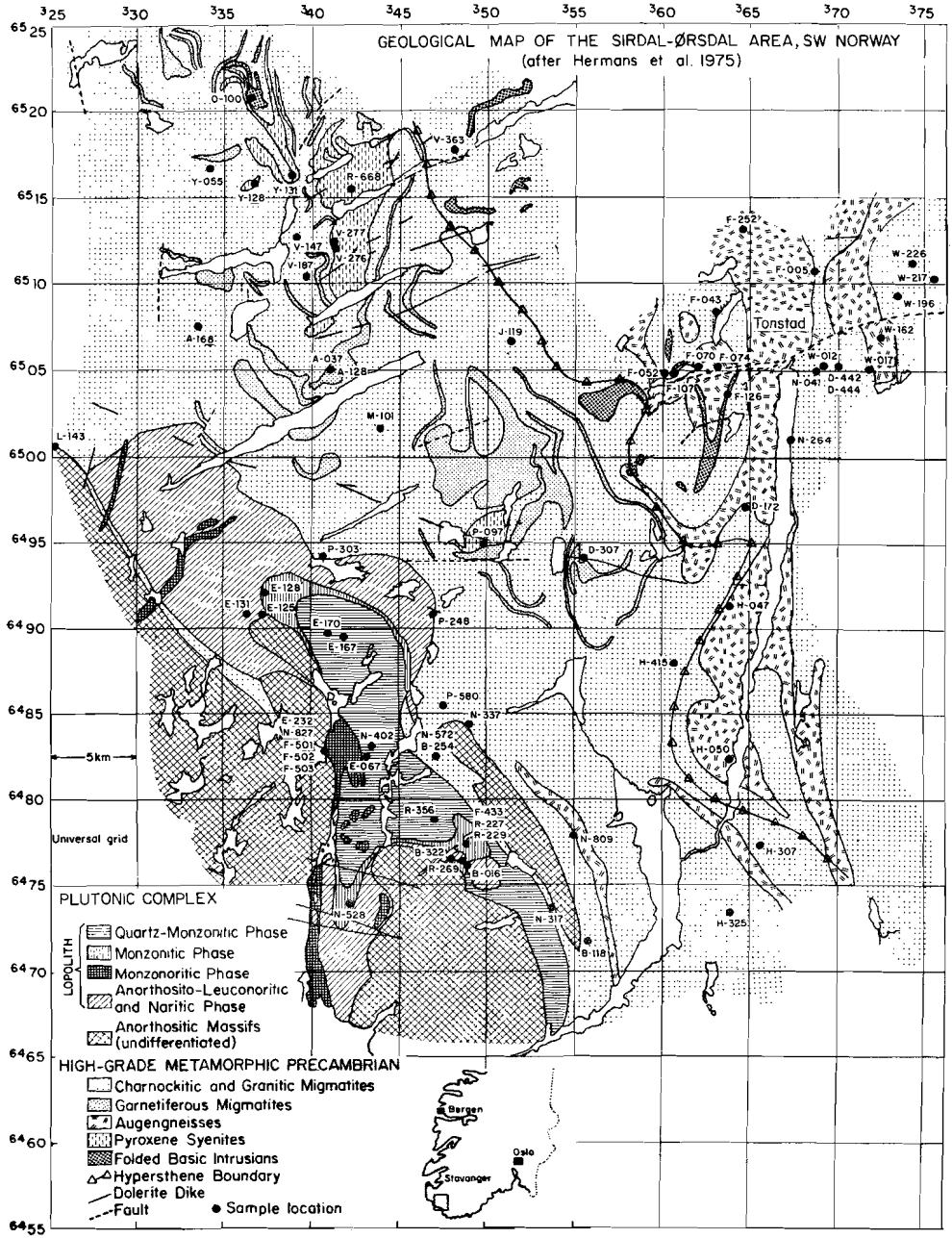

Figure I.1.: Geological sketch map of the investigated area, showing the locations of the analyzed samples.

The Ca-amphiboles are divided in a Mg-rich- and a Fe-rich group. The Mg-rich group contains all amphiboles from the metamorphic environment and phase A of the lopolith (the lowest, leuconoritic, part). The Fe-rich group is found in the higher parts of the lopolith and in the other igneous complexes, except the Egersund-Ogna anorthosite (section IV.3.2.). These groups are used to describe the changes in chemistry and physical parameters of the amphiboles in the area. If all Ca-amphiboles are lumped together (= Com or Combination), many relations become less clear. The pleochroic colours are described with the aid of a new numerical colour system (section IV.3.2.), which makes it possible to use the colour as a rough parameter for all kinds of calculations and graphical representations (table IV.14).

Besides rock- and amphibole analyses, some additional analyses on coexisting minerals, or amphiboles from comparable locations, were performed (Chapter V) to extend the picture where desired. They include clinopyroxene, plagioclase, spinel and opaque ore.

To investigate the influence of metamorphic grade on amphibole chemistry, it was also necessary to investigate the influence of the rock composition on the amphibole composition, and the mutual relations inside the rock groups and amphibole groups (Chapter VI). There appeared to be a rather intricate correlation pattern (section VI.7.). The petrography of every sample is given in the Appendix (Part III). This information will not be repeated in Part I.

I.2. : The colour pattern and its implications

I.2.1. : Amphibole pleochroic colours and metamorphic grades.

There is an irregular change in Ca-amphibole colour from brown to green with decreasing metamorphic grade. In many locations of the Rogaland area this pattern is disturbed by the coexistence of two differently coloured amphiboles, or by the occasional presence of green hornblende in an environment characterized by brown amphibole. To eliminate

disturbing samples several steps were taken : the amphiboles were divided in a main (primary)- and a secondary group (section VI.2.1.). The primary group consists, in general, of hornblende; the secondary group of actinolite. These are more bluish or greenish than the coexisting main amphiboles and were omitted in the discussion of the trend of the main phase of metamorphism. A second step was to exclude samples with a deviating colour if no free Ti-bearing ore phase was present in the handspecimen.

It is well known that Ti (in combination with Fe^{3+}) is the most important colour-determining element in the Ca-amphibole group; therefore, Ti should be present in excess in the rock to guarantee the maximum possible amount in amphibole (Leake, 1965-a, 1968).

It has also been established that the Ti-content in Ca-amphibole increases with temperature (Compton, 1958; Leake, 1965-a; Helz, 1973; Raase, 1974). Thus the change from green to brown pleochroic colours in fig. I.2 should indicate an increase in temperature, and so, an increase in metamorphic grade. However, this is only true if it is proved that the rock composition is not the main colour determining factor.

All rock types are represented in fig. I.2 and the colour change is obvious. In the greenest area (with colournumbers 2-5) there are two samples with higher n_y-values (W2226 L : 209, and W 196 B : 7), and in the brownish green (6-7) one (D 444 : 8). These are the most mafic rocks in that area with excess TiO_2, so there seems to be an influence of the rock composition. On the other side of the area there are two samples with more greenish colours in a brown (10-12) environment (P 303 : 9, and P 248 : 6). The last sample is relatively felsic : a granitic xenolith in the border zone of the lopolith.

I.2.2. : Relationships between amphibole pleochroic colours and rock composition.

From sections VI.3, -6, and -7 it may be concluded that niggli values are better parameters to correlate rock- and amphibole composition than

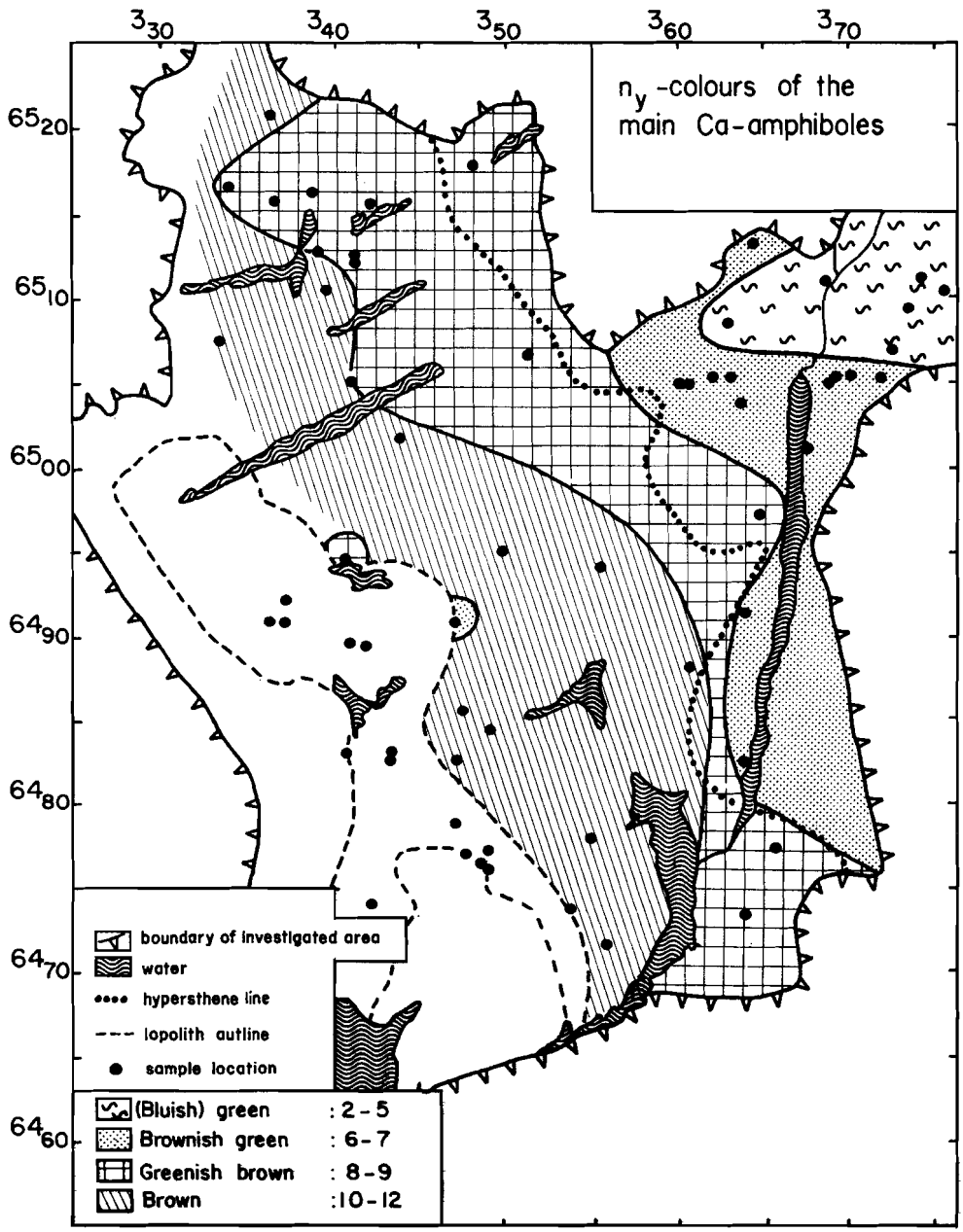

Figure I.2.: Distribution of amphibole colours (n_y) in the investigated migmatites. Colour numbers from section IV.3.2. Light-, normal-, and dark tinted colours are all included. Only main-phase amphiboles in rocks with excess TiO_2.

the bulk oxides. Therefore, niggli values were plotted against n_y- and n_z- colours, and the correlation coefficients calculated and judged.

For the migmatites and phase A rocks (Mg-rich amphiboles, table VI.3) n_y-colours give the best results (table I.2), while for the igneous rocks (Fe-rich amphiboles), and the combination of all amphiboles together, n_z-colours have higher correlation coefficients (calculation method after Davis, 1973). The strongest correlations ($|r| \geq .50$, or a special type, see fig. VI.2) for the various groups indicate a major importance of M (mafic mineral indicator), al (Al_2O_3-component) and alk (alkali-component) for the migmatitic group. The other niggli values have direct positive or negative correlations with the above mentioned M, al and alk. The n_z-colour of the igneous group has highest correlations with niggli-w (oxidation ratio of the rock) and niggli-h2o (H_2O component).

Mig. n_y		Ign. n_z		Com. n_z	
M	.62	w	-.59 A-type	M	.64
al	-.58 A-type	h2o	-.55 P-type	al	-.61
alk	-.56 A-type	T	-.52 P-type	fm	.60
L	-.55	π	-.42 A-type	L	-.58
fm	.54			alk	-.56 A-type
Q	-.53			t	-.53
si	-.53 A-type			Q	-.51
k	-.45 A-type			si	-.50 A-type
				π	.49 F-type
Mig. n_z				u	.48 C-type
π	.41 F-type			mg	.48 C-type
				c	.47 F-type
				k	-.46 A-type
				co2	-.25 A-type

Table I.2.: Correlation coefficients between niggli values and pleochroic colours of the main Ca-amphiboles in order of decreasing $|r|$-value. Mig., Ign., and Com., see section VI.3.1. Values from table III.4 and IV.4. Explanation of types, see fig.VI.2.

This means that in the migmatites a brown amphibole colour is positively influenced by mafic rocks with a relatively low Al_2O_3-content, and in the Fe-rich, igneous complexes by dry, poorly oxidized rocks. The A-type correlations for si, al and alk indicate that felsic rocks generally carry green amphibole, while mafic rocks may display every amphibole colour (fig. I.3).

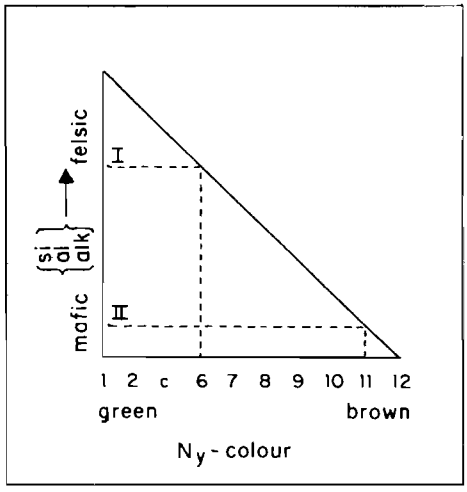

Figure I.3.: Correlation between n_y-colour and niggli si, al and alk in the migmatites. All samples plot within the triangle (fig.VI.2.: type A). The outward boundary is ideally drawn, and normally much more irregular. Felsic rocks (e.g. I) usually carry green amphibole while mafic rocks (e.g. II) have no bulk composition restriction for colour.

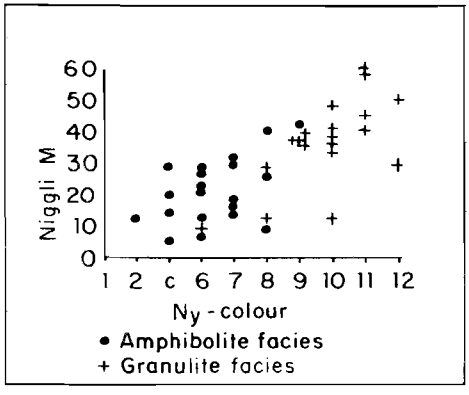

Figure I.4.: Correlation between niggli-M and n_y-colour in the migmatites. The r-value (.62) is the strongest for the correlation between bulk composition and amphibole colour.

Fig. I.4 shows the chemical differences between granulite- and amphibolite facies samples. Granulite facies samples, on an average, have more brownish colours than comparable amphibolite facies rocks. There is, of course, no sharp distinction between the two facies groups in the graph because of the gradual change in metamorphic grade. It is also clear from this graph that the higher grade amphibole carrying rocks are more mafic than the lower grade collection. This is quite logical due to the fact that the granulite facies is characterized by the presence of orthopyroxene instead of amphibole in the leucocratic rocks (Hermans et al, 1975).

Another important rock parameter is niggli al (table I.2). If a certain group of al values is compared the colours for n_y and n_z are higher in the granulite facies terrain.

al = 20 - 25	$\bar{n}_y$	$\bar{n}_z$	n
granulite facies	10	8	8
amphibolite facies	7	5	6

n = number of samples

Thus, in the granulite facies the samples are more mafic and the amphibole colours more brownish, and samples of comparable composition are more brown in the higher grade part. The colour difference cannot be explained

by rock composition only. The metamorphic conditions influence the amphibole pleochroic colours.

I.2.3. : Relationships between amphibole pleochroic colours and amphibole composition.

As argued in section IV.2. the amphibole structural formulae should be calculated on the basis of 23(O)(table IV.8). Fe^{3+}-, Fe^{2+}-, OH- and F-values may be derived from the 24(O,OH,F) calculation (table IV.10) and the 23(O)-including Fe^{2+}(Fe^{3+})-measurement method (table IV.12).

To understand the correlations between the various composition parameters which influence to amphibole colour, all correlations were calculated, tabulated, and graphically presented in section VI.5.

Table I.3 contains : a element parameters e.g. Ti, Na
b position parameters e.g. Sum Y, Ca+Sum Y
c combined parameters e.g. $(Fe^{3+} + Fe^{2+}/4)/Ti$.

The correlations are calculated for n_y- and n_z-colours, for the Mg-rich group of Ca-amphiboles (mainly from the migmatitic rocks), for the Fe-rich group of Ca-amphiboles (from the igneous complexes), and for all Ca-amphiboles together. The colour was plotted along the abscissa in all cases, with the lowest values for both axes in the lower left corner. The strongest correlations in table I.3 involve Ti- and Fe^{3+}-combined parameters. This is in agreement with most of the literature on amphibole colours (Deer, 1938: Ti; Rozenschweig and Watson, 1954 : $Fe^{3+}/(Fe^{2+} + Ti)$; Binns, 1965-a/b: Fe^{3+} versus 2Ti graph; Engel and Engel, 1962-b: Fe^{3+}/Fe^{2+}, OH and Ti; Henderson, 1968: Fe^{3+}/Ti; Raase, 1972: $(Fe^{3+} + \frac{1}{4}Fe^{2+})$ versus Ti graph and a review of amphibole colour literature). The parameter deduced from the work of Raase (1972) indicates that the total amount of Fe is also important but to a smaller extent than the Fe^{3+}-content : Fe-rich amphiboles prefer green colours (see table I.3 : Combination). The other parameters mentioned in literature: Fe^{3+}/Fe^{2+}, OH, and $Fe^{3+}/(Fe^{2+} + Ti)$(= Rozenschweig parameter), are of no real importance.

Parameter	Mg-rich n_y	n_z	Combination n_y	n_z	Fe-rich n_y	n_z
$(Fe^{3+} + Fe^{2+}/4)/Ti$	-.81	-.82	NA	NA	NA	NA
Fe^{3+}/Ti	-.79	-.79	NA	NA	NA	NA
Ti	.73	.73	.79	.75	.76	.58
$Al^{VI} + 2Ti$	.66	.64	.65	.66		
Ca + Sum Y	-.62	-.64	-.65	-.65	-.68	-.62
Mn	-.56	-.63 A	-.50	-.54		
Si	-.56	-.54	-.50	-.53		
Na + K	.54	.55		.55	.53 C	.61
Sum Y	-.52	-.56	-.65	-.67	-.55	-.57
Fe^{3+}	-.49	-.56	NA	NA	NA	NA
Sum X	.48 N	.47 C	.53	.55	.48 N	.62
$Fe^{3+}/(Fe^{2+} + Ti)$	-.45		NA	NA	NA	NA
Al-total	.43 B		.30 Q		-.46 A	
Na	.39 B	.45 B		.48 B	.60 N	.68
F/OH		.26 B	NA	NA	NA	NA
F		.25 B	NA	NA	NA	NA
F/(F + OH)		.18 B	NA	NA	NA	NA
Fe-total			-.48 A	-.52		
mg-ratio			.45 C	.49		
Mg			.40 C	.43 C		
Al^{VI}					-.75	-.57
A-site					.30 C	
K					.16 S	

Table I.3.: All determined main amphibole ion-, position-, and combined parameter relations with n_y- and n_z-colours, in order of decreasing |r|-value for the Mg-rich group, Fe-rich group and all amphiboles together (Combination). Fe^{3+}, Fe^{2+}, OH and F are only calculated for the Mg-rich group because of scarcity of data for the Fe-rich group. Letters, see types in fig.VI.2. NA: Fe^{3+} etc not analyzed, parameter not calculated.

The only "fluid influence" is expressed by F and F/OH : green amphiboles have low F and F/OH values, in brown amphiboles they may vary.

Seemingly important colour-influencing parameters (table I.3) other than Ti and Fe^{3+} (or combinations of both) are mainly related in the structural formula to Ti (table VI.7), sometimes by means of coupled substitutions (section VI.5.4.), or to Fe^{3+} (table VI.4). No clear correlation in the structural formula is found between Fe^{3+} and Ti, only a weak A-type. Parameters which form a combination of Ti and Al^{VI} (e.g. $Al^{VI} + 2Ti$) never give a better result than Ti alone. This means that the only important elements, which determine the colour, are Ti and Fe^{3+}, and, partly, Fe^{2+}. The most important correlations can be seen in fig.

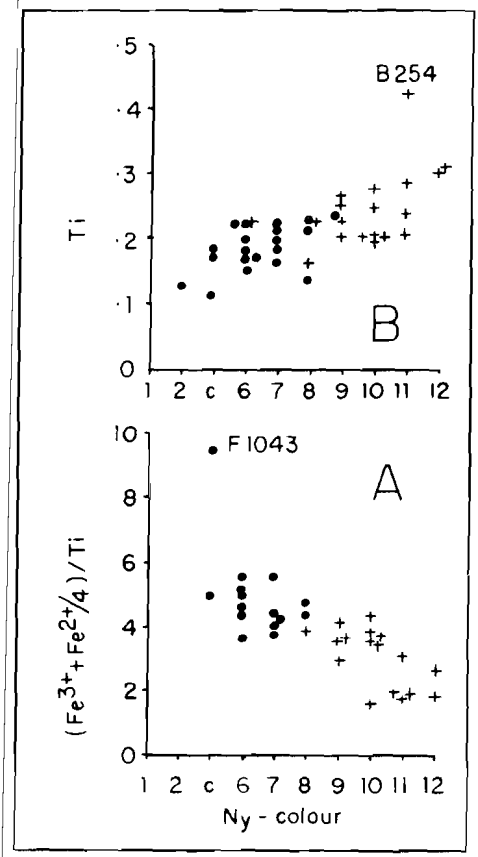

Figure I.5.: Correlations between n_y-colour and Ti, and the combined Fe-Ti parameter. Migmatites with excess Ti only. Crosses: granulite facies; dots: amphibolite facies. Values for A from table IV.12, for B from table IV.8. Correlation coefficients are -.81 and .73 resp. The use of n_z-colour as abscissa gives essentially the same picture.

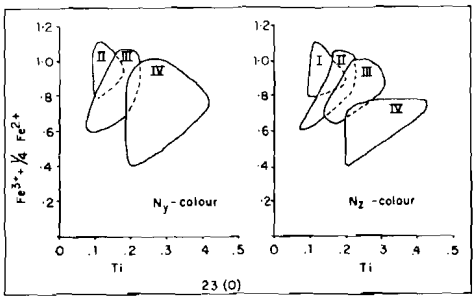

Figure I.6.: Rogaland/Vest-Agder equivalent of fig.1 from Raase (1972). I = bluish green (1-2), II = green (c). III = brownish green (6-8), and IV = brown (9-12).

I.5, and the Rogaland version of fig. 1 from Raase (1972) is fig. I.6. Mg-rich phase A samples can be plotted without any problem in the migmatite graphs. For the Fe-rich, igneous group, not enough Fe^{3+} analyses have been done, leaving only Ti (the other parameters are interrelated). The combined group confirms the correlations found for the migmatites and proves therefore the validity of the colour determining parameters.

Brown Ca-amphiboles are, on an average, richer in Ti, alkalies and Al-total. Green Ca-amphiboles are, on an average, richer in Mn, Si, and Fe^{3+}.

I.2.4. : Relationship between amphibole-colour determining Ti and Fe^{3+} and the rock composition.

Amphibole Ti and Fe^{3+} (or TiO_2 and Fe_2O_3) do not reveal high r-values in in relation to rock composition (section VI.3, 6 and 7). High TiO_2 is favoured in the more mafic rocks; Fe_2O_3 shows no relation. As far as TiO_2 is concerned, the findings in section I.2.2. are confirmed : in the granulite facies, where the samples are more mafic, the amphibole colours are more brownish, however, there is no strong rock control over Ti in amphibole as long as Ti-bearing ore phases are present in excess. Ti is free to respond to metamorphic circumstances.

I.2.5. : Chemical differences between Ca-amphiboles from the granulite- and amphibolite facies areas.

The granulite facies Ca-amphiboles of the main migmatitic group are
richer in : Al-total, Al^{VI}, Ti, K, (Na+K), Al^{IV}
poorer in : Si, Fe-total, Fe^{3+}, Mn.
equal in : Fe^{2+}, Mg, Ca, Na, OH, F.
compared to the amphibolite facies amphiboles.
Most of these differences can be explained by means of the difference in average rock composition, which was mentioned already in the preceding sections.

The granulite facies rocks are richer in : FeO, total Fe-oxides, MnO, MgO, CaO; poorer in : SiO_2, Na_2O, K_2O, P_2O_5, F; equal in : Al_2O_3, TiO_2, Fe_2O_3, H_2O^+, compared to the amphibolite facies rocks.

The most important amphibole composition influencing rock parameters (Chapter VI) are the niggli values :π, alk,μ. The first is higher, the second lower in the granulite facies area.μ is about equal for both parts. These differences in average rock values seem to cause the differences in average amphibole composition (sections VI.3, -6, -7), except for Ti and K.

To check the influence of the rock composition, the results of Chap-

ter VI were used. For every amphibole structural formula parameter the strongest related whole rock parameter was taken (e.g. Si-amph and π-rock, table I.4). Histograms of the rock parameters were made for both facies areas to find a range with as much samples as possible for both groups (e.g. π = .30-.40). Within this range the amphibole parameters from granulite and amphibolite facies were compared : table I.4.

Parameter			Facies			
Rock	Amphibole		Granulite		Amphibolite	
			$\bar{x}$	n	$\bar{x}$	n
		Si	6.46	3	6.48	6
π : .30- .40		Al-total	1.75	3	1.85	6
		Al^{VI}	.21	3	.33	6
alk : .10- .14		Mn	.035	4	.04	5
		Fe-total	1.85	7	1.89	8
μ : .30- .39		Mg	2.50	7	2.63	8
		mg-ratio	.57	7	.575	8
w : .20- .29		Fe^{3+}/Fe-tot.	.24	6	.20	5
		Fe^{3+}	.43	6	.42	5
FeO : 7.0 -9.0		Ti	.26	6	.20	5
MgO : 4.0 -6.0		Na	.47	4	.49	5
K_2O : 1.0 -2.0		K	.35	6	.25	5
Na_2O : 2.5 -3.0		Ca	1.81	6	1.76	5
F : .10- .20		OH	1.19	5	1.22	5
μ : .30- .40		F	.45	7	.35	8

Table I.4.: Average Ca-amphibole compositions for groups of granulite and amphibolite facies samples within certain compositional ranges for the host rocks. Amphibole values from table IV.12.

The only significant differences are found for Al-total (and hence Al^{VI}), Mg, Ti, K and F. Granulite facies amphiboles contain higher absolute values of Ti, K and F with respect to amphibolite facies amphiboles for a certain bulk rock composition. This causes a decrease of Mg (Tschermakite coupled substitution, section VI.5.4.) and Al^{VI} (charge compensator like Ti and K). The K-content has no significant correlation with the amphibole pleochroic colours as does Ti. The regional pattern for K is not clear. The F-content has a weak correlation with the colour (table I.3), there is also a slight positive correlation with amphibole K_2O. This results in (from) an irregular pattern for the F-distribution, which is not linked directly to the metamorphic pattern. Therefore, the average values of the F-content for granulite- and amphibolite facies amphiboles are about the same, while the highest values

are found the granulite facies.

Fe^{3+} and the oxidation ratio for Ca-amphiboles depend on the oxidation ratio of the rock (niggli w). The average w-values are about equal for both areas, but there is a large spread. The oxidation ratio of the amphiboles does not depend on the position in the metamorphic picture of granulite- and amphibolite facies, but has its own regional distribution (section I.3.). This implies that the influence of Fe^{3+} on the amphibole colours is rather small.

The final conclusion seems to be that the higher grade amphiboles contain, for a certain rock composition, higher amounts of Ti and K (and possibly F), and hence lower amounts of Mg and Al^{VI}. Ti is the most important element to determine the Ca-amphibole colour pattern, and indicates in this way a metamorphic temperature pattern. The absolute values for the temperature cannot be told from the Ti-content, because P_{H_2O}, P_{total} and f_{O_2} are also very important.

Comparison with part of the literature shows the following results :

	Higher values in granulite facies for:	amphibolite facies
Engel and Engel (1962-b) (regional investigation)	Na, K, Ti, F	Fluid, Fe^{3+}/Fe^{2+}, Mn, Fe/Mg
Kostyuk and Sobolev (1969) (literature compilation)	Al^{IV}, Al-total, Na, (Na+K), Ti	OH, Si
Raase (1974) (literature compilation)	(Na+K), Ti	Al^{VI}, Fe^{3+}
Dekker (this study) uncorrected for rock composition differences	Al-total, Al^{VI}, Al^{IV}, Ti, K, (Na+K)	Si, Fe-total, Fe^{3+}, Mn
Dekker (this study) corrected	Ti, K, (F), (Na+K)	Mg, Al^{VI}, Al-total

The conclusions of Kostyuk and Sobolev agree very well with the uncorrected results of the present author, while the information of Engel and Engel, and Raase is in good agreement with the corrected results, as far as the values higher in the granulite facies amphiboles are con-

cerned. High values in the amphibolite facies hornblendes do not agree very well, the Engel and Engel information seems to be affected by changes in rock composition.

I.3. : The amphibole oxidation ratio pattern

Fig. I.7 shows the oxidation ratio pattern for Ca-amphiboles of the main groups, based on the measurement of Fe^{2+} in mineral separates. These analyses were performed under special conditions to prevent oxidation during the process (section IV.1.). Not only samples from the migmatitic environment, but also from the igneous complexes were included.

The highest amphibole oxidation is found in a N-S trending zone along the Sirdalsvatn, and in a ENE-WSW zone north of Gyadalen. In the NW-part of the map, the hypersthene line crosses several oxidation ratio ranges. Therefore, the oxidation of the amphiboles is not connected with the main metamorphic event, but is of younger age, possibly connected with the great tectonic structures of Gyadalen and the Sirdalsvatn. However the tectonized sample V 187 has a low oxidation ratio.

There is only a weak positive correlation between the oxidation ratios of amphiboles and the host rocks (fig. I.8). In general the host rock value is higher than the amphibole ratio, except for the lowest host rock values. A plot of the rock values on the Rogaland map, like fig. I.7, creates a chaotic picture, not worth publishing. The ratios may differ very much for samples from the same region. This indicates that the amphiboles are more sensitive to certain oxidizing circumstances than the host rock. The amphiboles are able to reflect such an oxidizing (or reducing) phase in a regional picture, the host rocks cannot react as a uniform group, which is not remarkable in the light of the fact that the host rocks contain various ferro-magnesian minerals. These minerals all react in their own way, resulting in various oxidation ratios for various mineral assemblages.

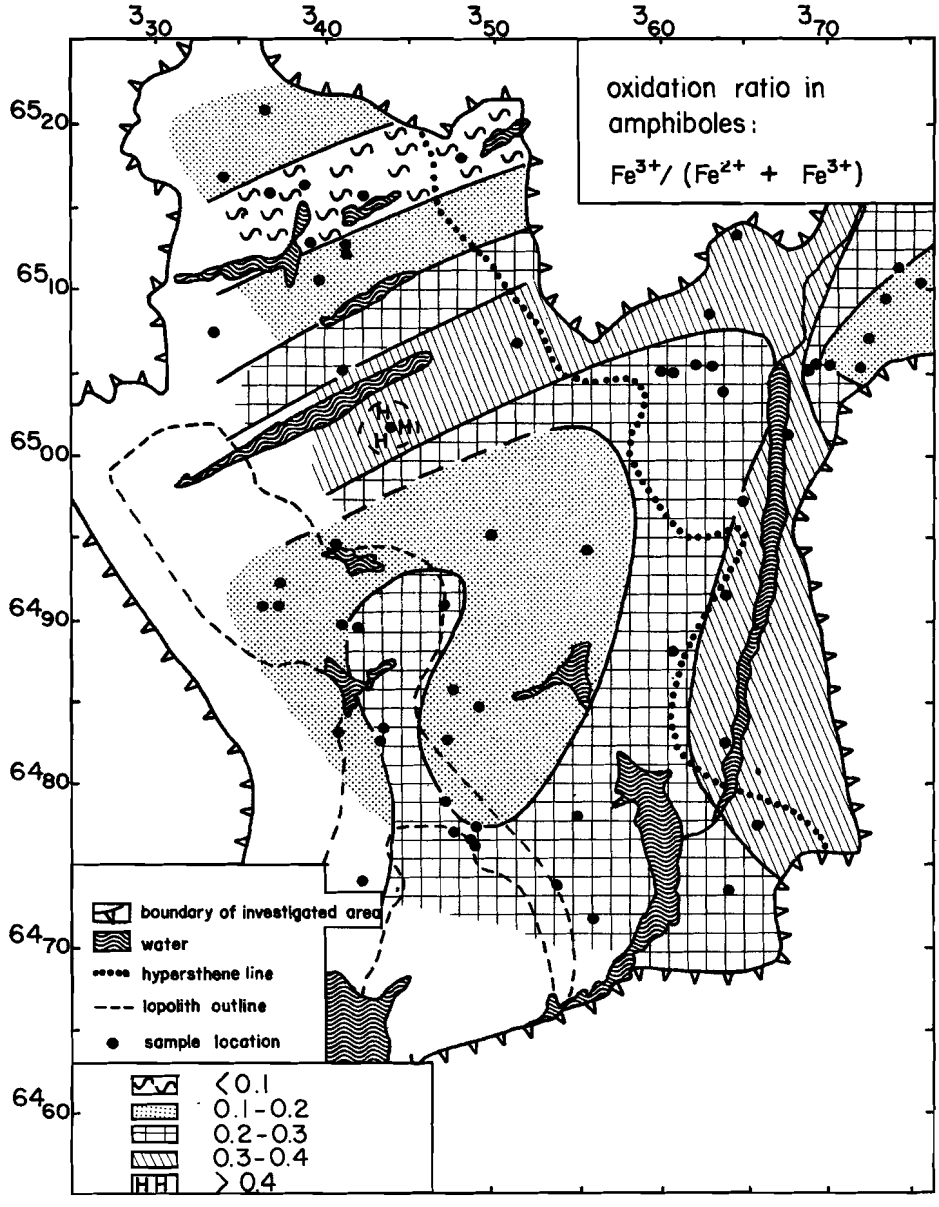

Figure I.7.: Regional distribution of the oxidation ratios in amphiboles. Values form table IV.10.

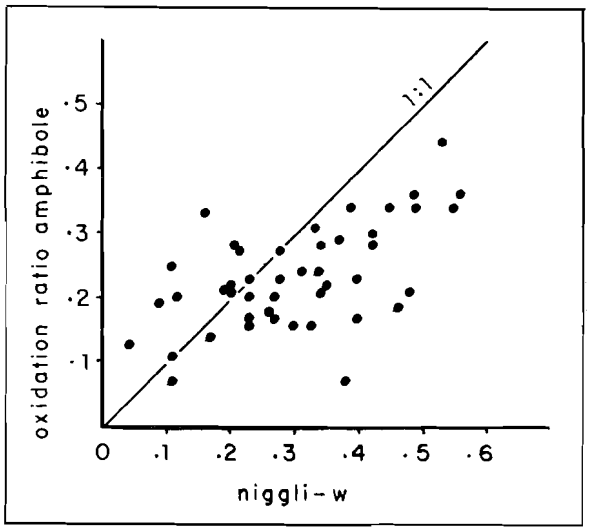

Figure I.8.: Correlation between the host rock oxidation ratio and the amphibole value. Niggli-w values, table III.4. Amphibole values, table IV.10.

I.4. : Ti distribution in the main- and secondary amphibole groups

Fig. I.9 contains Ti-histograms for amphiboles from various mineral facies (Raase, 1974) and for some Rogaland amphibole groups. The sloping line in the graph indicates the maximum Ti-content for a certain metamorphic (sub-)facies.

Group V includes the Mg-rich samples from the leuconoritic phase, and the intercalations in the lopolith, which were grouped with the Mg-rich (migmatitic) group for the correlation analyses (Chapter VI). Apart from the two extremely high Ti-values for E 125 and E 128, two groups can be distinguished : A from .26 to .155, B from .10 to .00. The A group lies in between the two main groups from the metamorphic environment (VI and VII), which coincide very well with the hornblende granulite- and higher-grade amphibolite facies of Raase. The B group lies in between I and II, in the lowest part of the amphibolite facies, with extremely low values for Y3131 (.00 and .01) and Y1131 (.03). Sample Y 131 from Gloppurdi igneous complex is also aberrant in other respects (Chapter VI). It seems to fit much better in group VIII. The question arises whether the B

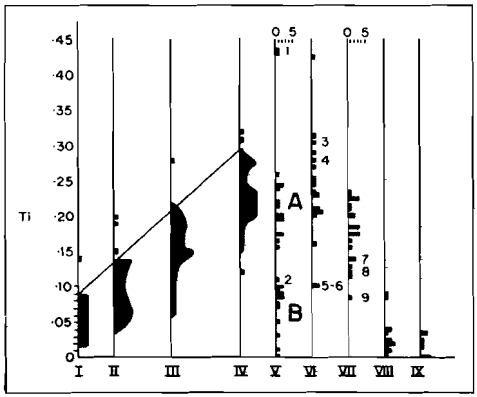

Figure 1.9.: Histograms of Ca-amphibole Ti-contents, 23(O). I-IV from Raase (1974), V-IX from this study.

I : greenschist-amphibolite transition facies
II : lower-grade amphibolite facies
III : higher-grade amphibolite facies
IV : hornblende granulite facies
V : Rogaland/Vest-Agder main amphiboles in the igneous complexes
VI : in the migmatites west of the hypersthene line
VII : in the migmatites east of the hypersthene line
VIII: Rogaland/Vest-Agder secondary amphiboles in the igneous complexes
IX : in the migmatites.
1-9 : Ti-undersaturated rocks (no free Ti-ore), resp.: E 128 1, F1433, D 307, O 100, P1580, P2580, D 442, W 012, W1226 D.

group of V and the secondary amphiboles of VIII should be grouped together. The last group (IX) covers the same range as VIII, there is no reason to assign these secondary amphiboles to separate events.

The position of the extreme high-Ti amphiboles points to an igneous origin (Leake, 1965-a; Raase, 1974). The maximum value allowed for metamorphic amphiboles lies between .30 and .35 (Leake, 1965-a).

It is interesting to see which samples of the igneous complexes fall into group A and B :

A (high temperature) : B 322, E 067, E 131, E1167, E 170, N1402, N1528, P1097, R 227, R1229, R 356, R1668, V 277, Y2131 (F1433, undersaturated).

B (lower temperature) : B1016, E1232, E3232, N3528, N1827, R1269, V 147, V 276, Y1128, (Y1131-Y3131, better fit in the secondary group).

These samples stand for :

A : all parts of the lopolith, including pegmatites; Botnavatnet- and Gloppurdi igneous complexes.

B : reaction products from pyroxene breakdown in various parts of the lopolith and anorthosite, and some fragmentary bluish green amphiboles in the lopolith and Gloppurdi I.C.

Amphiboles from group A and B do not show great mineralogical and chemical differences, they are all Fe-rich hornblendes. The secondary group is mainly lighter coloured, of actinolitic composition, and an

alteration product of hornblende from the main amphibole group. The Ti-content of the lower T group, however, resembles the Ti-content of the secondary group.

This results in the following picture :

--there appear to be at least some igneous amphiboles in the lopolith (E 125, E 128) as well as in the migmatites bordering the lopolith (B 254),

--the metamorphic environment of the igneous complexes, which was divided in granulite- and amphibolite facies areas by means of the hypersthene line, can be divided in the same way with the aid of amphibole Ti-contents,

--the igneous complexes show two groups : a high temperature group at granulite facies level, and a lower temperature group at lower amphibolite facies to greenschist facies level,

--after the last main metamorphic event, some parts were affected by retrograde metamorphism in greenschist facies. It is possible that there is a relation between this event and the regional oxidation pattern (section I.3.). The lower T group from the igneous complexes may also be part of this event,

--the fact that the highest Ti-value (E 128, 0.435) is found in an ultramafic xenolith in the lopolith with no free Ti-ore, indicates that kaersutites (Ti >0.50) might be found in other xenoliths richer in TiO_2.

I.5. : Al^{VI} distribution in the main- and secondary amphibole groups

In the Mg-rich Ca-amphibole group, Al^{VI} is strongly correlated to the niggli-π value (section VI.6.). The niggli-π stands for the An-percentage (section VI.3.), and therefore, the optically recognisable An % may be used to study the Al^{VI} behaviour (fig. I.10).

In the Fe-rich Ca-amphibole group Al^{VI} and niggli-π are not correlated significantly. This is perhaps caused by the Ti-behaviour (section I.4.). There appeared to be two temperature groups in the Fe-rich amphiboles. The low temperature group contains relatively little Ti and, therefore,

had to attract another charge compensator (Fe^{3+}, Al^{VI}, Na or K). From the relation Ti vs Al^{VI} (r=-.80) for the main Fe-rich Ca-amphibole group (section VI.5.) it is clear that Al^{VI} was preferred, although Fe and alkalies were present in excess in these rocks. This preference for Al^{VI} disturbed the correlation between Al^{VI} and niggli-π (= An%). The Fe-rich amphiboles which belong to the low temperature group (B) in section I.4. fall above the zone formed by Mg-rich amphiboles from the migmatites and the leuconoritic phase of the lopolith, and the Fe-rich amphiboles from the high T group (A) in section I.4.

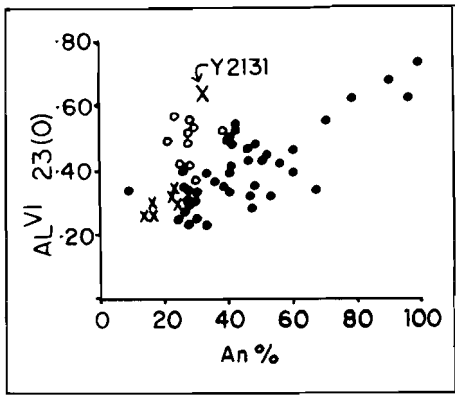

Figure 1.10.: Correlation between Al^{VI}, 23(0), and the An % of the coexisting plagioclase. Dots: Mg-rich amphiboles from the igneous complexes with high Ti (Group V-A of section I.4); open circles: low Ti, Fe-rich amphiboles, group V-B. Y2131 stands, as usually, apart.

The correlation between An% and Al^{VI} only holds for the high Ti (T) amphiboles (Mg- and Fe-rich). Low-Ti, Mg-rich amphiboles are secondary, and thus not included in the chart.

Now the Si vs Al^{VI} graph (Raase, 1974) can be drawn to estimate the pressure of formation. In fig. I.11 the graphs are plotted for the various groups of section I.4.

It can be seen that in the igneous complexes, the high Ti amphiboles (VA) lie further below the empirical 5 kb line than the low Ti-ones (VB). The migmatitic amphiboles from both sides of the hypersthene line lie at about the same distance from the 5 kb line as VA, except for some Ti-undersaturated samples. The amphibolite facies amphiboles lie slightly closer to the 5 kb line. In section I.2.5. it was already shown that granulite facies amphiboles are relatively low in Al^{VI}.

The secondary amphibole group VIII lies close to the 5 kb line, which is not continued below Al^{VI}= .45, Si= 7.0. Group IX coincides with the lower parts of VIII. All groups lie far below the line of maximum possible Al^{VI} from Leake (1965-b).

Combining of the six graphs of fig. I.11 results in fig. I.12.

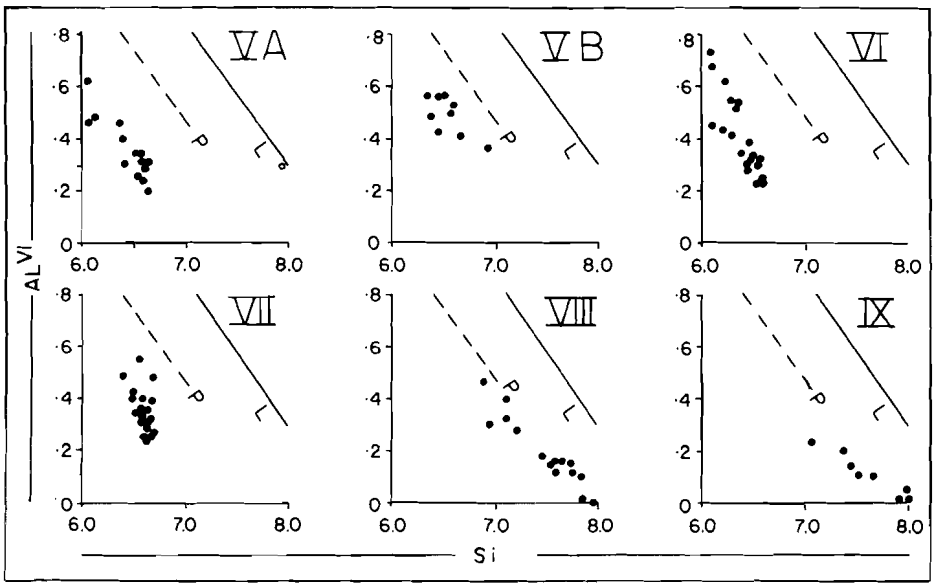

Figure I.11.: Si versus Al^{VI}, 23(0), graph for the various groups from fig.I.9. P = 5 kb line from Raase (1974), L = maximum possible Al^{VI} (Leake, 1965-b).

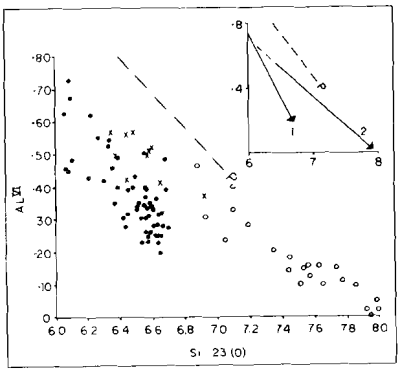

Figure I.12.: Combination of the six graphs from fig.I.11. Dots: group V-A, VI and VIII; open circles: group VIII and IX; crosses: group V-B. The inset shows the general trends for 1: dots, and 2: open circles and crosses.

The amphiboles of group VA, VI and VII form a group of dots more or less parallel to the 5 kb line and far below it. The trend from high Al^{VI}-low Si to low Al^{VI}-high Si is strongly determined by the An% of the coexisting plagioclase (fig. I.10). This also holds for the Ti-undersaturated samples, which lie closer to the 5 kb line. The general trend for this graph is represented by line 1 in the inset.

The secondary amphiboles (group VIII and IX) form a straight zone with a high correlation between Si and Al^{VI}, line 2 in the inset. There is no relation with An%. The low Ti group from the igneous complexes (group VA) lies at the interception of line 1 and 2. It does not fit in the group of

main amphiboles because the relation between An% and Al^{VI} is absent. This group with An% values between 20 and 40 falls in the 40 - 60% range of the main amphiboles.

There is no reason to place the low Ti amphiboles with the main amphiboles any longer (as was done in Chapter VI). They seem to fit the secondary trend much better, a trend which lies closer to the 5 kb line.

Thus Al^{VI} combined with Si 23(0) indicates :

--very low pressures for the main amphibole formation conditions in both the igneous complexes and the metamorphic environment. During this phase, Al^{VI} depended mainly on the An% of the coexisting plagioclase, which also determined the Si-contents,

--somewhat higher pressures, probably near 5 kb for the retrograde event, which not only includes actinolitization of pre-existing amphiboles, but also the breakdown of pyroxene to hornblende and actinolite (e.g. E 232) in and around the lopolith.

It should be realized that the Al^{VI} values from the 23(0) tables are maximum values (section IV.2.6.). When Fe^{3+} is measured, the Al^{VI}- (and Si-) values decrease. The size of the difference depends on the oxidation grade of the amphibole. For the completely analyzed samples in this study, the difference is largest in the low Al^{VI}-part, upto .15 and smaller in the high Al^{VI}-part, upto .10. However, Raase also used 23(0) values.

Hardly anyone ever mentiones whether P_{total} or P_{fluid} is meant. In most literature cases used by Raase (1974) to construct his diagram, the indicated P will have been P_{total}, leading to a 5 kb P_{total} line. P_{fluid} depends on the metamorphic facies and rock type. In Rogaland P_{total} seems to have been equally low for the whole terrain during the main amphibole forming event, but because of increasing T towards the west, dehydration occurred, resulting in a decreasing P_{fluid}.

Dehydration reactions all need quartz and, therefore, the mafic rocks will dehydrate more difficultly than felsic rocks : amphibolites may be preserved for a long time in granulite facies conditions. In that way P_{fluid} can differ strongly in a granulite facies formation : in banded series one often sees an alternation of amphibole carrying (-rich) mafic rocks and hypersthene carrying, amphibole- and biotite-free felsic rocks. The light bands are completely dry, the dark bands still have a certain fluid pressure, but this pressure will be well below the P_{total}. In the amphibolite facies terrain all rocks carry abundant amphibole and biotite, coexisting with quartz. P_{total} may be about the same as P_{fluid}.

An indication for the changing P_{fluid} from amphibole facies to granulite facies is the change in amphibolite mineralogy : biotite amphibolite → amphibolite → clinopyroxene amphibolite → two pyroxene amphibolite (→ hypersthene amphibolite).

I.6. : Conclusions

In the Rogaland/Vest-Agder area :

--the amphibole colours in Ti-saturated rocks of the migmatites change from (bluish-)green in the east to brown in the west. The lopolith of Bjerkreim-Sokndal shows this colour change from bottom to top,

--the amphibole colour is mainly determined by the Ti-content of the amphibole,

--brown amphiboles contain, on an average, more Ti, alkalies and Al-total, green amphiboles contain, on an average, more Mn, Si and Fe^{3+},

--the Ti-content in amphibole is not influenced strongly by the rock composition as long as Ti-bearing ore phases are present in excess. High Ti is favoured in mafic rocks,

--granulite facies amphiobles are richer in Al-total, Al^{IV}, Al^{VI}, Ti, K and (Na+K), and poorer in Si, Fe-total, Fe^{3+}, and Mn than amphibolite facies amphiboles. The amounts of Fe^{2+}, Mg, Ca, Na, OH and F do not differ significantly,

--corrected for rock composition the granulite facies amphiboles are richer in Ti, K, sum of alkalies and, possibly, F. They are poorer in Mg, Al^{VI} and Al-total than amphibolite facies amphiboles,

--the oxidation ratios of the Ca-amphiboles show a regional pattern which is not related to the main metamorphic event, but which seems to be dominated by great tectonic structures,

--the main amphibole forming phase was high T, low P (= Abukuma type) over the entire region, with an increase in T towards the west,

--the phase of secondary amphibole formation took place at lower T and somewhat higher P conditions, and is possibly related with a tectonic event.

II : Regional aspects and petrological implications.

II.1. : Introduction

In the Appendix all individual samples are described extensively. For each sample its field occurrence, macroscopic and microscopic information as well as those chemical- and optical properties which deserve special attention are given. These lead to certain ideas and conclusions about the origin of the amphiboles, and sometimes, their host rocks. The samples in this chapter are not arranged in alphabetic order as in the Appendix, but according to petrological environment. General descriptions of all formations are given by Hermans et al (1975).

II.2. : Migmatites

II.2.1. : General characteristics.

Formations treated in this section are, from the amphibolite facies :

--Granitic migmatites (D 172 D, D 442, D 444, F 005, F 043, F 052 D and -L, N 041 B, N 264, V 363, W 012 D, W 017 B, W 196 B, W 217, W 226 D and -L),

--Sirdalen augen gneisses (F 252, H 047 B, H 050 B, W 162 D),

--Espetveit augen gneisses (F 070 D), and, west of the hypersthene line:

--Charnockitic migmatites (B 118 L, B 254, D 307, H 307, H 325, H 415, J 119, M 101, N 317, N 337, N 572 D and -L, N 809, P 303, P 580 D and -L, V 147, V 187, Y 055).

The garnetiferous migmatites are only represented by a gabbroic sample in section II.4. Amphiboles are rare in this formation, only in the dark bands some amphibole may be present. The more leucocratic rocks contain garnet. Garnet and amphibole never appear together in a stable association, neither in the garnetiferous migmatites, nor in garnet-rich parts of other formations. This is a characteristic of the Abukuma type of regional metamorphism (e.g. Ernst, 1968 : figures 24 and 39). This HT-LP

type was already derived from the Ti- and Al^{VI}-information (sections I.4. and I.5.).

In the amphibolite facies area, the amphibole-bearing rocks range from from leucogranite to hornblendite (table I.1). Plagioclase An-percentages lie between 20 and 50% (table III.1); locally albite rims are found. Remarkable is the high alkalifeldspar content with respect to plagioclase in some of the samples (F 052 D and -L, see section II.2.5., and N 264). Retrograde minerals are not uncommon, especially around Tonstad (grid reference 3675-65055) : epidote, albite, chlorite, actinolite, titanite and sericite.

In the Sirdalen augen gneisses the constitution of the augen appears to be linked with the hornblende-biotite ratio. If the Ca-rich mafic mineral is abundant (hornblende more than biotite) the augen consist of aggregates of alkalifeldspar crystals with some quartz-, plagioclase-, biotite-, ore- and retrograde mineral crystals. If the K-rich mafic mineral dominates, the "eyes" are formed by one large alkalifeldspar crystal, in which all other minerals that are present in the rock may occur as inclusions. This phenomenon may be attributed to variations in Ca and K activities.

The main difference between the Espetveit- and Sirdalen augen gneiss is the smaller augensize of the former : normally 0.5-1 cm, while the Sirdalen augen may reach 10 cm (Dekker, 1973).

In the granulite facies area most amphibole-bearing rocks plot in the plagioclase corner of the QAP-triangle (fig. III.8). Two samples fall in the granite field : V 147 which presumably belongs to the Gloppurdi Igneous Complex (see section IV.3.2.) and B 118 L, the light part of a banded amphibolite sample with dehydrated rims. Some amphibole is still present in the contact zone between dark and light, and was assigned to the light band of B 118. New rock-sections showed the dehydrated character. So, no leucocratic rocks are present which belong to the charnockitic migmatite formation and contain amphibole. M 101

(quartz monzonorite) and Y 055 (enderbite) are the only other samples outside the diorite-norite field. Ultramafic rocks are represented by N 572 D (hypersthenite) and N 809 (hornblendite).

The An-percentages of the plagioclase are higher than in the amphibolite facies area : 30-90%, only the two granitic samples B 118 and V 147 are somewhat lower (27-28%).

Near the E-side of the lopolith, the migmatites form a mainly banded zone which contains olivine-bearing mafic and ultramafic rocks (B 254 and N 572 D). The only other occurrence of olivine in migmatites outside the igneous complexes is a locality east of Lundevatnet. Most forsterite-rich olivine is found in the leuconoritic phase of the lopolith and in some (ultra-)mafic xenoliths in the higher parts (e.g. E 128). Therefore, the presence of olivine in this migmatitic zone points to a magmatic origin, possibly related to the emplacement of phase A. It is also the only place with really kinked amphiboles (N 572 L). Everywhere else the amphiboles show no more deformation than a slightly undulatory extinction, even if the plagioclase is strongly fractured (N 317, V 187).

Retrograde minerals in amphibole-bearing rocks, as are found in the Tonstad area, are rare here.

In the amphibolite facies area, the amphiboles from the main group (section VI.2.1.) show only little variation (table IV.7 to -.12). They are common hornblendes (: Si=about 6.50; Ca+Na+K= about 2.50; mg-ratio= about 0.50; 23(0)), (fig. II.1-A). The secondary amphiboles are actinolites or actinolitic hornblende. The only deviating sample is N 041 B, which is not treated here because it is not clear whether it belongs to this formation or even this region (see Appendix). It is one of the few samples in the Rogaland/Vest-Agder area with exsolution lamellae.

The differences in chemical composition are mainly caused by differences in bulk composition (see Chapter I and VI).

In the granulite facies area the amphiboles show more variation (fig. II.1-B). The only amphiboles with Ca+Na+K less than 2.50 are of secondary origin (V2187, Y2055). The composition of the main amphiboles lies

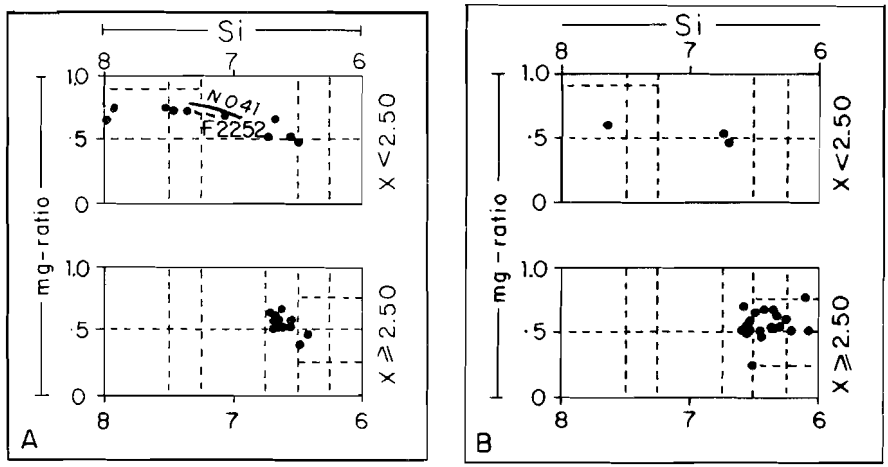

Figure II.1.: Plot of the amphiboles form the amphibolite (A) and granulite (B) facies areas, in Leake's diagram (1968). Compare with fig.IV.8. 23(O) structural formulae. X = Ca + Na + K.

between common hornblende and pargasite (N1572 R). This indicates the paucity of quartz in the samples, because pargasitic amphiboles only occur in quartz-free rocks (Ernst, 1968). V 147 deviates strongly with a mg-ratio of 0.25, this sample will not be treated here any further; it is described with the Gloppurdi Igneous Massif (section II.6.).

The three amphiboles poorest in Si (Si less than 6.25, 23(0)) : N1572 R, B 254 and N 317, are all derived from the olivine-bearing mainly banded zone near the lopolith.

K-Ar data on hornblendes all show ages of $\pm$ 950 Ma, except one sample in the south (Rog 43), see Chapter VII.

Biotite grows in most cases straight through all other minerals, indicating its late formation, sometimes it forms symplectitic intergrowths with quartz.

II.2.2. : Hydration and dehydration reactions

Various reactions are possible between pyroxene and amphibole (Martignole, 1975) :

I : hornblende + 4 quartz⇌3 orthopyroxene + clinopyroxene + 2 plagioclase + H_2O

II : hornblende + 2 biotite + 17 quartz⇌15 orthopyroxene + 4 orthoclase + 3 plagioclase + 5 H_2O

III : hornblende I + quartz⇌hornblende II + orthopyroxene + clinopyroxene + plagioclase + H_2O

Sen and Ray (1971-b) add some opaque ore on the right-hand side of the reactions.

In the amphibolite facies area all pyroxene- and amphibole-bearing samples are involved in hydration reactions. The amount of hydration depends on the availability of the components on the right-hand side of the above mentioned equations. It is not always possible to tell which one of the reactions produced the present assemblage.

Some examples are :

D 172 D : Amphibole-biotite-clinopyroxene-quartz clusters are present on the contact between a gabbronorite and a pegmatite. Orthopyroxene and alkalifeldspar are (now) only present in very small amounts. Plagioclase is omnipresent.

W 017 B : Orthopyroxene crystals may be surrounded by hornblende + quartz, which in turn are surrounded by biotite, growing through the amphibole.

Most samples in the amphibolite facies area show amphibole-quartz symplectites, thin quartz rims around amphibole, or amphibole fragments of equal optical orientation around quartz grains.

The last phenomenon looks like the dissolution of a formerly continuous hornblende crystal by quartz.[1] This possibly represents the recrystallization of hornblende-quartz aggregates formed by hydration. Pyroxene is not present in these samples.

In the granulite facies area quartz is absent in most amphibole-bearing samples, indicating the possibility of extensive dehydration of former amphibole-quartz assemblages. However, mineral reactions can hardly be proved.

1 : Plate 1, figure 1.

If only clinopyroxene is present, dehydration becomes problematic : all reactions involve orthopyroxene. These samples are H 307, H 415, P 303 and P 580 L. Both H-samples are biotite amphibolites near the hypersthene line where only the leucocratic rocks dehydrated. The amphibolites remained perfectly stable, except possibly for the outer rims, which were not incorporated in the samples.

P 303 is a biotite amphibolite near the contact with the lopolith. The amphibole is poikiloblastic, no quartz is present. The pleochroic colours are more greenish than those from the surrounding rocks (fig. I.2). The Ti-content is rather low (.20), even though some ilmenite is present. The amphibole may be due to fluid influx from the intrusion of the lopolith in a locally open system. P_{H_2O} rises and newly formed quartz from the hydration reaction can be removed. On the other hand, dehydration may have been ineffective in the central part of an amphibolite, as in B 118, but in that case the low Ti-values are not explained.

The last clinopyroxene-bearing sample is P 580 L, this diorite band contains only little amphibole from which nothing can be concluded. The accompanying dark band (P 580 D) appears to be strongly dehydrated, and contains much orthopyroxene + plagioclase. The green colour for these amphiboles results from Ti-undersaturation, no free ore is present.

Dehydration until a new equilibrium was reached is quite acceptable for B 118, D 307, H 325, J 119, N 809 and V 187. The amphibole now present may be the remnant of the original hornblende or a new one, according to reaction 3. For D 307 and N 809 this certainly seems to be the case : large (old) hornblendes are surrounded by a fine-grained orthopyroxene-clinopyroxene-plagioclase-hornblende matrix.[1] Opaque ore is almost absent in both samples, perhaps indicating that the reaction consumed ore.

Hydration is less easy to establish in this formation. Only M 101 shows an amphibole-quartz relation. It is also the most oxidized rock-

1 : Plate I, figure 2.

and amphibole sample in the charnockitic migmatites. Ti in the amphibole is relatively low, indicating that it formed at lower T than the other amphiboles from this unit.

In N 317 hornblendite-parts alternate irregularly with gabbronorite. On the contacts poikiloblastic amphiboles contain equally oriented pyroxene fragments[1], quartz is absent. This sample lies within 100 m of the lopolith.The hornblendite part seems to have formed from the original amphibole-(leuco)gabbronorite, due to the entrance of sulfur-carrying fluids, which might be linked to the intrusion of the lopolith. Orthopyroxene + clinopyroxene + plagioclase were replaced by amphibole and suphides, as can be seen from the poikiloblasts at the reaction fronts. Some pyroxene remnants are left in the amphibole due to plagioclase shortage. The orthopyroxene in these most hydrous parts is serpentinized during a, possibly later, tectonic phase, accompanied by the forming of a mylonite vein, uralitization of hornblende[2], and saussuritization and deformation of the plagioclase. This tectonic phase may be related to the folding of the lopolith. The banded migmatites were jammed between that body and the Outlier. The difference between the hornblendite and the gabbronorite seems to be caused only by differences in P_{fluid}. The penetrating fluid was concentrated along certain passegeways from which the quartz was carried away. The high Ti-content of the ferroan pargasite (.315) indicates a high T of forming, which is not remarkable in view of the intrusion of the lopolith at so short a distance. The main composition of the hornblende is comparable to those found in the leuconoritic phase of the lopolith. Little is known about the influence of sulfur fugacity on the stability of amphiboles. The only paper published sofar deals with Fe-Mg amphiboles (Popp et al, 1977).

II.2.3. : Retrograde metamorphism : actinolitization.

Actinolitization is commonly accompanied by the formation of epidote, chlorite, titanite, sericite and albite, and sometimes carbonate. The

1 : Plate I, figure 3; 2 : Plate I, figure 4.

actinolite is present at hornblende crystal margins, along cracks in the hornblende, and to a lesser extent as seemingly isolated blots in hornblende. In a few cases it forms small clusters with the other secondary minerals. The contacts between both amphiboles may be optically sharp, either straight, or irregular.[1] The hornblende does not show chemical zoning towards the actinolite (measured for F 052 D). The light coloured parts may be chemically different in various parts of one sample, without optical changes (F 252).

The newly formed assemblage represents the greenschist-amphibolite-facies transition (Ernst, 1968) and replaces the hornblende-intermediate plagioclase-biotite assemblage. There is no reason to believe in equilibrium between actinolite and hornblende : both amphiboles are not present as separate minerals in the sample, the only individual actinolite grains are surrounded by other secondary minerals. The Ti and Al^{VI} values point to different T and P conditions for the formation of both amphiboles (section I.4 and I.5.).

An extensive discussion of the actinolite-hornblende assemblage is given with its most remarkable occurrence in Rogaland at the contact between the lopolith of Bjerkreim-Sokndal and the Haaland Helleren anorthosite (section II.7.).

In F 252 (augen gneiss in the amphibolite facies) several "actinolite" spots have been measured by microprobe. They appeared to be rather varying in composition (table IV.8). This variation is caused by the incomplete transition from brownish hornblende (F1252) to actinolite (F2252 3), due to some retrogressive metamorphism. The amphibolite facies conditions remained dominant. It becomes clear from these measurements that the colour changes very quickly to the light actinolite colour (transitional types F2252 1 and 2), even before the actinolite chemistry is reached.

To see which element-changes determine the colour-change, and to illustrate the relative positions of the element percentage lines, the following graph was drawn (fig. II.2).

1 : Plate I, figure 1.

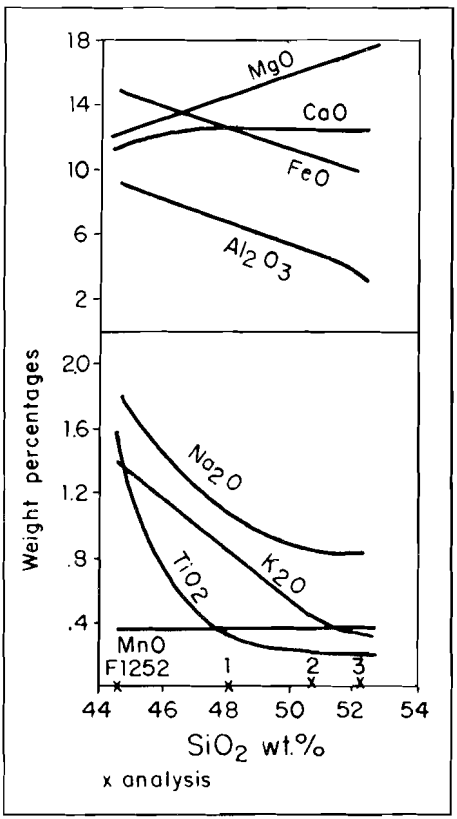

Figure II.2.: Oxide-changes due to the transition from hornblende to actinolite, with respect to SiO_2. 1, 2 and 3 are F2252 1, 2 and 3 resp. F1252 is brownish green, F2252 1/3 light indigo.

It is clear from the graph that TiO_2 changed relatively the fastest, and already reached a very low value in F2252 1. The data illustrate again that amphibole colour is primarily determined by Ti-content.

The fact that the F2252 analyses fall partly in the area normally ascribed to the miscibility gap (see actinolite discussion, section II.7) between hornblende and actinolite is not amazing. There is no equilibrium.

A similar graph can be drawn from the measurements on V 187 in the granulite facies area, where actinolitization is rare with respect to the amphibolite facies area (N 317, V 187 and Y 055 are the only high-grade samples with actinolite).

Several samples show a change of hornblende colour around enclosed ore grains or needles. Microprobe measurements of the ore needles in H 050 by F.J.M. Rietmeijer indicated a Fe/Ti-ratio of 10:1 for the intracrystalline ore needles, and 8:1 for the ore grains at crystal boundaries. This points to (titano-)magnetite. The needles are interpreted as a response to decreasing temperature (section IV.3.4.).[1] Measurements on the discoloured zones show a decrease in TiO_2, FeO and Na_2O (table II.3).

1 : Plate II, figure 1.

II.2.4. : The origin of amphibolites

In amphibolite facies terrains the question frequently arises whether the amphibolites and related rocks are of igneous or sedimentary origin. This is very difficult to establish. Many authors have worked on the distinction between ortho- and para-amphibolites; if structural evidence was absent, chemical characteristics were sought.

Walker et al (1960), Leake (1963, 1964, 1969) and Van der Kamp (1969), proposed methods involving the niggli-values of the amphibolites and trace element analyses. In this way igneous- and sedimentary origins could be distinguished, if a series of analyses from a certain area was present. It was made clear that a single analysis (or just a few) was mostly not conclusive.

Various investigators used this method and all but one (Winter, 1974) came to the conclusion that their amphibolites were ortho-amphibolites, even when field relations pointed to a sedimentary origin (Wakhaloo and Dahr, 1969; Kalsbeek and Leake, 1970; Preto, 1970; Rivalenti, 1970; Subbrarao, 1971; Herz and Bannerjee, 1973; Plimer, 1975; Mehta, 1976; and Weber-Diefenbach, 1976).

Orville (1969) states : "Any rock, whatever its origin, composed chiefly of hornblende with subordinate amount of plagioclase will approximate a basaltic composition, since the composition field for the two-phase assemblage hornblende-plagioclase closely mimics the composition field of basic igneous rocks. Chemical reaction between carbonate-rich rocks and carbonate-free pelitic rocks under open system conditions can produce a hornblende-plagioclase assemblage from a wide range of carbonate-rich pelite composition". This explaines the results found for the niggli-values, but he does not mention the trace element behaviour. However, not much is known about the trace elements in amphiboles and the degree of geochemical coherence with certain major elements.

The discrimination methods should be handeled with care, especially when only a few samples are used (Mehta; Subbrarao; Wakhaloo and Dahr,

all op.cit.). If all samples from this collection are plotted in the c-(al-alk) and in the c-mg graphs, all samples fall in the igneous field and follow the differentiation trend, except A 168 which is clearly from a metasedimentary formation. However, I should not dare to say that all these rocks are of an originally igneous origin.

II.2.5. : Some individual samples and their petrological problems

Amphibolite facies :

In the area east of Tonstad the amphibole colours are generally greenish, but some mafic rocks show more brownish colours. The metamorphic assemblage also varies over short distances, the most common assemblages indicate amphibolite facies, but in restricted zones granulite facies rocks are preserved. On the other hand greenschist facies minerals are present along faultzones. This resulted in a rather complex situation with abrupt changes over short distances.

D 442 - D 444 - W 012 D : three biotite amphibolites. The most important difference is the lack of free Fe-Ti-oxides in D 442 and W 012 D. Both samples have low Ti-values for the hornblendes with respect to D 444 (.14 and .12 versus .23). D 442 and D 444 are from the same location and comparison of the amphibole chemistry shows that D 444 contains less SiO_2, MgO, CaO and K_2O, and more Al_2O_3, TiO_2, FeO and Na_2O (table II.1). Most important is the difference in TiO_2, alkalies and mg-ratio.

This confirms Leake's (1965-a) remark that absence of free Ti-ore may indicate undersaturation of TiO_2 and FeO in the amphibole. These differences in amphibole chemistry depend completely on the bulk composition. If enough TiO_2 and FeO is present in the bulk, the amphibole can be saturated and a free Ti-ore phase will be formed.

F 005 - V 363 : this type of blastic leucocratic rock with irregular lineation is very common in the granitic migmatites. F 005 comes from a tectonized outcrop and contains retrograde minerals, V 363 does not. As shown lately by Maggetti and Nickel (1976), it is often very diffi-

	Δ	C
SiO_2	- 2.7%	1 %
Al_2O_3	+ 6	2.5
TiO_2	+63	6
Fe_2O_3	+ 5	5
FeO	+10	1
MgO	-10	1
CaO	- 7	1
Na_2O	+27	3.5
K_2O	-31	4
F	-40	15

Table II.1.: Differences between D 444- and D 442-amphibole. $\Delta = (X_{D\ 444} - X_{D\ 442})/X_{D\ 442}$. Values from table IV.7. C is the relative standard deviation deduced from fig. IV.5.

cult if not impossible, to establish the origin and history of a rock in migmatitic, polymetamorphic, area. A certain texture can be formed in various ways (= Konvergenz = structural convergence). For these samples one can think of an igneous, syntectonic, origin as well as of metablastic formation.

F 052 D and L : the most remarkable fact is the great amount of microcline in combination with ± 25% amphibole; one could almost speak of a microcline amphibolite (F 052 D) and a microcline amphibole pegmatite (F 052 L). Similar rocks have not been found anywhere else in Rogaland, only N 264 shows some resemblance. A comparison of the bulk compositions (see Appendix) indicates an increase in SiO_2 (quartz) and K_2O (microcline) in the veins (F 052 L) relative to the dark band, and a decrease of all other elements (mafic minerals).

The relation between the veins and the amphibole-rich zone is dubious; is F 052 D the paleosome which is partly mobilized as indicated by the resemblance with pictures from Mehnert (1968), and by the gradual transition which is often observed; or is the microcline-quartz syenite intruded alongside, and into, the dark band, as suggested by the partly sharp contacts, and the relative abundance of the leucocratic phase (light vs dark = 1:1)?

A quartz-feldspar zone on the eastside of this outcrop with vertical contacts, does not seem to influence the amphibole-rich zone, it probably intruded along a fault.

The presence of clinopyroxene remnants points to a possible original clinopyroxene-microcline-rock. Such rocks are occasionally found in the Faurefjell formation, northwest of the investigated area. Drury (1974) described diopside- and microcline-rich gneiss at the boundary between

highly deformed and recrystallized amphibolite facies gneisses and metasediment belts. He ascribed them to metasomatism during amphibolite facies metamorphism.

In the Björnestadvatn location, were these samples come from, no metasediments are recognisable, deformation and amphibolite facies metamorphism however are present. Conclusions to be drawn remain uncertain.

F 070 D : as written by Hermans et al (1975) : "The Espetveit augen gneisses form the uppermost unit of the synform east of Björnestadvatn". Apart from the tectonization caused by the formation of this structure, there are also two major faults crossing this formation and many small ones. A straight forward explanation of the mode of formation of the augen is hampered by this faulting.
Are the augen remnants of the original rock (protomylonite), are they newly formed (blastomylonite) or is it wrong at all to speak of a mylonite because the structure is independant of the fault tectonics? Hermans et al proposed an anatectic origin, caused by the intrusion of the Folded basic intrusions. The term augen gneiss is a compromise.

W 017 B - W 196 B : there are many thin layered amphibolitic/enderbitic rocks in the area east of Tonstad. This might be the result of an originally volcanic layering. After a granulite facies metamorphic event, H_2O was added to the rocks along certain levels, and amphibole + quartz formed at the expense of orthopyroxene + plagioclase (+ clinopyroxene) + H_2O.

Fletcher (1971) described a thin layered amphibolite series which did not originate from metamorphic segregation but from different starting material and a closed character for H_2O. That H_2O was not free to move through all rocks of the amphibolite facies terrain is furthermore demonstrated in the Tonstad area by the presence of charnockites and amphibole free, orthopyroxene- and plagioclase carrying mafic rocks. They are of course a minority.

The amphibolites also vary from watersaturated biotite amphibolites to 2-pyroxene amphibolites.

W 226 D and L : a hornblendite in sharp contact with a mela diorite. There is a great contrast between the two parts of the sample, mineralogically and chemically : SiO_2, CaO and Na_2O are more abundant in the diorite band; FeO, MgO, K_2O, H_2O and F in the melanocratic band, while TiO_2, Al_2O_3, MnO, P_2O_5 and CO_2 are about equal for both. The immobile elements (Fletcher, 1971) Fe, Mg and Ca are not concentrated in the same band. This points to an original chemical difference.

The presence of larger clinopyroxene and plagioclase crystals in the otherwise extremely fine-grained diorite seems to indicate a granulation proces. The equidimensional, angular ore crystals which are abundantly enclosed in all diorite minerals produce a unique picture which is strikingly different from other migmatitic rocks.[1]

Clinopyroxene + plagioclase remains stable beside hornblende in the amphibolite facies : lack of orthopyroxene prevents alteration of the diorite.

The chemical differences between the amphiboles from both layers (table II.2) show that Ti was a very immobile element while amphibole formed : there is a strong Ti-drop over the contact. The differences are essentially the same as between D 442 and D 444 except for K_2O (table II.1). The more greenish amphibole WI226 D contains less TiO_2, K_2O and "All Fe as FeO", and more SiO_2 and MgO.

	Δ	C
SiO_2	- 3.7%	1%
TiO_2	+182	7
MgO	- 19	1
FeO	+ 23	1
K_2O	+ 22	5

Table II.2.: Differences between WI226 D and W2226 L.
$\Delta = (X_{W2226\ L} - X_{WI226\ D})/X_{WI226\ D}$.
Values from table IV.7. C, see table II.1. Only differences greater than C are given.

Granulite facies :

B 254 : the Ti-content of the amphibole in this olivine amphibolite is one of the highest in Rogaland (.425), much higher than in the "normal" migmatitic amphiboles. This might indicate an igneous origin (Leake, 1965-a). The olivine has already been mentioned in section II.2.2.

Ernst (1968) states that primary hornblendes in igneous mafic rocks are Mg-rich and in ultra-

1 : Plate II, figure 2.

mafic rocks are typically pargasitic in composition. This is in good accordance with the chemical analyses of B 254 and N 572. A deep magmatic origin for amphiboles is no problem (see section II.4.2.).

Granulite facies metamorphism may have caused lineation and minor mineralogical changes (e.g. ore formation in olivine and amphibole).

From about the same location comes :

N 572 D and -L : this originally forsterite-rich rock (dunite or peridotite) recrystallized into an orthopyroxene-plagioclase-amphibole assemblage, without forming coronas. The whole rock recrystallized and reequilibrated, resulting in an ultramafic Fe-Mg-rich part (olivine hypersthenite)[1] and a mafic accumulation with all other elements.[2]

There is a spread in amphibole compositions in this small area, due to bulk composition differences : B 254-rock contains much more TiO_2 and less MgO; additional sample BA 92 (section V.2.) contains no free ore in the rock, and TiO_2 in the amphibole is very low, the pleochroic colours are soft greenish; N 572-rock is high in MgO and poor in TiO_2; whatever ilmenite present seems to have been introduced later. So the difference in Ti-content of the amphiboles in this case is not indicating T-differences. They accumulated as much Ti as possible.

Comparable amphibole compositons are found in the leuconoritic phase of the lopolith, and in xenoliths in the lopolith (e.g. E 128).

This all leads to the conclusion that at least part of the rocks in this environment (= banded migmatites near the E-side of the lopolith) seems to be related to the lower parts of the lopolith, and are of an igneous origin. Three km NW of this location a small extension of phase A is surrounded by banded migmatites. This intercalation probably has a further SE-ward extension than presently indicated in the map (Hermand et al, 1975).

H 325 : contains Huttenlocher intergrowths, see J.V. Smith (1974, V2, p. 540), and Wenk (1976, several authors report TEM-results obtained from bytownites). The occurrence of these intergrowths is restricted

1 : Plate II, figure 3; 2 : Plate II, figure 4.

to plagioclases with An-percentages of about 70%. The only other sample in this collection showing this phenomenon is O 100 from the Folded Basic Intrusions (section II.4.). These intergrowths are presently being investigated in our Department by Dr. C. Mayer.

N 337 : a sheared amphibole gabbronorite with long prismatic orthopyroxene crystals near the contact with the Outlier (anorthosite). The long prismatic pyroxene may be the result of a relatively high cooling rate (Lofgren et al, 1974), see also E 170 (section II.5). This high cooling rate might be due to the intrusion of the Outlier in the cooler environment, which also caused the sheared character of the rock. The amphibole has grown at the expense of pyroxene in distinct layers, probably due to the accumulation of the little fluid available in certain bands. The resulting rock is stable in the hornblende granulite facies.

Sulfide at orthopyroxene-margins and cleavage planes may have formed by the introduction of sulfur-carrying fluids derived from the Outlier or the lopolith (see N 317). Serpentinization is later.

On the other hand, dehydration caused by the intrusion of the anorthositic magma should not be ruled out, even though the texture seems to indicate partial overgrowth of amphibole on pyroxene. It is one of the few samples with bluish rims around ore grains in amphibole in the granulite facies (section IV.3.4.).

Y 055 : contains amphibole and quartz without any clear reaction relation. They appear in a random way together or separately in the sample, with or without pyroxene and plagioclase. The association is perfectly stable.

The location is rather far from the lopolith and seems to indicate the lowest grade of the granulite facies (hornblende granulite facies), unless the system was completely closed with respect to H_2O.

The secondary amphibole Y2055 is due to hydration of orthopyroxene.

II.3. : Faurefjell metasediments

The only sample from this formation is A 168 : magnesioriebeckite in alkalifeldspar granite.

The overall picture shows a recrystallized sandstone, which contains some alkalifeldspar-rich intercalations near the contact with the underlying marble. Upwards it grades into clinopyroxene granite, also very fine-layered (clinopyroxene determines the layering). Magnesioriebeckite only occurs near the contact with the marble.

In relatively fresh, quartz-rich samples the mainly fibrous amphibole is formed preferentially in the quartz[1], while in the alkalifeldspar-rich intercalations, with clouded sanidine-like feldspar, the amphibole grows in this feldspar.

From the rock analysis of A 168 (table III.3) it can be seen that the alkalifeldspar granite (with ca 50 modal percent alkalifeldspar) is almost free of Na_2O (0.15 wt%) and contains considerable amounts of K_2O (7.64 wt%). This confirms the K-rich character of the feldspar.

The only chemical components which the magnesioriebeckite derives from the host rock itself are Fe and Si (ilmenite and quartz). Its other main constituents Na and Mg have low concentrations in the bulk composition of the host rock (0.15 and 0.14 wt% oxides resp.), and presumably entered with the fluid from the marble. The fluid migrated apparently only over small distances, as indicated by the restricted occurrence of amphibole in the granite.

This explains the preferential growth of magnesioriebeckite from ilmenite into quartz in the fresh rocks. The rather different alkalifeldspar chemistry (with K and Al, which do not enter the amphibole chemistry) prevents extensive amphibole forming in this mineral.

In the intercalations of clouded alkalifeldspar, however, quartz is rare and ilmenite is absent, while alkalifeldspar is strongly contaminated. Riebeckite has to form in the alkalifeldspar which, together with

1 : Plate III, figure 1.

the contamination and the migrating fluid, supplies all elements. In the first reaction (ilmenite + quartz), the excess Ti forms rims of titanite around ilmenite.

Magnesioriebeckite formation is favoured by peralkalinity of the rock (Ernst, 1968). A 168 is closest to peralkalinity in this collection (fig. II.3), and Na addition from the marble will create peralkaline conditions. The temperature limit of the Mg-riebeckite depends on the Mg-content, P_{H_2O} and f_{O_2}. The increase of each one of these values increases the upper T-limit. It may be stable up to 900-950°C (Ernst, op.cit.). The P_{H_2O} may have been very low (less than 1 Kb).

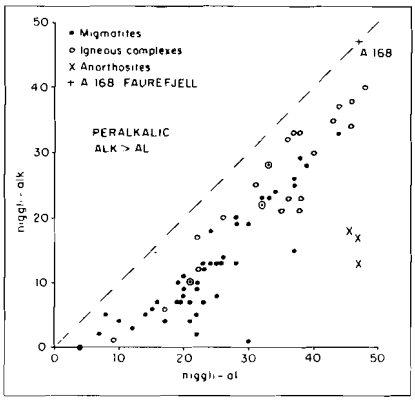

Figure II.3.: Niggli-al versus -alk for all rock compositions. All samples from the migmatites and the igneous complexes fall below the al = alk-line. A 168 is closest to peralkalinity.

The microcline amphibolite in the granitic migmatites may be an amphibolite facies equivalent of diopside-microcline rocks occurring in the Faurefjell formation northwest of the investigated area.

Outside the map area (fig. I.1), tremolite occurs in diopside rocks (Hermans et al, op.cit. p.71). It is thought to be retrograde and falls outside the scope of this study.

II.4. : Minor intrusions in the migmatites.

II.4.1. : Folded basic intrusions

Samples from this formation are : F 107 D, F 126 and O 100. The formation description by Hermans et al (1975) covers all rock characteristics, except for the An% of the plagioclase which is rather high in O 100 : An_{65-70}. This sample also contains Huttenlocher intergrowths (cf H 325, section II.2.5.). A remarkable feature in this formation is the occurrence of leucocratic lenses (or discs) of 10-20 cm in a regular

system parallel with the lineation (see Hermans et al, 1975 : fig. 6).

The igneous origin of these rocks is not very evident from their microscopic textures. They mainly show a granoblastic, equigranular, polygonal-interlobate texture. Only F 126 contains some porphyritic plagioclase crystals.[1] The clinopyroxene in this sample displays an intercumulus or embayment texture (see Schrijver, 1975, fig. 19). It is caused by plagioclase and quartz, but it is not possible to tell whether the clinopyroxene represents a former intercumulus phase in a now largely recrystallized rock, or if the texture is mainly the result of dissolution of the clinopyroxene by quartz during a late stage of crystallization. According to Spry (1969), embayment textures are rare in metamorphic rocks but common in volcanics. Sample O 100 is strongly tectonized.

The amphiboles from these samples fall in the transition range from the amphibolite facies amphiboles to those from the granulite facies (fig. II.4).

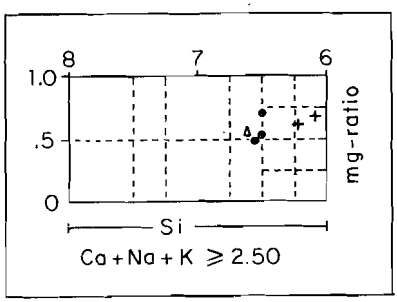

Figure II.4.: Plot of the amphiboles from the minor intrusions: 23(0).
• = Folded basic intrusion
+ = Gabbro in the garnetiferous migmatites
Δ = Meta-dolerite
See further fig.II.1.

This is not remarkable in view of the fact that F 107 D and F 126 lie close to the hypersthene line. O 100 lies in the northwestern part of the investigated area, well within the lower part of the granulite facies terrain (see nearby sample Y 055).

The mineral assemblages and amphibole colours are also in good agreement with the position of the samples in the metamorphic environment :

F 126 : amphibolite facies : amphibole + quartz + clinopyroxene + plagioclase,

F 107 D : near facies-transition : amphibole + quartz + orthopyroxene + clinopyroxene + plagioclase,

O 100 : granulite facies : amphibole + orthopyroxene + clinopyroxene + plagioclase.

1 : Plate III, figure 2.

The Ti-content in O 100 amphibole (0.28, 23(0)) is a minimum value because no free Ti-ore is present in the sample. This indicates relatively high temperatures during amphibole formation (section I.2.1.).

No special mineral relations can be seen in these samples.

As in the enveloping migmatites, retrograde metamorphism resulted in actinolitization (F 126), the formation of other secondary minerals (at crystal margins of orthopyroxene in F 107 D), and a more bluish colour around enclosed ore grains in hornblende (F2107 D versus F1107 D).

The chemical difference between the main hornblende F1107 D and the discoloured zone F2107 D is rather small (table II.3).

	Δ	C	
SiO_2	+ 0.4%	1	%
Al_2O_3	+ 2	2.5	
TiO_2	-21	5	
FeO	- 3	1	
MgO	+ 2.5	1	
Na_2O	-14.5	3.5	
CaO	+ 1.5	1	
K_2O	+ 0.6	3.5	

Table II.3.: oxide-changes between F1107 D and F2107 D.
$\Delta = (X_{F2107} - X_{F1107})/X_{F1107}$. See further table II.1.

Most important is the difference in TiO_2 and Na_2O, and to a lesser extent the Fe/Mg-ratio. This is, in general, in agreement with the changes found in F 252 (section II.2.3.). Si, Al, Ca and K do not differ markedly here. The colourchange in some biotite crystals from reddish brown to green in one crystal may also indicate loss of TiO_2.

The bulk composition of F 126 is more or less the same as for F 107 D, even though the mineralogy is quite different. The main chemical differences are the higher CaO and lower H_2O contents in F 107 D, which, therefore, prefers Ca-amphibole and alkalifeldspar above biotite.

The Folded basic intrusions are almost completely recrystallized and have lost their igneous textures. The amphiboles are perfectly comparable with the ones from the surrounding migmatites. The main metamorphic event has completely destroyed possible igneous amphibole characteristics. Biotite is late, showing cross cutting relations with all other minerals.

II.4.2. : $Anorthite_{99}$-bearing gabbro with amphibole xenocrysts.

The gabbro forms a layer of about 1 m thick in the garnetiferous migmatites, and contains fist-size xenocrysts of amphibole. An extensive description of the gabbro (A 037) and the xenocrysts (A 128) is given in the Appendix.

The amphiboles in the gabbro as well as in the xenocrysts are chemically similar to those found in the leuconoritic phase of the lopolith (section II.5.1.) and in the banded migmatites at the E-contact of the lopolith (section II.2.), see fig. II.4.

The An-percentages for A 037 (An_{99}) and A 128 (An_{96}) are the highest recorded in this area (section V.2.).

This set of samples is unique in the Rogaland area, both for the mineralogy and the chemistry of the bulk rock. These characteristics lead to the following reconstruction :

Cumulus crystals of clinopyroxene and apatite formed, followed by the intercumulus growth of amphibole, because of strong enrichment in volatiles of the melt (Larsen, 1976). In this way an (kaersutitic?) amphibole body, or layer, was formed, possibly in the upper mantle (Best, 1974, 1975; Ernst, 1968; LeMaitre, 1969; Oxburgh, 1964; Varne, 1968, 1970, 1971; Wilshire and Trask, 1971). Fragments of this amphibole body were picked up by a basaltic magma on its way upwards.

The high T of the magma caused the amphibole to react to plagioclase + orthopyroxene + ore,[1] but only to a certain extent because of the lack of SiO_2 (Sen and Ray, 1971-a; Yagi, in : Frisch and Schmincke, 1969). Yagi gives a temperature of 900°C for this prograde reaction without mentioning a P-value. This temperature is very well possible for a basaltic magma (see : Hess and Poldervaart, Ed., 1968, vol. 2).

A prograde reaction caused by metamorphic condition seems illogical because the gabbroic amphibole A 037 did not react at all, even though the compositions of A 128 and A 037 are comparable.

This lack of reaction also indicates a different origin for both amphiboles. A 037-amphibole formed at the intrusion level in a stable association.

1 : Plate III, figure 3.

The crystallization sequence seems to be : plagioclase, plagioclase + clinopyroxene, plagioclase + clinopyroxene + amphibole, clinopyroxene + amphibole, amphibole. Apatite, zircon, spinel and ore crystallized earlier, the main spinel and ore at the end. Banding may be caused by turbulence during crystallization.

During the intrusion the T and P decreased, causing exsolution of ore in amphibole (A 128) and apatite. The exsolution is interpreted to be the result of dropping temperature; Ti had to leave the amphibole and formed titano-magnetite (see section IV.3.4.). The present Ti-content is normal for medium- to high-grade metamorphic areas (section I.4.). A 037 is a little bit lower in Ti.

The Al^{VI}-content, a pressure indicator, is relatively high for both A 037 and A 128. This is caused by the extremely high Al_2O_3-content (results in high niggli π = high An%, see section I.5.) of the rock ($\pm$ 25%). However, if the prograde reaction products (plagioclase + orthopyroxene + ore) in A 128 are added to the remaining amphibole to obtain the presumed original amphibole composition, the Al^{VI}-content increases because of the extremely high An% of the plagioclase. The possibility of a deepseated origin (HP) for A 128 remains therefore open.

Besides the exsolution in amphibole, there appeared ore and plagioclase + orthopyroxene exsolutions in clinopyroxene.[1] Exsolution of plagioclase in pyroxene phenocrysts is described before by e.g. Emslie (1975) and Morse (1975) for anorthositic complexes. In both cases the pyroxene is an orthopyroxene. The exsolution of plagioclase is accompanied by ore exsolution.

As a reason for the high Al_2O_3-content of the original pyroxene, two possibilities are given :

1 : rapid growth under conditions of strong supersaturation, the large pyroxenes being part of the crystallization sequence of the host rock (Dowty et al, 1974) and

1 : Plate III, figure 4.

2 : high pressures, indicating lower crust or upper mantle as place of origin (Green and Ringwood, 1967 and Green, 1969). Thompson (1974) shows that the P_{total} in this case is more important than the magma composition.

The first possibility seems to contradict the cumulus character of the clinopyroxene in amphibole, while the alternative is in agreement with the amphibole information. Decompression causes the exsolution of plagioclase and ore (Emslie, op.cit.).

Falling T and P stimulate the exsolution of orthopyroxene. Therefore, if the orthopyroxene story may be applied to the clinopyroxene as well, it points to a deepseated origin for the clinopyroxene. The asset of the gabbro caused the exsolution.

Philpotts (1966) described clinopyroxene with plagioclase, orthopyroxene and ore lamellae in a noritic sample from the anorthosite-mangerite rocks in southern Quebec. He mentions several points to discriminate between exsolution and epitaxial intergrowth. None of his intergrowth criteria are applicable, but one of his exsolution criteria is (: no connection between plagioclase in the clinopyroxene, and plagioclase outside the clinopyroxene crystal). He concluded an intergrowth origin, mainly based upon the intermediate An-percentages.
In A 128 all An-percentages are very high, and therefore this criterion can not be used.

During a later deuteric phase part of the orthopyroxene was serpentinized, and some biotite, zoisite and diaspore were formed. Inclusion strings were formed in all minerals. Some quartz intruded via cracks, only at the outer rim of the xenocryst. Then the area was uplifted to the present level.

II.4.3. : Meta-dolerite in the amphibolite facies

Over a distance of 100 meters along the road, a dolerite is exposed in a very retrograde environment in the Espetveit augen gneiss formation. It could not be traced any further. The length of the outcrop may be due

to the almost parallellism of dolerite and road. Additional sample F 075 belongs to the centre, F 074 to the margin of the dolerite.

This dolerite might belong to the ENE-trending Hunnendal system. Versteeve (1975) measured rock ages (K-Ar) of 564-935 Ma for the Hunnendal system. The fact that the hornblendes in this rock are in complete chemical agreement with the amphiboles from the surrounding migmatites, and the fact that hornblende formation all happened over 950 Ma ago (Chapter VII) in the Rogaland/Vest-Agder area, indicates that this meta-dolerite is older than the ones measured by Versteeve.

The mineralogy of the meta-dolerite changes from centre to rim, from almost alkali-free (plagioclase-ore-actinolite-chlorite-epidote-carbonate-apatite) to relatively alkali-rich (F 074 : plagioclase-ore-hornblende-alkalifeldspar-quartz-chlorite-epidote-apatite-zircon).

Influx of alkalies from the augen gneisses made it possible for hornblende and some microcline to form in the margin, while in the centre amphibole without alkalies (= actinolite) formed during amphibolite facies metamorphism. Because hornblende contains less SiO_2 than actinolite, some free quartz formed as a by-product of the reaction :

pyroxene + plagioclase I + H_2O + alkalies $\longrightarrow$ hornblende + plagioclase II + quartz + microcline

which occurred in the margin, and not from the reaction :

pyroxene + plagioclase I + H_2O $\longrightarrow$ actinolite + plagioclase II

which occurred in the centre.

So,the presence of actinolite in the centre of the dolerite does not indicate other physical but other chemical conditions.

The chemistry of the hornblende varies rather irregularly in Fe/Mg-ratio and Ti-content. This variation coincides with a colour variation. Brownish crystals contain more Mg and Ti, the more bluish green amphiboles are richer in Fe. This irregularity is due to retrograde metamorphism, by which the secondary minerals in this environment were also formed.

II.5. : The Bjerkreim-Sokndal lopolith.

The following samples from the lopolith are included :
--leuconoritic phase (phase A) : B 016, B 322, E 125, E 131 and P 248,
--monzonoritic phase (phase B) : R 269,
--(quartz-)monzonitic phase (phase C) : E 067, E 128, E 167, E 170, F 433, N 402, N 528, R 227, R 229, R 356.

II.5.1. : Leuconoritic phase

II.5.1.-1 : General characteristics.

The amphibole-carrying rocks which certainly belong to the magmatic phase (B 016, B 322, E 125 and additional samples R 179, R 313 and R 385) vary from dioritic to pyroxenitic compositions. Quartz and alkalifeldspar are normally absent (except small amounts in B 016). The An-content of phase A rocks varies mostly between 35 and 50%, and the present samples show values of 29 (B 016) and 45-50% (other samples).

A real xenolith is P 248 (granite) which originally belonged to the surrounding migmatites (An_{27}). More problematic is E 131 (norite) with properties of the leuconoritic phase but also of ultramafic samples from the banded migmatites at the eastern contact of the lopolith (N 572 L and -D, section II.2.5.). The An-value is very high (An_{78}). It will not be used to describe the general characteristics of phase A but is compared with this phase at the end of this section.

Phase A consists of five rhythms, which differentiate from anorthosite at the bottom to diorites/norites at the top of each rhythm. Graded layering is also present. This all leads to a series of rapidly changing mineralogical compositions. However, it is difficult to tell which rhythm a certain sample belongs to. Brown amphiboles are only found in the fourth and fifth rhythm. About 20% of the leuconorites and norites contains some amphibole, mainly as a minor phase (upto 5 modal percent). The amphibole

may form at crystal margins of orthopyroxene or ore as small greenish crystals. More important are the samples with considerable amounts of brown hornblende, which are rather rare in phase A. They are the subject of this section.

The mineralogy and amphibole composition of the additional samples can be seen from table V.1 (section V.2.). Not only mineralogy and amphibole chemistry change, but also the texture. R 179, a plagioclase-rich sample, shows beautiful deformation features in all minerals, without fracturing, except in amphibole. This could be due to syntectonic emplacement. B 322 only shows deformation features in part of the sample.

Magnetite and ilmenite form mosaic textures with polygonal contacts, due to recrystallization. A spinel exsolution in ilmenite formed afterwards. Green spinel is a normal constituent of the leuconoritic phase in the northern part of the lopolith (Van Riel, 1973-b), it is absent in the southern part (Rietmeijer, 1973).

When the samples are arranged in order of decreasing pyroxene content, ilmenite decreases too, while plagioclase and amphibole increase. This is associated with an increase in Fe- and Si-content and a decrease of Na and Mg (and hence mg-ratio) of the amphibole. The amphibole becomes less pargasitic. A real pargasitic composition is not found, however, not even in the ultramafic members. This is caused by the high Fe-content of the rocks : niggli-mg = 0.27 - 0.37 (section VI.3.2.).

Brown amphibole occurs mainly as anhedral crystals, dispersed through the rock or, sometimes, in pockets and zones. The compositions are rather Mg-rich (fig. II.5), except for B 016 (see subsection II.5.1.-2), and are comparable to those from the charnockitic migmatites (fig. II.1-B). The Ti-content varies from 0.215 to 0.42 (23(0)). The high values are indicative of an igneous origin of the amphiboles (section I.4.).

The brown hornblendes do not show any clear reaction relations. The absence of quartz and the overal presence of orthopyroxene indicate granulite facies associations. The hornblende may be of igneous origin, possibly due to the enrichment in volatiles at the end of the crystalli-

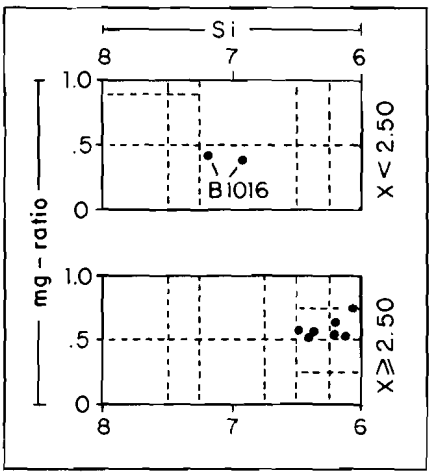

Figure II.5.: Plot of the Ca-amphiboles from the leuconoritic phase of the lopolith. See further fig.II.1.

zation of a certain rhythm, which caused partial replacement of orthopyroxene, or the primary crystallization of hornblende.

II.5.1.-2 : Retrograde metamorphism : cummingtonite and green hornblende

B 016 is the only phase A sample with green hornblende and cummingtonite (see also L 143 from the anorthosites, section II.7.3.). The combination cummingtonite-hornblende-plagioclase is not uncommon in metamorphosed basic rocks (Shido, 1958 : Abukuma Plateau; Watters, 1959 : New Zealand; Himmelberg and Phinney, 1967 : Granite Falls, Montana; Ernst, 1968; Deer et al, 1963, v.2, p. 243). The last group of authors gave a review of the occurrences and the possible modes of origin :

--1 : Ca-amphibole + SiO_2 ⟶ cummingtonite + plagioclase,

--2 : primary crystallization, no metamorphic influence,

--3 : replacement of orthopyroxene : orthopyroxene ⟶ cummingtonite ⟶ hornblende, which is by far the most common genesis.

The first possibility should give cummingtonite rims around hornblende, whereas the reverse is found. In the second case no pseudomorphs after orthopyroxene should occur. The third is in good accordance with the phenomena described in the Appendix : relic pyroxene texture[1] and a retrograde environment.

The hornblende rims around cummingtonite may be explained by the reverse of the first reaction or it may be contemporaneous with the cummingtonite formation. Both modes of origin consume anorthite, resulting in zoned plagioclase; quartz drops in the green hornblende are a by-

1 : Plate IV, figure 1.

product of the hydration reaction. The plagioclase zoning only occurs in the retrograde samples in the Mydland tunnel.

The paragenesis described above is found nowhere else in the lopolith. R 229 shows a slight resemblance, but belongs to another phase. This points to the abnormality of this sample B 016, and supports the proposed, retrograde, formation. Both Watters' (op.cit.) description and his proposed mode of origin are very similar.

The variation in cummingtonite-hornblende ratio may be due to the original pyroxene composition and depends on the neighbouring minerals. Pure cummingtonite crystals are found, surrounded by green hornblende crystals, isolating the first from the plagioclase. However, a few cummingtonite crystals in plagioclase do not have green hornblende rims. This can be explained by the influence of biotite (for K) and ore (for Ti) on the reaction. In thin section both minerals seem to affect the reaction, green colouring is often intensified in their immediate surroundings. Three minerals (plagioclase, biotite, ore) are needed in the reaction, besides cummingtonite or orthopyroxene. Their degree of availability will influence the cummingtonite/hornblende-ratio.

Biotite-quartz symplectites may be derived from older biotites, which are involved in the reaction (Si-rich biotite $\longrightarrow$ Al-rich biotite + quartz), or from orthopyroxene, together with cummingtonite (+ hornblende).

So, the cummingtonite-bearing assemblages are not stable. The cummingtonite is more or less an armored relict.

Another point supporting the proposed genesis comes from sections I.4. and I.5. : the hornblende falls in the higher P, lower T group of the igneous complexes. The association of amphibole + quartz represents amphibolite facies conditions.

Amphibole exsolution is rare in phase A, no occurrences other than B 016 are known. The very fine lamellae found here in both amphiboles are presumably actinolite or tremolite : that is the only kind of amphibole which may be exsolved from cummingtonite as well as from a

hornblende.[1] In the lower T-range there is a miscibility gap between actinolite-tremolite and hornblende (see extensive discussion of the actinolite-hornblende association in section II.7.).

See further Ross et al (1969). Stout (1972) published a picture (his fig. 12-B) from Telemark which is similar to some crystals in B 016. Robinson et al (1971-b) explained the small angles between the exsolution planes and the $(\bar{1}01)$ and (100) directions. Amphibole exsolution patterns and mechanisms are discussed extensively by Gittos et al (1974, 1976).

A difference in amphibole colour between the various samples is accompanied by differences in Ti-content. A more bluish colour near ilmenite inclusions inside an amphibole grain is chemically expressed by a decrease in TiO_2, alkalies, FeO and SiO_2, and an increase in MgO and Al_2O_3 (table II.4).

	Δ	C	
SiO_2	- 2.5%	1	%
Al_2O_3	+ 7	2.5	
TiO_2	-25	5	
FeO	- 4	1	
MgO	+ 7.5	1	
Na_2O	- 6.5	3	
K_2O	-10	5	

Table II.4.: Oxide-changes between normal B 322 amphibole and the discoloured zone near ilmenite.
$\Delta = (X_{B\ 322\text{-blue}} - X_{B\ 322\ brown}) / X_{B\ 322\text{-brown}}$.
Values for the bluish parts are not given in table IV.7. See further table II.1. Compare with table II.3, which also shows a decrease in mg-ratio.

These changes may indicate that the relatively low Ti-amphiboles B 322 and R 313 suffered an element loss, due to interaction with ilmenite, while R 179 and R 385 have kept (all?) their elements. The last two samples do not show discoloured zones, and are dark brown. They probably belong to another rhythm than B 322 and R 313, or they are influenced less by metamorphism. The almost kaersutitic Ti-values of the dark brown hornblendes, together with the small $Z \wedge c$ values (10^o) and the possibility of Ti-loss during retrograde metamorphism indicate that an original kaersutitic composition for hornblendes from this phase is not impossible.

Actinolitization has not been encountered in this phase. Retrograde metamorphism did not proceed beyond hornblende formation in the amphibolite facies.

1 : Plate IV, figure 2.

II.5.1.-3 : Some individual samples and their petrological problems

E 125 : the apparent xenolithic character of this sample may have been suggested by the bad exposure of the outcrops in the swampy field (see Appendix). The mineralogy points to a normal phase A position. The presence of zircon indicates the last (fifth) rhythm.

E 131 : as mentioned in subsection II.5.1.-1, this ore-rich amphibole-bearing norite has somewhat deviating properties with respect to other phase A samples : An_{78}, rather small grainsize, exceptional rock chemistry (table III.3 and fig. III.6), low amphibole Ti (.195). The amphibole has a very light colour; it is the only Ca-amphibole with positive optical angle. The rock composition is very low in SiO_2 and alkalies, low in F and CO_2, normal in MgO, P_2O_5 and H_2O, high in TiO_2, FeO and CaO, and very high in Fe_2O_3, MnO, Al_2O_3 and total Fe-oxides. The large amount of opaque ore (12 modal %) is mainly magnetite. Only B 322 is richer in iron.

The mineralogy is in good agreement with several other phase A samples, only the apatite content is rather low and the plagioclase content high (apatite concentrates with the mafic minerals). Therefore, several factors indicate a normal phase A position for E 131, while others point to a more or less xenolithic character. The amphibole composition lies between phase A compositions and the pargasitic composition of xenolith E 128 and sample N 572 from the banded migmatites (section II.2.).

According to Gierth and Krause (1973), the orthopyroxene-ore symplectites (called Myrmekit I in their paper), which occur frequently surrounded by amphibole, are due to exsolution.[1] In an early stage of the intercumulus crystallization, orthopyroxene contained much Fe-oxide; later, orthopyroxene and Fe-oxide crystallized apart while excess oxides were exsolved from the earlier formed orthopyroxene. Because of relatively quick cooling, the ore could not leave the pyroxene crystal with

1 : Plate IV, figure 3.

which it formed a symplectitic structure.

Other possible modes of origin for orthopyroxene-ore symplectites as mentioned in literature are : eutectic crystallization (Haselton and Nash, 1975), subsolidus oxidation (ibid.), and the oxidation of olivine (Mueller, 1969; Irvine, 1974).

P 248 : granitic xenolith at the contact with the charnockitic migmatites. The amphibole colour is much too green for this environment (fig. I.2), while the Ti-content (.23 ion) is high enough to create a brown colour. Unfortunately the Fe^{3+}/Fe^{2+} ratio is unknown, but in view of the colour and the Ti-value it should be very high. This might mean that in fig. I.7, the 0.2-0.3 zone continues to the north from the lopolith onwards. On the other hand the high oxidation ratio may be caused by the interaction with the leuconoritic melt. Pseudomorphs indicate the former presence of orthopyroxene.

The amphibole does not fit in the group of higher P, lower T amphiboles, as found in the igneous complexes. It is believed to have formed from orthopyroxene + plagioclase + fluid (from the lopolith). The colour and Ti-content are in good agreement with the same properties from amphiboles of the higher phases of the lopolith, but the mg-ratio is much higher.

The combination of ilmenite grains with haematite exsolution, and magnetite grains with ilmenite exsolution is found nowhere else in this collection. Generally only one of these exsolutions is found.

II.5.2. : Monzonoritic phase

Only one sample is described from this intermediate phase : R 269. The location is about the same as for B 016 (section II.5.1.).

The monzonorites frequently contain some amphibole, mainly as brownish green to greenish rims around pyroxene and ore, and in many cases associated with some quartz (symplectite). Bluish green alteration rims are also present. The An-percentage normally lies between 22 and 36%.

R 269 contains zoned plagioclase, core = An_{26}, rim = An_{16}. Quartz is present in about half of the samples from this formation, usually in minor quantities.

The association amphibole + quartz + orthopyroxene + clinopyroxene + plagioclase indicates conditions of hornblende granulite facies. If more fluid had been present, more (or all) of the orthopyroxene might have been altered to the amphibole + quartz assemblage of the amphibolite facies. However, the conditions are less severe than for the leuconoritic phase (section II.5.1.).

The analysed sample contains green ferro-hornblende rims around light bluish ferro-actinolite cores (fig. II.6), which may contain some pyroxene remnants. Quartz drops are abundant in parts of the green hornblende near the centre of an amphibole aggregate. There is a great resemblance with E 232/ N 827 from the Eia outcrop (section II.7.), and some affinity with B 016 which shows colourless cummingtonite cores and green ferro-hornblende rims (section II.5.1.).

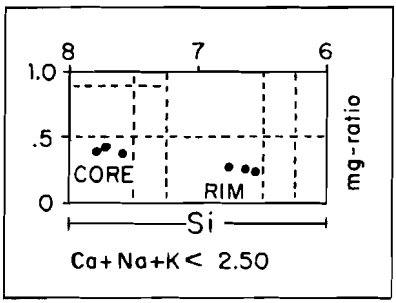

Figure II.6.: Plot of the amphiboles from R 269. See further fig. II.1 and II.5.

The $2V_x$ value for the ferro-hornblende (R1269) is very small for this collection (40°), and the amphiboles are much more Fe-rich than in the leuconoritic phase (mg-value rock = 0.23).

All amphibole is formed from pyroxene + plagioclase, as indicated by the pyroxene remnants inside the amphibole aggregates,[1] the zoned plagioclase (which is not a common feature in this formation), and the amphibole-quartz relation.[2] Actinolite is the result of clinopyroxene alteration in a partly closed system. See section II.7. for an extensive discussion of the reaction.

The hornblende R1269 (as well as B1016, E1232, E3232 and N1827) belongs to the higher P, lower T group of section I.4. and I.5. The loca-

1 : Plate IV, figure 4; 2 : Plate V, figure 1.

lity is strongly tectonized.

A presumed xenolith (E 256) in the northern part of the lopolith (3411-64919) is the subject of a special study at our department. The monzonoritic zone, at the contact between the leuconoritic- and (quartz-) monzonitic phase, contains many xenoliths.

This specific sample is rich in biotite, plagioclase, olivine, ilmenite and apatite, and contains amphibole rims around the mafic phases in certain parts of the sample. These rims consist of small fragments of about equal orientation, and are comparable to the local amphibole occurrences in e.g. E 131 (section II.5.1.). This amphibole may represent a late magmatic product. The composition is about equal to E 131-amphibole. The grainsize of the rock is extremely fine, plagioclase is ca An_{80}.

The most remarkable phenomenon is the presence of very thin garnet rims around biotite, olivine and ore at the contacts with plagioclase. Garnet is abundant in the amphibole-free parts of the rock, and amphibole-garnet contacts are restricted to the outer rims of amphibole-rich spots.

This is the only sample in the Rogaland/Vest-Agder area were amphibole and garnet appear together in this way. A few samples in the NW-part of the map contain garnet rims around mafic minerals, with bluish green amphibole as small flakes (e.g. Y 131).

Equilibrium between garnet and amphibole is questionable in these samples. Amphibole and garnet seem never to have been in equilibrium within the investigated area (see section II.2.).

II.5.3. : (Quartz-) monzonitic phase

II.5.3.-1 : General characteristics

Apart from the samples from the main sequence (E 067, E 167, N 402, N 528, R 229, R 356), some others were collected : E 128 (mela-trocto-

lite), E 170 (a dubious amphibolite band), F 433 (pegmatite with amphibole crystals up to 30 cm) and R 227 (monzonorite which may be part of a chilled margin of phase C (Rietmeijer, 1978), or which may belong to phase B; because of its outcrop relation with R 229 and F 433 at the Orrestadvatn location, it is taken with this formation).

Rietmeijer (1978) describes this phase extensively. Rietmeijer and Dekker (1978) describe and explain the extreme amphibole- and pyroxene poikiloblasts in these rocks.

The samples from this formation change from monzonites (and monzonorites) at the base to syenites and granites at the top. The mineralogical compositions of E 128 and E 170 do not fit in this sequence, while F 433 (found near the base) might compositionally be related to the very top. Amphibole is omnipresent in small quantities and becomes more abundant towards the top, often associated with quartz to form the large extreme poikiloblasts type II (Rietmeijer and Dekker, op.cit. and section II.5.3.-2) : E 067, E1167, N1402, R1229 and R 356. Pyroxene and ore decrease towards the top.

The chemistry of the rocks shows an increased Fe/Mg-ratio (niggli-mg = 0.26 - 0.06) with respect to the lower phases. Inside this phase SiO_2 and K_2O increase from the base to the top; Al_2O_3, H_2O^+ and CO_2 are variable, and all other elements decrease (fig. II.7). See further Chapter VI for the changes in rock- and amphibole chemistry, and all interrelations in the igneous complexes.

The amphiboles are also low in mg-ratio (fig. II.8), and more Si-rich than the amphiboles from the leuconoritic phase. They become richer in Na, Mn and Fe towards the top of this phase, while Al_{total}, K and Ti do not change significantly, and Si, Ca and Mg (and thus mg-ratio) decrease.

R 227 has the highest mg-ratio of this Fe-rich group : 0.36, due to its position near the base of this phase. Near the top the ratio may be about 0.10 (E1167 and F 433-pegmatite). A small crystal of ferro-actinolite (E2167) goes down to 0.04. These Fe-rich hornblendes are also characterized by low $2V_x$-values (fig. IV.24).

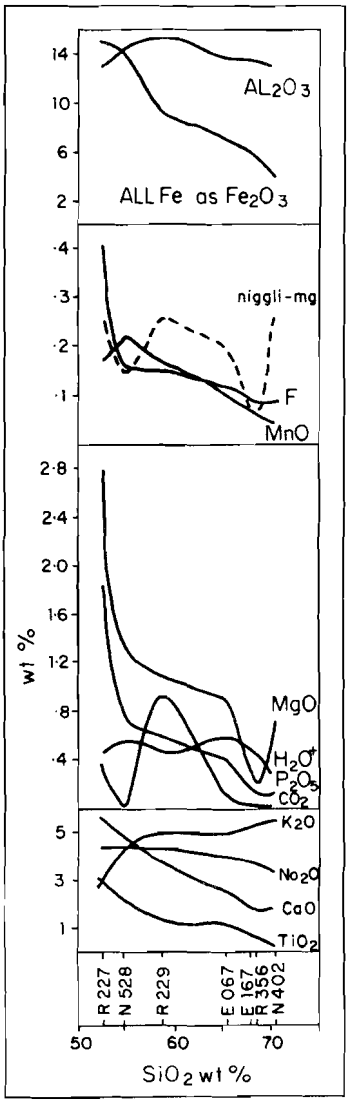

Figure II.7.: Chemical changes in the (quartz-)monzonitic phase of the lopolith, as a function of the SiO_2-content. The quartz-poor part forms the base (R 227, N 528, R 229), the quartz-rich phase the top of the lopolith (E 067, E 167, R 356, N 402). No rock composition was measured for F 433-pegmatite. The lines are best fits through seven points. A remarkable feature is the flattening of several curves in the SiO_2 = 60 - 65 % region.

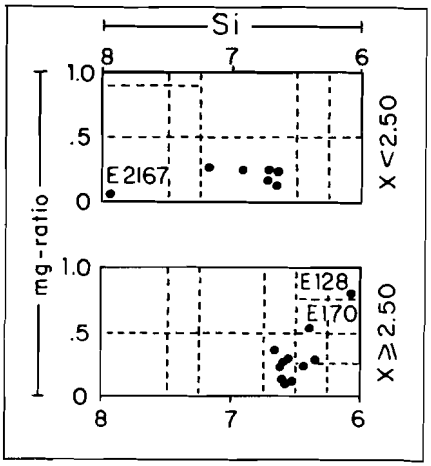

Figure II.8.: Plot of the Ca-amphiboles from the (quartz-)monzonitic phase of the lopolith. See further fig.II.1.

The colours of E 128 and E 170 amphibole are much too brown for this phase. Their chemistry is also rather distinct : they are the only amphiboles with mg-ratios greater than 0.40 and they fit much better in fig. II.5 from the leuconoritic phase or fig. II.1-B from the charnockitic migmatites (see detailed discussion on E 128 in section II.5.3-4).

Exsolution lamellae of a second amphibole in the main amphibole has been found in a few locations in this phase :
--near Orrestadvatn (R 94 and R 98 from the collection of Rietmeijer),[1]

1 : Plate V, figure 2.

--NE of Barstadvatn (F 441, additional sample from this collection, 3417-64785, no chemical analyses),
--in the northern part of the lopolith (E 167, this collection).

All exsolutions are extremely fine (less than 1 micron thick), and consist of colourless lamellae, irregularly distributed in the (bluish-) green Ca-amphibole host. They may consist of actinolite or cummingtonite in ferro-hornblende or ferro-edenitic hornblende. Unfortunately no analyses of the lamellae are available at this moment.

The exsolutions are mainly found in smaller crystals or rims around pyroxene or ore, while the larger crystals are devoid of it. See Plate V, figure 2 and for further information : subsection II.5.1-2, section IV.3.4. and in the Appendix sample N 041 from the migmatites which also contains very fine exsolution lamellae, and where the composition of host and lamellae is calculated.

II.5.3.-2 : Autometamorphism : formation of extreme poikiloblasts

According to Rietmeijer and Dekker (1978) an extreme poikiloblast is : "a group of at least three sections of the same mineral, with the same optic orientation and separated by a fabric consisting of other minerals." Most important are the poikiloblasts of orthopyroxene and clino-amphibole in the upper part of the lopolith.

Two groups of amphibole poikiloblasts have been distinguished :
--group I : clino-amphibole occurring in very fine-grained rocks of more or less monzonoritic composition (e.g. R 227).
--group II : clino-amphibole in coarse-grained rocks, with poikiloblasts up to 50 x 100 cm. These are all more or less related to quartz-bearing coarser-grained veinlets and pockets.

It was concluded that the crystals nucleated with great difficulty at widely spaced points in the host rock, during recrystallization in high temperature, low pressure environments. The Fe/(Fe+Mg)-ratio has to be very high for these textures to develop. This was confirmed by the later chemical analysis of W 175, one of the few extreme poikilo -

blasts of amphibole in the migmatites (section V.2.-A).

Group I poikiloblasts are only present in granulated rocks. The relation between granulation and extreme poikiloblast formation can be seen in a series of samples near the location of N 528 : dark quartz-poor mangerites (N 528 as well as additional samples F 419 and F 420) are locally transected by a finer-grained, darker "dike" (additional sample F 421), which is 2-3 meters wide. Contacts could not be seen due to outcrop overgrowth.

N 528 is the only sample in this collection with 4 optically different amphiboles, however, the rock is heterogeneous : a mangeritic part contains N2528 (arfvedsonite, see next section) and N3528 (magnesian hastingsitic hornblende), a thin pyroxenite band contains N1528 (titaniferous hastingsitic hornblende) and N2528; the last amphibole N4528 (colourless, not analyzed) is only found in the contact zone between these two parts.

The mortar structure of N 528, with larger mesoperthite and clinopyroxene crystals in a very fine-grained matrix which contains all minerals, indicates granulation. This is supported by the additional samples F 419-F 421, where F 419 is similar to N 528. There is an increased granulation from the rather coarse mangerite F 419 to the very fine-grained dike-like zone of F 421.[1] The mineralogy of F 421 is comparable to that of F 419/F 420.

The granulation is accompanied by a tendency of all mafic minerals (especially orthopyroxene) to form extreme poikiloblasts. Mesoperthite decreases while separate alkalifeldspar and plagioclase increase. Orthopyroxene dominates and amphibole is absent in the part showing the strongest granulation. The "dike" is a zone of strong granulation and recrystallization.

As N3528 is only present in the fine-grained, granulated parts, it must have formed during or after granulation.The most fine-grained sample F 421 was completely dehydrated, the rest of the mangerites contained still some fluid.

1 : Plate V, figure 3 and 4; Plate VI, figure 1.

N1528 and N3528 are only slightly different hornblendes, their most important chemical differences are given in table II.5. The more brownish hornblende in the pyroxenite (N1528) contains more TiO_2, Na_2O and FeO, and less MgO and Al_2O_3. This resembles the oxide changes in the discoloured zones (table II.3 and II.4), and both N3528 and the discoloured zones belong to the lower T, higher P phase of retrograde metamorphism.

	Δ	C
Al_2O_3	+17%	3%
TiO_2	-65	5
MgO	+20	2
Na_2O	-10	3
FeO	- 5	1

Table II.5.: Oxide-differences between N1528 and N3528. $\Delta = (X_{N3528} - X_{N1528})/X_{N1528}$. See further table II.1.

N1528 may have formed before the granulation, together with the group II poikiloblasts in the top of the lopolith.

Group II poikiloblasts (E 067, E1167, N1402, R1229, and R 356) and the associated quartz are thought to have resulted from the reaction : orthopyroxene ± clinopyroxene + plagioclase I + alkalifeldspar + H_2O ⟶ amphibole + plagioclase II + quartz (the An-percentage of plagioclase I is higher than that of plagioclase II). The water could derive from the final stage of the magmatic period.

The K-Ar age of the amphibole (E1167) is 950 Ma, and proves that amphibole formation and the intrusion of phase C are closely related in time (Chapter VII). All group II poikiloblasts belong to the HT, LP event of amphibole formation (section I.4. and I.5.).

E 067 is from a somewhat lower level than E 167. In E 167 the amphibole contains less mafic minerals (modal %) and the rock is richer in quartz. This may be caused by an originally more felsic rock for E 167, or by an accumulation of fluid in the top level of this phase, resulting in more amphibole + quartz formation out of pyroxene + plagioclase.

N 402 is the most extreme form of poikiloblast-formation in the top of the lopolith. The rock is almost completely re-equilibrated, which resulted in a relatively simple mineralogy. In E 067 and E 167 some pyroxene remnants still remain, while in the similar sample N 402 they are completely absent. Enough fluid was intruded to complete the amphibole forming reaction, the quartz did not leave the system and the al-

ready coarse alkalifeldspar remained about the same. This created a pegmatite-like appearance.

II.5.3.-3 : Retrograde metamorphism

Besides the granulation and formation of group I amphibole poikiloblasts, some arfvedsonite-riebeckite formed in N 528. This Na-amphibole is connected with the presence of carbonate, which is a very local feature. According to Tröger (1969), arfvedsonite may form in a postmagmatic -hydrothermal stage, together with carbonate in monzonites. If this hydrothermal proces has taken place, than the P_{fl} must have been very low because orthopyroxene continued to grow : the clinopyroxene component of an exsolved pyroxene crystal is replaced by carbonate + orthopyroxene + ore. The orthopyroxene lamellae have broadened in the carbonate, creating a set of equally oriented long prismatic orthopyroxene fragments in a carbonate + ore matrix. The orthopyroxene forming reaction may have been :

$$Ca(Mg,Fe)Si_2O_6 + MgCO_3 \longrightarrow CaCO_3 + (Mg,Fe)_2Si_2O_6$$

The fourth amphibole (N4528) seems to form a bufferzone between the Ca-amphibole and the Na-amphibole, but is generally absent. Too little is known about it.

Ferro-actinolite (E2167), or ferrotremolite according to Ernst (1968), is a relatively late phase, presumably related to the lower T, higher P event which formed amphibole in various places in and around the lopolith (section I.4. and I.5). Temperature of formation and oxygen fugacity are low (T less than 600°C), P_{H_2O} is less important (Ernst, 1966; Hellner and Schürmann, 1966).

This amphibole is extremely rare : only metamorphosed iron-formations contain amphiboles approaching this composition (Mueller, 1960; Ernst, 1968; Morey et al, 1972; Floran, 1975; Immega and Klein, 1976).

The Fe^{3+}/Fe-total value is dubious because it is calculated, but it should be very low (table IV.9). The calculation based on Z+Y=13 does

not differ in this case from Z+Y+X=15, because of the vacant A-site. This indicates that the value of 0.04 may be reliable (section IV.2.5.). The ferro-actinolite may have formed from clinopyroxene and olivine, which are still present in the sample.

Thin rims of hornblende around other mafic constituents (pyroxene, olivine, ore, or main hornblende) are common in this phase (N3528, R2229, part of R 356). Their composition may vary towards the more Si-rich side, loosing Ca in the case of R2229 which results in cummingtonite (R3229). Ti is normally lower than for the poikiloblastic hornblendes, this is clearly shown in R 356. Measurements on part of a poikiloblast shows Ti = .20 (23(0), R 356 1), while rims result in values of .10-.12 (R 356 2/4). These rims will mainly belong to the lower T, higher P group, and are therefore of later origin (section I.4. and I.5). A direct relation with quartz is sometimes present, sometimes absent.

A colour change in N 402 amphibole from a brownish green core (N1402) to a bluish green rim (N2402) shows chemical changes comparable to those found in B 322 (table II.4) and F 107 (table II.3) : table II.6.

	Δ	C
SiO_2	+ 0.7%	1 %
Al_2O_3	- 3	2.5
TiO_2	-43	4
FeO	+ 2.5	1
MgO	- 8	2
Na_2O	-26	3
CaO	+ 0.9	1
K_2O	-10	4

Table II.6.: Oxide-changes between N1402 2 (core) and N2402 (rim) in analogy with table II.3 and II.4. $\Delta = (X_{N2402} - X_{N1402\ 2})/X_{N1402\ 2}$. See further table II.1.

There is not much chemical difference between N1402 1 and -2 (respectively measured halfway between core and rim, and in the core).

Ti, Na, K and Mg decrease and Fe increases from N1402 2 to N2402. This is in agreement with the other measurements (B 322 and F 107) as far as Ti and the alkalies are concerned. Mg and Fe act opposite to former findings, possibly because in this case biotite caused the measured discolouring instead of Fe(Ti)-oxides. This leads to the conclusion that the Fe-Mg change does not influence this colour change, which leaves only Ti and Na (K did not react in F 107).

Another sample with these colour changes (F 433) only shows a significant decrease in MgO and Na_2O in the more bluish parts, however, the

measurements of the F2433 spots were troubled by the omnipresence of very fine ore needles.

Retrograde metamorphism in the lopolith of Bjerkreim-Sokndal resulted in higher-grade mineral assemblages than retrograde metamorphism in the amphioblite facies area.

This all leads to the following picture : after the intrusion of the lopolith the main amphiboles formed all over the top of the lopolith (extreme poikiloblasts group II). Granulation, caused by dynamometamorphism, appeared along certain zones and locally some amphibole formed at the cost of mafic minerals (extreme poikiloblasts group I and more bluish green amphibole rims); (later?) hydrothermal fluids circulated through certain parts of the lopolith, causing the formation of carbonate (and for instance Na-amphibole) under very low fluid pressures.

II.5.3.-4 : Some individual samples and their petrological problems.

E 128 : The structure and mineralogy of this mela-troctolite indicate a deep-seated igneous origin. The amount of olivine is much greater than in any known sample from the loplith. This may indicate that the sample does not belong to the described phases of the lopolith, or that it represents a special crystal accumulation in the leuconoritic phase. Local occurrences of ultramafics are not uncommon in the leuconoritic phase (B 322). The olivine in E 128 is more Mg-rich than in B 254, which is thought to be related to the emplacement of phase A (section II.3.). The amphibole is really pargasitic, with a very high Na- and Ti-content and the highest mg-ratio for this Si-poor group. It also contains more than 1% Cr_2O_3, which is not uncommon in many alpine ultramafic complexes in the final magmatic stages (Windley et al, 1973). The origin of the amphibole may be due to intercumulus crystallization. First the cumulus olivine crystallized (possibly with some plagioclase), than the trapped

liquid was enriched in H_2O and amphibole-anorthite-clinopyroxene-spinel started to crystallize. Clinopyroxene is only a minor phase, it was immediately surrounded by amphibole, then amphibole, plagioclase, and spinel crystallized. Yoder (1966) mentioned a temperature of 800-900°C and P_{H_2O} greater than 7 kb for such an intercumulus phase. Irvine (1974) states : "Addition of water to alumina-bearing basic melts delays the crystallization of plagioclase relative to the mafic minerals (especially clinopyroxene) and, under some conditions, may suppress it completely by producing hornblende."
A metamorphic origin, as proposed by Robins (1975) for a more or less similar sample from northern Norway, can not be established here. The reaction relationship or pseudomorphism, as described by Robins is not visible in this case.
E 128 certainly is a xenolith in the (quartz-)monzonitic phase.

E 170 : the brown amphibole in this xenolithic lens is chemically comparable with those in the leuconoritic phase, or in the surrounding migmatites, but not with amphiobles from the (quartz-)monzonitic phase. The sample consists mainly of a fine-grained amphibolite with thin layers of dioritic mineralogy. These thin layers are relatively coarse-grained in the centre (mainly clinopyroxene) and very fine-grained near the contact with the amphibolite. In the very fine-grained zone orthopyroxene is present with a long prismatic form. Plagioclase is completely altered in the amphibolite and rather fresh in the diorite. The larger clinopyroxene crystals are partly resorbed to skeletal crystals.
This seems to point to an old amphibolite in which the diorite intruded in various thin layers, along a system of parallel joints (lit-par-lit injection). The extreme fine grainsize of the contact zone and the pyroxene crystal forms indicate a relatively high cooling rate (Lofgren et al, 1974). The uralite (comparable with N 317) is relatively late. Explanation of the layering by assuming hydration of a diorite, or dehydration of an amphibolite seems less probable. Both do not explain the textures. Where the sample comes from originally (roof or bottom) is not clear.

F 433 : the amphiboles from this pegmatite, near the base of phase C, show a most remarkable feature. The more bluish zones (F2433), which lie mainly parallel to the c-axis in the main amphibole (F1433), have another orientation of the optic axial plane than the rest of the crystal. The optic axial plane in the main part of the crystal is oriented $\perp$ c (as in crossite) which is uncommon for Ca-amphibole. In the altered zones (F2433) the orientation is normal for Ca-amphibole (//010).
The chemical differences between F1433 and F2433 are rather small (table IV.7).
Pegmatite F 433 is a relatively young phase, intruded after the emplacement of the main parts of the lopolith. The Ca-amphiboles belong to the most Fe-rich found in Rogaland/Vest-Agder. The composition is very similar to samples E1167 and R 356 1 from the top of the (quartz-) monzonitic phase. However, the pegmatitic amphiboles are richer in alkalies and Mn, and contain less Ti. The last may be the result of a lack of Ti in the late pegmatite phase (no ilmenite is present). Whole rock analysis has not been performed because of the coarse grainsize, and the irregular distribution of the amphibole, so information on the Ti-content of the system is lacking. The strong resemblance to the above men-mentioned amphiboles indicates a related origin. The wallrock alteration creates the extreme amphibole poikiloblasts (cf. II.5.3.-2), supporting the proposed genesis (: orthopyroxene + clinopyroxene + alkalifeldspar + plagioclase ^{1} + $H_2O \longrightarrow$ amphibole + quartz + plagioclase.^{2} Plagioclase^{1} has a higher An-percentage than plagioclase ^{2}. Fluid derived from the final magmatic stage).Originally several minerals seem to have been enclosed during amphibole formation in the pegmatite : titanite, allanite, magnetite and plagioclase plates. A small pocket in amphibole shows some pyroxene remnants : the above mentioned reaction seems to have taken place here too. Probably at the end of the magmatic stage some biotite formed inside the amphibole by partial replacement due to rising alkalinity. Still later biotite-quartz-symplectites were formed (as in B 016, section II.5.1.-2). The relation between F1433 and F2433 is not quite clear. The needle-rich more bluish zones seem to be the

result of exsolution in all of the amphibole, as is indicated by the lack of a clear chemical difference between F1433 and F2433. This is in contradistinction to the normal behaviour of these "group A" ore exsolutions (section IV.3.4.). Ore microscopical investigation suggests magnetite for the needles as well as for the primary enclosed crystals, confirming the overall lack of Ti in the pegmatite.

II.6. : Pyroxene syenite massifs

II.6.1. : Gloppurdi

Samples from this massif are : R 668, V 276, V 277, Y 128, Y 131, and presumably V 147.
This massif, the (quartz-)monzonitic phase of the lopolith (section II.5.3.) and the Botnavatnet massif (section II.6.2.) are described by Rietmeijer (1978).
The samples consist of monzonites, syenites and some granites, not only from the main body, but also from two offshoots (Y 128 and Y 131). The chemical character is comparable with that of the top of the lopolith (section II.5.3.). On basis of SiO_2, the contents of TiO_2, "All Fe as FeO", MgO and P_2O_5 are lower, and Al_2O_3 and H_2O are higher than for the phase C samples. Other elements are more or less the same. The mg-ratio lies between .23 and .04 which is in good agreement with the top of the lopolith (.26-.06), and stresses the relatively Fe-rich character. The K_2O values for V 277 and R 668 are the highest measured in this collection (8.06 and 7.06 wt% resp.). See further section VI.1. for rock chemistry information.
The amphibole chemistry (fig. II.9) is also in good accordance with the phase C amphibole chemistry (fig. II.8). The mg-ratio values may even be lower.
Amphibole is a minor constituent, mainly present as small bluish-green rims around (former) pyroxene and olivine, together with various retrograde minerals and quartz. In non-retrograde rocks the small rims are

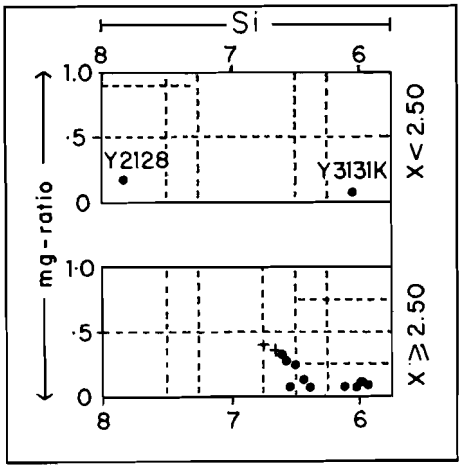

Figure II.9.: Plot of the amphiboles from the Gloppurdi- (•) and Botnavatnet (+) massifs. See further fig.II.1 and II.8.

present as well. Only locally a grey-brown, subhedral amphibole (e.g. R 668), occurs together with the bluish green variety. Extreme amphibole poikiloblasts as found in the lopolith (section II.5.3.) are absent in Gloppurdi. The relation with quartz is generally of symplectitic character, pointing to the formation from (ortho-)pyroxene, as is supported by their presence as rims around this mineral. However, rims are also found around olivine and opaque ore.

Primary magmatic amphiboles cannot be recognized. The only samples which fall in the HT, LP group (sections I.4. and I.5) are R1668, V 277 and Y2131. All other amphiboles belong to the lower T, higher P group (the Y 131 amphiboles are difficult to group, due to their extreme chemistry). However, also the HT, LP amphiboles often show a relation with quartz, indicating their derivation from pyroxene. Whether this happened during the final stages of the intrusion of this massif, or during the granulite facies metamorphism is not clear. It seems logical to assume that granulite facies metamorphism should have destroyed the Fe-rich amphibole + quartz association in favour of orthopyroxene + plagioclase, and thus to assume that the amphiboles formed later. The rather low Ti-values (.165-.195) fall in the amphibolite facies range (fig. I.9) and therefore also point to a metamorphic origin. On the other hand it is true that rocks in this environment, close to the hypersthene line, suffered less from metamorphism than rocks nearer to the lopolith. In hornblende granulite subfacies, amphibole + quartz might survive (e.g. Y 055, section II.2.5., also from this region). All bluish green amphiboles seem to have formed later, not only do they rim pyroxene and olivine, but also brown amphibole (e.g.

R1668), and their chemistry points to a more actinolitic composition : TiO_2 and alkalies decrease, MgO and SiO_2 increase (R2668). Afterwards the retrograde minerals formed, indicating conditions of greenschist facies.

A thin zone of ferro-actinolite was formed in some cracks (Y2128) in the main amphibole (Y1128). Uralite fibres can be found on amphibole rims. Some very thin, colourless to light bluish, zones at olivine-Ca-amphibole contacts may be of the same composition, and contemporaneous with the retrograde minerals.

For the smallest amphibole fragments it is dangerous to draw conclusions regarding the metamorphic conditions from their chemical compositions. In Y 128 it is shown that the chemical and optical properties of the amphibole change with the size of the investigated fragment. The smallest parts still bear many of the pyroxene characteristics while the coarser fragments become real amphiboles instead of wet pyroxenes.

This may also explain the strange chemistry of Y 131 amphiboles and their extreme high Al_2O_3 contents. Alumina has to take the place of other elements which are not sufficiently available.

The analyses of the differently coloured Y 131 grains mainly resulted in decreasing TiO_2, Na_2O and MgO, and increasing FeO from brownish via bluish to colourless crystals (see Appendix). The amphiboles from this sample are extremely poor in SiO_2.

The presence of, late formed, garnet and amphibole in the same specimen (Y 131) is a rare phenomenon in Rogaland (section II.2 and II.5.2.), however, both minerals formed in different parts of the sample, and never appear in contact. Reactions cannot be written for this sample because the original mineralogy of the garnet-rimmed ore-aggregates is unknown. The conditions for Abukuma type metamorphism remain fulfilled, amphibole and garnet do not coexist.

II.6.2. : Botnavatnet.

The only sample from this massif is P 097. There is a very close

resemblance between this massif and the Gloppurdi massif (Rietmeijer, 1978). The amphibole chemistry and optics are also similar, as far as can be concluded from the one measured sample. P1097 and R1668, and P2097 and R2668 are very similar (fig. II.9). The difference between the brownish main amphibole (P1097) and the more bluish amphibole (P2097) is mainly a matter of TiO_2 and MgO (table II.7).

	Δ	C
SiO_2	+ 1.6%	1 %
Al_2O_3	- 4	3
TiO_2	-57	6
MgO	+11.5	1.5
FeO	- 1.9	1

Table II.7.: Oxide differences between P1097 and P2097. $\Delta = (X_{P2097} - X_{P1097})/X_{P1097}$. See further table II.1. Compare with table II.3, II.4 and II.5.

In contrast to other measurements on bluish rims around brownish or greenish amphiboles (B 322, F 107, N 402), the alkalies do not decrease. The bluish amphibole again represents a change towards a more actinolitic composition.

II.7. : Anorthosites

II.7.1. : Introduction

According to literature, amphibole is not a common mineral in anorthosite. De Waard and Romey (1969) mention paracrystalline hydration, in the Adirondacks, resulting in the local development of hornblende at the expense of pyroxene and plagioclase. They also describe the "streaky arrangement of dark minerals" due to deformation, which may be compared with the strings of mafic minerals in L 143 from the Egersund-Ogna anorthosite (section II.7.3.). De (1969) found hornblende coronas around iron ore and diopside, formed during metamorphic reconstitution, probably by circulating fluids (Eastern Ghats, India). Windley et al (1973) described hornblende anorthosites from the Fiskenaesset Complex, in W. Greenland, with, at least partially, metamorphic hornblendes. It is not quite clear from their paper whether igneous amphibole was present, as was concluded from this paper by Leake et al (1976). Myers et al (1977) concluded to a metamorphic origin for amphiboles from anorthosites just outside the region described by Windley et al. They leave the point open whether the amphibole derived from igneous hornblende or pyroxene.

It can be seen from this review that, while an igneous origin for

anorthositic amphibole is never really established, a metamorphic origin is widely accepted.

II.7.2. : Haaland Helleren anorthosite

Samples from this complex are : E 232, F 501, F 502, F 503, and N 827. Amphibole is not a common constituent in the anorthosite, and mainly occurs NW of Eia, near the contact with the lopolith. All samples are from one location (fig. II.10), where pegmatites, noritic bands, leucocratic and mesocratic xenoliths occur in the anorthosite.

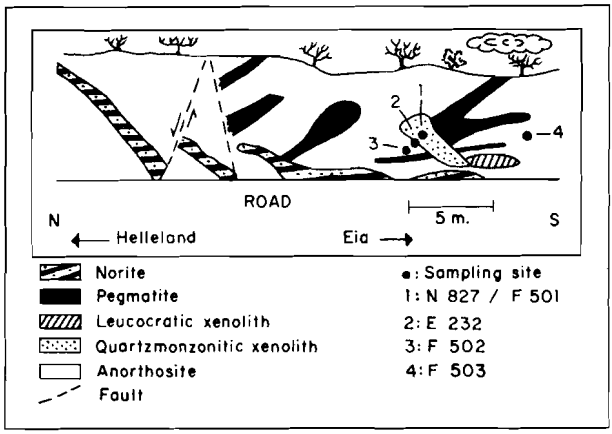

Figure II.10.: General view of the E 232-outcrop, 500 m NW of Eia. Drawing after van Riel (1973-a) and Maijer (pers.comm.).

The rocks have suffered strong retrograde metamorphism. The pyroxene that normally occurs in the anorthosite is replaced by biotite and amphibole. The contacts between the anorthosite and the noritic bands and the xenoliths are sharp. The mesocratic, quartzmonzonitic, xenolith (E 232 F, N 827, F 501) is medium-grained, with a slight variation in grainsize independent of the distance to the contact. It is vaguely banded with a concentration of mafic minerals along the upper contact with the anorthosite. It contains small green-coloured ferro-hornblendes and larger amphibole-quartz symplectites. The symplectites frequently have a homogeneous green mantle (ferro-hornblende) and a lighter coloured core (more actinolitic composition)[1]. The colourchange is gradual. Biotite also forms symplectites with quartz. Titanite rims part of the opaque ore (mainly magnetite). Deformation features are present in plagioclase and biotite. In the anorthosite the amphibole forms aggregates of crystals

1 : Plate VI, figure 2

which may grown through one another[1]. The aggregates all have a light-blue core (actinolite) and a green rim (ferro-hornblende), and are much larger than in the quartzmonzonitic xenolith (several cm). Symplectitic intergrowths of amphibole or biotite with quartz are present. Part of these symplectites are recrystallized into a fine-grained, granoblastic-polygonal aggregate. Remnants of clinopyroxene, coated by carbonate and partly overgrown by amphibole are rarely preserved. Deformation is shown by bent amphibole aggregates and by cracks transecting the samples; these cracks may contain fine-grained amphibole.

The amphibole analyses from this location are plotted in fig. II.11.

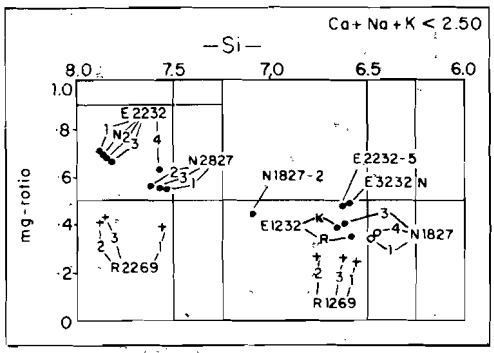

Figure II.11.: Plot of the amphiboles from the E 232-outcrop in Leake's system. Values from table IV.8, 23(0). o = Ca+Na+K ≥ 2.50; • = Ca+Na+K < 2.50; + = R 269 values, see fig. II.6. R 269 is a sample from the monzonoritic phase with comparable phenomena.
E1232 K and R: 3 microprobe points each; E2232 N and E3232 N: 6 points; E2232 1/5, N1827 1/4 and N2827 1/3: 1 point each.

They represent : core and rim measurements in E 232 F (quartzmonzonite, E1232 K = lighter coloured core; E1232 R = green rim), in E 232 N, including stepscanning (anorthosite, E2232 1/5 = light blue core; E3232 N = green rim), and in N 827 (quartzmonzonite, N1827 1/4 = rim; N2827 1/3 = light coloured symplectitic core).

It is clear from this diagram that the mg-ratio for the quartzmonzonitic amphiboles is lower than for the anorthositic amphiboles. This is in agreement with the whole rock analyses :

	niggli-mg	amphibole-mg
quartzmonzonite	.16 - .17	$.34^5$ - .57
anorthosite	.45 - .51	$.48^5$ - .70

The transition from ferro-hornblende to actinolite in the quartzmonzonite and anorthosite is compared in fig. II.12.
Except for TiO_2, all trendlines for a certain oxide are parallel. The level of the lines may differ considerably. The anorthositic amphiboles

1 : Plate VI, figure 3

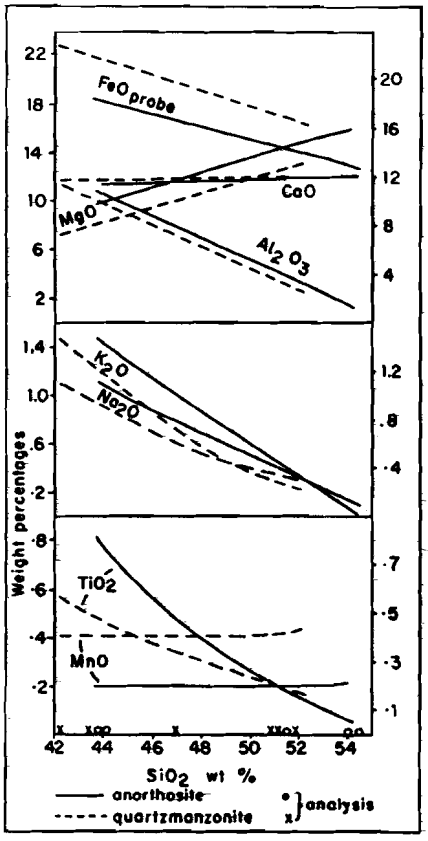

Figure II.12.: Comparison between the oxide-changes, with respect to SiO_2, for the amphiboles from the quartzmonzenites and the anorthosite from the E 232-outcrop.
See also fig.II.2.

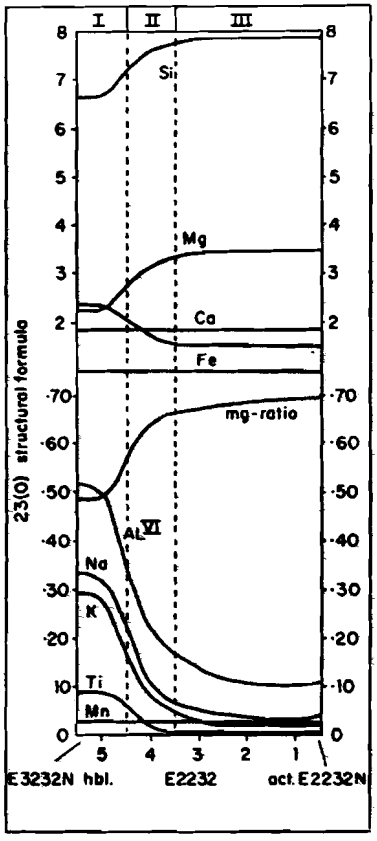

Figure II.13.: Stepscanning profile from actinolite core to ferro-hornblende rim in an anorthositic amphibole aggregate.
I : green rim; II : transition zone;
III : soft coloured core. The five analysis spots (E2232 1/5) are connected by smooth curves.

are higher in MgO, K_2O, Na_2O, and TiO_2, and lower in FeO and MnO for a certain SiO_2-value. The coupling of higher alkali- and Ti-contents with a higher Mg-content follows from the fact that a Mg-rich amphibole gives less Si in the structural formula than a Fe-rich amphibole, and hence more Al^{IV}. It therefore needs more charge compensators (section VI.5.2.). CaO and Al_2O_3 are about equal.

From core to rim, from ferro-hornblende to actinolite, SiO_2 and MgO increase, CaO and MnO increase very little, and the other oxides decrease. In fig. II.13 the element changes from rim to core appear to be rather abrupt. The curves are drawn rather smoothly but are possibly much steeper in zone II. It is clear that the complex chemistry of the ferro-hornblende abruptly changes into a very simple chemistry for the actinolite. Only Mn and Ca remain constant. The hornblende belongs to the lower T, higher P group of section I.4. and I.5.

The hornblende-actinolite assemblage

The hornblende-actinolite assemblage is not uncommon. The last ten years many authors reviewed and extended the knowledge of this paragenesis (Klein, 1968 ; Ernst, 1968, 1972; Cooper and Lovering, 1970; Cooper, 1972; Jasmund and Schäfer, 1972; Choudhury, 1972, 1974; Beach, 1974; Brady, 1974; Graham, 1974; Hietanen, 1974; Wenk et al, 1974; Wetzel, 1974; Grapes, 1975; Misch and Rice, 1975). A summary of the occurrences of actinolite-hornblende pairs is given by Grapes, who divides them in two environmental groups : (1) from metamorphic aureoles and (2) from regionally metamorphosed terrains. The possible existence of a miscibility gap, and the question if the amphiboles are in equilibrium were the greatest problems encountered. Various conclusions were reached for various areas. A miscibility gap is claimed at low to intermediate pressures, and for temperatures below 600°C (e.g.: Ernst, 1968; Klein, Hietanen, Misch and Rice). At elevated pressures a complete miscibility is possible if ΔV_{mixing} is negative (Ernst, 1968), as is demonstrated by Ernst (1972) for glaucophane schist conditions in the Shirataki District, Japan. The scarcity of analyses in between actinolite and hornblende might be explained by : "... the rapid but continuous change of stable amphibole compositions .... over a small range of increased metamorphic grade." instead of by a miscibility gap, in the "... rather high pressure metamorphism ..." of the Scottish Dalradian (Graham). Most authors interpret the actinolite rimmed by bluish-

green hornblende as a prograde reaction near the greenschist facies-amphibolite facies transition. Equilibrium may be indicated by :
(1) a sharp contact between both amphiboles (Becke line),
(2) a discontinuous chemical transition,
(3) exsolution lamellae of hornblende in actinolite and vice versa,and
(4) the coexistence of separate grains of both minerals.

If all four conditions are fulfilled in a sample, equilibrium may exist. For most occurrences only one or two of these conditions are found. In many cases green hornblende is the only separate homogeneous amphibole, indicating a stable phase. The prograde reaction is than said to be uncompleted, possibly because of the low P_{H_2O}, which influences the speed of the reaction (Akella and Winkler, 1966; Liou, Kuniyoshi and Ito, 1974).

The stability limits for both amphiboles are influenced by the whole rock composition too (especially for metamorphic amphiboles, while P and T are the main determining factors in magmatic circumstances (De Albuquerque, 1974)). MgO-rich systems increase the stability of actinolite, while high Al_2O_3 values for the bulk chemistry enlarge the hornblende stability field (Brown, 1967; Cooper and Lovering, 1970).

Beach (1974) described a, more or less, similar phenomenon as found here as the result of a retrograde reaction. Ortho- and clinopyroxene are replaced by hornblende rims and hornblende-quartz intergrowths with a lighter coloured, less aluminous, core. The alteration is restricted to zones of deformation. The hornblende forms rims around pyroxene if the alteration is not completed, and is intergrown with quartz in the centre when the pyroxene is replaced completely. This is explained by the inability of the Si-surplus, from the pyroxene core, to diffuse out of the hornblende. In the centre the hornblende is richer in Si and Mg, and lower in Al, Fe and Na. Ca remains constant. A model is given for the element interchange between the various reacting minerals (amphibole, pyroxene, feldspars, ores and quartz) and the intergranular fluid. The alteration results in a lower An-content for the plagioclase (Si and Na in, and Al and Ca out), loss of perthite (K for amphibole),

decrease in opaques (Fe and Ti for amphibole), disappearance of pyroxene (amphibole forming, Si for plagioclase), forming of amphibole and quartz, and Mg removal by the intergranular fluid, which should have introduced Na. The close relation between the disappearance of pyroxene and the presence of deformation zones is explained by the penetration of fluids by hydraulic fracturing. The description and explanation given by Beach seem to fit the Rogaland samples from the E 232-outcrop very well. Small crystals never have an actinolite core, but only some quartz in the centre. The large crystals were incapable of diffusing Si and Mg from the reaction plane out of the newly formed hornblende, and Al no longer could get in. Therefore, the centre of the newly formed amphibole becomes a Mg-rich, Al-poor system, which increases the stability of actinolite over hornblende. First the actinolite component in hornblende increases and quartz forming is reduced, than a quick overstep is made to actinolite forming. This paragenesis is clearly not in equilibrium, ferro-hornblende is the stable phase, actinolite is present because of the corona texture. So, nothing can be said about a miscibility gap, the changing chemistry of the system caused the actinolite to form.

The contact between the anorthosite and the lopolith is rather disturbed in this location, as can be seen from fig. II.11, so the relationship between deformation and pyroxene alteration also holds for this example. The fluid may be derived from the final stages of the magmatic differentiation. The pegmatites indicate a rather high final activity in these surroundings.

The quartzmonzonitic xenolith, which is thought to be derived from the top of the lopolith (phase C), seems to have recrystallized almost completely : very fine grainsize, microcline as the alkalifeldspar which is uncommon in the lopolith, and the "intrusion" of the F 502 vein in the anorthosite. Recrystallization in the anorthosite is indicated by the fine-grained, granoblastic-polygonal, quartz-biotite and quartz-amphibole textures, which replace the irregular symplectites locally. A complete recrystallization after amphibole formation has not taken place,

because in that case no actinolite should be present anymore in this medium to high grade, Al_2O_3-rich, metamorphic environment.

The other explanation for actinolite-hornblende coronas, being the result of a prograde reaction is unacceptable in this case, because actinolite is not present farther away from this locality as should have been the case if the lopolith heated a regionally metamorphic terrain in greenschist facies.

Only one comparable sample is found in or around the lopolith : R 269 (section II.5.2.), a monzonorite from the intermediate phase, found in the Mydland tunnel. This rock is also recrystallized and occurs in a tectonized zone. The fact that the rest of the lopolith contains only ferro-hornblende replacing pyroxene (section II.5.3.) indicates that the alteration there was a quiet open system reaction in contrast to the partly closed system effect which caused the formation of actinolite.

For further information on the Haaland-Helleren anorthosite the reader is referred to J. Michot (1961). See also section II.2.3. for secondary amphiboles in the migmatites and section II.5.1.-2 and II.5.3.-3 for retrogressive metamorphism in the lopolith.

II.7.3. : Egersund anorthosite (Michot and Michot, 1969; Michot, 1969).

The only sample from this anorthosite is L 143. Plagioclase is anhedral and inequigranular, it looks like an adcumulate. These properties are common in the outer zones of the anorthosites. The term adcumulate is erroneous because the anorthosite is recrystallized in this zone. The grainsize diminishes from the centre of the anorthosites to the contact with the lopolith, and the mafic minerals become arranged in strings. The zone may be several kilometers wide. Amphibole is uncommon.

The strings of mafic minerals consist of ortho- and clinopyroxene rimmed by serpentine, ore needle zones, cummingtonite and light coloured,

greenish hornblende. Cummingtonite only appears between orthopyroxene and hornblende, and the contacts between both amphiboles are sharp. Very fine exsolution lamellae are found in some of the hornblende rims, and they seem to continue into the cummingtonite. Ilmenite needle zones are omnipresent in the cummingtonite (fig. II.14). See also section II.5.1.-2 : cummingtonite in B 016 from phase A.

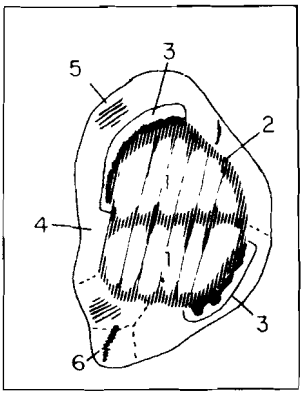

Figure II.14.: L 143 relation scheme, a combination of various natural examples.
1: orthopyroxene; 2: serpentine; 3: cummingtonite with ore needle systems; 4: magnesiohornblende/actinolitic hornblende; 5: colourless exsolution lamellae; 6: ore needle zone. See Plate VI, figure 4.

Several microprobe measurements in a certain hornblende rim resulted in slightly varying compositions, supporting the inhomogeneous character of the hornblende which could already be deduced microscopically. The oxide changes with varying SiO_2 contents are approximately the same as for E 232 and F 252 : fig. II.15. The only exception is TiO_2 which increases with rising SiO_2-content. The cummingtonite is plotted on the right side of the transition zone. From microprobe information it is not clear if the highest SiO_2-values for L1143 are indeed found at the contact with cummingtonite, and if the chemical difference represents real zoning, or inhomogeneity between subgrains. Therefore, the position of L2143 in the diagram is only determined by the SiO_2 content.

The composition of the colourless amphibole is reached more or less continuously for MgO, Al_2O_3, and K_2O and discontinuously for CaO, Fe-total, Na_2O, TiO_2 and MnO, with rising SiO_2-content. This chemical discordance causes a sharp contact between both amphiboles. They could not form a solid solution under the final conditions of metamorphism.

The chemical composition of this hornblende (L1143 : fig. II.16) deviates strongly from the composition of anorthosite amphibole E3232 etc. (section II.7.2.) and from the amphiboles from the igneous complexes (section II.5. and II.6.). L1143 is much more Mg-rich and, therefore, not used in the igneous group in Chapter VI. It belongs to the lower T,

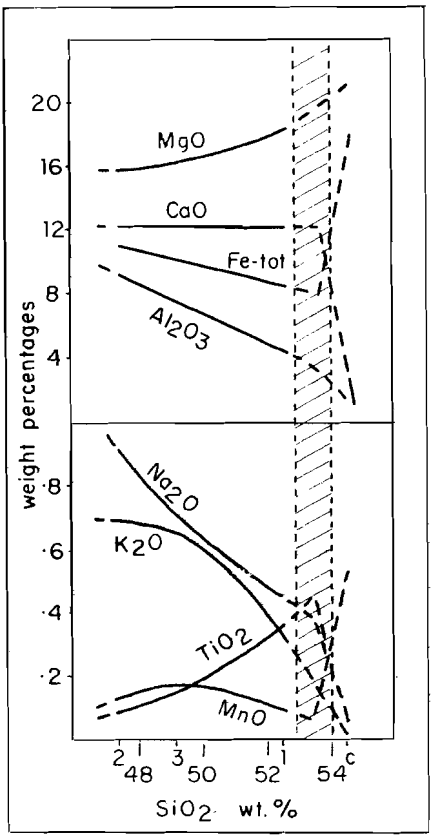

Figure II.15.: Oxide-changes with respect to SiO_2 in L 143-hornblende (L1143). The shaded zone represents the transition from L1143 to cummingtonite (L2143), the position is arbitrary. 1: L1143 1; 2: L1143 2; 3: L1143 3; c: L2143. Compare with fig.II.2 and II.12.

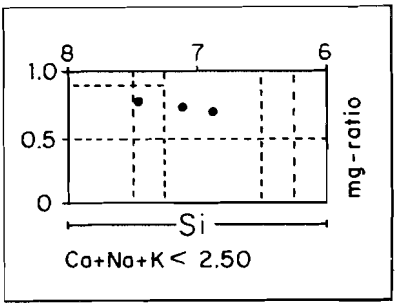

Figure II.16.: Plot of the Ca-amphibole compositions from L 143. See further fig.II.1.

higher P group of sections I.4. and I.5. The low Ti values are not due to a lack of TiO_2 : ilmenite needles and grains are present in the amphibole.

The variation in composition is almost the same as for N 041 (section II.2.). The cummingtonite is also much more Mg-rich than the cummingtonites from the lopolith (fig. IV.10).

Another cummingtonite-hornblende assemblage has been described in section II.5.2. (B 016). The origin by replacement of orthopyroxene and reaction with plagioclase during retrograde metamorphism seems to fit this occurrence too (lower T, higher P group). Cummingtonite never appears in contact with plagioclase, and is not present in clinopyroxene-enveloping rims.

The exsolution lamellae are dubious as to their composition. TEM investigation by Dr. Champness (section IV.3.4.) might solve this problem. The ore needles in the colourless amphibole are the result of the inability of the cummingtonite to incorporate the TiO_2 of the orthopyroxene. The hornblende can only accept a small amount of TiO_2 due to the metamorphic condition. The actinolitic hornblende composition is indicative

of amphibolite facies conditions (or of the lack of certain elements to form a common hornblende, however, the most important element Al is abundant). The low Al^{IV}-values fall in the range of the miscibility gap of Misch and Rice (1975), and this should indicate temperatures of at least 600°C at 5 ± 1 kb, if the empirical gap from the Skagit Metamorphic Suite is applicable in this area. A pressure of ± 5 kb was already proposed in section I.5., and a temperature of 600°C does not seem unreasonable for the phase of secondary amphibole formation in the westside of the investigated area near the lopolith.

The pyroxene remnants and the general lack of amphibole in surrounding anorthosite samples stress the lack of water, and the local character of this paragenesis.

A primary magmatitic origin is highly unlikely in the light of the recrystallization of the anorthosite, and the restriction of Fe-Mg-amphiboles to metamorphosed rocks (Ernst, 1968).

The increase in TiO_2 with rising SiO_2-content in L1143 is caused by the lack of other charge compensators. In fig. II.17-A the behaviour of the charge compensators Al^{VI}, Na, K with increasing Si content is compared for E2232 and L1143.

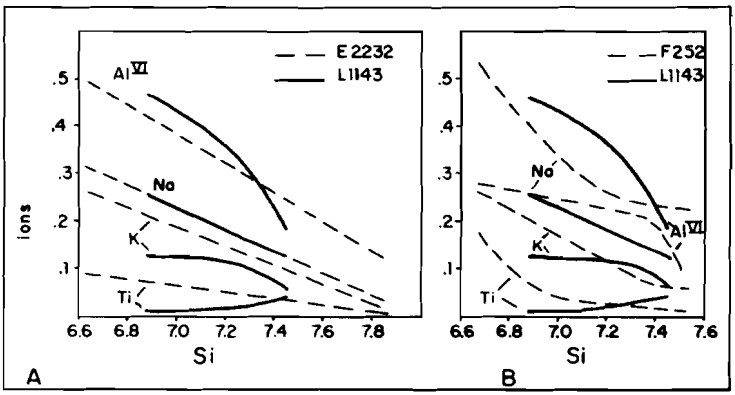

Figure II.17.: Change of charge compensator ion quantities with increasing Si-content in the 23(O) structural formula. A : L1143 versus E2232; B : L1143 versus F1252 and F2252.
E2232: 3 microprobe spots (fig.II.13); F 252: 4 spots (fig.II.2); L1143: 3 spots (fig.II.15).

Na is exactly the same for both amphiboles. K is less abundant in L1143 (the niggli k is lowest for the host rock, K_2O has to be received from the antiperthite). Al^{VI} is somewhat higher for L1143 at the lower Si side, but decreases more rapidly at higher Si values (highest Al_2O_3 in bulk composition of L 143). Therefore, an extra charge compensator is needed. Ti deals with the problem, or at least part of it. Fe^{3+} is unknown from the 23(O) formula and could not be analysed because of material shortage. The Ti is probably added from the ilmenite needles in the cummingtonite.

Compared to F 252 (augen gneiss, section II.2.) the trends are different (fig. II.17-B). F 252-amphibole contains more alkalies and Ti, and less Al^{VI}. This also holds for the bulk composition. The decrease of these elements is not as regular as in E2232. The alkalies control the charge compensation and Ti decreases rapidly with increasing Si.

II.8. : Conclusions

In the Rogaland/Vest-Agder area :

--it is not possible to see through the metamorphic event of about 1000 Ma ago, as far as the amphibole compositions are concerned. All Ca-amphiboles belong to either the HT, LP group which is related to the granulite-amphibolite facies metamorphism and the intrusion of the lopolith of Bjerkreim-Sokndal, or to the lower T, higher P phase of amphibole formation (between 1000 and 950 Ma ago). This means that eventual older amphiboles were reequilibrated,

--igneous amphiboles are difficult to recognize. Primary crystallization is assumed on chemical grounds for some Mg-rich, Si-poor hornblendes occurring in phase A of the lopolith, in the banded migmatites at the eastern contact of the lopolith, and in a thin gabbro layer in the garnetiferous migmatites. Crystallization due to autometamorphism at the end of the igneous activity is assumed for the top of the lopolith,

--xenoliths in the lopolith are highly comparable in mineralogy and amphibole characteristics with samples from the banded migmatites at the eastern boundary of the lopolith,

--the syenite massifs of Gloppurdi and Botnavatnet do not contain recognisable igneous amphibole,

--a better facies division than just granulite and amphibolite facies with the aid of the hypersthene line, can be made by means of the following assemblages (De Waard, 1965) :

I : orthopyroxene-plagioclase-quartz (granulite facies)

II : orthopyroxene-plagioclase-quartz-hornblende (hornblende-granulite facies)

-------present position of the hypersthene line-------

III : hornblende-plagioclase-quartz (amphibolite facies).

The greenschist facies influences are too local to map, and the former facies can still be recognized in most of the retrograde samples. This new division requires a careful check on the complete sample collection,

--deformed amphiboles are rare,

--dehydration reactions are common west of the hypersthene line. In the quartz-bearing rocks amphibole is generally absent; only near the hypersthene line, rocks with amphibole and quartz in contact may be found,

--older amphiboles can be recognized petrographically in partly dehydrated amphibolites in the granulite facies area,

--the occasional presence of watersaturated rocks in the mainly dry granulite facies area proves that at least part of the rocks formed a closed system. The fluid-free and -rich layers may be very thin,

--amphibole-quartz relations (e.g. symplectites) are common in mafic rocks east of the hypersthene line. They point to hydration reactions in (formerly) pyroxene carrying mafic and intermediate layers (area east of Tonstad),

--a former granulite facies metamorphism has been present in at least part of the area east of Tonstad,

--amphibole and garnet never appear in equilibrium (as in the Barrovian type of metamorphism). The orthopyroxene-anorthite tieline prevents their coexistence and indicates the Abukuma type metamorphism,

--exsolution lamellae are rare,

--the anorthosites only locally contain some amphibole in the lower T, higher P group. The conditions of forming may have been 600-700°C at about 5 kb in the western part of the investigated area, while the same event produced greenschist facies assemblages in the eastern part. This implies that during the second amphibole formation event, the temperature division in the area was of the same type as in the main amphibole formation event, but a few hundred degrees lower,

--cummingtonite is only present in disequilibrium assemblages, rimmed by hornblende, and originated from orthopyroxene,

--actinolite rimmed by hornblende in and around the lopolith is not an indication of prograde metamorphism, but the result of pyroxene alteration in a partly closed system,

--the more bluish rims around hornblendes of the HT, LP group are a response to the lower T, higher P event. The colourchange is mainly the result of Ti and alkali decrease,

--greenschist facies assemblages are locally formed, mainly around Tonstad, and may be a final stage of the lower T, higher P metamorphic event which formed amphibole under amphibolite facies conditions near and in the igneous complexes,

--the alteration from hornblende to actinolite in the retrograde samples is characterized by a quick decrease of TiO_2. The other elements change more gradually,

--magnesioriebeckite formed only in a peralkaline rock,

--all K-Ar measurement on hornblendes, from various formations all over the area, give the same result : about 950 Ma. This age is though to represent a cooling age (cf. Chapter VII). Hornblende formation must have been earlier.

AMPHIBOLES AND THEIR HOST ROCKS IN THE HIGH-GRADE METAMORPHIC PRECAMBRIAN OF ROGALAND/VEST-AGDER, SW. NORWAY

Part II

Methods and data

Introduction.

This part contains all relevant data on the investigated amphiboles and rocks of the Rogaland/Vest-Agder area (see for locations fig. I .1). It also holds information on the methods used and on the accuracy and reliability on the measurements.
An effort is made to give information on the background of the tables presented here, including some statistical information on the limits of their trustworthiness. Too often geologists publish impressive tables of meaningless data. Meaningless, because no information at all is given concerning the reliability of the data; because the geologist does not know or understand the reliability himself; or because the analysts do now know or understand what the geologist wants, and thus provide him with information which in itself may be good, but does not fit the specific geological problem.
I think that a closer contact between the laboratory, the geologist and the statistician is needed in many cases to guard against injudicious use of data, and thus against the publication of meaningless data.

III : Investigations on the whole rock

III.1. : Modal analyses.

Modal analyses were carried out with a J. Swift and Son pointcounter, using the cogwheels a, b and h, which results in a pointdistance of 1/6th mm. Line spacing was taken as 1 mm.
For each sample one thousand points were counted in thin section, sometimes several thin sections were used for one sample. The volume percentages found in this way and given in table III.1 are only indicative and should never be used as exact values. Again, the rocks may not be homogeneous, several thin sections of the same handspecimen giving varying percentages.

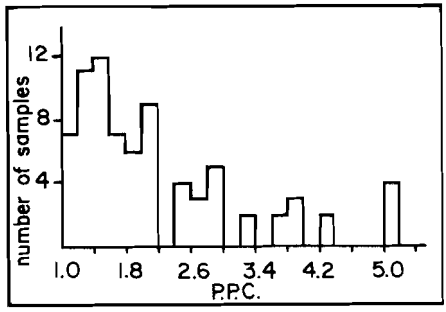

Figure III.1.: P.P.C.-histogram according to table III.1.

The P.P.C. (= points per crystal, Kalsbeek (1969)), varies mostly between 1.0 and 2.1 (fig.III.1, table III.1), which means that the "golden rule" of Frangipane and Schmid (1974)(P.P.C.=1.0) has been disregarded by the author. However, I think that the point-counter analyses presented in this table give a reasonably good idea of the modal composition. If more information is needed concerning the accuracy range the graph of Kalsbeek (op.cit.) is recommended in which the accuracy level is also indicated for "P.P.C. values" greater than 1.0.

Table III.1.: Modal composition, An% and P.P.C. of the rocks under discussion.
A : less than 1 percent; X : mineral present, grainsize too coarse for modal analysis.
Total pyroxene : sum of ortho- and clinopyroxene; it was not always possible to tell opx from cpx during pointcounting if both are present, in these cases only the sum is given.
An% of plagioclase is determined in sections a, after Tobi (1963).

SAMPLE	AMPHIBOLE 1	AMPHIBOLE 2	AMPHIBOLE 3	AMPHIBOLE 4	ORTHOPYROXENE	CLINOPYROXENE	TOTAL PYROXENE	QUARTZ	ALKALI FELDSPAR	PLAGIOCLASE	MESOPERTHITE	TOTAL LEUCOCRATIC	BIOTITE	STILPNOMELANE	CHLORITE	MUSCOVITE	OLIVINE	APATITE	ZIRCON	ORE	SPINEL	ALLANITE	SPHENE/TINE	ZOISITE	EPIDOTE	TITANITE	CARBONATE	DIASPORE	GARNET	-- 100 % -- QUARTZ	ALKALI FELDSPAR	PLAGIOCLASE	AN %	P.P.G.
A 037' B	8					25	25			50		50	A			A	A	A	A	6	3	A	A	6			A	I		0	0	100	99	2.7
A 128	65				4	13	17			7		7	A					5		5	A		A	A						0	0	100	96	>5
A 168	1							45	51			96		2				A	A	A										47	53	0		1.4
B 016	20	6						2	1	49		52	17					2	A	3							A			4	2	94	29	1.2
B 118 L	4						14	20	39	20		79	A					A	A	2			A				A			25	25	50	27	1.1
B 254	42						2			38		38	A				12	A		5			A							0	0	100	51	1.6
B 322	14				35	A	35			2		2	1					6		42										0	0	100	46	1.6
C 172 D	4				1	18	19	8		56		64	7					A		4			A							13	0	87	30	1.7
D 307	19						22	A		57		58	2			A		A		A							A			1	0	99	60	1.5
D 442	46									36		36	17					1	A											0	0	100	40	1.5
D 444	51									32		32	10					A	A	4			2							0	0	100	40	1.5
E 067	12				4	4	8	10	37	30		77	1			A	A	A	A	2		A	A				A			13	48	39	14	3.9
E 125	5						30			54		54	A					A	A	10			A							0	0	100	48	1.2
E 128	20					A	A			15		15					61			2	2		2							0	0	100	60	1.4
E 131	4				22		22			56		56	4					1		32	2									0	0	100	78	1.5
E 167	9	A				A	A	26	32	30		88	A	1			A	A	A	1										33	36	34	16	4.3
E 170	43	A					13			43		43	A					A	A	1			A							0	0	100		1.2
E 232 F	8							10	30	40		80	5				A			5		A	A							13	37	50	27	1.8
E 232 N	4	8					2	A		76		77	9				A			3			A			A	A			1	0	99	38	3.8
F 005	6							16	26	44		86	5			A	A	A	A	1		A			A	A				19	30	51	27	1.8
F 043	8	A						21	31	29		81	3			A	A	A	A	2		A			A	3				26	38	36	26	1.4
F 052 D	25	2				A	A	2	52	7		61	3			3		2	A	2			A		A	2	A			3	85	12		1.9
F 052 L	25	4				A	A	11	52	4		67	1			1		1	A	1		A	A		A	1				16	78	6		>5
F 070	10							22	38	20		80	5			A		2	A	3		A			A		A			27	48	25	27	1.5
F 074	24							3	A	55		59			10			3	A	6					A					5	1	94		1.1
F 107 D	17	A					14	7	11	40		58	1			A	A	6	A	6			A				A			12	19	69	38	1.2
F 126	7	A					3	24		40		67	19	A	5	A		2	A	4			A		A					38	0	62	35	1.2
F 252	10	A				2	2	22	8	53		83	4			A		A	A	2		A			A	A				27	10	63		2.5
F 433	x	x				x	x	x	x	x			x	x						x		x					x	x		x	x	x	8	>5
F 501	2							7	26	49		82	7				A	1	A	6		A				1				9	32	59	26	1.6
F 507 F	16	1					A	11	32	17		60	2				A	5	A	6			9			A				18	53	29	-	1.1
F 502 N	2	1					A	2		83		85	9		A	A		A		2			A			A				2	0	98	35	3.9
F 503	4	1					A	1		84		85	5				1	A		1			2			A				1	0	99	39	4.2
H 047 B	11	A				2	2	15	25	40		80	4	A	A			A	A	3					A					19	31	50	27	2.0
H 050	16	A				1	1	18	26	34		78	A		A	A		A	A	2			2		A		A			23	33	44	30	2.0
H 307	36					10	10			40		40	12					1	A	1							A			0	0	100	55	1.9
H 325	37				20		20			42		42						A		A					A		A			0	0	100	70	2.4
H 415	56					1	1			34		34	4					1	A	4										0	0	100	33	1.4
J 119	23						23			50		50	2			A		A	A	3			A							0	0	100	48	1.2
L 143	3	A					3	A	A	92		92					A			A				J	A					1	1	98	54	3.8
M 101	12				5	1	6	4	14	45		63	2	A			A	4	A	9			4							6	22	72	30	1.3
N 061 B	30	50			8		8	2		A		3	10					A	A	A			A							66	0	34		3.3
N 264	10	A						14	48	12		74	10			1		2	A	2					A	A	1			19	65	16	24	1.9
N 317	49						14	A		31		32	A			A		3	A	3			A							1	0	99	46	1.1
N 337	12						27		2	50	A	53	A			A		1	A	8			A							0	4	96	29	1.1
N 402 F	x	x						x	x	x		x	x	x				x	x	x			x							x	x	x	14	>5
N 528 B	A	A	A	A			9	3	20	1	60	84	A				4	2		3			A				3			4	59	37	23	2.6
N 572 L	40				21		21			14		14					23			2	A		A	A						0	0	100	90	2.8
N 572 O	12				73		73			2		2	A				13			A			A	A						0	0	100	90	2.8
N 809	56						34			9		9	A					A		A			A							0	0	100	47	1.3
N 827 F	4	A						10	30	42		82	5		2	1		1	A	4		A			A	A				12	37	51	27	1.8
O 100	20				16	7	23			53		53	3			A		A	A				A							0	0	100	67	2.0
P 097	6	1						22	43	A	26	92	A	A	A	A		A	A	A			A							24	61	15		2.1
P 248	4							22	56	12		90	2		A			A	A	3		A	A		A	A				24	63	13	27	1.2
P 303	40					4	4			46		46	9		A	A		A	A	A			A				A			0	0	100	40	1.4
P 580 D	17				25	A	26			50		50	7		A	A				A										0	0	100	42	1.2
P 580 L	1				A	35	36	A		60		61	1		A	A				A			A				A			1	0	99	42	2.4
R 227	5				10	10	20	A	14	50		65	2			A		2	A	4							A			1	22	77	23	1.0
R 229	1	A	A				12	1	51	29		81	1			A		A	A	2							1			1	63	36	27	1.7
R 269	10	5					3	3	19	44		66	11					3		2						A	A			5	28	67	20	1.5
R 356	1					5	5	24		5	61	90	A				7	A	A	1			A							27	34	39	23	2.5
R 668	13	1				A	A	1	47	29	5	82	A	A				A	A	A			A							1	61	38	25	2.9
V 147	1						A	30	42	20		92	A	A				A	A	A		A	3		A	A				33	45	22	28	2.0
V 187	15	A					34	A		46		47	1		A	A		A	A	2										1	0	90	53	1.7
V 276	1							34	40	10	13	97	A	A	A				A	A										35	49	16	25	2.1
V 277	3							9	30		15	91	A	A		A		2	A	A			3		A					10	42	48	15	2.1
V 363	4							30	27	34		91	2		3			1	A	2					A					33	30	37	26	3.2
W 012 D	40							9	A	45		55	5					A	A	A		2			A					16	1	83	33	2.1
W 017 B	11						3	20		56		76	8			A		A	A	A			A		A					26	0	74	40	2.8
W 162 D	A							13	14	52		79	12		A			2	A	4		A				Z				16	18	66	23	1.5
W 196 B	20				5	A	6	30		35		65	A			A		2	A	5		A	A							46	0	54	50	1.2
W 217	4							28	30	31		89	6					A	A	A			A							31	34	35	25	3.7
W 226 D	88					A	A			10		10	2					1	A											0	0	100	40	1.7
W 226 L	7					44	44			46		46	A					A	A	3										0	0	100	40	1.1
Y 055	1	A			8	1	9	18	4	66		88	A			A		A	A	1										20	5	75	46	2.0
Y 128	1	A					5	10	51	21		82		5	2			A	A	A		A	A	A		A				12	62	26	27	2.9
Y 131	A	A	A			2		5	33	46		84	A		A	2	A	A	A	3		A				A	2		3	6	39	55	31	2.6

III.2. : Chemical analyses.

III.2.1. : Introduction

Whole rock chemical analyses were carried out in the Petrochemical Laboratory of the Institute of Geology and Mineralogy, University of Leiden, under supervision of Mr. K. Stephan. A single solution method as proposed by Shapiro and Brannock (1962) and Shapiro (1967) was used. All samples were analysed in duplicate by three analysts.

III.2.2. : Sample preparation

The samples were crushed in a jawcrusher to parts smaller than 5 mm. A hand sample splitter was used to separate the sample in a whole rock analysis sample and an amphibole analysis sample. The amphibole sample preparation is further described in section IV.1.2. The whole rock sample was ground in a Braun pulverizer, fitted with ceramic plates, and finally in a Fritsch Pulverisette, type 601, for one hour. Samples were homogenized with a Turbula mixer before weighing.

III.2.3. : Analytical methods, their accuracy and precision

Several methods were used, depending on the element to be measured :
SiO_2, Al_2O_3, TiO_2, Fe_2O_3-tot, P_2O_5 : colorimetric
MgO, CaO, Na_2O, K_2O, MnO : atomic absorption
FeO : titrimetric
H_2O : Penfield
CO_2 : gas volumetric
F : method of Huang and Johns (1967)

The samples were grouped in batches of 15 : 1 blank, 2 reference samples, 10 samples, 2 reference samples. The reference samples are a basalt (BN 01) and a granite (GN 02). They are used as an accuracy

(= quality) control, by checking them regularly against the U.S.G.S. reference samples W1, G2, PCC1 and DTS1. The precision or reproducibility depends on various factors. Wernimont (1951) concluded that, as long as the analyses are performed in one laboratory, the precision is rather high; if several laboratories are used, the st.dev.(s) increases a lot (.07→.25). The accuracy, however, may vary widely between the laboratories. These results were confirmed by Fairbairn (1953), who divided precision in three groups : (1) replicate analyses by the same analyst in a given laboratory and using the same procedure, (2) by different analysts in a given laboratory and using the same procedure and (3) different analysts, different laboratories and using different methods. The first two groups give a high precision for experienced analysts, the last is distinctly lower. In our case, group 2 was applied over an extended period of time. Mercy (1956) worked extensively with the rapid methods of Shapiro and Brannock (op.cit) and found that accuracy and precision : "... compare very favourably with both conventional chemical and with spectrographic procedures." He also checked the results over a longer period of time (eight months) and concluded : "In general, the results are very satisfactory..." Ahrens (1954) presented the information of Fairbairn (op.cit) in a graph with relative deviation (=C =st.dev/ mean) and percent constituent as parameters on a log-log-scale. It was perfectly clear that there was a negative correlation between these two parameters. Or as Burri (1959, p.17) stated : "Als allgemeine Gesetzmässigkeit ergibt sich daraus, dass die Genauigkeit der Bestimmung einer Komponente mit ihrer Konzentration zu- bzw. abnimmt." ("As a common rule hence it follows, that the precision of the determination of a component increases resp. decreases with its concentration.").
In table III.2 the precision for the reference samples BN 01 and GN 02 is indicated as st.dev. and relative st.dev. These results are compared with Ahrens'graph, see fig. III.2.
It is clear that the precision in our case is distinctly better than for the experiments of Fairbairn. But that is in good agreement with

Wernimonts results : one laboratory has a much higher precision than a combination of laboratories, as in this case with Fairbairn (34 laboratories). This does not say anything about the accuracy.

	BN 01	s	C	GN 02	s	C
SiO_2	44.59	.09	.20	70.32	.07	.10
TiO_2	3.01	.007	.23	.33	.03	9.09
Al_2O_3	15.27	.19	1.24	14.59	.03	.21
Fe_2O_3	4.11	.16	3.89	1.24	.11	8.87
FeO	7.66	.16	2.09	1.06	.07	6.60
MnO	.10	.013	6.96	.08	.012	15.00
MgO	6.78	.13	1.92	.88	.03	3.41
CaO	10.54	.15	1.42	2.22	.18	8.11
Na_2O	3.29	.11	3.34	3.51	.10	2.84
K_2O	1.68	.08	4.76	4.23	.07	1.65
P_2O_5	.79	.008	1.01	.11	.006	5.45
H_2O^+	1.31	.13	9.92	1.01	.14	13.86
Fe_2O_3-tot	12.60	.10	.80	2.41	.10	4.14

Table III.2.: Absolute (s) and relative (C) standard deviations for reference basalt BN 01 and granite GN 02, as an indication of the precision. Number of measurements is 16.

The direction of the tie-lines may vary from Ahrens' directions. In these cases the absolute st.dev. varied less in this research between high and low oxide values than with Ahrens. This results in a steeper line. FeO and Fe_2O_3 were measured by classical methods and show more or less the same direction in both cases. Interesting is the orientation of the Al_2O_3 tie-line which is in both cases the same and reversed to the general, and expected, trend. The reason for this orientation is unknown. The distance between the various lines for a certain percent constituent range (e.g. MgO and CaO) may depend on the optimal measurement range for the various elements with a certain instrument (in this case A.A.). As a conclusion it can be said that the precision obtained in this case is not disappointing. The error cause

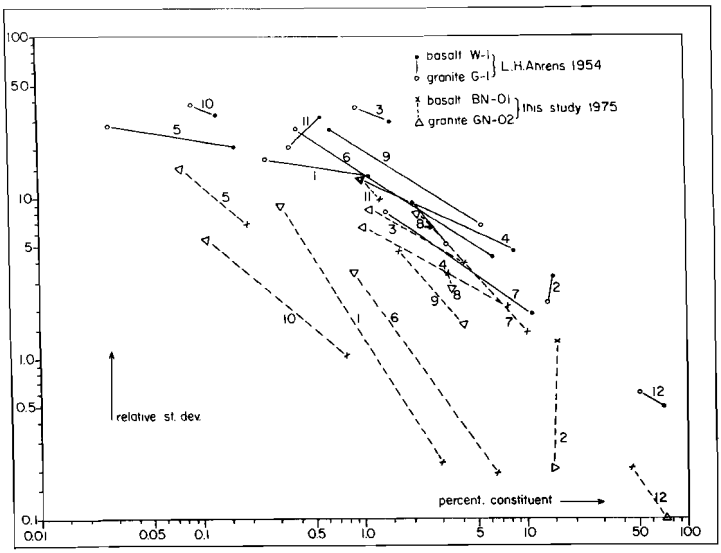

Figure III.2.: Precision of the whole rock chemical analyses as a function of relative st.dev. and percent. constituent, and compared with the results of Ahrens (1954). 1: TiO_2; 2: Al_2O_3; 3: Fe_2O_3; 4: FeO; 5: MnO; 6: MgO; 7: CaO; 8: Na_2O; 9: K_2O; 10: P_2O_5; 11: H_2O^+; 12: SiO_2.

changed from a great personal influence for the classical methods to instrumental for the "rapid rock" methods.

However :

"There have been some marked advances in both instrumentation and technique during the last two decades and one could assume that our overall abilities in rock analysis might have improved but this assumption is not always warranted by the conclusions in Table 7. Significant improvements are noted for FeO, Fe_2O_3 and Al_2O_3. The improvement for Al_2O_3 is probably due to the increased use of direct methods rather than the indirect method of obtaining this oxide by difference." (Flanagan, 1969). This agrees well with the findings of Mercy (op.cit).

It is not clear if one may extrapolate the tie-lines of fig. III.2. Therefore, there is no indication of the precision for the percent constituents outside the basalt and granite reference sample range. An indication for the size of the error bars is found by means of the deviation and relative deviation from the mean for all analysed samples

of the Rogaland collection. The deviation is : (value 1 - value 2) : 2. The rel.deviation is : (value 1 - value 2) : (value 1 + value 2) x 100%. This is : deviation divided by the mean and multiplied by 100%. Fig. III.3 shows the rel.deviation in histograms. It is directly clear that the most frequent rel.deviation (= mode) is normally lower than the rel.deviation mean, which shows that it is not sufficient to give the rel.deviation mean for a series of analyses with different values for one oxide (e.g.: SiO_2, rel.deviation is 0.21%) if one did not determine reference samples with each batch (in that case the only information on the precision is received from the duplicate measurements, which can not give a standard deviation). Fig. III.4 shows the relation between the rel.percent. deviation and the percent.constituent, more or less an equivalent of fig. III.2 but for a greater spread in values. The highest values of the rel.percent.deviation are connected by smooth curves. These curves indicate the maximum deviation found for a certain percentage of an element-oxide in this collection and indicates precision for the laboratory in Leiden. Their direction coincides with Ahrens' lines (fig. III.2). In some cases (e.g. MnO) the absolute deviation values and constituents percentages are very low and a curve is formed by every abs.dev. value. They are indicated in these cases as : absolute deviation, with the value given in the graph. To determine whether the second figure behind the decimal point for the various elements is significant a simple method can be used in this case. The so-called 2FSC (= Two Figure Significance Curve) is drawn in a modified version of fig. III.2, see fig. III.5. The 2FSC connects the points at which the absolute standard deviation equals 0.10% oxide. At the right side of this curve the abs.st.dev. is greater than 0.10 and therefore the second figure behind the decimal point for the oxide becomes meaningless. At the other side of the curve it may be significant. From the graph it can be seen that the oxides can be divided into three groups :

1. oxides always below 2FSC; the second figure may be significant :
   TiO_2, MnO, K_2O and P_2O_5

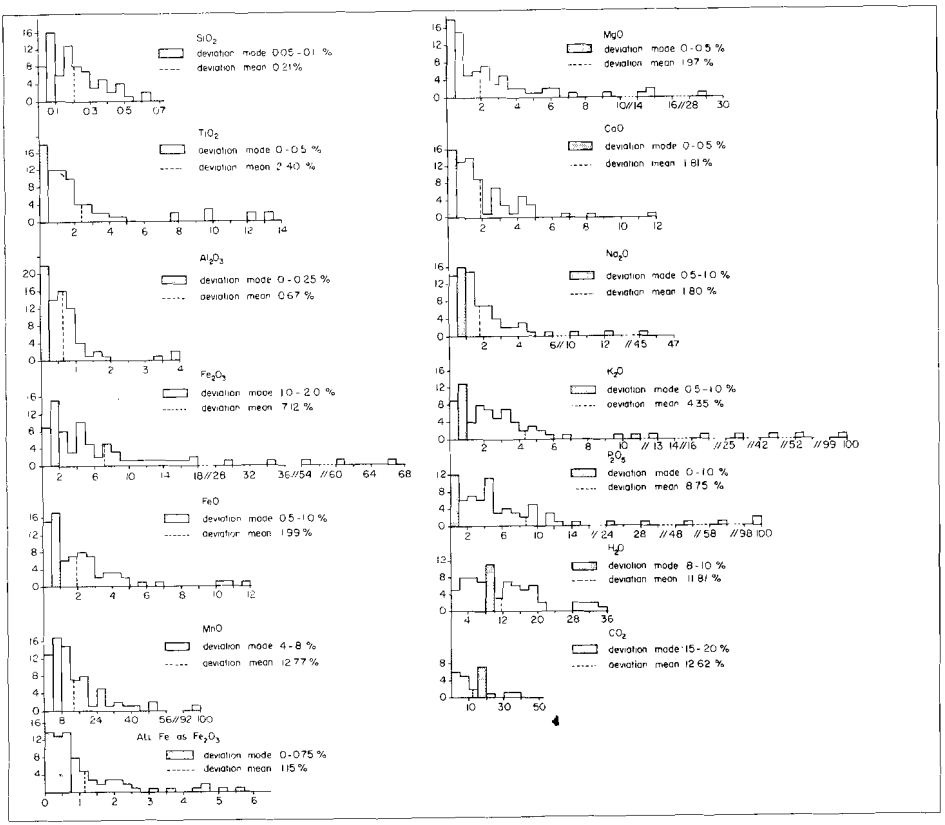

Figure III.3.: Relative percentage deviation in whole rock duplicates.
Relative % deviation = $\frac{\text{value 1 - value 2}}{\text{value 1 + value 2}} \times 100\%$
Deviation mode : most frequent deviation; Deviation mean : arithmetic mean. This only indicates the variation for the laboratory in Leiden.

2. oxides always above 2FSC; a meaningless second figure : Fe_2O_3, CaO and H_2O
3. oxides partly above and partly below the 2FSC. The critical value is not known because we do not know the course of the curve between granite- and basalt value : SiO_2, Al_2O_3, FeO, MgO, Na_2O and Fe_2O_3-total.

The variation between these groups is caused by the different methods of determination and element properties.

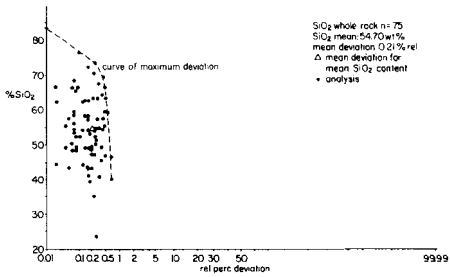
SiO2 whole rock n=75
SiO2 mean:54.70 wt%
mean deviation 0.21% rel
Δ mean deviation for mean SiO2 content
• analysis
curve of maximum deviation
%SiO2
rel perc deviation

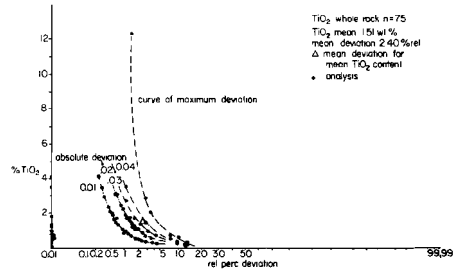
TiO2 whole rock n=75
TiO2 mean 1.51 wt%
mean deviation 2.40% rel
Δ mean deviation for mean TiO2 content
• analysis
curve of maximum deviation
absolute deviation
%TiO2
rel perc deviation

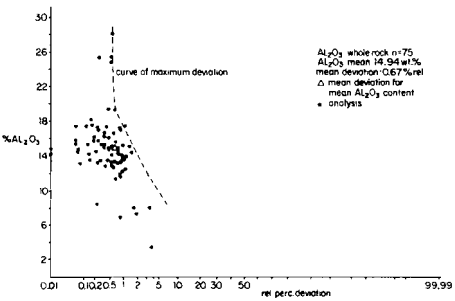
Al2O3 whole rock n=75
Al2O3 mean 14.94 wt%
mean deviation 0.67% rel
Δ mean deviation for mean Al2O3 content
• analysis
curve of maximum deviation
%Al2O3
rel perc deviation

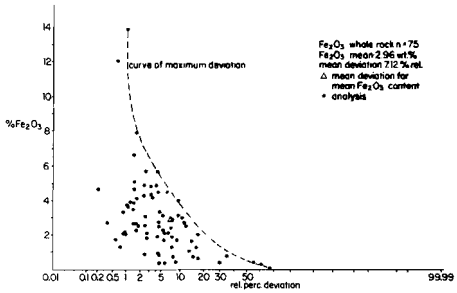
Fe2O3 whole rock n=75
Fe2O3 mean 2.96 wt%
mean deviation 7.12% rel.
Δ mean deviation for mean Fe2O3 content
• analysis
curve of maximum deviation
%Fe2O3
rel perc deviation

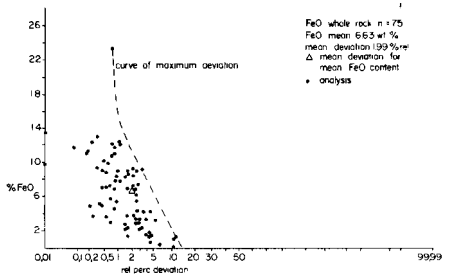
FeO whole rock n=75
FeO mean 6.63 wt %
mean deviation 1.99% rel
Δ mean deviation for mean FeO content
• analysis
curve of maximum deviation
%FeO
rel perc deviation

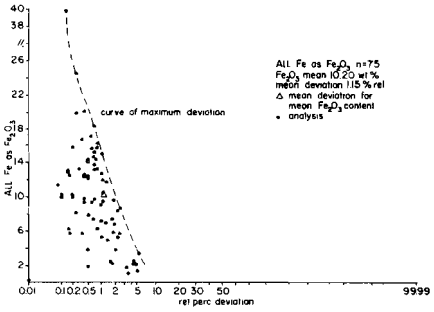
ALL Fe as Fe2O3 n=75
Fe2O3 mean 10.20 wt%
mean deviation 1.15% rel
Δ mean deviation for mean Fe2O3 content
• analysis
curve of maximum deviation
ALL Fe as Fe2O3
rel perc deviation

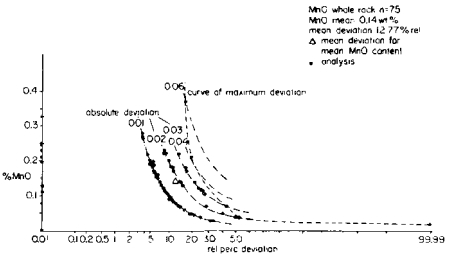
MnO whole rock n=75
MnO mean: 0.14 wt%
mean deviation 12.77% rel
Δ mean deviation for mean MnO content
• analysis
curve of maximum deviation
absolute deviation
%MnO
rel perc deviation

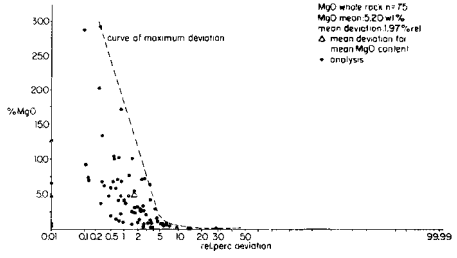
MgO whole rock n=75
MgO mean 5.20 wt%
mean deviation 1.97% rel
Δ mean deviation for mean MgO content
• analysis
curve of maximum deviation
%MgO
rel perc deviation

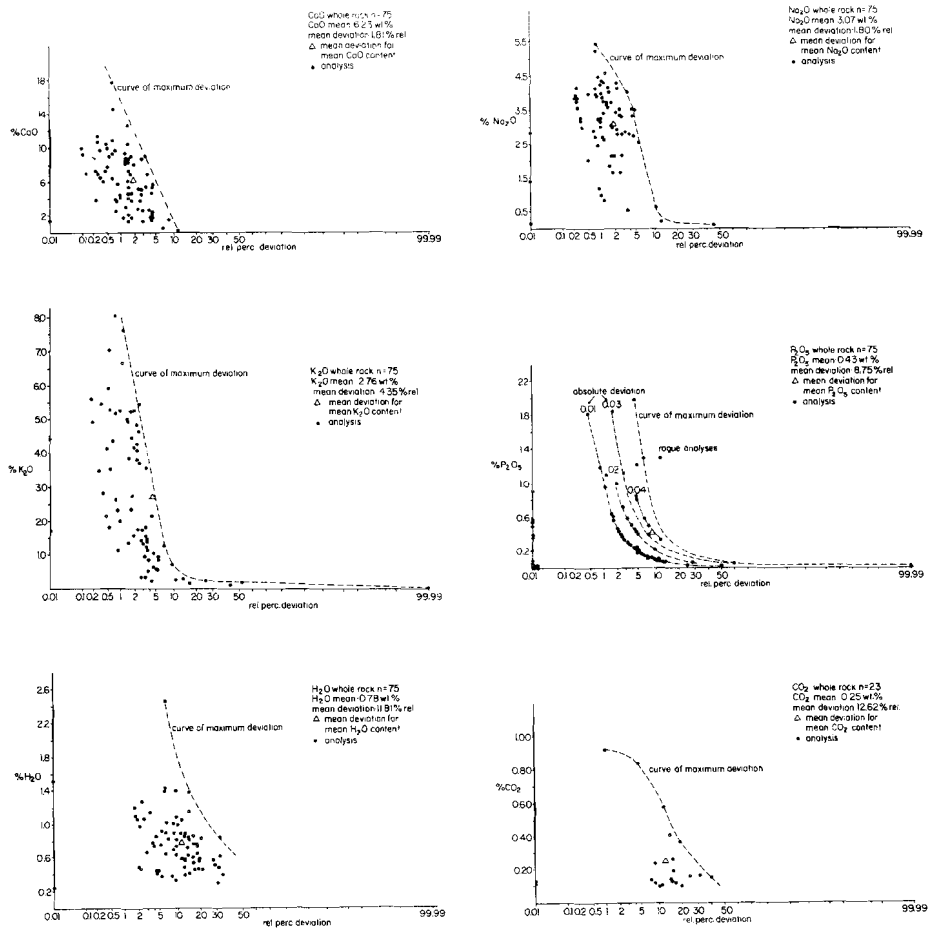

Figure III.4.: Relative percentage deviation versus oxide percentage. The "curve of maximum deviation" connects the highest values of deviation found for certain oxide percentages, it is very subjective. The MnO-curve shows clearly that the rel.perc. deviation diminishes with increasing MnO-content, even though the absolute deviation on the curve of maximum deviation increases. These graphs make it possible to compare the results of various laboratories. Each point is the result of 2 analyses of one sample. Mean deviation is derived from fig. III.3.

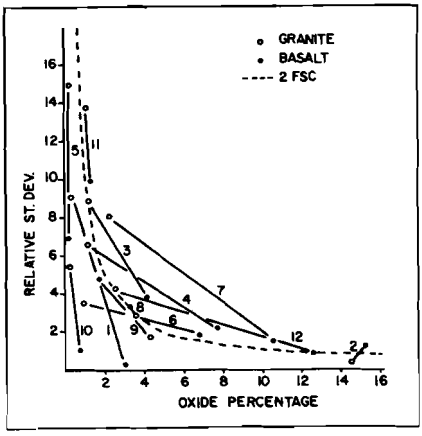

Figure III.5. : Modified version of fig.III.2 to determine the significance of the second figure behind the decimal point. 1: TiO_2; 2: Al_2O_3; 3:Fe_2O_3; 4: FeO; 5: MnO; 6: MgO; 7: CaO; 8: Na_2O; 9: K_2O; 10: P_2O_5; 11: H_2O^+; 12: all Fe as Fe_2O_3.

III.2.4. : Results

In table III.3, the means of the whole rock duplicate analyses are given with two figures behind the decimal point, because it is the normal routine of the laboratory, and because they are needed for statistical calculations. However, one should be very careful in using these second figures behind the decimal point, especially for Fe_2O_3, CaO and H_2O.

In fig. III.6 it is possible to place a certain sample value quickly in the general picture of this collection. It also gives an indication of the differences between samples from igneous parts (shaded) and samples from migmatitic areas (rest of the histogram). Extraordinary values are immediately recognized (e.g. Al_2O_3-content of A 037).

H_2O-determinations of samples rich in hydrous minerals are too low because no flux was used in the Penfield method. This can be seen from fig. III.7. From 0-50% hydrous minerals, or 0-42% amphibole, the whole rock total varies around 100%. Above 50% hydrous minerals, or 42% amphibole, all totals are less than 100%. This error becomes $\pm$ 2% at 90% hydrous minerals.

III.3. : Niggli value calculation.

According to the description of Burri (op.cit); H_2O, F and CO_2 are not incorporated in the Q, L and M values. Decimals are omitted in most of the values because they are not significant. See table III.4.

WHOLE ROCK ANALYSES

	A 037 B	A 128	A 168	B 016	B 118 L	B 254	B 322	D 172 B	D 172 D	D 307	D 442	D 444	E 067	E 125
SiO_2	39.87	40.98	83.39	47.37	66.67	41.22	23.90	58.91	54.56	52.30	47.35	44.51	65.28	43.64
TiO_2	.98	1.28	.21	4.14	.99	4.11	12.32	1.37	1.76	.53	1.07	2.95	1.08	3.46
Al_2O_3	24.95	15.25	8.50	14.21	13.43	15.09	8.16	14.84	15.27	17.48	16.33	15.19	13.60	13.62
Fe_2O_3	4.18	4.89	.03	2.41	3.47	5.19	13.91	3.36	3.64	.84	3.12	3.38	1.88	7.95
FeO	5.15	11.02	.19	12.47	3.36	13.44	23.31	5.71	7.01	7.80	9.13	12.09	4.67	10.78
MnO	.11	.18	.00	.19	.11	.22	.37	.13	.12	.14	.20	.19	.10	.25
MgO	4.64	10.06	.14	3.71	.94	6.75	7.55	3.24	4.03	7.20	7.04	6.28	.94	5.98
CaO	17.73	10.83	.17	7.32	2.86	9.05	8.07	6.09	6.53	9.06	8.73	8.56	2.52	10.59
Na_2O	.24	1.20	.15	3.60	3.07	2.64	.55	4.14	3.98	2.99	3.05	3.17	3.69	2.46
K_2O	.24	1.40	7.64	1.58	4.35	.93	.30	1.34	1.44	.60	2.12	1.39	4.86	.27
P_2O_5	.18	.09	.02	1.82	.27	.81	1.31	.40	.57	.11	.24	.34	.40	.60
H_2O^+	1.27	.90	.33	.92	.25	1.03	.46	.39	.65	.72	.86	1.16	.59	.56
H_2O^-	.15	.15	.04	.10	.09	.16	.11	.07	.15	.13	.23	.20	.19	.18
CO_2	.24	.00	.00	.84	.00	.00	.00	.00	.00	.16	.00	.00	.10	.00
F	.05	.48	.07	.35	.09	.24	.86	.15	.25	.17	.37	.18	.12	.13
Sum	99.98	99.21	100.88	101.03	99.95	100.88	101.18	100.14	99.96	100.23	99.84	99.59	100.02	100.47
-F=0	.02	.20	.03	.15	.04	.10	.36	.06	.11	.07	.16	.08	.05	.05
Total	99.96	99.01	100.85	100.88	99.91	100.78	100.82	100.08	99.85	100.16	99.68	99.51	99.97	100.42
Total Fe as Fe_2O_3	9.90	17.12	.24	16.25	7.20	20.11	39.79	9.69	11.42	9.30	13.26	16.80	7.06	19.91

	E 128	E 131	E 167	F 170	E 232 B	F 005	F 043	F 052 D	F 052 L	F 070	F 074	F 107 D	F 107 B	F 126
SiO_2	40.35	35.07	67.80	49.66	57.37	62.63	59.71	52.49	65.39	63.55	49.14	53.45	56.26	54.49
TiO_2	.73	2.85	.72	1.42	1.20	.85	1.88	1.89	.50	1.40	3.56	3.05	2.69	3.14
Al_2O_3	7.51	19.38	13.58	14.83	19.32	15.40	13.80	14.51	13.62	14.35	15.90	13.32	13.38	14.14
Fe_2O_3	2.64	12.05	2.12	2.09	3.86	2.58	5.74	3.97	1.34	2.78	4.69	4.83	4.38	4.74
FeO	11.89	11.16	3.76	9.12	3.64	2.80	4.19	4.93	2.32	3.68	7.73	8.36	7.28	7.28
MnO	.18	.33	.08	.17	.08	.07	.13	.19	.08	.10	.16	.18	.15	.15
MgO	29.33	7.04	.26	6.32	.86	2.34	2.00	4.70	2.28	1.57	4.27	3.05	2.57	3.27
CaO	4.04	9.25	1.81	9.75	4.61	3.87	4.23	5.80	3.02	3.90	5.54	6.48	6.08	5.59
Na_2O	.99	.68	3.87	3.56	4.31	4.87	3.79	2.89	2.70	3.76	4.05	3.02	3.19	3.35
K_2O	.21	.18	5.22	.97	3.49	3.80	2.75	5.60	6.68	3.52	1.71	2.02	2.34	1.87
P_2O_5	.05	.40	.12	.10	.21	.30	.85	1.01	.45	.58	.62	1.31	1.19	.96
H_2O^+	1.52	.90	.37	1.43	.89	.85	.63	1.19	.83	.74	2.47	.38	.37	1.07
H_2O^-	.16	.14	.07	.15	.20	.12	.14	.08	.06	.06	.13	.24	.09	.13
CO_2	.20	.00	.00	.00	.12	.00	.00	.00	.00	.00	.00	.13	.12	.00
F	.05	.15	.08	.36	.08	.18	.33	.48	.33	.28	.35	.31	.34	.34
Sum	99.85	99.58	99.86	100.02	100.24	99.66	100.17	99.93	99.60	100.27	100.32	100.13	100.43	100.52
-F=0	.02	.06	.03	.15	.03	.08	.14	.20	.14	.12	.15	.13	.14	.14
Total	99.83	99.52	99.83	99.87	100.21	99.58	100.03	99.73	99.46	100.15	100.17	100.00	100.29	100.38
Total Fe as Fe_2O_3	15.84	24.43	6.29	12.21	7.90	5.68	10.38	9.44	3.91	6.86	13.27	12.46	14.11	12.82

	F 252	F 507	F 502	F 503	H 047 B	H 050	H 307	H 325	H 415	J 119	L 143	M 101	N 041 B	N 264
SiO_2	66.18	59.29	55.74	55.09	59.63	57.61	44.53	47.03	46.95	50.11	53.31	48.62	49.53	54.95
TiO_2	.60	1.04	.56	.48	1.27	1.59	1.83	.99	2.03	1.57	.08	3.47	.27	1.82
Al_2O_3	15.89	17.76	25.53	25.74	16.18	15.73	17.19	17.42	13.83	14.85	28.28	14.50	6.99	14.11
Fe_2O_3	1.68	3.64	.40	.41	3.07	4.55	4.53	2.49	4.19	2.08	.38	6.65	1.33	3.01
FeO	1.58	3.43	1.33	1.38	2.87	3.22	8.42	8.55	9.49	9.75	.65	5.39	10.16	4.18
MnO	.04	.05	.03	.03	.12	.09	.27	.20	.22	.21	.02	.14	.27	.11
MgO	1.46	.77	.82	1.01	2.67	2.92	6.79	10.06	6.92	6.75	.78	4.79	17.27	2.77
CaO	2.79	3.79	8.57	8.28	4.58	5.15	9.78	10.00	8.96	10.45	11.52	7.04	6.98	5.13
Na_2O	3.75	3.96	5.44	5.21	3.88	3.76	2.55	2.16	3.53	2.93	4.49	3.29	.84	2.77
K_2O	4.66	4.13	.72	.89	4.09	3.70	2.16	.14	1.29	.58	.28	2.81	2.36	5.44
P_2O_5	.23	.40	.05	.04	.51	.63	.34	.08	.47	.22	.00	1.99	.00	1.22
H_2O^+	.47	.73	.74	.86	.57	.48	.83	.56	.84	.61	.63	.83	.84	1.08
H_2O^-	.14	.15	.10	.15	.23	.11	.09	.19	.29	.13	.16	.13	.15	.44
CO_2	.12	.26	.19	.10	.00	.12	.00	.00	.00	.00	.00	.00	.16	.13
F	.12	.14	.01	.02	.19	.32	.76	.12	.77	.15	.01	.68	.85	.90
Sum	99.71	99.54	100.23	99.69	99.86	99.98	100.07	99.99	99.78	100.39	100.59	100.33	98.00	99.66
-F=0	.05	.06	.00	.01	.08	.14	.32	.05	.32	.06	.00	.29	.36	.21
Total	99.66	99.48	100.23	99.68	99.78	99.84	99.75	99.94	99.46	100.33	100.59	100.04	97.64	99.45
Total Fe as Fe_2O_3	3.43	7.44	1.87	1.94	6.25	8.12	13.87	11.98	14.72	12.90	1.09	12.63	12.61	7.64

Table III.3.: Means of whole rock duplicate analyses. A correction is made for fluorine on oxygen positions, according to Deer, Howie and Zussman (1974), p.517 : -F=O equals (16/38)xF.

WHOLE ROCK ANALYSES

	N 317	N 337	N 402	N 528 B	N 572 L	N 572 D	N 809	N 827	O 100	P 097	P 248	P 303	P 580 B	R 227
SiO_2	43.21	49.63	70.54	54.67	43.30	49.51	47.62	57.94	49.39	68.99	66.75	49.43	50.91	52.66
TiO_2	2.31	2.41	.31	2.08	1.46	.16	1.76	1.21	.60	.23	.72	1.22	.23	3.03
Al_2O_3	12.53	13.82	12.89	14.73	11.59	3.59	8.03	17.88	16.09	15.13	14.67	14.98	17.03	12.83
Fe_2O_3	5.75	4.96	.77	1.26	2.11	1.84	2.52	4.00	.40	.46	2.62	2.69	2.00	1.75
FeO	11.33	9.23	2.86	11.84	9.93	12.39	8.80	4.25	8.92	1.74	2.11	8.28	6.87	12.01
MnO	.21	.25	.04	.22	.14	.23	.13	.11	.15	.07	.09	.23	.18	.17
MgO	9.19	4.81	.71	1.29	20.41	28.71	13.42	.85	10.36	.51	.90	7.44	10.13	2.75
CaO	9.52	8.38	1.82	4.75	7.35	1.50	12.79	3.88	10.05	1.76	2.08	8.65	7.94	5.64
Na_2O	2.01	3.55	3.28	4.35	1.40	.11	1.67	4.06	1.62	4.15	2.82	3.45	2.70	4.30
K_2O	1.45	1.55	5.43	4.13	.36	.05	.84	4.42	.63	4.93	5.93	1.75	1.06	2.67
P_2O_5	.44	.51	.14	.72	.02	.00	.01	.44	.02	.08	.21	.18	.00	1.85
H_2O^+	1.41	.77	.29	.54	1.09	.86	.49	.67	1.14	.44	.42	1.02	.97	.44
H_2O^-	.08	.16	.12	.07	.16	.11	.14	.15	.14	.07	.11	.16	.15	.11
CO_2	.00	.00	.00	.00	.14	.00	.00	.10	.00	.15	.00	.13	.00	.37
F	.34	.33	.09	.16	.04	.00	.73	.13	.17	.13	.09	.57	.13	.41
Sum	99.78	100.36	99.19	100.79	99.50	99.06	98.95	99.89	99.68	98.84	99.52	100.19	100.30	100.98
-F=O	.14	.14	.04	.07	.02	.00	.31	.05	.07	.05	.04	.24	.05	.17
Total	99.64	100.22	99.15	100.72	99.48	99.06	98.64	99.84	99.61	98.79	99.48	99.95	100.25	100.81
Total Fe as Fe_2O_3	18.32	15.20	3.94	14.40	13.13	15.59	12.28	8.72	10.29	2.39	4.96	11.88	9.62	15.08

	R 229	R 269	R 356	R 668	V 147	V 187	V 276	V 277	V 363	W 012 D	W 017 B	W 162 D	W 196 B	W 217
SiO_2	58.57	54.80	68.51	64.04	73.58	48.98	76.38	62.79	66.66	54.56	58.14	63.85	55.83	72.11
TiO_2	1.29	1.66	.59	.51	.27	1.76	.02	.22	.94	.71	.83	1.07	2.14	.35
Al_2O_3	15.45	17.22	13.34	17.53	13.20	13.26	12.16	18.25	14.25	15.40	15.85	15.57	12.01	14.00
Fe_2O_3	1.05	1.89	1.61	.28	.75	1.72	.85	.87	2.03	2.34	2.28	2.05	4.30	.71
FeO	7.33	6.84	3.72	2.05	1.27	12.88	.46	1.12	2.91	7.13	5.52	3.29	8.97	1.59
MnO	.17	.12	.07	.04	.06	.27	.05	.05	.11	.20	.17	.07	.16	.05
MgO	1.05	1.46	.22	.40	.20	5.97	.07	.20	1.05	5.59	4.04	1.51	3.76	.57
CaO	3.81	4.79	1.62	1.82	1.34	9.29	.59	1.69	2.73	6.93	6.85	2.62	7.39	1.39
Na_2O	4.26	4.58	3.75	4.18	2.78	2.17	2.79	3.91	3.42	3.65	3.56	4.01	2.15	2.89
K_2O	4.91	3.58	5.25	7.06	4.98	1.14	5.19	8.06	4.27	1.76	1.27	3.84	.52	5.28
P_2O_5	.57	.92	.12	.11	.07	.40	.00	.60	.37	.10	.20	.50	1.12	.10
H_2O^+	.46	.75	.41	.51	.69	1.40	.56	.64	.46	.77	.89	.75	1.06	.61
H_2O^-	.12	.09	.12	.10	.11	.16	.12	.14	.14	.12	.15	.15	.24	.14
CO_2	.92	.41	.00	.00	.00	.00	.00	.00	.00	.00	.00	.00	.00	.00
F	.15	1.02	.09	.15	.04	.30	.46	.17	.23	.37	.12	.26	.35	.13
Sum	100.11	100.13	99.42	98.78	99.34	99.70	99.70	98.71	99.57	99.63	99.87	99.54	100.00	99.92
-F=O	.06	.43	.04	.06	.02	.13	.19	.07	.10	.16	.05	.11	.15	.05
Total	100.05	99.70	99.38	98.72	99.32	99.57	99.51	98.64	99.47	99.47	99.82	99.43	99.85	99.87
Total Fe as Fe_2O_3	9.18	9.48	5.74	2.55	2.15	15.89	1.36	2.11	5.26	10.15	8.40	5.71	14.25	2.47

	W 226 D	W 226 L	Y 055	Y 128	Y 131
SiO_2	45.93	51.51	63.18	62.81	57.77
TiO_2	.68	.66	.60	.46	.58
Al_2O_3	11.54	11.71	17.26	16.68	16.85
Fe_2O_3	2.94	2.54	.62	2.73	3.14
FeO	8.91	6.83	4.83	2.34	6.21
MnO	.19	.19	.11	.12	.22
MgO	12.60	7.09	2.06	.41	.26
CaO	10.88	14.62	5.31	2.30	4.32
Na_2O	1.83	2.81	3.26	4.14	3.32
K_2O	1.14	.31	1.81	5.25	4.46
P_2O_5	.28	.22	.15	.07	.15
H_2O^+	1.00	.48	.56	1.20	1.01
H_2O^-	.10	.14	.11	.20	.13
CO_2	.00	.00	.00	.00	.58
F	.53	.08	.04	.02	.02
Sum	98.55	99.19	99.91	98.73	99.02
-F=O	.22	.03	.02	.01	.01
Total	98.33	99.15	99.89	98.72	99.01
Total Fe as Fe_2O_3	12.83	10.12	5.97	5.32	10.03

Table III.3. : continued.

	si	al	fm	c	alk	h_2o	f	co_2	ti	p	k	mg	w	Q	L	M	°	r	b	T	t
											100 x								100 x		
A 037 B	82	30	30	39	1	8.7	0.3	0.7	1.5	0.2	40	48	42	28.4	43.5	28.2	95	23	35	29	-10
A 128	84	17	56	23	4	6.0	3.0	0.0	2.6	0.1	43	54	29	19.7	31.9	48.4	62	14	45	13	-10
A 165	789	47	4	2	47	10.2	4.1	0.0	1.5	0.1	97	54	13	70.1	28.9	1.0	0	26	30	0	-02
B 015	122	22	46	20	12	7.9	2.8	2.9	8.1	2.0	23	31	15	25.8	36.5	37.6	30	15	21	10	-10
B 116 L	382	34	29	13	24	3.6	1.2	0.0	3.0	0.5	48	20	48	49.0	39.1	12.0	12	7	17	10	-03
B 254	86	19	54	21	7	7.3	1.7	0.0	6.5	0.7	19	40	26	19.9	34.8	45.2	48	10	32	12	-09
B 322	43	9	75	16	1	2.8	4.9	0.0	16.7	1.0	26	27	35	0.3	17.3	82.3	74	6	22	8	-08
D 172 D	153	25	42	20	13	6.1	2.2	0.0	3.7	0.7	20	41	32	34.7	39.3	26.1	31	11	33	12	-08
D 307	126	25	44	23	8	5.8	1.3	0.6	1.0	0.1	12	59	9	32.9	37.8	29.4	52	12	51	17	-06
D 442	108	22	47	21	10	6.6	2.6	0.0	1.8	0.2	31	51	23	25.0	39.2	35.6	38	15	42	12	-09
D 444	101	20	50	21	9	8.7	1.2	0.0	5.0	0.3	23	42	20	22.6	37.1	40.2	39	13	33	11	-10
E 067	270	33	28	11	28	8.2	1.5	0.5	3.5	0.8	46	20	27	45.7	41.8	12.6	9	10	16	5	-06
E 125	95	17	52	25	6	4.0	0.9	0.0	5.6	0.5	7	37	40	23.1	30.7	46.2	52	16	28	11	-14
E 128	61	7	85	7	2	7.7	0.3	0.5	0.8	0.0	11	78	17	8.8	14.6	76.6	61	2	76	5	-02
E 131	68	22	56	19	2	5.8	0.9	0.0	4.2	0.3	15	36	49	19.3	32.4	48.1	85	0	28	19	00
E 167	305	36	24	9	32	5.7	1.1	0.0	2.4	0.3	47	7	34	47.8	42.8	9.4	6	13	5	4	-05
E 170	118	21	45	25	10	11.3	2.7	0.0	2.6	0.2	15	50	17	27.8	36.4	35.7	36	22	38	11	-14
E 232 B	191	38	24	16	21	9.8	0.8	0.6	3.0	0.3	35	17	48	38.7	49.4	11.9	26	0	11	19	+01
F 005	230	33	29	15	23	10.4	2.0	0.0	2.4	0.4	39	45	45	43.3	43.2	13.5	19	10	36	10	-05
F 043	206	28	38	16	19	7.3	3.5	0.0	5.0	1.2	32	27	55	41.3	38.9	19.8	20	5	22	9	-05
F 052 D	148	24	40	18	18	13.0	4.2	0.0	4.1	1.2	56	49	42	29.6	42.5	27.9	15	14	36	6	-12
F 052 L	266	33	26	13	28	11.2	4.2	0.0	1.5	0.7	62	53	34	45.1	42.2	12.6	8	17	39	5	-08
F 070	243	32	29	16	23	9.4	3.4	0.0	4.1	0.9	38	31	41	45.0	40.7	14.1	18	9	23	9	-07
F 074	133	26	45	16	14	22.3	2.9	0.0	7.3	0.7	22	39	35	29.4	41.7	28.9	30	4	32	12	-04
F 107 D	155	23	45	20	12	3.7	2.8	0.5	6.6	1.6	31	30	34	35.4	35.0	29.5	30	8	22	11	-09
F 126	163	25	44	18	13	10.6	3.2	0.0	7.0	1.3	27	33	37	36.4	36.9	26.6	30	5	26	12	-06
F 252	278	39	20	13	28	6.6	1.5	0.8	2.0	0.4	45	45	49	47.7	44.6	7.6	17	0	39	11	-02
F 501	215	38	25	14	23	8.9	1.5	1.3	2.8	0.7	41	17	49	41.0	47.0	11.9	21	0	8	15	+01
F 502	171	46	8	28	18	7.5	0.1	0.7	1.3	0.1	8	45	21	39.4	56.2	4.5	44	0	29	28	00
F 503	169	47	9	27	17	8.8	0.2	0.4	1.1	0.1	11	51	21	39.3	55.1	5.5	44	0	18	30	+03
H 047 B	202	32	30	17	22	6.5	2.0	0.0	3.2	0.7	41	45	49	39.4	44.8	15.9	20	10	35	10	+07
H 050	184	30	34	18	19	5.2	3.3	0.6	3.8	0.9	40	41	36	37.4	43.3	19.2	21	10	32	11	-07
H 307	98	22	46	23	9	6.1	5.3	0.0	3.1	0.3	36	49	33	23.3	39.8	37.0	45	14	39	13	-10
H 325	99	22	51	23	5	3.9	0.8	0.0	1.5	0.1	4	82	21	27.2	34.7	38.0	64	9	55	17	-06
H 415	108	19	50	22	10	6.5	5.7	0.0	3.4	0.5	19	48	28	24.0	35.5	40.6	31	18	36	9	-13
J 119	116	20	46	26	8	4.7	1.1	0.0	2.8	0.2	11	50	16	29.1	33.7	37.2	46	20	40	14	-12
L 143	151	47	6	35	12	5.9	0.1	0.0	0.7	0.0	4	58	34	39.2	57.8	3.0	57	6	53	34	-01
M 101	129	23	44	20	13	7.3	5.7	0.0	6.8	2.2	36	43	53	28.3	38.9	32.9	26	7	31	10	-10
N 041 B	100	8	72	15	5	5.7	5.5	0.5	0.4	0.0	64	23	11	23.1	18.2	58.7	28	14	62	3	-12
N 264	184	28	34	18	20	12.0	5.2	0.6	4.6	1.7	56	41	40	36.2	42.7	21.3	15	12	29	8	-10
N 317	90	15	57	21	6	9.7	2.7	0.0	3.6	0.4	32	49	31	20.2	29.7	50.2	44	15	39	9	-12
N 337	123	20	47	22	11	6.4	2.5	0.0	4.5	0.5	22	38	33	27.7	36.6	36.2	29	18	28	9	-13
N 402 F	346	38	20	9	33	4.7	1.5	0.0	1.2	0.3	52	26	20	52.0	40.5	7.4	7	15	20	5	-04
N 528 D	163	26	39	15	20	5.4	1.4	0.0	4.6	0.9	39	15	9	31.4	44.0	24.7	12	14	11	6	-09
N 572 L	76	12	71	14	3	6.5	0.2	0.3	1.9	0.0	15	75	16	17.0	23.0	59.9	62	6	20	9	-05
N 572 D	85	4	93	3	0	4.9	0.0	0.0	0.2	0.0	23	78	12	20.0	5.3	74.8	83	0	22	4	+01
N 809	95	10	59	27	4	3.2	4.6	0.0	2.6	0.0	25	68	21	21.8	19.6	58.5	37	27	48	6	-21
N 827 F	197	36	27	14	23	7.6	1.4	0.4	3.1	0.6	42	16	46	38.4	48.7	13.2	21	0	12	13	-01
O 100	109	21	51	24	4	8.4	1.2	0.0	1.0	0.0	20	66	4	30.1	32.2	37.6	66	12	58	17	-07
P 097	335	43	13	9	35	7.0	2.0	0.9	0.9	0.1	44	30	20	50.4	45.9	3.8	11	5	29	8	-01
P 248	295	38	23	10	29	6.1	1.3	0.0	2.4	0.4	57	26	53	48.5	43.4	8.2	13	0	22	9	-01
P 303	116	21	47	22	10	8.0	4.2	0.4	2.1	0.2	25	55	23	26.4	37.5	36.2	33	18	43	11	-11
P 580 B	115	23	51	19	7	7.3	0.9	0.0	0.4	0.0	21	67	21	29.7	36.8	33.6	51	7	62	16	-03
R 227	150	22	44	17	17	4.1	3.8	1.4	6.5	2.2	29	26	11	30.6	38.4	31.0	13	9	19	5	-12
R 229	201	31	33	14	25	5.4	1.6	4.3	3.3	0.8	43	18	11	37.1	46.5	16.3	11	13	13	6	-08
R 269	174	32	13	16	22	8.0	9.9	1.7	4.0	1.2	34	23	20	34.6	48.2	17.3	20	5	18	10	-06
R 356	321	37	22	8	33	6.5	1.4	0.0	2.0	0.3	48	6	28	49.4	42.3	8.2	6	11	5	4	-04
R 668	272	44	11	8	37	7.1	2.0	0.0	1.5	0.3	53	23	12	42.7	53.0	4.2	9	0	19	7	-01
V 147	430	46	12	8	34	13.3	0.7	0.0	1.1	0.2	54	15	33	59.2	37.1	3.6	10	0	0	12	+04
V 187	117	18	51	24	7	11.2	2.3	0.0	3.2	0.4	26	42	11	29.5	30.9	39.6	47	17	33	11	-13
V 276	510	48	8	4	40	12.5	9.7	0.0	0.1	0.0	55	10	62	61.2	36.5	2.2	5	0	0	8	+04
V 277	267	46	8	8	38	9.2	2.3	0.0	0.8	1.0	58	15	41	41.6	53.2	5.0	6	0	0	8	00
V 363	290	37	24	13	26	6.8	3.1	0.0	3.1	0.7	46	28	38	49.2	41.3	9.5	16	2	23	11	-02
W 012 D	146	24	43	20	13	6.9	3.0	0.0	1.4	0.1	24	51	23	33.6	38.8	27.7	32	15	43	11	-09
W 017 B	174	28	37	22	13	8.8	1.1	0.0	1.8	0.3	19	48	27	40.0	38.5	21.6	37	13	39	15	-07
W 162 D	256	37	26	11	25	10.1	3.4	0.0	3.1	0.8	39	34	36	45.8	42.3	11.9	15	0	19	12	+01
W 196 B	165	21	49	23	7	10.4	3.2	0.0	4.8	1.4	15	34	30	14.2	27.9	30.9	49	9	27	14	-09
W 217	385	44	15	8	33	10.9	2.2	0.0	1.3	0.2	54	30	29	55.8	39.0	5.2	10	0	4	11	+03
W 226 D	93	14	58	23	5	6.8	3.4	0.0	1.1	0.2	29	66	23	21.9	26.4	51.7	46	19	52	9	-14
W 226 L	117	16	42	35	7	9.7	0.5	0.0	1.1	0.2	7	58	25	29.0	27.9	43.1	40	38	35	9	-26
Y 055	226	37	28	26	15	6.7	0.4	0.0	1.7	0.2	26	40	11	48.0	39.9	12.2	39	0	31	22	+02
Y 128	257	40	19	10	30	16.5	0.2	0.0	1.5	0.1	46	13	51	43.7	48.9	7.3	14	0	10	10	00
Y 131	201	35	28	16	21	11.7	0.2	2.7	1.5	0.2	47	4	31	40.1	46.6	13.2	24	6	4	14	-02

Table III.4.: Niggli values, according to Burri (1959).

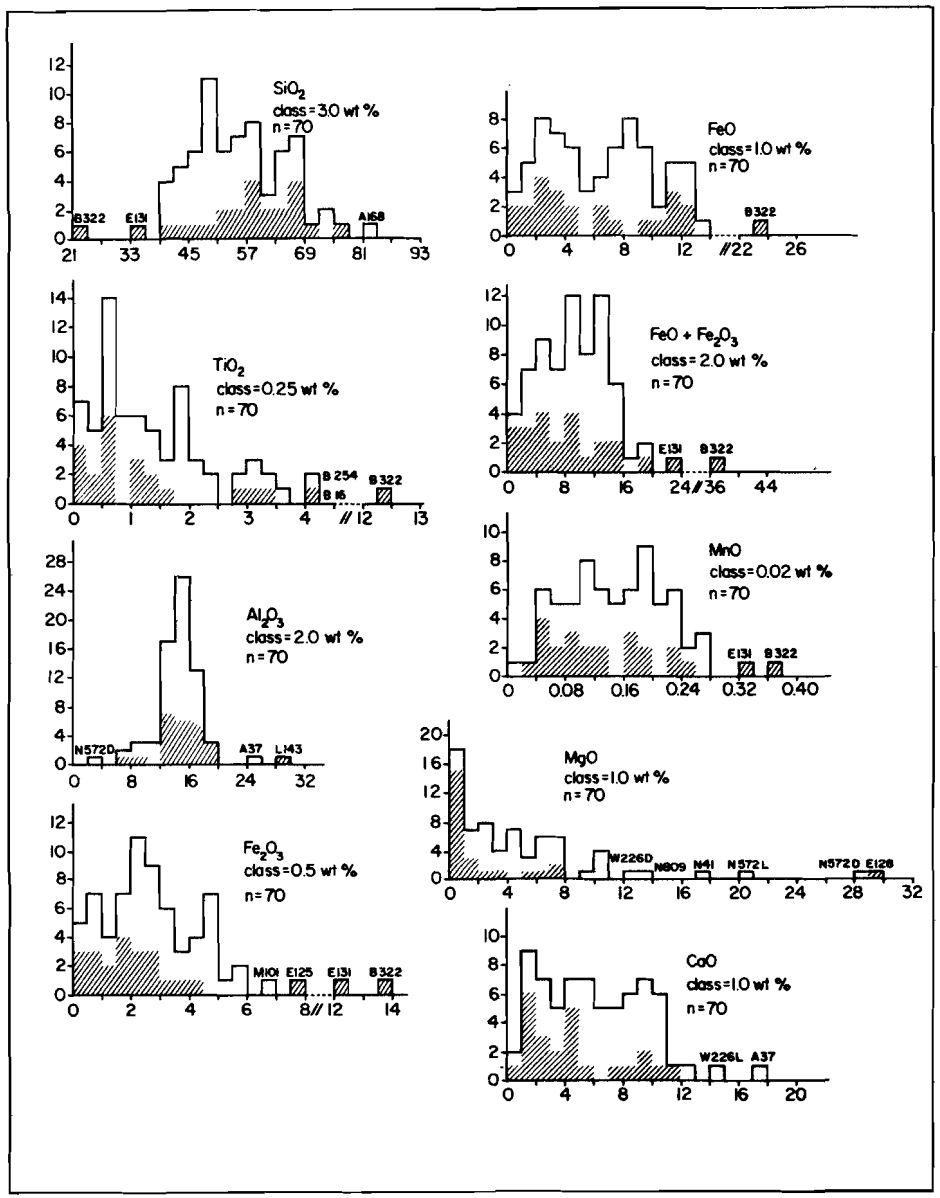

Figure III.6.: Whole rock histograms, derived from table III.3. Abscissa : oxide wt%, ordinate : number of samples. The shaded area concerns all samples from igneous complexes, i.e. the igneous rocks as well as their inclusions. The rest represents all other samples. F 501 - F 503 are not included.

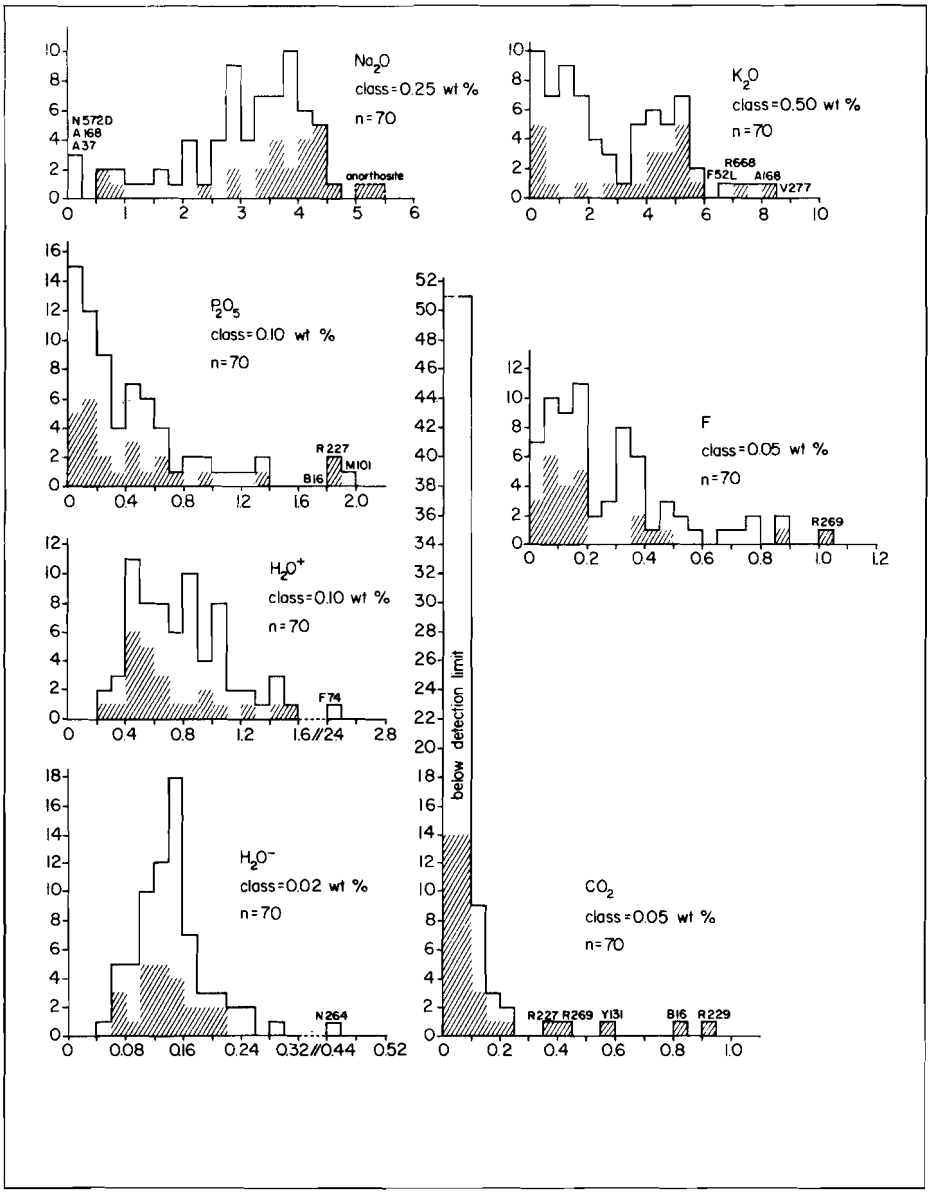

Figure III.6.: continued

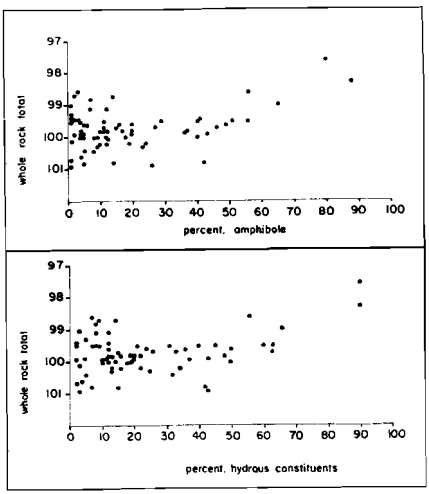

Figure III.7.: Influence of the percentage amphibole, and total of hydrous minerals on the whole rock analysis sum, because of incomplete H_2O-measurements.

III.4. : Microscopic description : general petrography.

Several types of microscopes have been used in the course of each description. General features were studied with a Leitz SM-Pol, using **Tröger's** determination tables (1969, 1971). Closer examination, if needed, was carried out with the aid of a Leitz Ortholux. Structural phenomena were observed with a Zeiss stereomicroscope. The descriptive terminology for the textures is mostly according to Moore (1970). The rock nomenclature is after Hermans et al. (1975), except for the name gabbronorite, which indicates a norite-like rock with more clinothan orthopyroxene. The rock descriptions of all samples used in this study can be found in the Appendix. Names derived by modal analysis, and microscopic description and determination are listed in table I.1. Fig. III.8 shows the QAP-triangle for M<90, with the samples given in the previous tables and the nomenclature list of Hermans et al. (op. cit).

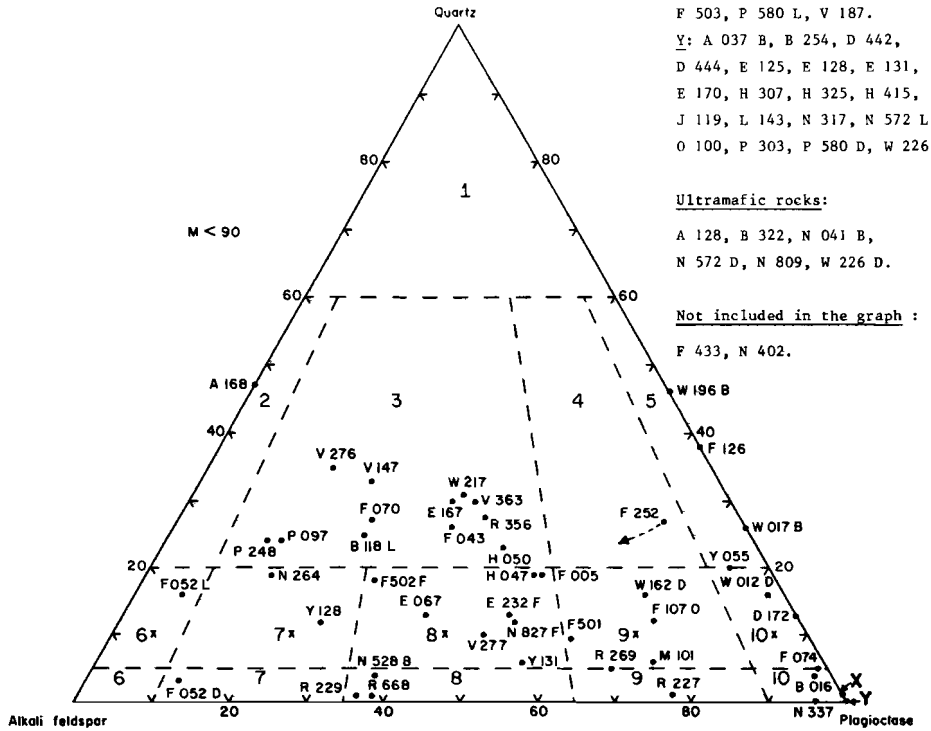

Plagioclase corner:

X: D 307, E 232 N, F 502 N, F 503, P 580 L, V 187.

Y: A 037 B, B 254, D 442, D 444, E 125, E 128, E 131, E 170, H 307, H 325, H 415, J 119, L 143, N 317, N 572 L, O 100, P 303, P 580 D, W 226 L.

Ultramafic rocks:

A 128, B 322, N 041 B, N 572 D, N 809, W 226 D.

Not included in the graph :

F 433, N 402.

Figure III.8.: Modal compositions of the rocks from this study in the QAP-diagram. F 252 is an augengneiss, the modal composition refers to the matrix, the real composition should be more in the direction of the alkalifeldspar corner.

Plutonic rocks	Charnockitic rock suite
1	1
2 alkali-feldspar granite	2 alkali-feldspar charnockite
3 granite	3 charnockite
4 granodiorite	4 charno-enderbite
5 tonalite	5 enderbite
6 alkali-feldspar syenite	6 hypersthene alkali-feldspar syenite
7 syenite	7 hypersthene syenite
8 monzonite	8 hypersthene monzonite; if mesoperthite is the main feldspar: mangerite
9 monzodiorite	9 jotunite or monzonorite
10 diorite (An<50) gabbro (An>50) anorthosite (M<10)	10 norite anorthosite (M<10)

6^{x} - 10^{x} as 6-10 with prefix quartz
Rocks with a clearly metamorphic texture received appropriate names.

IV : Investigations on the amphiboles

IV.1. : Chemical analyses.

IV.1.1. : Introduction

The amphiboles were analysed with a Geoscan electron microprobe. Fe^{2+}, H_2O and F were obtained by wet-chemical methods. Fe^{2+} was also estimated with the aid of the structural formula, and compared with the analytical data (section IV.2.4.).

IV.1.2. : Sample preparation

After splitting the jawcrusher sample (section III.2.2.), the part of the sample for amphibole analyses was sieved. Everything smaller than 0.15 mm was thrown away because of possible oxidation in the jawcrusher, the remainder was ground under a N_2-atmosphere. During a testseries, it was shown that amphiboles ground in normal atmosphere contained on an average more Fe^{3+} than the same sample ground in a N_2-atmosphere (internal report). This agrees with the findings of French and Adams (1972), who state that :
"There is little doubt that one of the largest sources of error in the determination of iron (II) oxide is the preparation of the sample before extraction". They show that the longer you grind in normal atmosphere, the higher your Fe (III) oxide is going to be. To reduce the oxidation they moist the sample with aceton during grinding.
For this study we developed a simpler method :
A Fritsch Pulverisette, type P-0150, was provided with two gastaps in its plexiglass cover. The first tap was connected with a N_2-gas cylinder, the other led to a ventilation system. Thirty seconds before grinding started, N_2-gas was led into the Pulverisette and through it to the ventilation system, so that the normal atmosphere was transformed into a N_2-atmosphere by the time the grinding started. An extra

advantage is the removal of the dust fraction during the grinding proces (if one is not interested in that fraction). Grinding products are sieved and everything between 0.15 and 0.05 mm is collected for analysis. Coarser material is ground again, the finer fraction is thrown away.

After grinding, the samples were purified by means of a LOC-separator (Laboratory Overflow Centrifuge) (IJlst, 1973-a and -b). This was done by the author under the supervision of Mr. IJlst and by courtesy of Prof. H. Priem in the Z.W.O. Laboratory for Isotope Geology, Amsterdam. Only 46 samples were treated this way. The remaining samples did not contain enough amphibole to purify, and were not analysed for Fe^{2+}, OH and F. The separation procedure also gave some information on the density of the amphiboles (table IV.1).

The number of separations needed to get a rather pure sample depends on the accompanying minerals; amphiboles from complex whole rocks, therefore, show a more accurate density value than the amphiboles from simpler host rocks. From this table IV.1 and the mg-ratio values from table IV.8 one can construct a curve for the relation : density versus mg-ratio (fig. IV.1).

Now it is possible to find a much better density value for all the Rogaland Ca-amphiboles. Halfway through the separation, the partly purified sample is washed on a 32 micron sieve. Before the washing all minerals with a density less that 3.14 were removed. This reduces the sample to be washed, especially for leuco- and mesocratic rocks. The washing is needed because the fine dust may clog the separation of small sample quantities in the centrifuge as well as in the Frantz Magnetometer, which is used repeatedly to purify the centrifuged sample to its utmost. This sequence was chosen because in this way only little sample material has to pass through the time-consuming magnetometer. At the end of the magnetic separation the samples were 95 till 100% pure.

Apart from this purification, the magnetometer also tells us something about the magnetic properties of the amphiboles. It will be difficult

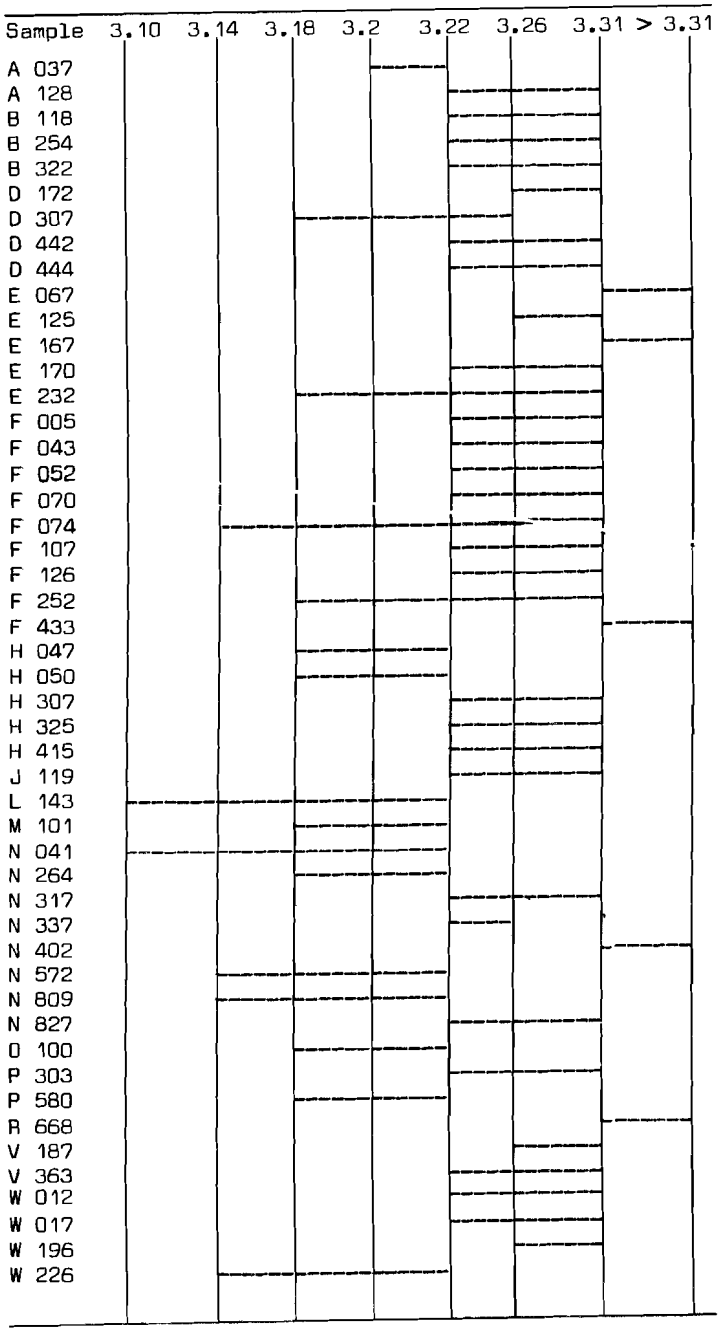

Table IV.1.: Density ranges of the Ca-amphiboles.

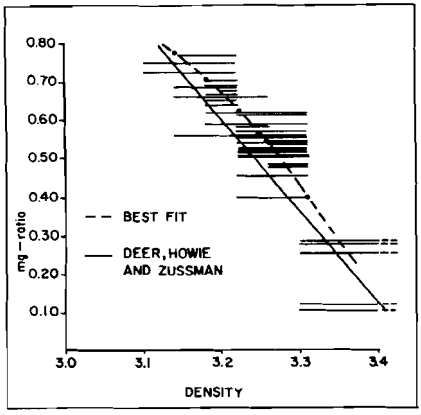

Figure IV.1. : Experimentally determined curve for the relation mg-ratio versus density (=Best fit). The line from Deer, Howie and Zussman (1974, fig.63) does not fit the Rogaland amphiboles completely. The dots represent the mg-ratio limit values for the density groups from table IV.1. A calculated straight line through these five points is: D = 3.5 - 0.457 mg; r (=correlation coefficient) = -.995.

to get exact, internationally recognisable and checkable, values, because many Frantz Magnetometers are adapted in one way or another to the special wishes of the laboratory. The figures presented in table IV.2 only have a relative significance. For technical reasons, not all separated samples are presented in this table.

From table IV.2 and table IV.8 it is possible to construct a diagram in the way fig. IV.1 was designed : fig. IV.2. Herewith we can construct a density versus ampère diagram : fig. IV.3. These diagrams may help to speed up sample preparation and purification if the microprobe determined mg-ratio is known, or to establish the approximate mg-ratio if one of the above mentioned physical properties is known. Handpicking to get every sample 100% pure was discarded as too time-consuming. The remaining impurities were identified under the microscope and the chemical analyses were corrected for them, assuming the following values as a mean for the contaminating crystals : table IV.3. These samples were used for the wet-chemical methods. Polished thin sections were prepared for the microprobe.

IV.1.3. : Geoscan electron microprobe measurements and their reliability

The Geoscan electron microprobe of the Institute of Earth Sciences, Free University , Amsterdam was used, under supervision of Dr. C. Kieft of the Research Group for Analytical Chemistry of Minerals and Rocks (WACOM), subsidized by the Netherlands Organization for the Advancement

Sample	Ampère range
B 322	0.30-0.45
F 433	0.20-0.25
N 572	0.52-0.58
N 809	0.40-0.50
N 827	0.20-0.35
O 100	0.46-0.50
P 303	0.37-0.40
P 580	0.45-0.50
R 668	0.29-0.32
V 187	0.36-0.39
V 363	0.30-0.40
W 012	0.30-0.40
W 017	0.36-0.41
W 196	0.34-0.38
W 226	0.30-0.50

Table IV.2.:
Ampère range at a tilt angle of 15°.

of Pure Scientific Research (Z.W.O.). Most of the analyses were carried out by the author, using as standards : wollastonite or diopside (Ca), corundum (Al), synthetic TiO, Fe-metal, rhodonite (Mn), olivine (Mg), orthoclase (K), albite (Na)and diopside (Si). Wollastonite, kyanite, olivine (Fe) and periclase were used as secondary standards. Accelerating potential was 20 KV. The counting time was 50 seconds for each spot, 5-6 spots were measured for each mineral. The apparent data were corrected for mass absorption, atomic number effects and fluorescence, using a modified version of a computer program by

Contamination	FeO	H_2O	F
Orthopyroxene	amph.^{x}	1/2 amph.^{x}	0.0
Clinopyroxene	amph.^{x}	1/2 amph.^{x}	0.0
Apatite	0.0	amph.^{x}	amph.^{x}
Biotite	amph.^{x}	2.5%	1.0%
Microcline	0.0	0.25%	0.0
Zoisite	0.0	1.5%	0.0
Epidote	0.0	1.0%	0.0
Hydroxides	81%	10%	0.0
Serpentine	0.0	13%	0.0
Plagioclase	0.0	0.0	0.0
Olivine	10%	0.0	0.0

amph.^{x} : same value as amphibole.

Table IV.3.: Assumed element content in weight percentages for contamination correction. All values are chosen in accordance with microscopic observations, combined with Deer, Howie and Zussman (op. cit) analyses.

Springer (1967) (Kieft and Maaskant, 1969). For Pulsrates see table IV.4. Sometimes eight rock samples were measured in one run, because each of the two polished thin sections might contain as much as four samples. This could of course only be done if enough amphibole was

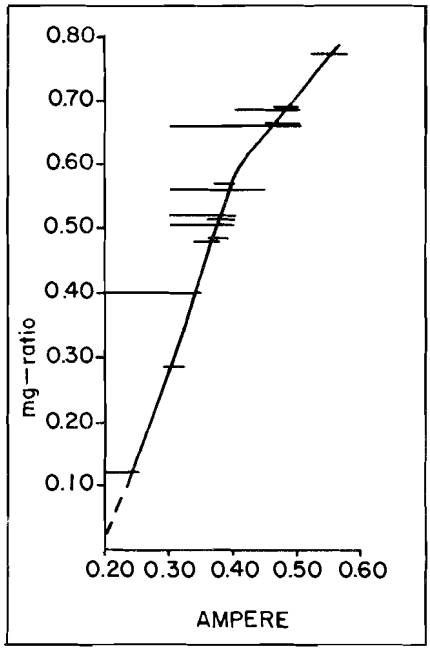

Figure IV.2.: Mg-ratio versus magnetic property.

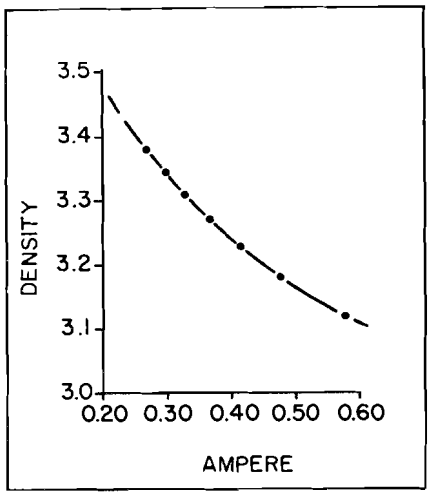

Figure IV.3.: Density versus magnetic property, a combination of fig. IV.1 and IV.2.

present in each sample. For a more extensive description of the procedures used, the reader is referred to Maaskant (1970).

Fe	100
Mg	59
Ca	351
Si	151 (PET)
Si	87 (KAP)
Al	89
Na	46
K	565
Ti	44
Mn	86

Table IV.4.: Pulsrates. Pulsrates = counts per second : element % (standards only).

The precision and reliability of the analyses can be indicated in several ways, two of which are given here. The first is a measurement of the stability of the microprobe itself, called precision by the author because it greatly depends on the stability of the machine and the skill of the operator.

$$\text{Precision in \%} = \left| \left(\frac{\text{standard counts before measurement}}{\text{standard counts after measurement}} \right) \times 50 \right| - 50$$

Example : before Fe measurement 100.000 counts, after 102.000 counts.

$$\text{Precision} = \left(\frac{100.000}{102.000} \times 50 \right) - 50 = (.9804 \times 50) - 50 = 49.02 - 50 = -0.98\%$$

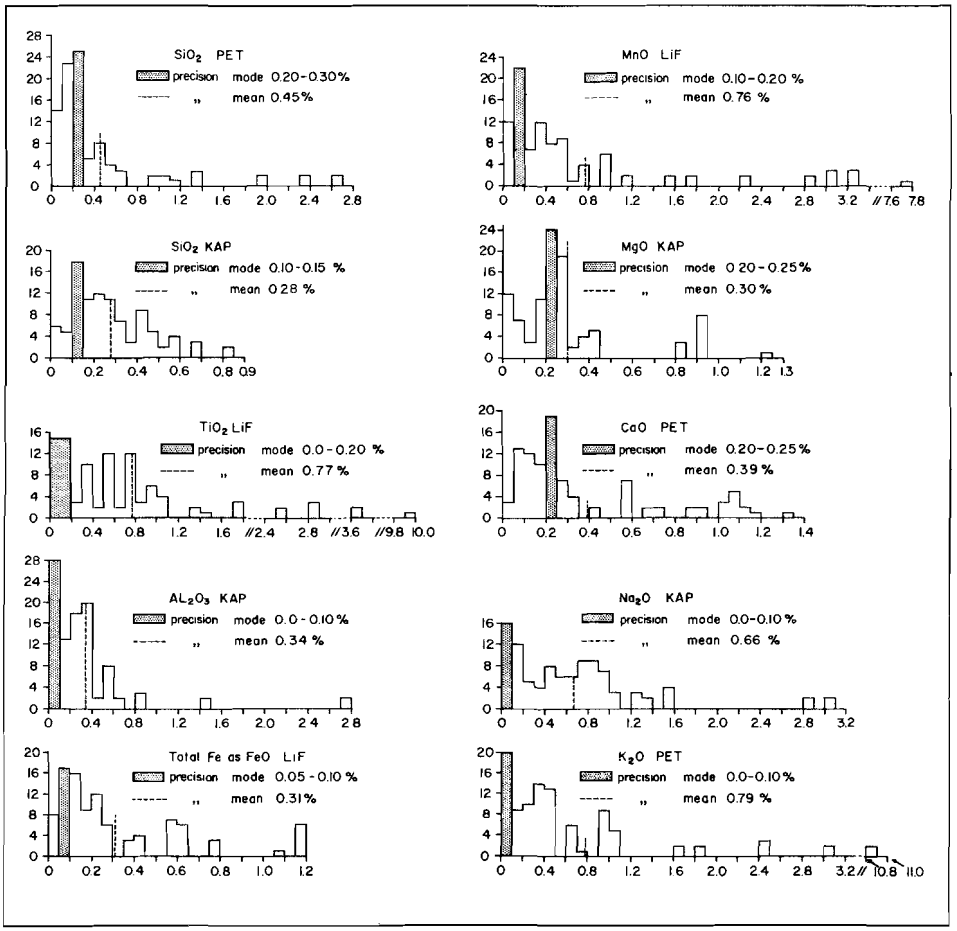

Figure IV.4. Microprobe precision in relative **percentages.** Abcis : rel. % precision, ordinate : number of samples. Compare with fig. III.3.

The minus sign can be neglected because it is not important which of the two measurements is the highest. The value is expressed in relative percentages. The precision for the oxides as measured with the various crystals (PET, KAP and LiF) is shown in fig. IV.4.
The means of all measurements are smaller than 1.00%. However, this does not mean that the amphibole measurements have an error of less than 1%. The real error range is much greater. This is shown by the second method.

The reliability of the measurements was examined with the aid of a hornblende standard considered to be homogeneous. During each run with a set of samples this amphibole-standard was measured too. This resulted in 33 to 36 standard values (in a few runs not all standard values were measured). For a homogeneous amphibole this should give a normal distribution for each element, which tallies in this case as good as can be expected with ± 35 determinations. Therefore a standard deviation can be calculated which is an expression of the reliability of the amphibole measurements. See table IV.5.

Amphibole standard		Rel.st.dev.
SiO_2	42.75%	0.85%
Al_2O_3	13.8 %	2.35%
TiO_2	1.05%	6.26%
FeO	11.6 %	1.06%
MnO	0.2 %	9.06%
MgO	14.3 %	0.96%
CaO	10.9 %	1.20%
Na_2O	2.7 %	2.67%
K_2O	.35%	5.80%

Table IV.5.: Standard amphibole analysis and the reliability of the microprobe measurements.

In accordance with section III.2.3, fig. IV.5 is constructed. It shows the dependence of the relative standard deviation on the oxide percentages of the standard amphibole. Seven points out of nine determine the relative standard deviation curve (RSDC), in accordance with Burri's statement (section III.2.3). Al and, possibly, Ti (the curve can be drawn in various ways at the left side) are more difficult to determine than the other seven elements. A reason might be their high valence in combination with their position in the amphibole structural formula as charge compensators, or probably incomplete homogeneity of the amphibole standard. It is clear that the seven elements determining the curve have no element influence on the standard deviation. Only the amount present determines the st.dev. Al and Ti have their own extra influence, which increases the st.dev. The 2 figure significance curve (2FSC) intersects the rel.st. dev. curve at approximately 6-9 oxide percents. At 10% a clear distinction of the two curves is visible. Therefore 10% may be taken as 2 figure significance point (2FSP). Above this value the second figure behind the decimal point is meaningless. Although it may be a 100%

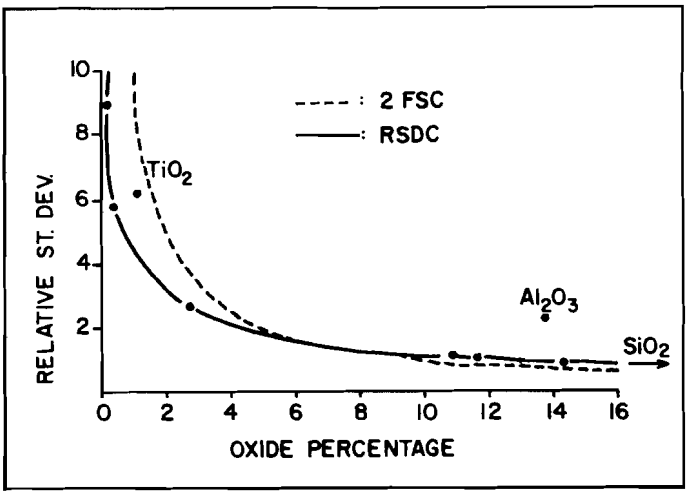

Figure IV.5.: Standard deviation determination curve for the Rogaland amphiboles. For every amount of SiO_2, MgO, FeO, CaO, Na_2O, K_2O, and MnO the rel. st.dev. can be found directly from the RSDC. Al_2O_3 and TiO_2 will have higher st.dev.'s. See also fig. III.5.

accurate, we cannot judge it to be so.

For Al_2O_3 and TiO_2 the 2FSP will be lower, but it is not possible to draw st.dev. lines for these oxides and therefore to determine the 2FSP.

The tabled amphibole oxides are given with 2 figures behind the decimal point in accordance with the whole rock analyses, but it should be clear by now that some figures should be handled with care.

IV.1.4. : Complementary laboratory measurements

Fe^{2+}, OH and F were analysed in the Vening Meinesz Laboratory, Department of Geochemistry, State University of Utrecht, under supervision and responsibility of Mr. Anten and Mr. Belle. The Fe^{2+} was determined according to the method of French and Adams (1972). This method minimizes the oxidation possibilities during the analytical process. Instead of the normal polypropylene bottle, the new bottle of Perkin Elmer can be used which is an improvement for this method. Its metal wall with thermo couple protects the sample in case of melting of the

polypropylene bottle as may sometimes happen with the conventional bottle on a sandbath. Because Fe-total is known from microprobe measurements, Fe^{3+} can be calculated.
The Penfield method was used to estimate the water content, on 0.25 gramme sample with PbO_2 as flux and SnO_2 instead of CaO to bind the fluorine. CaO gave too great a variation in the measurements, possibly because not all the fluorine could be captured. The fluorine analyses were done with the aid of an Orion specific ion meter, equipped with an ion selective fluorine electrode.

Analytical procedure : Method developed by L. Belle from the Vening Meinesz Laboratory, Department of Geochemistry.
Reagents : NaOH, Na_2CO_3, NaF, NaCl, HCL, glacial acetic acid, Titriplex^R-IV (all chemicals analytical grade).
Buffer Solution : 58 g of NaCl, 4 g of Titriplex^R-IV and 75 ml acetic acid are dissolved in 500 ml distilled water. The pH of this solution is adjusted to 5-5.5 by the addition of a NaOH solution. Then 2-5 drops of a solution of methylorange (1% in ethanol) is added and the volume is made up to 1 l in distilled water.
Standard Series : A standard series of 0, 2, 4, 6, 8, 10 $mg.l^{-1}$ F is prepared from a 1000 $mg.l^{-1}$ stock solution of F (as NaF). To 25 ml of each of these solutions 5 ml of the buffer solution is added.
Apparatus : Orion specific ion meter, model 407A; Orion F electrode, 940900; Orion reference electrode, 900100.
Procedure : Of the sample 250 mg is mixed with 3 g of Na_2CO_3 in a Pt crucible. This crucible is placed over a Meker gas burner and its content fused for 15 minutes. The crucible is then taken from the flame and carefully swirled in order to spread out the melt onto the wall. Thus cooled, the carbonate cake is leached in 40 ml hot distilled water. The solution is cooled, washed into a volumetric flask, made up to 100 ml with distilled water, and homogenized. After undissolved material is allowed to settle onto the bottom of the flask, 25 ml of the supernatant solution is pipetted into a 100 ml beaker. Addition

of about 0.25 ml concentrated HCl brings the pH down to about 6 after which 5 ml of the buffer solution is added. The F electrode and the reference electrode are placed into the stirred solution. The potentiometric signal indicated on the specific ion meter is stable after 3-5 minutes. The measured value is interpolated in the calibration curve, obtained by analogous measurement of the standard series.

To calculate the error of the FeO and F measurements (H_2O has no duplicates) a formula for standard deviation from Tooms (1959) can be used :

$$s = \sqrt{\frac{\sum d^2}{2n}}$$ (d = deviation from the mean of the duplicates, n = total number of sample)

If the distribution is normal, 68 percent of the samples will fall within a range of one standard deviation at both sides of the mean. If not, the distribution is not normal and the s-value may not be used. For FeO and F these percentages are 86 and 80 respectively, so that in these cases the relative mean deviations are preferred, fig. IV.6, although it has been stated before (section III.2.3) that it is a very poor indicator.

The 2FSP-values for FeO and F are $\pm$ 8% and 3% respectively. Fe_2O_3 is obtained by subtraction of the microprobe FeO-value and the wet chemical FeO-value, and is therefore less precise. The error will probably vary between 0 and 5% relative. A 2FSP of 5% seems reasonable, although it can not be proved statistically.

(Fe_2O_3 = (FeO-probe - FeO-wet) x 1.11)

H_2O is the most problematic determination, no estimation of the error can be made on experimental grounds for the values presented here. No duplicates were made, because of shortage of material. According to the laboratory, the values might be up to 20 percent too low for the following reasons :

1 : it is very difficult, if not impossible, to remove all crystal-water from the sample by heating,

2 : it is not easy to precipitate all liberated water in the widening of the Penfield tube.

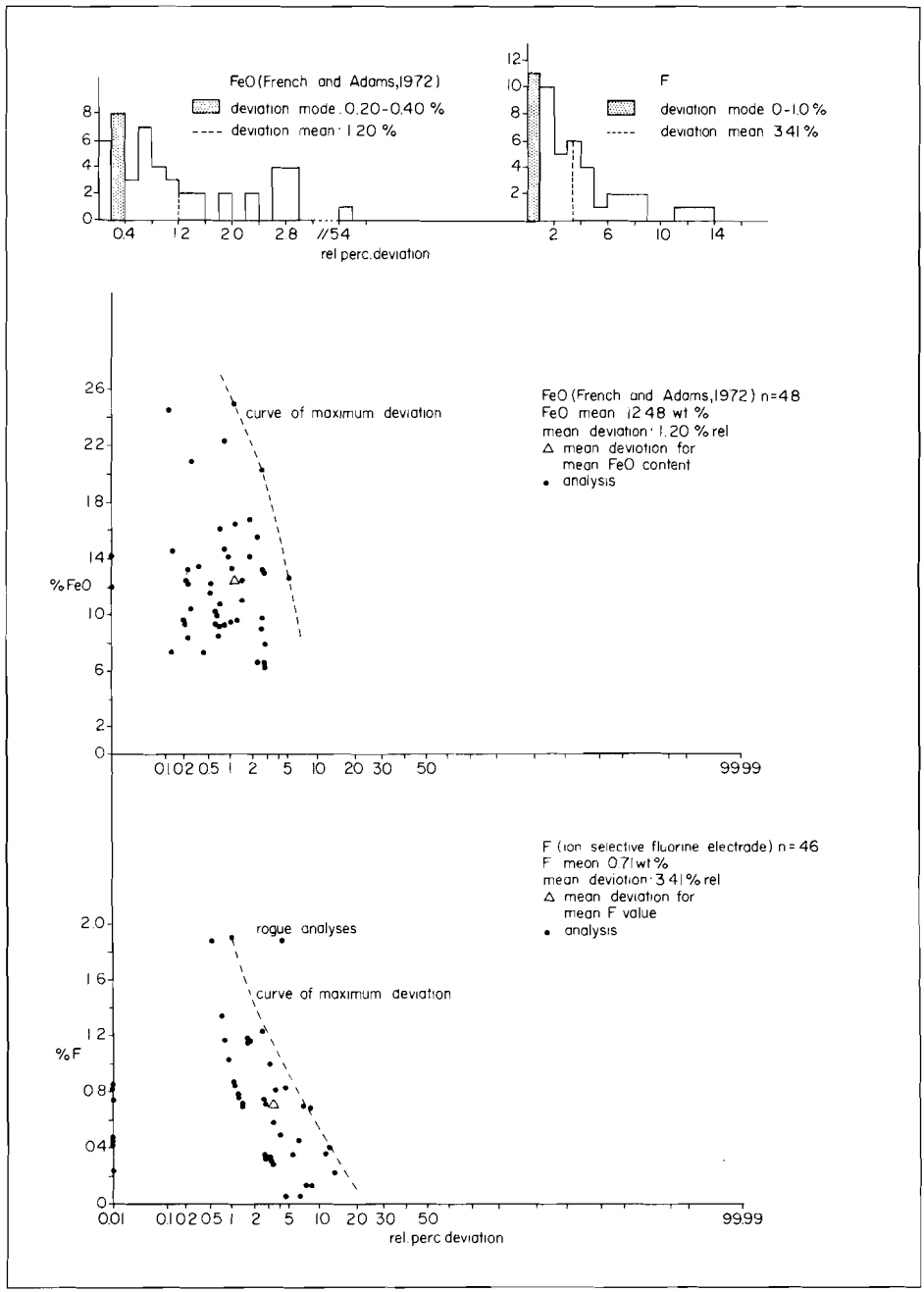

Figure IV.6.: FeO and F relative percentages deviation versus number of samples and versus weight percentages FeO and F. Compare with fig.III.3 and III.4.

On the other hand, the amount of H_2O^- should be subtracted. According to literature the amount should be very low, but the fact that the weight of the sample increases by oxidation of FeO while heating at 110^o is seldom mentioned. The samples from this study have not been analysed for the H_2O^- content.
Therefore the H_2O-values are rather dubious, and in addition, also the sum of fluids. Several samples were analysed for Cl because the presence of this element may be a reason for a low sum (H_2O + F). Seven of the lowest "sum of fluid" samples were selected, ranging from ultramafic host rock to pegmatites (table IV.6).

No.	H_2O + F	Cl	Sum	host rock
A 128	1.57 wt%	0.00	1.57	Phenocryst in gabbro
B 254	1.17	0.14	1.31	Olivine amphibolite
F 433	1.43	0.58	2.01	Pegmatite
N 402	1.42	0.30	1.72	Granite
W 017 B	1.03	0.26	1.29	Schistose enderbite
W 196 B	1.07	0.14	1.21	Schistose enderbite
W 226 D	1.30	0.07	1.37	Plagioclase-bearing hornblendite

Table IV.6.: Additional Cl-analyses for low (H_2O+F) samples.

It is clear from the table that in some cases the Cl seems to complete the fluid analysis, while in other samples no Cl can be detected and possibly O^{2-} has to be added to fill up the empty space in the $(OH,F,Cl)_2$-group of the structural formula. The highest Cl-values are found in pegmatitic amphiboles, a result that is not unexpected.
Analytical procedure : titration according to the "Volhard"-method.
The duplicates are analysed separately and show a complete similarity.

IV.1.5. : Results

The results of the microprobe analyses and the wet-chemical measurements are presented in table IV.7. Sometimes two results are given for a certain amphibole (e.g. B1016 1 and B1016 2). This depends on the (in-) homogeneity found with the microprobe. The total is corrected for

fluorine. The Cl-values are not inserted in the table, the reader is referred to table IV.6. For completeness, all amphiboles mentioned in table I.1. are presented in this table, even if they could not be analysed (e.g. F2052 D).
In accordance with fig. III.6, the analytical information is transformed into histograms, which show immediately the deviating values, and the difference or similarity between igneous and migmatitic samples, see fig. IV.7.

IV.2. : Calculations of structural formulae.

IV.2.1. : Introduction

Several papers have appeared in literature which are discussing the various calculation methods, mostly in the sixties (e.g. Borneman-Starynkevich, 1960; Phillips, 1963; Borg, 1967; Leake, 1968; Binns, 1965-a). The western petrologists concluded that the 24(O,OH,F,Cl) method gives the best results, if the fluid content is somewhere near 2.00 (1.7-2.3). Lower or higher values are probably wrong, so the fluid content then should not be incorporated in the calculation and the 23(O) method is used.
The eastern geologists, Russians as well as Japanese, preferred the 23(O) method in all cases, because of the poor quality of the fluid determinations (see chapter IV.1.3.). Nowadays, some critical geologists in the western world are changing to the eastern point of view, for the same reason the Russians used years ago : the unreliable fluid determinations (Robinson et al, 1971-a; Goff and Czamanske, 1972). However, most of the geologists still use the 24(O,OH,F,Cl) method if the fluids are determined, and the 23(O) method if not, without discussing the reason why they use it for their special investigation.
In this thesis the following three methods are used :
1 : 23(O) basis, microprobe information only

	A 037 B	A 128	A 168	B1016 1	B1016 2	B2016	B 118 L	B 254	B 322	D 172 D	D 307	D 442
SiO_2	41.28	41.90	55.60	45.43	47.74	52.73	43.39	40.55	42.64	43.98	43.72	43.54
TiO_2	1.49	1.75	1.03	0.84	0.71	0.09	1.84	3.77	1.90	1.90	2.74	1.23
Al_2O_3	15.20	13.65	0.28	8.00	6.34	0.93	9.36	13.33	11.96	9.81	11.12	11.02
Fe_2O_3*	3.67	3.39	-	-	-	-	4.06	3.19	3.78	-	2.50	4.47
FeO*	7.65	10.05	-	-	-	-	14.13	13.23	12.26	-	9.42	13.37
MnO	0.20	0.20	0.00	0.28	0.32	0.89	0.26	0.19	0.13	0.25	0.13	0.31
MgO	12.88	12.05	9.37	8.23	9.23	11.95	10.94	9.34	11.24	10.94	12.96	10.13
CaO	12.20	11.85	0.18	10.67	10.83	1.80	10.78	11.05	11.20	11.31	11.66	11.23
Na_2O	1.38	1.60	7.05	1.14	1.09	0.08	2.00	2.37	2.11	1.67	1.85	1.78
K_2O	2.03	1.50	0.13	0.65	0.44	0.04	1.59	1.56	1.12	1.45	1.49	1.32
H_2O^+	1.47	0.86	-	-	-	-	0.81	0.95	1.75	-	1.38	1.51
F	0.93	0.71	-	-	-	-	1.92	0.22	0.59	-	1.22	0.40
FeO**	10.96	13.10	23.64	22.72	21.78	30.59	17.44	16.10	15.66	16.61	11.67	17.39
-F=O	0.39	0.30	-	-	-	-	0.81	0.09	0.25	-	0.51	0.17
Total	99.99	99.01	97.28	97.96	98.48	98.90	100.27	99.66	100.43	97.92	99.68	109.14

	D 444	E 067	E 125	E 128 1	E 128 2	E 131	E1167	E2167	E 170	E1232 K	E1232 R	E2232 N
SiO_2	42.36	41.84	40.99	42.05	42.42	41.46	40.81	49.17	42.38	43.40	42.38	54.50
TiO_2	2.01	1.87	3.82	4.01	3.85	1.79	2.01	0.07	2.10	0.77	0.64	0.06
Al_2O_3	11.74	9.93	13.44	14.01	13.78	14.88	8.75	0.22	11.31	9.77	10.63	1.46
Fe_2O_3*	4.71	5.98	2.89	-	-	-	7.04	-	2.61	-	-	-
FeO*	14.75	20.99	12.31	-	-	-	24.49	-	14.29	-	-	-
MnO	0.32	0.31	0.21	0.07	0.08	0.29	0.54	0.43	0.22	0.37	0.37	0.21
MgO	9.11	5.09	9.95	14.40	14.90	14.67	2.00	0.83	10.36	8.12	9.66	16.19
CaO	10.44	9.90	10.97	11.55	11.62	11.34	9.72	11.21	11.11	11.54	11.44	12.00
Na_2O	2.26	2.03	2.37	2.71	2.68	2.56	2.02	0.15	2.23	1.02	1.04	0.16
K_2O	0.91	1.26	1.57	1.26	1.23	1.20	1.35	0.05	1.14	1.18	1.27	0.09
Cr_2O_3	-	-	0.03	1.43	1.28	0.00	-	-	0.12	-	-	-
H_2O^+	1.55	1.70	1.89	-	-	-	1.63	-	1.62	-	-	-
F	0.24	0.35	0.36	-	-	-	0.34	-	0.29	-	-	-
FeO**	18.99	26.37	14.91	6.21	6.03	9.33	30.63	35.47	16.64	21.72	23.02	12.65
-F=O	0.10	0.15	0.15	-	-	-	0.14	-	0.13	-	-	-
Total	100.30	100.50	100.65	97.80	97.88	97.52	100.39	97.60	99.95	97.89	98.27	97.26

	E2232 1	E2232 2	E2232 3	E2232 4	E2232 5	E3232 N	F 005	F1043	F2043	F1052 D	F2052 D	F3052 L
SiO_2	54.50	54.13	54.13	51.60	43.95	43.72	44.57	43.28	54.94	43.89	NA	44.11
TiO_2	0.06	0.06	0.06	0.12	0.79	0.75	1.66	1.01	0.00	1.62	-	1.77
Al_2O_3	1.31	1.65	1.70	3.72	10.48	10.80	9.36	9.77	0.39	9.07	-	8.95
Fe_2O_3*	-	-	-	-	-	-	5.67	6.62	-	4.83	-	4.70
FeO*	-	-	-	-	-	-	9.83	11.62	-	11.09	-	11.09
MnO	0.21	0.22	0.20	0.21	0.19	0.21	0.30	0.75	0.69	0.45	-	0.51
MgO	16.28	15.81	15.82	14.46	10.00	10.05	12.31	10.38	15.36	11.79	-	11.99
CaO	11.96	11.82	11.91	11.91	11.41	11.39	11.49	11.44	12.48	11.20	-	11.12
Na_2O	0.10	0.17	0.14	0.34	1.09	1.12	1.91	1.66	0.15	2.12	-	2.15
K_2O	0.09	0.12	0.12	0.37	1.41	1.53	1.38	1.42	0.05	1.46	-	1.45
H_2O^+	-	-	-	-	-	-	1.31	1.40	-	1.43	-	1.43
F	-	-	-	-	-	-	0.75	0.69	-	1.01	-	1.01
FeO**	12.31	12.68	12.89	14.04	18.64	18.30	14.93	17.58	12.75	15.44	-	15.44
-F=O	-	-	-	-	-	-	0.32	0.29	-	0.43	-	0.43
Total	96.82	96.66	96.97	96.82	97.96	97.87	100.21	99.76	96.80	99.55	NA	99.85

	F4052 L	F 070	F 074	F1107 0	F2107 D	F1426	F2126	F1252	F2252)	F2252 2	F2252 3	F1433
SiO_2	51.39	43.62	44.37	43.01	43.19	43.27	NA	44.65	48.06	50.66	52.17	40.84
TiO_2	0.32	1.47	1.38	1.99	1.57	1.97	-	1.54	0.12	0.22	0.19	0.89
Al_2O_3	4.14	9.80	9.90	10.25	10.45	10.14	-	9.12	6.86	4.99	3.50	9.20
Fe_2O_3*	-	4.51	-	4.47	-	5.60	-	5.94	-	-	-	5.47
FeO*	-	13.89	-	13.07	-	12.69	-	9.53	-	-	-	24.97
MnO	0.46	0.41	0.23	0.23	0.22	0.36	-	0.36	0.36	0.35	0.37	0.67
MgO	16.67	10.65	11.54	10.55	10.83	10.10	-	12.38	14.78	16.07	17.42	2.30
CaO	11.82	11.42	11.63	10.99	11.15	11.14	-	11.50	12.55	12.58	12.49	10.23
Na_2O	1.13	1.79	1.57	1.65	1.41	1.44	-	1.81	1.09	0.86	0.83	2.26
K_2O	0.59	1.59	1.51	1.66	1.67	1.49	-	1.37	0.85	0.41	0.34	1.55
H_2O^+	-	-	-	1.54	-	1.39	-	1.42	-	-	-	1.15
F	-	-	-	0.84	-	0.43	-	0.36	-	-	-	0.28
FeO**	10.69	17.75	16.06	17.09	16.64	17.53	-	14.88	12.72	10.99	10.00	29.89
-F=O	-	-	-	0.35	-	0.18	-	0.15	-	-	-	0.12
Total	97.21	98.95	98.19	99.90	97.13	99.64	NA	99.83	97.59	97.13	97.31	99.69

Table IV.7.: Amphibole analyses : oxides and fluorine. Fluorine correction, see teble III.3.

* : Fe_2O_3 and FeO are only given if measured.

** : Total Fe as FeO.

If H_2O, Fe_2O_3 and F are not measured, the total will be ebout 2% too low. NA : not analyzed.

	F2433	H1047 B	H2047 B	H1050	H2050	H 307	H 325	H 415	J 119	L1143 M	L1143 1	L1143 2
SiO_2	40.34	45.28	NA	44.82	NA	41.84	42.56	43.48	42.37	48.52	52.48	47.41
TiO_2	0.91	1.65	-	1.93	-	2.01	2.31	2.21	2.40	0.21	0.36	0.09
Al_2O_3	9.60	9.04	-	9.33	-	11.90	13.21	9.53	11.13	8.30	4.40	9.25
$Fe_2O_3^*$	-	5.00	-	4.96	-	5.47	4.17	5.09	5.85	-	-	-
FeO*	-	8.59	-	7.93	-	10.81	9.75	12.22	10.53	-	-	-
MnO	0.68	0.34	-	0.25	-	0.43	0.17	0.31	0.18	0.12	0.09	0.13
MgO	2.07	13.34	-	14.03	-	10.77	12.35	11.21	11.07	16.14	18.44	15.80
CaO	10.46	11.44	-	11.39	-	11.58	10.84	11.07	11.37	12.18	12.49	12.13
Na_2O	2.05	1.96	-	1.94	-	1.64	2.66	1.94	1.67	0.85	0.45	0.91
K_2O	1.62	1.33	-	1.52	-	2.09	0.49	1.60	1.82	0.68	0.33	0.69
H_2O^+	-	1.14	-	0.95	-	1.02	1.30	1.03	1.55	-	-	-
F	-	0.85	-	1.35	-	0.79	0.13	1.21	0.86	-	-	-
FeO**	30.58	13.09	-	12.39	-	15.73	13.50	16.80	10.70	8.48	10.98	
-F=O	-	0.35	-	0.57	-	0.33	0.05	0.52	0.36	-	-	-
Total	98.31	99.81	NA	99.83	NA	100.07	99.89	100.40	100.44	97.70	97.52	97.39

	L1143 3	L2143	M 101	N1041 1	N1041 2	N1041 3	N2041 1	N2041 2	N2041 3	N1264	N2264 M	N2264 1
SiO_2	49.12	54.86	44.49	47.59	47.11	48.31	48.62	49.78	51.47	45.05	55.98	56.78
TiO_2	0.15	0.04	1.85	0.71	0.76	0.28	0.15	0.00	0.00	1.57	0.00	0.00
Al_2O_3	7.64	1.20	9.56	8.22	8.24	7.70	7.79	6.94	5.62	9.14	0.56	0.19
$Fe_2O_3^*$		-	5.32	3.16	2.43	2.10	2.54	2.76	3.00	5.46	-	-
FeO**	-	-	6.17	9.28	10.02	8.67	8.40	7.31	6.00	9.37	-	-
MnO	0.18	0.51	0.20	0.33	0.33	0.27	0.27	0.25	0.24	0.27	0.25	0.20
MgO	16.34	21.29	14.97	14.48	14.86	15.93	15.85	16.84	18.24	13.27	18.06	18.72
CaO	12.09	1.26	11.40	11.34	11.23	11.30	11.26	11.37	11.44	11.45	12.75	12.88
Na_2O	0.71	0.07	1.89	1.25	1.42	1.50	1.37	1.22	1.11	1.94	0.23	0.11
K_2O	0.66	0.02	1.88	0.78	0.89	0.77	0.70	0.62	0.55	1.32	0.06	0.02
H_2O^+	-	-	0.86	1.29	1.19	1.37	1.40	1.55	1.72	1.16	-	-
F	-	-	1.92	0.70	0.65	0.74	0.76	0.84	0.93	0.75	-	-
FeO**	10.22	18.12	10.96	12.12	12.21	10.56	10.69	9.79	8.70	14.28	10.08	9.06
-F=O	-	-	0.81	0.29	0.27	0.31	0.32	0.35	0.39	0.32	-	-
Total	97.11	97.37	99.70	98.84	98.86	98.63	98.78	99.13	99.93	100.44	97.97	97.96

	N 317	N 337	N1402 1	N1402 2	N2402	N1528 B	N2528 B	N3528 B	N4528 B	N1572 R	N1572 X	N2572 D
SiO_2	41.55	43.67	42.18	42.28	42.81	40.53	NA	40.39	NA	42.08	42.73	NA
TiO_2	2.78	1.81	2.10	2.32	1.33	2.18	-	0.76	-	1.91	1.93	-
Al_2O_3	12.63	10.03	9.27	9.11	8.85	10.14	-	11.94	-	15.02	15.05	
$Fe_2O_3^*$	4.26	2.67	6.12	5.62	-	-	-	-	-	1.80	1.72	-
FeO**	12.11	12.62	10.42	10.42	-	-	-	-	-	6.60	6.59	-
MnO	0.19	0.25	0.38	0.41	0.37	0.25	-	0.22	-	0.10	0.10	
MgO	10.49	12.16	5.68	5.79	5.33	4.43	-	5.30	-	15.24	15.35	-
CaO	11.20	11.23	9.83	9.89	9.98	10.40	-	10.53	-	11.29	11.16	-
Na_2O	2.14	1.91	2.17	2.20	1.64	1.94	-	1.75	-	2.98	2.87	-
K_2O	1.64	1.79	1.32	1.38	1.24	1.53	-	1.57	-	0.55	0.55	-
H_2O^+	1.17	0.87	0.97	0.97	-	-	-	-	-	1.77	1.48	-
F	0.42	1.92	0.45	0.45	-	-	-	-	-	0.07	0.06	-
FeO**	15.94	15.02	25.93	25.48	26.06	26.59	-	25.22	-	8.22	8.14	-
-F=O	0.18	0.81	0.19	0.19	-	-	-	-	-	0.03	0.03	-
Total	100.40	100.12	100.70	100.65	97.41	97.99	NA	97.68	NA	99.38	99.56	NA

	N 809	N1827 1	N1827 2	N1827 3	N1827 4	N2827 1	N2827 2	N2827 3	Q 100	P1097	P2097	P 248
SiO_2	43.79	42.10	46.98	43.39	42.06	50.89	51.77	51.23	44.02	42.74	43.41	43.58
TiO_2	2.61	0.36	0.35	0.45	0.60	0.18	0.18	0.24	2.50	1.51	0.65	2.03
Al_2O_3	10.60	11.38	6.92	10.32	11.88	3.57	3.05	3.49	10.53	8.46	8.11	10.36
$Fe_2O_3^*$	2.67	4.92	4.37	4.59	4.79	-	-	-	1.55	-	-	-
FeO**	9.00	18.64	16.59	17.38	18.11	-	-	-	9.67	-	-	-
MnO	0.12	0.41	0.41	0.41	0.40	0.44	0.43	0.40	0.09	0.19	0.19	0.35
MgO	14.09	6.96	9.63	8.30	7.72	12.74	12.86	12.64	13.79	7.40	8.26	11.80
CaO	11.65	11.57	11.73	11.59	11.55	11.81	11.87	11.97	11.78	10.71	10.61	11.27
Na_2O	2.25	1.07	0.61	1.04	1.12	0.35	0.32	0.35	1.84	2.05	2.02	1.77
K_2O	1.32	1.41	0.69	1.27	1.46	0.32	0.27	0.34	1.43	1.69	1.65	1.55
H_2O^+	0.77	-	-	-	-	-		-	1.16	-	-	-
F	1.10	0.13	0.13	0.13	0.13	-	-	-	0.74	-	-	-
FeO**	11.40	23.07	20.53	21.51	22.41	17.32	16.89	17.14	1.07	23.17	22.74	15.41
-F=O	0.46	0.05	0.05	0.05	0.05	-	-	-	0.31	-	-	-
Total	99.51	98.90	98.36	98.82	99.57	97.62	97.64	97.80	98.79	97.92	97.64	98.12

Table IV.7.: continued

	P 303 1	P 303 2	P1580 D	P2580 L	R 227	R1229	R2229 1	R2229 2	R2229 3	R3229	R1269 1	R1269 2
SiO_2	44.29	43.88	42.70	42.45	43.24	41.82	43.90	42.16	46.03	50.69	42.12	43.25
TiO_2	1.75	1.84	0.89	0.89	1.71	1.29	0.29	1.26	0.78	0.02	0.41	0.38
Al_2O_3	9.56	10.04	12.46	12.53	9.09	9.23	7.39	8.92	5.93	0.52	10.51	9.16
$Fe_2O_3^*$	2.88	2.89	3.71	3.84	-	-	-	-	-	-	-	-
FeO^*	13.33	13.61	8.74	9.31	-	-	-	-	-	-	-	-
MnO	0.40	0.39	0.12	0.18	0.18	0.25	0.28	0.25	0.25	0.68	0.41	0.43
MgO	11.58	11.23	13.73	13.01	7.37	4.83	5.21	4.95	5.88	6.91	5.09	5.64
CaO	11.33	11.21	11.65	11.47	10.43	10.38	10.62	10.39	8.37	0.52	10.99	10.58
Na_2O	1.92	1.99	1.89	1.91	1.80	1.67	1.28	1.44	0.50	0.09	1.38	1.49
K_2O	1.42	1.43	1.64	1.74	1.27	1.33	0.91	1.25	0.56	0.01	1.16	0.92
H_2O^+	0.77	0.77	0.63	0.63	-	-	-	-	-	-	-	-
F	0.83	0.83	0.35	0.35	-	-	-	-	-	-	-	-
FeO^{tot}	15.88	16.21	12.08	12.87	22.96	27.01	27.80	27.23	29.59	38.45	26.60	26.03
-F=O	0.35	0.35	0.15	0.15	-	-		-	-	-	-	-
Total	99.66	99.76	98.36	98.16	98.05	97.81	97.68	97.85	97.89	97.89	98.67	97.88

	R1269 3	R2269 1	R2269 2	R2269 3	R 356 1	R 356 2	R 356 3	R 356 4	R1668	R2668	V 147	V1187
SiO_2	42.36	49.96	51.69	51.39	40.71	41.87	42.13	41.38	41.93	42.00	41.51	42.55
TiO_2	0.54	0.73	0.22	0.16	1.65	0.82	0.98	0.89	1.50	0.69	0.81	2.13
Al_2O_3	10.12	3.10	1.97	2.33	9.44	8.71	8.82	8.98	8.98	9.24	11.25	10.43
$Fe_2O_3^*$	-	-	-	-	-	-	-	-	1.83	-	-	2.23
FeO^*	-	-	-	-	-	-	-	-	23.53	-	-	16.06
MnO	0.41	0.22	0.52	0.47	0.36	0.29	0.28	0.35	0.43	0.45	0.16	0.14
MgO	5.29	8.78	9.31	9.54	2.37	3.44	3.72	2.50	5.79	5.97	5.05	9.68
CaO	10.67	10.92	10.87	10.89	9.49	9.92	9.75	9.80	10.54	10.62	10.42	11.71
Na_2O	1.47	0.51	0.42	0.24	1.89	1.39	1.41	1.33	2.08	1.99	1.49	1.32
K_2O	1.06	0.23	0.13	0.12	1.49	1.22	1.09	1.21	1.53	1.49	1.62	2.31
H_2O^+	-	-	-	-	-	-	-	-	0.86	-	-	0.89
F	-	-	-	-	-	-	-	-	1.23	-	-	1.28
FeO^{tot}	26.13	23.52	23.22	22.68	30.63	29.51	29.54	31.57	25.18	25.79	25.82	18.07
-F=O	-	-	-	-	-	-	-	-	0.52	-	-	0.54
Total	98.05	97.97	98.35	97.82	98.03	97.17	97.72	98.01	99.61	98.24	98.13	100.19

	V2187 1	V2187 2	V 276	V 277	V 363	W 012 0	W 017 8	W 162 D	W 196 8	W 217	W1226 0	W2226 L
SiO_2	52.22	44.44	40.02	42.36	43.68	44.69	43.83	43.88	43.08	41.98	45.30	43.64
TiO_2	0.15	0.74	0.69	1.43	1.21	1.08	1.99	1.16	1.74	1.49	0.74	2.09
Al_2O_3	2.61	9.12	10.42	9.13	9.35	9.67	10.38	9.26	10.87	10.52	10.34	10.46
$Fe_2O_3^*$	-	-	-	-	1.41	3.39	3.34	-	3.30	-	2.75	-
FeO^*	-	-	-	-	16.52	14.62	14.22	-	15.61	-	10.05	-
MnO	0.17	0.15	0.56	0.26	0.55	0.45	0.33	0.55	0.25	0.62	0.22	0.22
MgO	13.79	10.82	2.68	6.52	10.61	10.92	10.44	10.68	9.82	8.20	13.99	11.29
CaO	12.19	11.78	9.85	10.22	11.07	10.93	11.27	11.01	11.02	10.29	11.30	11.07
Na_2O	0.40	0.91	1.80	1.89	1.73	1.61	1.52	1.71	1.61	1.76	1.64	1.69
K_2O	0.34	1.47	1.65	1.53	1.36	1.24	1.25	1.32	1.02	1.34	1.02	1.24
H_2O^+	-	-	-	-	1.02	0.94	0.72	-	0.61	-	0.81	-
F	-	-	-	-	1.17	0.68	0.31	-	0.46	-	0.49	-
FeO^{tot}	15.96	17.78	30.50	24.86	17.79	17.67	17.23	17.79	18.58	21.18	12.53	15.43
-F=O	-	-	-	-	0.49	0.29	0.13	-	0.19	-	0.21	-
Total	97.83	97.21	98.17	98.20	99.21	99.93	99.47	97.36	99.20	97.38	98.44	97.13

	Y1055	Y2055 1	Y2055 2	Y1128 1	Y1128 2	Y2128	Y1131 1	Y1131 2	Y2131	Y3131 R	Y3131 K
SiO_2	42.37	43.24	43.48	39.15	40.47	49.77	37.16	36.98	36.72	37.73	37.46
TiO_2	2.02	0.07	1.22	0.80	1.07	0.23	0.23	0.20	1.60	0.09	0.02
Al_2O_3	10.35	10.96	8.91	10.97	9.83	0.94	14.59	14.49	14.10	13.25	15.64
$Fe_2O_3^*$	-	-	-	-	-	-	-	-	-	-	-
FeO^*	-	-	-	-	-	-	-	-	-	-	-
MnO	0.13	0.10	0.12	0.48	0.52	0.67	0.34	0.33	0.34	0.43	0.45
MgO	10.04	10.48	9.71	1.09	1.31	3.55	1.47	1.93	1.78	1.44	1.26
CaO	11.46	11.22	10.12	10.18	10.09	10.86	10.92	11.05	11.06	11.15	10.36
Na_2O	1.35	0.79	1.01	1.77	1.77	1.20	0.89	1.04	1.34	0.82	0.51
K_2O	2.30	2.45	1.99	1.83	1.58	1.06	2.25	2.18	2.29	2.36	1.16
H_2O^+	-	-	-	-	-	-	-	-	-	-	-
F	-	-	-	-	-	-	-	-	-	-	-
FeO^{tot}	17.67	18.61	20.34	31.53	31.66	30.22	30.05	29.26	28.37	30.97	30.13
-F=O	-	-	-	-	-	-	-	-	-	-	-
Total	97.69	97.92	96.90	97.80	98.30	98.50	97.80	97.46	97.60	98.24	96.99

Table IV.7.: continued

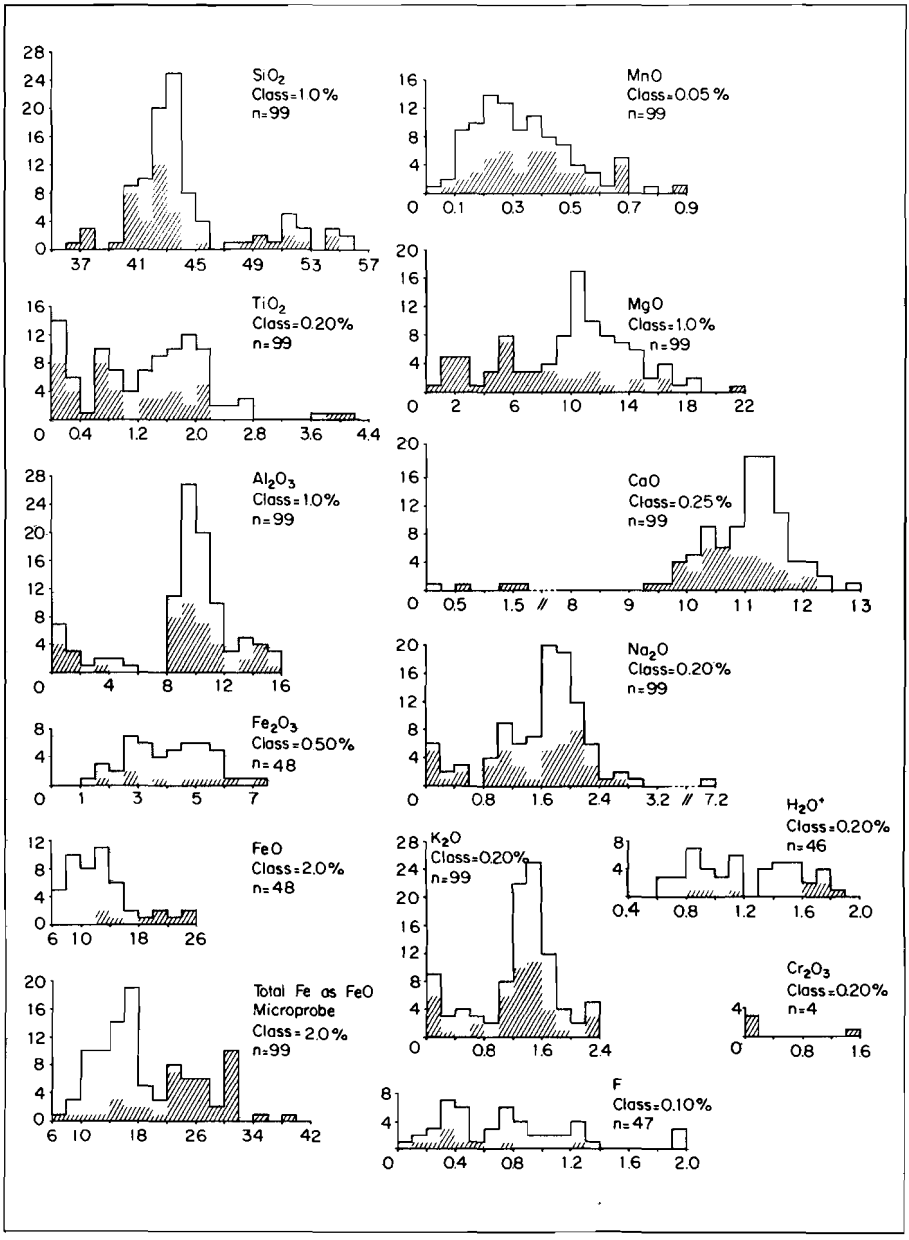

Figure IV.7.: Amphibole histograms, derived from table IV.7. Abscissa : oxide wt %, ordinate : number of samples. The shaded area concerns all samples from igneous complexes, i.e. the igneous rocks as well as their inclusions. The clear area concerns all other samples.

2 : 23(O) basis, Z + Y brought to 13 (idealisation of the formula)

3 : 24(O,OH,F) basis, all analytical information used to create the formula.

Where possible, i.e. for those samples where Fe^{2+}, OH and F were analysed, the results of these three methods are compared by computer, calculating correlation coëfficients for all formula positions and elements (section IV.2.6.).

IV.2.2. : Only microprobe information, 23(O) method

This is the simplest and quickest method. The scheme of Deer, Howie and Zussman (1974, p. 515) is followed, using 23 instead of 24(O), because fluid analyses are lacking. The structural formulae are shown in table IV.8.

As basis for the grouping of the elements into the structural formula, the following scheme is adopted :

General formula : $A_{0-1}X_{2-3}Y_{\pm 5}Z_8O_{22}(OH,F,Cl)_{\pm 2}$

Z : Si + (8.0 - Si) Al

Y : Al(rest) + Ti + Fe + Mn + Mg + Cr

X : Ca + Na + K

A : not mentioned normally, if needed : A = X + Y - 7

For more detailed information concerning the structural formulae and their site-occupancy, see Ernst (1968), Hawthorne and Grundy (1973a and b, 1975, 1976, 1977) and Hawthorne (1976).

Names are given according to Leake (1968) for the Ca-amphiboles and Ernst (1968) for the Na- and Fe-Mg-amphiboles.

Fig. IV.8 contains all Ca-amphibole analyses, divided in several groups depending on origin and character of the host rock. The alkali- and iron-magnesian amphiboles cannot be plotted in the Ernst diagram, because no Fe^{3+}/Fe^{2+} ratio is known. The histograms for the ions are given in fig. IV.9.

	A 037 B	A 128	A 169	B1016 1	B1016 2	B2016	B 118	B 254	B 322	D 172 D	D 307	D 442
Si	6.09	6.23	8.30	6.935	7.18	7.915	6.58	6.095	6.36	6.60	6.46	6.55
Al	1.91	1.77	.00	1.065	.82	.085	1.42	1.905	1.64	1.40	1.54	1.45
Al	.73	.62	.05	.375	.305	.08	.235	.455	.465	.335	.395	.505
Ti	.165	.20	.115	.095	08	.01	.21	.425	.215	.215	.305	.14
Fe^{2+}	1.35	1.63	2.95	2.90	2.74	3.84	2.21	2.025	1.955	2.085	1.44	2.19
Mn	.025	.03	.00	.035	.04	.115	.035	.025	.015	.03	.015	.04
Mg	2.03	2.67	2.085	1.87	2.07	2.675	2.475	2.095	2.505	2.45	2.855	2.27
Ca	1.93	1.86	.03	1.745	1.745	.26	1.75	1.78	1.79	1.82	1.845	1.81
Na	.395	.46	2.04	.34	.32	.025	.59	.69	.61	.485	.53	.52
K	.385	.28	.025	.125	.085	.005	.305	.30	.215	.28	.28	.255
Z	8.00	8.00	8.30	8.00	8.00	8.00	8.00	8.00	8.00	8.00	8.00	8.00
Y	5.09	5.15	5.20	5.275	5.235	7.00	5.165	5.025	5.155	5.115	5.01	5.145
X	2.71	2.60	2.095	2.23	2.15	.005	2.645	2.77	2.615	2.585	2.655	2.585
mg	.675	.62	.41	.39	.425	.40	.525	.505	.56	.535	.66	.505

	D 444	E 067	E 125	F 128 1	E 128 2	E 131	E1167	E2167	E 170	E1232 K	E1232 R	E2232 N
Si	6.40	6.58	6.12	6.075	6.11	6.06	6.59	7.945	6.395	6.66	6.59	7.855
Al	1.60	1.42	1.88	1.925	1.89	1.94	1.41	.045	1.605	1.34	1.41	.145
Al	.49	.31	.485	46	.45	.625	.26	.00	.405	.415	.515	.105
Ti	.23	.22	.43	.435	.415	.195	.245	.01	.24	.09	.075	.005
Fe^{2+}	2.40	3.47	1.86	.75	.725	1.14	4.135	4.795	2.10	2.785	2.965	1.525
Mn	.04	.04	.025	.01	.01	.035	.075	.06	.03	.05	.05	.025
Mg	2.055	1.19	2.215	3.10	3.20	3.20	.48	.20	2.33	1.835	1.605	3.48
Cr			.005	.165	.145	.00			.015			
Ca	1.69	1.67	1.755	1.785	1.795	1.78	1.68	1.94	1.755	1.90	1.885	1.855
Na	.655	.62	.685	.76	.75	.725	.635	.045	.655	.305	.31	.03
K	.175	.255	.30	.235	.225	.225	.275	.01	.20	.23	.25	.015
Z	8.00	8.00	8.00	8.00	8.00	8.00	8.00	7.99	8.00	8.00	8.00	8.00
Y	5.215	5.23	5.015	4.93	4.945	5.195	5.195	5.065	5.12	5.195	5.21	5.15
X	2.53	2.545	2.735	2.77	2.77	2.73	2.59	1.995	2.67	2.435	2.445	1.90
mg	.435	.255	.54	.80	.815	.73	.105	.04	.525	.395	.365	.69

	E2232 1	E2232 2	E2232 3	E2232 4	E2232 5	E3232 N	F 005	F1043	F2043	F1052 D	F2052 D	F3052 L
Si	7.88	7.855	7.835	7.57	6.63	6.60	6.04	6.595	7.985	6.635	.NA	6.64
Al	.12	.145	.165	.43	1.37	1.40	1.36	1.405	.015	1.365		1.36
Al	.105	.14	.125	.215	.495	.52	.285	.35	.05	.25		.23
Ti	.005	.005	.005	.02	.09	.085	.185	.115	.00	.185		.20
Fe^{2+}	1.49	1.54	1.56	1.72	2.35	2.31	1.86	2.24	1.55	1.95		1.93
Mn	.025	.025	.025	.025	.025	.025	.05	.095	.085	.08		.065
Mg	3.51	3.42	3.415	3.16	2.25	2.26	2.735	2.36	3.33	2.66		2.69
Ca	1.855	1.835	1.85	1.87	1.845	1.84	1.835	1.87	1.945	1.815	.	1.795
Na	.03	.045	.04	.095	.32	.33	.525	.49	.045	.62		.63
K	.015	.02	.02	.07	.27	.295	.265	.275	.01	.28		.28
Z	8.00	8.00	8.00	8.00	8.00	8.00	8.00	8.00	8.00	8.00		8.00
Y	5.135	5.13	5.13	5.14	5.21	5.20	5.315	5.16	5.015	5.105		5.115
X	1.90	1.905	1.91	2.04	2.435	2.465	2.82	2.635	2.00	2.72		2.70
mg	.70	.685	.68	.645	.485	.49	.59	.505	.67	.57	.NA	.575

	F4052 L	F 070	F 074	F1107 D	F2107 D	F1126	F2126	F1252	F2252 1	F2252 2	F2252 3	F1433
Si	7.44	6.565	6.625	6.57	6.545	6.56	.NA	6.675	7.05	7.35	7.505	6.595
Al	56	1.435	1.375	1.48	1.455	1.44		1.325	.95	.65	.495	1.405
Al	.145	.305	.365	.35	.41	.37	.	.28	.235	.205	.10	.345
Ti	.035	.165	.155	.225	.18	.225	.	.175	.035	.025	.02	.11
Fe^{2+}	1.295	2.215	2.005	2.165	2.11	2.22		1.86	1.56	1.335	1.205	4.035
Mn	.055	.055	.03	.03	.03	.045		.045	.045	.045	.045	.09
Mg	3.60	2.39	2.57	2.385	2.445	2.285		2.76	3.235	3.475	3.735	.555
Ca	1.835	1.84	1.86	1.785	1.81	1.81	.	1.84	1.975	1.955	1.925	1.77
Na	.32	.525	.455	.485	.415	.425	.	.525	.31	.24	.20	.77
K	.11	.305	.285	.32	.335	.29		.26	.16	.075	.06	.32
Z	8.00	8.00	8.00	8.00	8.00	8.00		8.00	8.00	8.00	8.00	8.00
Y	5.13	5.15	5.125	5.155	5.175	5.145		5.12	5.11	5.085	5.105	5.135
X	2.26	2.67	2.60	2.59	2.545	2.52		2.63	2.44	2.27	2.22	2.80
mg	.725	.51	.56	.52	.535	.50	.NA	.59	.67	.715	.75	.12

Table IV.8.: Amphibole analyses : half-unit cell contents; 23 O, Microprobe information only. Total Fe as Fe^{2+}, NA : not analyzed.

	F2433	H1047 B	H2047 B	H1050	H2050	H 307	H 325	H 415	J 119	L1143 M	L1143 1	L1143 2	L1143 3
Si	6.51	6.70	.NA	6.625	.NA	6.305	6.265	6.54	6.375	7.00	7.45	6.88	7.10
Al	1.49	1.30	.	1.375	.	1.695	1.735	1.46	1.625	1.00	.55	1.12	.90
Al	.335	.275	.	.25	.	.42	.555	.23	.35	.41	.185	.465	.40
Ti	.11	.185	.	.215	.	.23	.255	.25	.27	.02	.04	.01	.015
Fe^{2+}	4.13	1.62		1.53		1.98	1.66	2.115	1.99	1.29	1.005	1.335	1.235
Mn	.095	.04	.	.03	.	.055	.02	.04	.02	.015	.01	.015	.02
Mg	.50	2.985	.	3.095		2.42	2.71	2.515	2.485	3.47	3.905	3.42	3.52
Ca	1.81	1.815		1.805	.	1.87	1.71	1.785	1.835	1.88	1.90	1.885	1.875
Na	.645	.56	.	.555	.	.48	.76	.565	.49	.235	.125	.26	.20
K	.335	.25	.	.285	.	.40	.09	.305	.35	.125	.06	.125	.12
Z	8.00	8.00	.	8.00	.	8.00	8.00	8.00	8.00	8.00	8.00	8.00	8.00
Y	5.17	5.105	.	5.12	.	5.105	5.20	5.15	5.115	5.205	5.145	5.245	5.19
X	2.785	2.625	.	2.65		2.75	2.56	2.655	2.67	2.245	2.085	2.27	2.195
mg	.105	.64	.NA	.665	.NA	.545	.615	.54	.555	.725	.795	.715	.735

	L2143	M 101	N1041 1	N1041 2	N1041 3	N2041 1	N2041 2	N2041 3	N1264	N2264 M	N2264 1	N 317	N 337
Si	7.855	6.58	6.99	6.92	7.055	7.085	7.195	7.345	6.66	7.925	7.99	6.21	6.535
Al	.145	1.42	1.01	1.08	0.945	.915	.805	.655	1.34	.075	.01	1.79	1.465
Al	.06	.245	.41	.345	.38	.42	.38	.29	.25	.02	.02	.435	.305
Ti	.005	.205	.08	.085	.03	.015	.00	.00	.175	.00	.00	.315	.205
Fe^{2+}	2.17	1.355	1.49	1.50	1.29	1.305	1.185	1.04	1.765	1.195	1.065	1.99	1.88
Mn	.06	.025	.04	.04	.035	.035	.03	.03	.035	.03	.025	.025	.03
Mg	4.545	3.30	3.17	3.255	3.47	3.445	3.63	3.88	2.925	3.81	3.925	2.34	2.715
Ca	.195	1.805	1.785	1.77	1.77	1.76	1.76	1.75	1.815	1.935	1.94	1.795	1.80
Na	.02	.54	.355	.405	.425	.385	.345	.30	.555	.065	.03	.62	.555
K	.005	.355	.145	.17	.145	.13	.115	.10	.25	.01	.005	.315	.34
Z	8.00	8.00	8.00	8.00	8.00	8.00	8.00	8.00	8.00	8.00	8.00	8.00	8.00
Y	7.035	5.13	5.19	5.225	5.205	5.22	5.225	5.24	5.15	5.055	5.035	5.105	5.135
X	.025	2.70	2.285	2.34	2.335	2.275	2.22	2.155	2.62	2.01	1.975	2.73	2.695
mg	.67	.705	.675	.68	.725	.72	.75	.78	.62	.755	.785	.535	.585

	N1402 1	N1402 2	N2402	N1528	N2528	N3528	N4528	N1572 K	N1572 R	N2572 D	N 809	N1827 1	N1827 2
Si	6.56	6.57	6.71	6.415	.NA	6.355	.NA	6.15	6.105	.NA	6.44	6.49	7.10
Al	1.44	1.43	1.29	1.585		1.645	.	1.85	1.895	.	1.56	1.51	.90
Al	.26	.24	.355	.305		.57	.	.705	.675		.28	.56	.33
Ti	.245	.27	.16	.26		.09		.21	.21		.29	.04	.04
Fe^{2+}	3.375	3.31	3.435	3.52		3.32	.	.98	.995	.	1.40	2.975	2.595
Mn	.05	.055	.05	.035		.03		.015	.015	.	.015	.055	.055
Mg	1.32	1.34	1.255	1.045		1.245	.	3.295	3.295	.	3.09	1.60	2.17
Ca	1.64	1.645	1.685	1.765	.	1.775	.	1.72	1.755	.	1.835	1.91	1.90
Na	.655	.66	.50	.595	.	.525	.	.80	.835	.	.64	.32	.18
K	.26	.275	.25	.31		.315		.10	.10		.245	.275	.135
Z	8.00	8.00	8.00	8.00		8.00	.	8.00	8.00	.	8.00	8.00	8.00
Y	5.25	5.215	5.255	5.165		5.255		5.305	5.19	.	5.075	5.23	5.19
X	2.555	2.58	2.435	2.67		2.62	.	2.625	2.69		2.725	2.505	2.21
mg	.28	.285	.265	.225	.NA	.27	.NA	.77	.765	.NA	.685	.345	.45

	N1827 3	N1827 4	N2827 1	N2827 2	N2827 3	O 100	P1097	P2097	P 248	P 303 1	P 303 2	P1580 D	P2580 L
Si	6.625	6.45	7.53	7.63	7.56	6.505	6.65	6.745	6.505	6.62	6.565	6.345	6.34
Al	1.375	1.55	.47	.37	.44	1.495	1.35	1.255	1.495	1.38	1.435	1.655	1.66
Al	.485	.56	.15	.16	.165	.34	.20	.23	.335	.305	.335	.525	.545
Ti	.05	.07	.02	.02	.025	.28	.175	.075	.23	.195	.205	.10	.10
Fe^{2+}	2.745	2.875	2.145	2.08	2.115	1.37	3.015	2.955	1.925	1.985	2.03	1.50	1.61
Mn	.055	.05	.055	.055	.05	.01	.025	.025	.045	.05	.05	.015	.025
Mg	1.89	1.66	2.81	2.825	2.78	3.04	1.72	1.915	2.625	2.58	2.505	3.04	2.90
Ca	1.895	1.90	1.875	1.875	1.89	1.865	1.785	1.765	1.80	1.815	1.80	1.855	1.835
Na	.305	.335	.10	.09	.10	.525	.62	.61	.51	.555	.58	.545	.555
K	.25	.285	.06	.05	.06	.27	.335	.325	.295	.27	.27	.31	.33
Z	8.00	8.00	8.00	8.00	8.00	8.00	8.00	8.00	8.00	8.00	8.00	8.00	8.00
Y	5.225	5.215	5.18	5.14	5.135	5.04	5.135	5.20	5.16	5.115	5.125	5.18	5.18
X	2.45	2.515	2.035	2.015	2.055	2.665	2.74	2.70	2.61	2.64	2.645	2.71	2.72
mg	.403	.36	.56	.57	.56	.69	.36	.39	.57	.56	.545	.665	.64

Table IV.8.: continued

	R 227	R1229	R2229 1	R2229 2	R2229 3	R3229	R1269 1	R1269 2	R1269 3	R2269 1	R2269 2	R2269 3	R 356 1
Si	6.665	6.61	6.93	6.655	7.19	7.985	6.57	6.76	6.625	7.57	7.765	7.74	6.55
Al	1.335	1.39	1.07	1.345	.81	.015	1.43	1.24	1.375	.43	.235	.26	1.45
Al	.32	.33	.305	.315	.28	.08	.50	.45	.49	.125	.115	.155	.34
Ti	.20	.155	.035	.15	.09	.00	.05	.045	.065	.085	.025	.02	.20
Fe^{2+}	2.96	3.57	3.67	3.595	3.865	5.065	3.47	3.40	3.42	2.98	2.92	2.85	4.12
Mn	.025	.035	.035	.035	.035	.09	.055	.055	.055	.03	.065	.06	.05
Mg	1.695	1.135	1.225	1.165	1.37	1.62	1.185	1.315	1.235	1.985	2.085	2.14	.565
Ca	1.725	1.76	1.795	1.76	1.40	.09	1.835	1.77	1.79	1.775	1.75	1.78	1.635
Na	.54	.51	.395	.44	.15	.025	.42	.45	.445	.15	.12	.07	.59
K	.25	.27	.185	.25	.11	.00	.23	.185	.21	.045	.025	.02	.305
Z	8.00	8.00	8.00	8.00	8.00	8.00	8.00	8.00	8.00	8.00	8.00	8.00	8.00
Y	5.20	5.225	5.27	5.26	5.64	6.855	5.26	5.265	5.265	5.205	5.21	5.23	5.275
X	2.51	2.54	2.37	2.45	1.66	.115	2.485	2.41	2.445	1.97	1.895	1.85	2.535
mg	.36	.24	.25	.245	.26	.24	.25	.275	.26	.395	.41	.425	.12

	R 356 2	R 356 3	R 356 4	R1668	R2668	V 147	V1187	V2187 1	V2187 2	V 276	V 277	V 363	W 012 D
Si	6.725	6.715	6.655	6.585	6.595	6.495	6.45	7.65	6.74	6.445	6.805	6.64	6.69
Al	1.275	1.285	1.345	1.415	1.405	1.505	1.55	.35	1.26	1.555	1.195	1.36	1.31
Al	.375	.37	.36	.25	.305	.57	.315	.10	.37	.425	.285	.315	.395
Ti	.10	.12	.11	.175	.08	.10	.245	.015	.085	.085	.165	.14	.12
Fe^{2+}	3.965	3.935	4.25	3.315	3.385	3.38	2.29	1.955	2.255	4.11	3.245	2.26	2.215
Mn	.04	.035	.05	.055	.06	.02	.02	.02	.02	.075	.035	.07	.055
Mg	.825	.885	.60	1.36	1.40	1.175	2.19	3.01	2.465	.645	1.515	2.405	2.44
Ca	1.71	1.665	1.69	1.78	1.785	1.745	1.90	1.915	1.915	1.70	1.71	1.805	1.755
Na	.435	.435	.415	.635	.605	.45	.39	.115	.265	.565	.575	.51	.47
K	.25	.22	.25	.305	.30	.325	.45	.065	.285	.34	.305	.285	.24
Z	8.00	8.00	8.00	8.00	8.00	8.00	8.00	8.00	8.00	8.00	8.00	8.00	8.00
Y	5.305	5.345	5.37	5.155	5.23	5.245	5.06	5.10	5.175	5.34	5.245	5.19	5.225
X	2.39	2.32	2.355	2.72	2.69	2.52	2.74	2.09	2.465	2.60	2.585	2.575	2.46
mg	.17	.18	.12	.285	.29	.255	.485	.605	.52	.135	.315	.505	.52

	W 017 B	W 162 D	W 196 B	W 217	W1226 D	W2226 L	Y1055	Y2055 1	Y2055 2	Y1128 1	Y1128 2	Y2128	Y1131 1
Si	6.565	6.665	6.50	6.485	6.685	6.555	6.455	6.56	6.70	6.385	6.54	7.83	6.025
Al	1.435	1.335	1.50	1.515	1.315	1.445	1.545	1.44	1.30	1.615	1.46	.17	1.975
Al	.395	.32	.435	.40	.485	.40	.315	.52	.32	.49	.415	.005	.815
Ti	.225	.13	.20	.175	.085	.235	.23	.01	.14	.10	.13	.03	.03
Fe^{2+}	2.16	2.26	2.345	2.74	1.545	1.94	2.25	2.36	2.62	4.30	4.28	3.98	4.075
Mn	.04	.07	.035	.08	.03	.03	.015	.015	.015	.065	.07	.09	.045
Mg	2.33	2.42	2.17	1.89	3.08	2.53	2.28	2.37	2.23	.265	.315	.83	.33
Ca	1.81	1.79	1.78	1.705	1.785	1.78	1.87	1.825	1.67	1.78	1.745	1.83	1.895
Na	.44	.505	.47	.525	.47	.49	.40	.23	.30	.56	.555	.365	.28
K	.24	.255	.195	.265	.19	.24	.45	.475	.39	.38	.325	.21	.465
Z	8.00	8.00	8.00	8.00	8.00	8.00	8.00	8.00	8.00	8.00	8.00	8.00	8.00
Y	5.15	5.20	5.225	5.285	5.225	5.14	5.09	5.275	5.325	5.22	5.21	4.935	5.295
X	2.49	2.55	2.45	2.515	2.445	2.51	2.72	2.53	2.365	2.715	2.625	2.41	2.64
mg	.515	.51	.48	.40	.66	.565	.50	.50	.46	.055	.07	.17	.075

	Y1131 2	Y2131	Y3131 K	Y3131 R
Si	6.00	5.945	6.05	6.125
Al	2.00	2.055	1.95	1.875
Al	.77	.635	.99	.66
Ti	.025	.195	.00	.01
Fe^{2+}	3.97	3.84	4.07	4.205
Mn	.045	.045	.06	.06
Mg	.465	.43	.305	.35
Ca	1.92	1.97	1.79	1.94
Na	.33	.42	.16	.255
K	.45	.475	.24	.49
Z	8.00	8.00	8.00	8.00
Y	5.275	5.145	5.46	5.285
X	2.70	2.815	2.19	2.685
mg	.105	.10	.07	.075

Table IV.8.: continued

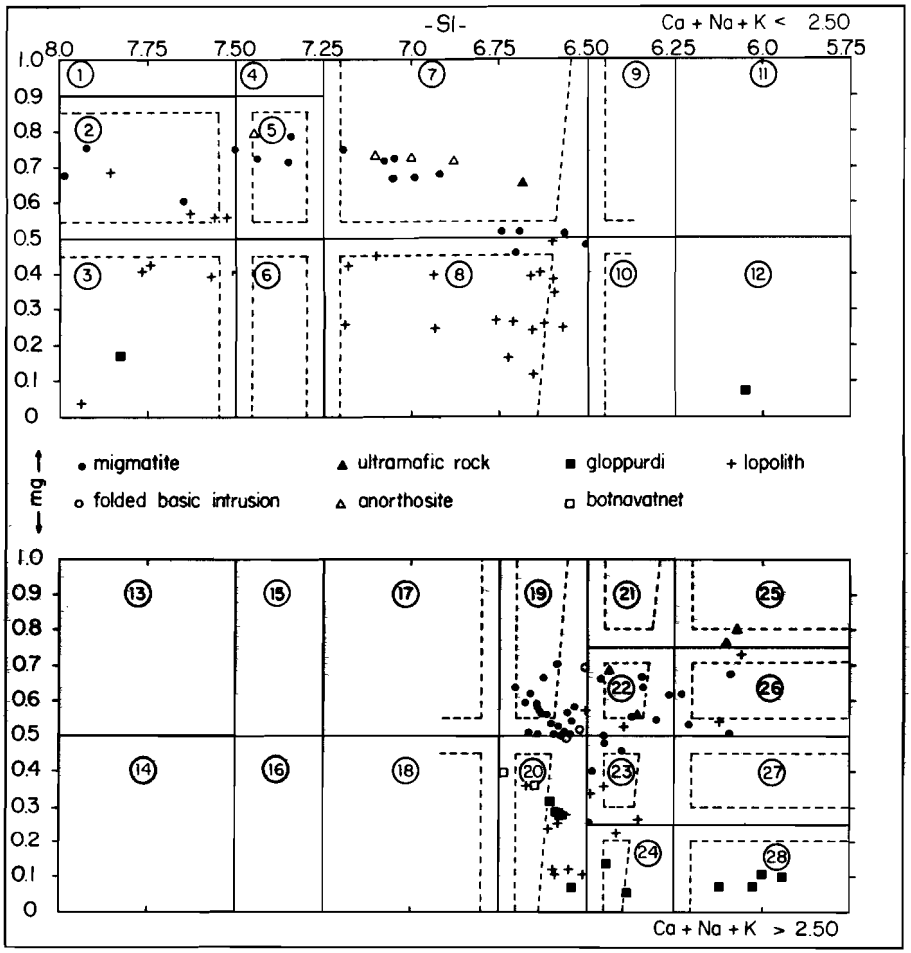

Figure IV.8.: Plotting of 137 amphibole analyses in Leake's system (1968). Only microprobe information on basis of 23(O) (table IV.8).
--- : border zone on both sides of a name transition line.

Names after Leake (1968) :

1: Tremolite
2: Actinolite
3: Ferro-actinolite
4: Tremolitic hornblende
5: Actinolitic hbl.
6: Ferro-actinolitic hbl.
7: Magnesio-hbl.
8: Ferro-hbl.
9: Tschermakitic hbl.
10: Ferro-tschermakitic hbl.
11: Tschermakite
12: Ferro-tschermakite
13: Richterite
14: Ferro-richterite
15: Richteritic edenite
16: Ferro-richteric edenite
17: Edenite
18: Ferro-edenite
19: Edenitic hbl.
20: Ferro-edenitic hbl.
21: Pargasitic hbl.
22. Ferroan pargasitic hbl.
23: Magnesian hastingsitic hbl.
24: Hastingsitic hbl.
25: Pargasite
26: Ferroan pargasite
27: Magnesian hastingsite
28: Hastingsite

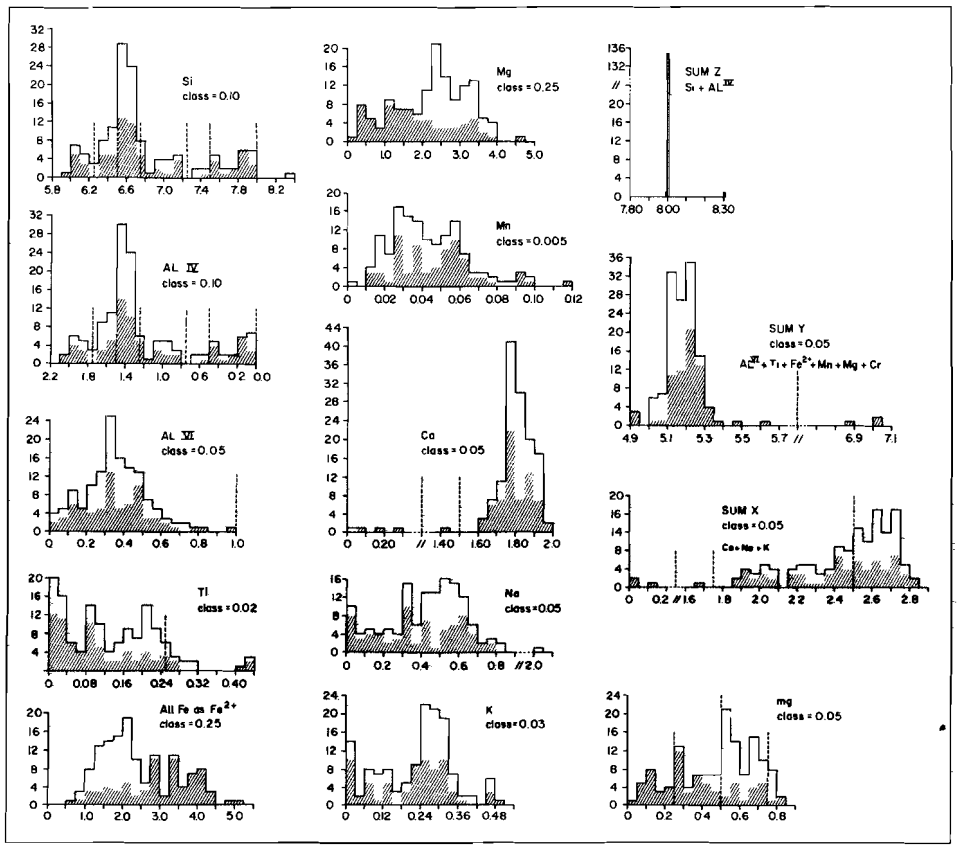

Figure IV.9.: 137 amphibole structural formulae as histograms of number of positions in half-unit cell (23 O) versus number of samples. Microprobe only.

--- : name transition according to Leake (1968). Shaded : samples from magmatic complexes; clear : other samples.

In the table (IV.8), the values are given in three figures behind the decimal point with the last figure rounded off to zero or five. Normally the third figure has no meaning at all, but for series of measurements in mineral transitions it may be useful to indicate small changes. The second figure behind the decimal point is needed because otherwise the name systems can not be used. This does not mean that the plot in the diagram is 100% accurate, a small spread around the plotted point must be taken into consideration. The reliability of the values is difficult to express in standard deviations because the formula is the result of a calculation based on nine element analyses, all influencing the formula to some extent. Anyway it should be realized that the given values may vary in the second figure behind the decimal point.

According to fig. IV.8 the names are determined for the Ca-amphiboles as presented in table I.1. To indicate the possibility of variations in the second figure behind the decimal point, border zones are drawn in fig. IV.8, with an arbitrary width of 0.05 ions for the mg-ratio, and calculated maximum variation widths of 0.05 and 0.05-0.15 ions for Ca + Na + K and Si respectively, the broad Si zone only holds on the low **Si-side** (section IV.2.6 for an extensive discussion). Samples situated within the border zones have been given two names in table I.1 (e.g., B 254). If the sample lies near a crossing of name transition lines, only one name is given with the addition : near cross (e.g., B 118 L). Names are dubious"facts"for solid solution series, especially when there are several systems to deduce these names. It is, therefore, advisable to give, beside the name, also the system used to derive the name, and eventually a second name if the sample is located near a name transition line. The Ca-amphiboles in this thesis are named according to this group of structural formulae, because it is the most reliable system (section IV.2.6). Non Ca-amphiboles are named in conformity with the 23(0), Z+Y= 13 group, because Fe^{3+} information is needed and wet chemical analyses were not possible for these amphiboles, due to material shortage.

IV.2.3. : Idealisation of the 23(0) structural formulae, calculation of the Fe^{3+} values

To get an idea of the Fe^{3+}/Fe^{2+} (or Fe^{3+}/Fe-total) ratio from microprobe measurements only, some authors calculate the Fe^{3+} value (Finger, 1972; Papike et al, 1974; Kroonenberg, 1976; De Roever et al, 1976). One of the methods, as used by Kroonenberg and De Roever et al (op.cit) is tried out here. It is assumed that no important elements are missing (the sum of the analyses should be about 98%).

Calculation method : Ions found in chapter IV.2.2 in Z- and Y-site are summed :

Si + Al + Fe + Mg + Mn + Ti + Cr = sum Z + Y

$$\frac{13.00}{\text{sum } Z+Y} = \text{"a"}$$

All cations, including Ca, Na and K, are multiplied by "a", to bring Z+Y to the ideal sum of 13 ions, and next by their valence. The sum of the last values (valence sum) will be 46 or, normally, less. The Fe^{3+} content is thought to be responsible for the missing charges, each Fe^{3+} ion adding one charge unit to the total. So 46.00 - valence sum = Fe^{3+}. The Fe^{2+} = Fe-Fe^{3+}. The wanted ratio can now be calculated. The values for the elements found after multiplying by "a", give the new structural formula values (see table IV.9 and fig. IV.10). This also makes it possible to plot the alkali- and Fe-Mg-amphiboles. The difference between fig. IV.8 and fig. IV.10 lies in the fact that Ca+Na+K and Si are lowered for most of the samples by this procedure, because Z+Y for 23(0) normally exceeds the ideal sum of 13. Therefore several samples went from the Ca+Na+K > 2.50 figure to the <2.50 figure, and to the right side of both figures (see section IV.2.4., IV.2.5. and IV.2.6. for a discussion).

	A 037 B	A 128	A 168	B1016 1	B1016 2	B2016	B 118	B 254	B 322	D 172 D	D 307	D 442
Si	6.04	6.16	7.99	6.79	7.055	7.915	6.49	6.085	6.29	6.54	6.45	6.48
Al	1.96	1.84	.01	1.21	.945	.085	1.51	1.915	1.71	1.46	1.55	1.52
Al	.66	.52	.04	.20	.16	.08	.14	.44	.37	.26	.385	.41
Ti	.165	.20	.11	.095	.08	.01	.205	.425	.21	.215	.305	.14
Fe^{3+}	.375	.515	1.70	.95	.81	.00	.62	.085	.565	.41	.06	.49
Fe^{2+}	.965	1.095	1.14	1.89	1.88	3.84	1.56	1.935	1.365	1.66	1.38	1.675
Mn	.025	.03	.00	.035	.04	.115	.035	.025	.015	.03	.015	.04
Mg	2.81	2.64	2.01	1.83	2.03	2.675	2.44	2.09	2.475	2.425	2.855	2.245
Ca	1.91	1.84	.025	1.71	1.715	.255	1.725	1.775	1.77	1.80	1.845	1.79
Na	.39	.455	1.965	.33	.315	.025	.58	.69	.605	.48	.53	.515
K	.38	.275	.025	.125	.08	.005	.305	.30	.21	.275	.28	.25
Z	8.00	8.00	8.00	8.00	8.00	8.00	8.00	8.00	8.00	8.00	8.00	8.00
Y	5.00	5.00	5.00	5.00	5.00	7.00	5.00	5.00	5.00	5.00	5.00	5.00
X	2.68	2.57	2.015	2.165	2.11	.005	2.61	2.765	2.585	2.555	2.655	2.555
mg	.675	.62	.41	.39	.425	.405	.525	.505	.56	.535	.66	.505

	D 444	E 067	E 125	E 128 1	E 128 2	E 131	E1167	E2167	E 170	E1232 K	E1232 R	E2232 H
Si	6.295	6.465	6.11	6.07	6.11	5.97	6.49	7.915	6.335	6.555	6.485	7.77
Al	1.705	1.535	1.89	1.93	1.89	2.03	1.51	.04	1.665	1.445	1.515	.23
Al	.355	.165	.47	.455	.45	.495	.135	.00	.33	.295	.38	.015
Ti	.225	.215	.425	.435	.415	.195	.24	.01	.235	.085	.07	.005
Fe^{3+}	.755	.805	.07	.00	.00	.705	.69	.185	.425	.715	.725	.485
Fe^{2+}	1.605	2.605	1.79	.755	.725	.42	3.385	4.59	1.655	2.025	2.20	1.025
Mn	.04	.04	.025	.01	.01	.035	.075	.06	.03	.05	.05	.025
Mg	2.02	1.17	2.215	3.12	3.20	3.15	0.475	.20	2.31	1.83	1.575	3.445
Cr			.005	.165	.145	.00			.015			
Ca	1.665	1.64	1.755	1.785	1.795	1.75	1.655	1.935	1.78	1.87	1.855	1.835
Na	.655	.605	.685	.755	.75	.715	.625	.045	.645	.30	.305	.03
K	.17	.255	.30	.235	.225	.22	.275	.01	.215	.225	.245	.015
Z	8.00	8.00	8.00	8.00	8.00	8.00	8.00	7.955	8.00	8.00	8.00	8.00
Y	5.00	5.00	5.00	4.94	4.945	5.00	5.00	5.045	5.00	5.00	5.00	5.00
X	2.49	2.50	2.74	2.775	2.77	2.685	2.555	1.99	2.64	2.395	2.405	1.88
mg	.455	.255	.54	.80	.815	.73	.105	.04	.525	.40	.345	.69

	E2232 I	E2232 2	E2232 3	E2232 4	E2232 5	E3232 M	F 005	F1043	F2043	F1052 D	F2052 O	F3052 L
Si	7.80	7.775	7.755	7.49	6.53	6.50	6.585	6.515	7.975	6.585	NA	6.58
Al	.20	.225	.245	.51	1.47	1.50	1.415	1.485	.025	1.415	.	1.42
Al	.02	.055	.045	.125	.36	.39	.21	.25	.04	.19	.	.155
Ti	.005	.005	.005	.02	.09	.085	.185	.115	.00	.185	.	.20
Fe^{3+}	.45	.45	.47	.48	.725	.71	.425	.565	.05	.36	.	.38
Fe^{2+}	1.025	1.075	1.075	1.225	1.59	1.56	1.42	1.65	1.50	1.575	.	1.53
Mn	.025	.025	.025	.025	.025	.025	.05	.09	.085	.055	.	.065
Mg	3.475	3.39	3.38	3.125	2.21	2.23	2.71	2.33	3.325	2.635	.	2.67
Ca	1.835	1.82	1.83	1.85	1.815	1.81	1.815	1.845	1.94	1.80	.	1.79
Na	.03	.045	.04	.095	.315	.325	.52	.485	.045	.615	.	.62
K	.015	.02	.02	.07	.27	.29	.26	.275	.01	.28	.	.28
Z	8.00	8.00	8.00	8.00	8.00	8.00	8.00	8.00	8.00	8.00	.	8.00
Y	5.00	5.00	5.00	5.00	5.00	5.00	5.00	5.00	5.00	5.00	.	5.00
X	1.88	1.885	1.89	2.015	2.40	2.425	2.595	2.60	1.995	2.695	.	2.69
mg	.70	.69	.68	.64	.49	.49	.59	.505	.67	.57	.	.57

	F4052 L	F 070	F 074	F1107 D	F2107 D	F1126	F2126	F1252	F2252 1	F2252 2	F2252 3	F1433
Si	7.365	6.495	6.56	6.44	6.46	6.485	NA	6.616	6.985	7.305	7.445	6.525
Al	.635	1.505	1.44	1.56	1.56	1.515	.	1.385	1.015	.695	.555	1.475
Al	.065	.215	.28	.25	.30	.275	.	.205	.16	.155	.035	.26
Ti	.035	.165	.155	.225	.175	.22	.	.17	.035	.025	.02	.105
Fe^{3+}	.445	.51	.43	.545	.595	.52	.	.42	.41	.295	.38	.48
Fe^{2+}	.835	1.70	1.545	1.59	1.485	1.675	.	1.42	1.135	1.03	.81	3.515
Mn	.055	.05	.03	.03	.025	.045	.	.045	.045	.045	.045	.09
Mg	3.565	2.36	2.55	2.36	2.42	2.265	.	2.74	3.215	3.45	3.71	.55
Ca	1.815	1.82	1.84	1.76	1.785	1.785	.	1.825	1.955	1.945	1.91	1.75
Na	.315	.515	.45	.48	.41	.42	.	.52	.31	.24	.23	.70
K	.11	.30	.285	.315	.32	.285	.	.26	.155	.075	.06	.315
Z	8.00	8.00	8.00	8.00	8.00	8.00	.	8.00	8.00	8.00	8.00	8.00
Y	5.00	5.00	5.00	5.00	5.00	5.00	.	5.00	5.00	5.00	5.00	5.00
X	2.24	2.635	2.575	2.555	2.515	2.49	.	2.605	2.42	2.26	2.20	2.765
mg	.725	.51	.56	.52	.53	.50	.	.59	.67	.735	.75	.12

Table IV.9.: Amphibole analyses : half-unit cell contents; 23 O, Z+Y=13, Fe^{3+} calculated, NA : not analyzed.

	P2439	M1047 B	M2047 B	M1050	M2050	M 307	M 325	M 415	J 119	LJ143 M	LJ143 1	LJ143 2
Si	6.43	6.845	.NA	6.565	.NA	6.255	6.17	6.465	6.32	6.89	7.365	6.755
Al	1.57	1.355	.	1.435		1.745	1.83	1.535	1.68	1.11	.635	1.245
Al	.235	.21	.	.175	.	.35	.425	.14	.275	.28	.095	.31
Ti	.11	.18	.	.21	.	.325	.25	.245	.27	.02	.04	.01
Fe^{3+}	.585	.38		.435	.	.365	.705	.515	.38	.73	.525	.84
Fe^{2+}	3.49	1.225	.	1.08	.	1.60	.93	1.575	1.59	.54	.47	.47
Mn	.09	.04	.	.03	.	.055	.02	.04	.025	.015	.01	.015
Mg	.49	2.965	.	3.07	.	2.405	2.675	2.485	2.46	3.415	3.86	3.355
Ca	1.785	1.805	.	1.785	.	1.855	1.685	1.765	1.815	1.855	1.88	1.85
Na	.635	.555	.	.55	.	.475	.745	.56	.485	.235	.12	.25
K	.33	.25	.	.285	.	.40	.09	.305	.345	.12	.06	.125
Z	8.00	8.00	.	8.00	.	8.00	8.00	8.00	8.00	8.00	8.00	8.00
Y	5.00	5.00	.	5.00	.	5.00	5.00	5.00	5.00	5.00	5.00	5.00
X	2.75	2.605	.	2.62	.	2.73	2.52	2.63	2.645	2.21	2.06	2.225
mg	.105	.645	.	.67	.	.54	.62	.54	.55	.73	.795	.715

	LJ143 3	L2143	M 101	N1041 1	N1041 2	N1041 3	N2041 1	N2041 2	N2041 3	N1264	N2264 M	N2264 J
Si	6.995	7.84	6.515	6.89	6.80	6.945	6.965	7.075	7.215	6.585	7.895	7.965
Al	1.005	.16	1.485	1.11	1.20	1.055	1.035	.925	.785	1.415	.095	.03
Al	.275	.045	.165	.29	.205	.25	.28	.235	.145	.16	.00	.00
Ti	.015	.005	.205	.075	.085	.03	.015	.00	.00	.175	.00	.00
Fe^{3+}	.69	.09	.455	.655	.795	.70	.745	.78	.815	.535	.195	.13
Fe^{2+}	.525	2.075	.885	.81	.68	.57	.535	.385	.205	1.21	.995	.935
Mn	.02	.06	.025	.04	.04	.035	.04	.03	.025	.03	.03	.025
Mg	3.47	4.535	3.265	3.13	3.195	3.415	3.385	3.57	3.81	2.89	3.79	3.91
Ca	1.845	.19	1.79	1.76	1.74	1.74	1.73	1.73	1 715	1.79	1.925	1.935
Na	.195	.02	.535	.35	.395	.42	.38	.335	.30	.55	.06	.03
K	.12	.005	.35	.145	.765	.14	.13	.11	.10	.245	.01	.005
Z	8.00	8.00	8.00	8.00	8.00	8.00	8.00	8.00	8.00	8.00	7.99	7.995
Y	5.00	7.00	5.00	5.00	5.00	5.00	5.00	5.00	5.00	5.00	5.01	5.005
X	2.16	.025	2.675	2.255	2.30	2.30	2.24	2.175	2.115	2.585	1.995	1.97
mg	.735	.67	.705	.675	.68	.725	.72	.75	.785	.62	.755	.78

	N 317	N 337	M1402 1	N1402 2	N2402	N1528	N2528	N3528	N4528	N1572 R	N1572 K	N2572 O
Si	6.16	6.47	6.44	6.465	6.585	6.335	.NA	6.215	.NA	6.02	6.06	.NA
Al	1.84	1.53	1.56	1.535	1.415	1.665	.	1.765	.	1.98	1.94	.
Al	.365	.225	.105	.105	.20	.20	.	.405	.	.55	.575	.
Ti	.31	.20	.24	.265	.155	.255	.	.09	.	.205	.205	.
Fe^{3+}	.365	.46	.855	.735	.865	.575	.	.R7	.	.635	.68	.
Fe^{2+}	1.61	1.40	2.455	2.52	2.505	2.90	.	2.385	.	.35	.285	.
Mn	.025	.03	.05	.05	.045	.035	.	.03	.	.01	.01	.
Mg	2.325	2.685	1.295	1.325	1.23	1.035	.	1.22	.	3.25	3.245	.
Ca	1.78	1.785	1.61	1.62	1.655	1.74	.	1.74	.	1.73	1.695	.
Na	.615	.55	.64	.65	.49	.585	.	.515	.	.825	.79	.
K	.31	.355	.255	.27	.245	.305	.	.31	.	.10	.10	.
Z	8.00	8.00	8.00	8.00	8.00	8.00	.	8.00	.	8.00	8.00	.
Y	5.00	5.00	5.00	5.00	5.00	5.00	.	5.00	.	5.00	5.00	.
X	2.705	2.69	2.505	2.54	2.39	2.63	.	2.565	.	2.655	2.585	.
mg	.535	.585	.28	.265	.265	.225	.	.27	.	.765	.77	.

	N 809	N1827 1	N1827 2	N1827 3	N1827 4	N2827 1	N2827 2	N2827 3	O 100	P1097	P2097	P 248
Si	6.405	6.38	7.00	6.515	6.345	7.425	7.55	7.48	6.49	6.58	6.64	6.43
Al	1.595	1.62	1.00	1.485	1.655	.575	.45	.52	1.51	1.42	1.36	1.57
Al	.235	.41	.215	.34	.425	.04	.075	.08	.32	.115	.10	.235
Ti	.285	.04	.04	.05	.07	.02	.02	.025	.275	.175	.075	.225
Fe^{3+}	.255	.785	.66	.775	.75	.55	.49	.485	.125	.475	.70	.525
Fe^{2+}	1.14	2.14	1.895	1.925	2.075	1.565	1.57	1.61	1.24	2.51	2.21	1.375
Mn	.015	.055	.05	.05	.05	.055	.05	.05	.01	.025	.025	.045
Mg	3.07	1.57	2.14	1.86	1.63	2.77	2.795	2.75	3.03	1.70	1.89	2.59
Ca	1.825	1.88	1.875	1.865	1.865	1.845	1.855	1.87	1.86	1.765	1.74	1.78
Na	.64	.315	.175	.30	.33	.10	.09	.10	.525	.615	.60	.505
K	.245	.27	.13	.24	.28	.06	.05	.06	.27	.33	.32	.295
Z	8.00	8.00	8.00	8.00	8.00	8.00	8.00	8.00	8.00	8.00	8.00	8.00
Y	5.00	5.00	5.00	5.00	5.00	5.00	5.00	5.00	5.00	5.00	5.00	5.00
X	2.71	2.465	2.18	2.405	2.475	2.005	1.995	2.03	2.655	2.71	2.66	2.58
mg	.685	.345	.45	.405	.36	.56	.57	.56	.69	.36	.39	.57

Table IV.9.: continued

	P 303 1	P 303 2	P1580 D	P2580 L	R 227	R1229	R2229 1	R2229 2	R2229 3	R3229	R1269 1	R1269 2
Si	6.56	6.505	6.255	6.255	6.565	6.495	6.79	6.525	7.165	7.975	6.435	6.625
Al	1.44	1.495	1.745	1.745	1.435	1.515	1.21	1.475	.835	.025	1.565	1.375
Al	.23	.26	.405	.43	.195	.175	.135	.15	.255	.07	.33	.28
Ti	.195	.205	.10	.10	.195	.15	.035	.145	.09	.00	.05	.045
Fe^{3+}	.405	.43	.64	.615	.68	.79	.93	.90	.13	.00	.89	.91
Fe^{2+}	1.565	1.58	.84	.97	2.235	2.72	2.665	2.625	3.715	5.06	2.515	2.425
Mn	.05	.045	.015	.025	.025	.035	.035	.035	.035	.09	.055	.055
Mg	2.555	2.48	3.00	2.86	1.67	1.12	1.20	1.145	1.365	1.62	1.16	1.285
Ca	1.80	1.78	1.83	1.81	1.70	1.73	1.76	1.725	1.40	.09	1.80	1.735
Na	.55	.57	.535	.545	.53	.50	.385	.43	.15	.025	.41	.445
K	.27	.27	.305	.325	.245	.265	.18	.245	.11	.00	.225	.18
Z	8.00	8.00	8.00	8.00	8.00	8.00	8.00	8.00	8.00	8.00	8.00	8.00
Y	5.00	5.00	5.00	5.00	5.00	5.00	5.00	5.00	7.00	6.955	5.00	5.00
X	2.82	2.62	2.67	2.68	2.475	2.495	2.325	2.40	.26	.00	2.435	2.36
mg	.56	.545	.665	.64	.36	.24	.25	.245	.26	.24	.25	.275

	R1269 3	R2269 1	R2269 2	R2269 3	R 356 1	R 356 2	R 356 3	R 356 4	R1668	R2668	V 147	V1187
Si	6.495	7.455	7.645	7.605	6.415	6.575	6.54	6.475	6.505	6.48	6.375	6.425
Al	1.505	.545	.345	.395	1.585	1.425	1.46	1.525	1.495	1.52	1.625	1.575
Al	.325	.00	.00	.01	.165	.185	.155	.13	.155	.16	.41	.28
Ti	.06	.08	.025	.02	.195	.095	.115	.105	.175	.08	.095	.24
Fe^{3+}	.905	.69	.735	.805	.95	1.04	1.195	1.25	.55	.805	.835	.195
Fe^{2+}	2.445	2.245	2.135	2.00	3.085	2.835	2.64	2.885	2.725	2.52	2.48	2.09
Mn	.055	.03	.065	.06	.05	.04	.035	.045	.055	.06	.02	.02
Mg	1.21	1.955	2.05	2.105	.555	.805	.86	.585	1.34	1.375	1.155	2.175
Ca	1.755	1.745	1.72	1.725	1.605	1.67	1.62	1.645	1.755	1.755	1.715	1.895
Na	.44	.15	.12	.07	.58	.425	.425	.405	.63	.595	.445	.385
K	.205	.045	.025	.02	.30	.245	.215	.24	.305	.295	.315	.445
Z	8.00	8.00	7.99	8.00	8.00	8.00	8.00	8.00	8.00	8.00	8.00	8.00
Y	5.00	5.00	5.01	5.00	5.00	5.00	5.00	5.00	5.00	5.00	5.00	5.00
X	2.40	1.94	1.865	1.815	2.485	2.34	2.26	2.29	2.69	2.645	2.475	2.725
mg	.26	.395	.41	.425	.12	.17	.18	.125	.285	.29	.255	.485

	V2187 1	V2187 2	V 276	V 277	V 363	W D12 D	W D17 8	W 162 D	W 196 B	W 217	W1226 D	W2226 L
Si	7.39	6.65	6.285	6.485	6.54	6.575	6.49	6.565	6.395	6.35	6.575	6.485
Al	.41	1.35	1.715	1.515	1.46	1.425	1.51	1.435	1.605	1.65	1.425	1.515
Al	.035	.265	.215	.13	.19	.255	.30	.195	.295	.225	.345	.32
Ti	.015	.085	.08	.165	.14	.12	.22	.13	.195	.17	.08	.235
Fe^{3+}	.37	.605	1.15	.845	.67	.79	.58	.71	.825	.98	.76	.48
Fe^{2+}	1.57	1.62	2.855	2.34	1.56	1.385	1.555	1.515	1.48	1.70	.76	1.435
Mn	.02	.02	.075	.035	.07	.055	.04	.07	.035	.08	.025	.03
Mg	2.99	2.415	.625	1.485	2.37	2.395	2.305	2.38	2.17	1.845	3.03	2.50
Ca	1.90	1.89	1.655	1.675	1.775	1.725	1.79	1.765	1.75	1.665	1.755	1.765
Na	.115	.265	.55	.56	.50	.46	.435	.495	.465	.515	.46	.485
K	.06	.28	.33	.30	.26	.235	.235	.25	.195	.26	.19	.235
Z	8.00	8.00	8.00	8.00	8.00	8.00	8.00	8.00	8.00	8.00	8.00	8.00
Y	5.00	5.00	5.00	5.00	5.00	5.00	5.00	5.00	5.00	5.00	5.00	5.00
X	2.075	2.435	2.535	2.535	2.535	2.42	2.46	2.51	2.41	2.44	2.405	2.485
mg	.605	.52	.135	.315	.305	.52	.515	.51	.68	.40	.66	.56

	Y2055	Y2055 1	Y2055 2	Y3128 1	Y3128 2	Y2128	Y3131 1	Y3131 2	Y2131	Y3131 R	Y3131 K
Si	6.41	6.425	6.535	6.275	6.435	7.83	5.89	5.875	5.88	5.995	5.95
Al	1.59	1.575	1.465	1.725	1.565	.17	2.11	2.12	2.12	2.005	2.05
Al	.255	.345	.115	.35	.28	.005	.615	.585	.54	.475	.875
Ti	.23	.01	.14	.095	.13	.03	.03	.025	.19	.01	.005
Fe^{3+}	.325	.95	1.135	.76	.725	.00	.995	.965	.52	.985	.78
Fe^{2+}	1.91	1.36	1.42	3.47	3.485	3.98	2.99	2.925	3.28	3.13	3.22
Mn	.015	.015	.015	.065	.07	.09	.045	.045	.045	.06	.06
Mg	2.265	2.32	2.175	0.26	.31	.83	.325	.455	.425	.34	.30
Ca	1.855	1.785	1.63	1.75	1.72	1.83	1.855	1.88	1.895	1.90	1.76
Na	.395	.225	.295	.55	.545	.365	.275	.32	.415	.25	.155
K	.445	.465	.38	.375	.315	.21	.455	.445	.47	.48	.235
Z	8.00	8.00	8.00	8.00	8.00	8.00	8.00	8.00	8.00	8.00	8.00
Y	5.00	5.00	5.00	5.00	5.00	4.935	5.00	5.00	5.00	5.00	7.00
X	2.695	2.475	2.305	2.675	2.58	2.34	2.585	2.645	2.78	2.63	.39
mg	.50	.50	.46	.055	.07	.165	.075	.105	.10	.073	.07

Table IV.9.: continued

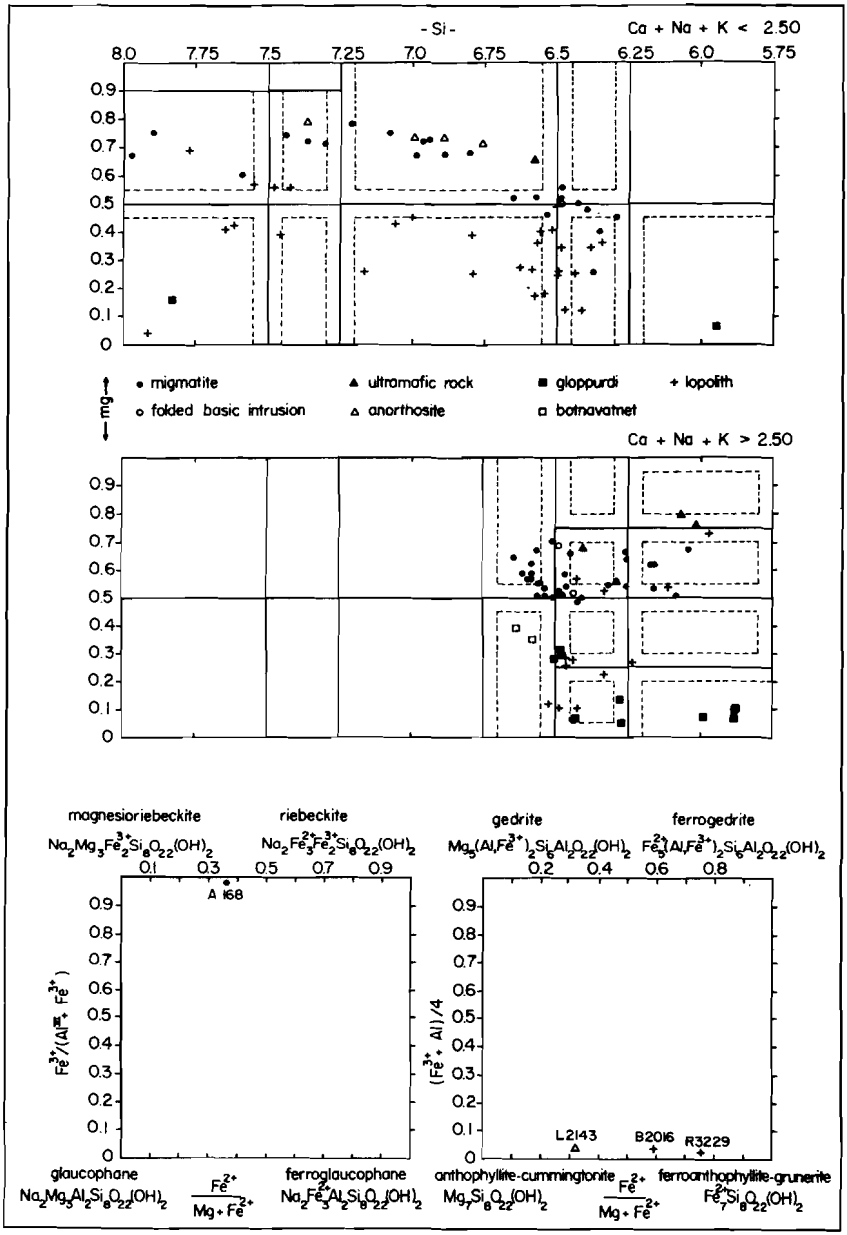

Figure IV.10.: Plotting of 137 amphibole analyses in Leake's system (above), and Ernst's (below) (1968). Microprobe information on basis of 23(O), Z+Y=13 and Fe^{3+} calculated. Names : see fig. IV.8.

IV.2.4. : Complete analysis; 24(O,OH,F) method.

Calculation again according to Deer, Howie and Zussman, using the F-correction (op.cit, p. 517). See table IV.10.
All analytical errors (as discussed in section IV.1.3. and IV.1.4.) influence this formula, see section IV.2.1.
Most important is the Fe^{3+} information, which may be compared with the calculated value (section IV.2.3.). The oxidation ratios are inserted in the table. Fig. IV.11 shows the "relation" between the calculated and measured ratios. No clear relationship is to be seen. The reason for the deviation (assuming that the measured value is about right) must be plural, which means that the calculated value does not give a direct reliable indication. This result shows that the statement of De Roever (op.cit, p. 232) about this Fe^{3+} calculation procedure is not well-founded, especially because he uses the Fe^{3+}-content for all kinds of graphs and conclusions. He stated : "The validity of this procedure was checked previously (De Roever et al, 1974) by wet chemical determination of the FeO content of one amphibole, giving $Fe^{2+}/Fe^{2+}+Fe^{3+}$ 0.65 and $0.68_{av.}$ respectively for wet chemical and calculated microprobe analysis". His 1974-paper does not give any more information about the reliability, only some vague passage : "... proved to be in good accordance ...". If De Roever wants to use this calculation method for the blue amphiboles, he will have to state a better case about the reliability.

IV.2.5. : Evaluation of the Fe^{3+} calculation method

The main cause of the difference between the calculated and measured Fe^{3+}/Fe-total is the assumption that SUM Y contains exactly 5.00 cations of Al^{VI}, Ti, Fe^{3+}, Fe^{2+}, Mn, (Cr), and Mg, and that none of these elements is located, partly, in the X-position, or some Ca in the Y-site. A second reason is the fact that the microprobe analysis is supposed to be 100% exact.

	A 037 B	A 128	B 118	B 254	B 322	D 307	D 442	D 444	E 067	E 125	E1167	E 170
Si	6.055	6.29	6.54	6.17	6.31	6.43	6.52	6.375	6.49	6.07	6.485	6.355
Al	1.945	1.71	1.46	1.83	1.69	1.57	1.48	1.625	1.51	1.93	1.515	1.645
Al	.685	.705	.20	.56	.395	.36	.465	.455	.195	.415	.125	.355
Ti	.165	.20	.21	.43	.21	.305	.14	.225	.22	.425	.24	.235
Fe^{3+}	.405	.385	.46	.365	.42	.275	.505	.535	.70	.32	.84	.295
Fe^{2+}	.94	1.26	1.78	1.685	1.515	1.16	1.675	1.855	2.72	1.525	3.23	1.79
Mn	.025	.025	.035	.025	.015	.015	.04	.04	.04	.025	.075	.03
Mg	2.815	2.695	2.455	2.315	2.48	2.84	2.26	2.04	1.175	2.195	.475	2.315
Cr										.005		.02
Ca	1.915	1.875	1.74	1.80	1.775	1.84	1.80	1.685	1.645	1.74	1.655	1.785
Na	.395	.465	.585	.70	.605	.53	.515	.66	.61	.68	.62	.65
K	.38	.285	.305	.305	.21	.28	.25	.175	.25	.295	.275	.22
Z	8.00	8.00	8.00	8.00	8.00	8.00	8.00	8.00	8.00	8.00	8.00	8.00
Y	5.035	5.27	5.14	5.18	5.035	4.955	5.085	5.15	5.05	4.91	4.985	5.04
X	2.69	2.625	2.63	2.805	2.59	2.65	2.565	2.52	2.505	2.715	2.55	2.655
mg	.675	.615	.52	.505	.56	.66	.505	.455	.255	.54	.105	.525
OH	1.44	.86	.815	.965	1.725	1.355	1.51	1.555	1.76	1.865	1.73	1.62
F	.43	.335	.915	.105	.275	.57	.19	.135	.17	.17	.17	.375
Σ Fluid	1.87	1.215	1.73	1.07	2.00	1.925	1.70	1.67	1.93	2.035	1.90	1.995
I	.30	.23	.21	.18	.22	.19	.23	.22	.20	.17	.21	.14
II	.28	.32	.28	.04	.29	.04	.23	.32	.24	.04	.17	.20

	F 005	F1043	F1052 D	F3052 L	F 070	F1107 D	F1126	F1232	F1433	H1047 B	H1050	H 307
Si	6.605	6.525	6.57	6.58	6.495	6.455	6.525	6.64	6.59	6.69	6.61	6.30
Al	1.395	1.475	1.43	1.42	1.505	1.545	1.475	1.36	1.41	1.31	1.39	1.70
Al	.24	.26	.17	.155	.215	.27	.33	.24	.34	.265	.23	.41
Ti	.185	.115	.185	.20	.165	.225	.225	.17	.11	.185	.215	.23
Fe^{3+}	.63	.75	.545	.53	.505	.505	.635	.665	.665	.555	.55	.62
Fe^{2+}	1.22	1.465	1.39	1.385	1.705	1.64	1.575	1.185	3.37	1.06	.98	1.36
Mn	.05	.095	.055	.065	.05	.03	.045	.045	.09	.045	.03	.055
Mg	2.72	2.33	2.63	2.665	2.36	2.36	2.27	2.745	.555	2.98	3.085	2.42
Ca	1.825	1.85	1.795	1.78	1.82	1.765	1.80	1.83	1.77	1.81	1.80	1.87
Na	.52	.485	.615	.62	.515	.48	.42	.52	.71	.56	.555	.48
K	.26	.275	.28	.275	.30	.315	.285	.26	.32	.25	.285	.40
Z	8.00	8.00	8.00	8.00	8.00	8.00	8.00	8.00	8.00	8.00	8.00	8.00
Y	5.045	5.015	4.975	5.00	5.00	5.03	5.08	5.05	5.13	5.09	5.09	5.095
X	2.605	2.61	2.69	2.675	2.635	2.56	2.50	2.61	2.80	2.62	2.64	2.75
mg	.59	.50	.57	.575	.51	.52	.50	.59	.12	.64	.665	.545
OH	1.295	1.41	1.43	1.42	NA	1.54	1.40	1.41	1.24	1.125	.93	1.025
F	.35	.33	.48	.475	NA	.40	.203	.17	.145	.395	.63	.375
Σ Fluid	1.645	1.74	1.93	1.895	NA	1.94	1.603	1.58	1.385	1.52	1.56	1.40
I	.34	.34	.28	.28	.23	.24	.29	.36	.16	.34	.36	.31
II	.23	.26	.19	.20	.23	.26	.24	.23	.12	.24	.29	.19

	H 325	H 415	J 119	M 101	N1041 1	N1041 2	N1041 3	N2041 1	N2041 2	N2041 3	N1264	N 317
Si	6.29	6.515	6.295	6.53	7.00	6.96	7.07	7.085	7.17	7.285	6.645	6.23
Al	1.71	1.485	1.705	1.47	1.00	1.04	.93	.915	.83	.715	1.355	1.77
Al	.59	.20	.245	.185	.425	.395	.40	.425	.35	.225	.235	.465
Ti	.255	.25	.27	.205	.08	.085	.03	.015	.00	.00	.175	.315
Fe^{3+}	.465	.575	.655	.59	.35	.27	.23	.28	.30	.32	.605	.48
Fe^{2+}	1.205	1.53	1.31	.76	1.14	1.24	1.06	1.025	.88	.71	1.155	1.52
Mn	.02	.04	.02	.025	.04	.04	.035	.035	.03	.03	.035	.025
Mg	2.72	2.50	2.45	3.275	3.17	3.27	3.475	3.44	3.615	3.85	2.915	2.345
Ca	1.715	1.775	1.81	1.795	1.785	1.775	1.77	1.76	1.755	1.735	1.81	1.80
Na	.76	.565	.48	.54	.355	.405	.425	.385	.34	.305	.555	.62
K	.09	.305	.345	.355	.145	.165	.145	.13	.115	.10	.25	.315
Z	8.00	8.00	8.00	8.00	8.00	8.00	8.00	8.00	8.00	8.00	8.00	8.00
Y	5.255	5.105	4.95	5.04	5.205	5.30	5.23	5.22	5.175	5.135	5.12	5.15
X	2.565	2.645	2.635	2.69	2.285	2.345	2.335	2.275	2.21	2.14	2.615	2.735
mg	.615	.54	.55	.705	.675	.68	.725	.72	.75	.785	.62	.535
OH	1.28	1.03	1.535	.84	1.265	1.17	1.335	1.36	1.49	1.625	1.14	1.17
F	.06	.58	.405	.89	.325	.305	.34	.35	.385	.415	.35	.20
Σ Fluid	1.34	1.61	1.94	1.93	1.59	1.475	1.775	1.71	1.875	2.04	1.49	1.37
I	.28	.27	.33	.44	.23	.18	.18	.21	.25	.31	.34	.24
II	.43	.25	.19	.34	.43	.54	.55	.57	.67	.80	.31	.18

Table IV.10.: Amphibole analyses : half-unit cell contents; 24(O), including Fe_2O_3, H_2O^+ and F analyses. I : Fe^{3+}/Fe^T measured. II : Fe^{3+}/Fe^T calculated.

	N 337	N1402 1	N1402 2	N1572 R	N1572 K	N 809	N1827 1	N1827 2	N1827 3	N1827 4	O 100	P 303 1
Si	6.525	6.57	6.585	6.11	6.195	6.50	6.41	7.025	6.55	6.345	6.55	6.69
Al	1.475	1.43	1.415	1.89	1.805	1.50	1.59	.975	1.45	1.655	1.45	1.31
Al	.29	.27	.255	.68	.77	.355	.455	.245	.385	.42	.40	.395
Ti	.205	.245	.27	.21	.21	.29	.04	.04	.05	.07	.28	.20
Fe^{3+}	.30	.715	.66	.195	.19	.30	.565	.49	.52	.545	.175	.32
Fe^{2+}	1.575	2.66	2.66	.80	.80	1.12	2.375	2.075	2.195	2.285	1.205	1.685
Mn	.03	.05	.055	.01	.01	.015	.055	.05	.055	.05	.01	.05
Mg	2.71	1.32	1.345	3.30	3.315	3.12	1.58	2.145	1.865	1.735	3.06	2.61
Ca	1.80	1.64	1.65	1.755	1.735	1.85	1.885	1.88	1.875	1.865	1.88	1.835
Na	.555	.655	.665	.84	.805	.65	.315	.175	.305	.33	.53	.565
K	.34	.26	.275	.10	.10	.25	.275	.13	.245	.28	.27	.275
Z	8.00	8.00	8.00	8.00	8.00	8.00	8.00	8.00	8.00	8.00	8.00	8.00
Y	5.11	5.26	5.245	5.195	5.295	5.20	5.07	5.045	5.07	5.105	5.13	5.26
X	2.695	2.555	2.59	2.695	2.64	2.75	2.475	2.185	2.425	2.475	2.68	2.675
mg	.585	.28	.285	.765	.77	.685	.345	.45	.405	.375	.69	.56
OH	.87	1.005	1.005	1.715	1.43	.76	NA	NA	NA	NA	1.15	.775
F	.91	.22	.22	.03	.03	.515	.06	.06	.06	.06	.35	.40
Σ Fluid	1.78	1.225	1.225	1.745	1.46	1.275	NA	NA	NA	NA	1.50	1.175
I	.16	.21	.20	.20	.19	.21	.19	.19	.19	.19	.13	.16
II	.25	.26	.23	.64	.72	.18	.27	.26	.29	.27	.09	.21

	P 303 2	P1580 D	P2580 L	R1668	V1187	V 363	W 012	W017 B	W 196 B	W1226 D
Si	6.635	6.45	6.45	6.62	6.48	6.675	6.74	6.67	6.61	6.78
Al	1.365	1.55	1.55	1.38	1.52	1.325	1.26	1.33	1.39	1.22
Al	.425	.67	.695	.295	.355	.355	.46	.53	.575	.605
Ti	.21	.10	.10	.18	.245	.14	.12	.23	.20	.085
Fe^{3+}	.33	.42	.44	.22	.255	.16	.385	.38	.38	.31
Fe^{2+}	1.72	1.105	1.185	3.115	2.045	2.11	1.845	1.81	2.005	1.26
Mn	.05	.015	.025	.06	.02	.07	.055	.045	.03	.03
Mg	2.53	3.09	2.945	1.365	2.20	2.415	2.455	2.365	2.245	3.12
Ca	1.815	1.885	1.865	1.785	1.91	1.81	1.765	1.84	1.81	1.81
Na	.585	.555	.56	.64	.39	.51	.47	.45	.48	.475
K	.275	.315	.34	.31	.45	.265	.24	.245	.20	.19
Z	8.00	8.00	8.00	8.00	8.00	8.00	8.00	8.00	8.00	8.00
Y	5.265	5.40	5.39	5.235	5.12	5.25	5.32	5.36	5.435	5.41
X	2.675	2.755	2.765	2.735	2.75	2.585	2.475	2.535	2.49	2.475
mg	.545	.665	.64	.285	.485	.51	.52	.515	.48	.66
OH	.775	.635	.64	.905	.905	1.04	.945	.73	.625	.81
F	.405	.165	.17	.615	.615	.565	.325	.15	.225	.23
Σ Fluid	1.18	.80	.81	1.52	1.52	1.605	1.27	.88	.85	1.04
I	.16	.28	.27	.07	.11	.07	.17	.17	.16	.20
II	.21	.43	.39	.17	.09	.30	.36	.27	.36	.50

Table IV.10.: continued

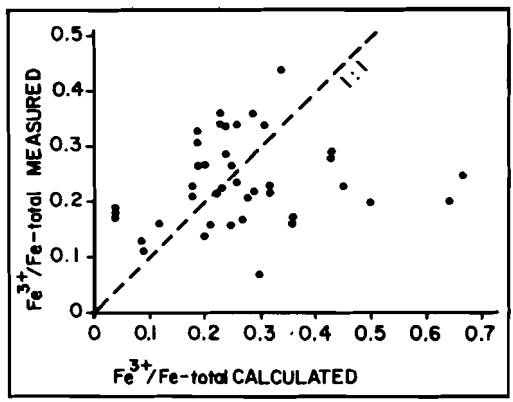

Figure IV.11.: Fe^{3+}/Fe-tot. : measured versus calculated. Only two samples fall on the equality line. The negative range (measured smaller than calculated) contains 21 samples, the positive 23. This indicates that there is no systematic error.

And a third reason may be the inaccuracy of the measured ratio. Starting with the last point : Fe_2O_3 depends on microprobe- and wet chemical FeO analyses (section IV.1.4). The ratio is therefore influenced by inaccurate measurements. If the standard deviation is added to (or subtracted from) the tabled microprobe-FeO value, and the mean deviation is subtracted from (or added to) the tabled wet chemical FeO value, the difference in $Fe^{3+}/(Fe^{3+}+Fe^{2+})$ is never more than 0.02. Low ratios can have a greater value than high ratios.

The second reason is probably the least problematic in this case, because in section IV.1.3. it is shown that the microprobe measurements have a rather good precision and reliability. If the standard deviation from fig. IV.5 is added to the main elements for a certain sample (in this case A 037) and the difference in Fe^{3+}/Fe-total is calculated, this is never more than 0.02. This indicates that errors in the microprobe- and wet chemical measurements are not the main causes of the difference between measured and calculated Fe^{3+}/Fe-total (= ΔFe). In fig. IV.12 the difference between the measured and the calculated value of the Fe-ratio (table IV.10) is compared with the SUM Y values of both the 23(0) method with only microprobe information ($SUM\ Y_{cal}$) (table IV.8), and the 23(0) method with combined microprobe information and the measured FeO (and thus Fe_2O_3), without the inaccurate fluid determinations ($SUM\ Y_{mea}$) (table IV.12).

It can be seen that the ΔFe is 0.00 for $SUM\ Y_{mea}$ = 5.00 and $SUM\ Y_{cal}$ = ± 5.10-5.20. The first value is to be expected because it was the assumption for the calculation. The spread in the second value for a given ΔFe depends on the oxidation ratio and the mg-ratio. The $mean\text{-}line_{cal}$ represents samples with an average mg-ratio and an average oxidation grade (see fig. IV.13/14).

These average values are .50 - .55 and ± .20 resp. If the mg-ratio is higher (less FeO to be oxidized), or the oxidation grade is lower, than the average, the difference between $SUM\ Y_{cal}$ and $SUM\ Y_{mea}$ will be less and vice versa. This ΔSUM Y has an average value of about .15 (see fig. IV.15).

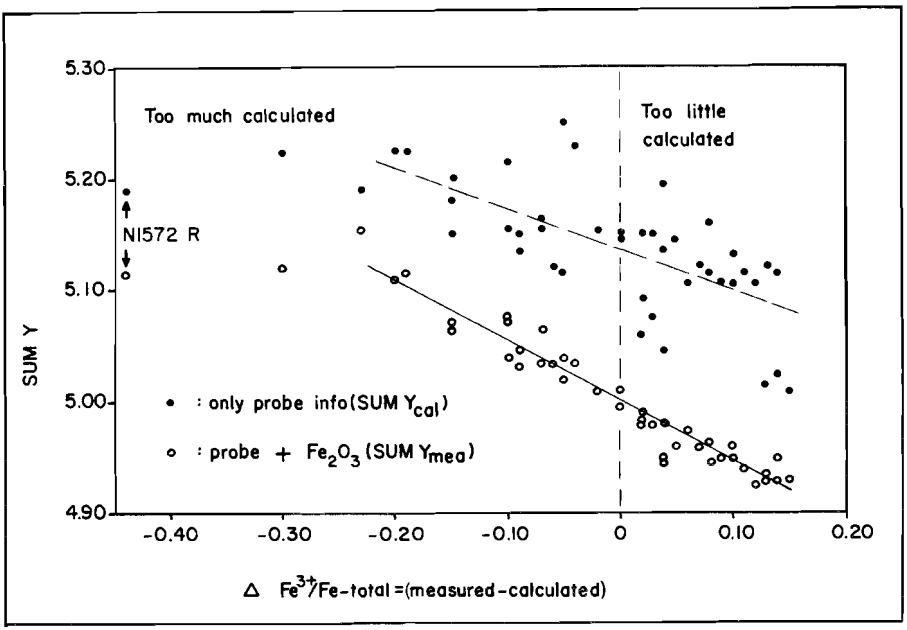

Figure IV.12.: Relation between SUM Y_{cal} and SUM Y_{mea} on one side and the difference between measured and calculated Fe-ratio on the other side. Line functions are : mean-line$_{cal}$: SUM Y_{cal}=5.135-.37 (ΔFe); mean-line$_{mea}$: SUM Y_{mea}=5.00-.53 (ΔFe). N1572 R was omitted for the calculation of the lines.

Negative ΔFe-values in fig. IV.12 are combined with SUM Y_{mea} greater than 5.00, because the calculation method counted on a larger ΔSUM Y, and hence lowered every Y-position cation too much, which resulted in a lower positive charge (valence sum, see section IV.2.3.). This automatically led to a higher Fe^{3+} content (and thus ratio). The opposite goes for SUM Y_{mea} less than 5.00. This leads to the conclusion that the calculation method described in section IV.2.3. is principally unreliable because it depends upon an equation with four parameters of which only two can be determined with the microprobe :

$$\text{SUM } Y_{cal} = \text{SUM } Y_{mea} + C. \frac{Fe^{3+}/\text{Fe-total}}{\text{mg-ratio}} \qquad (1)$$

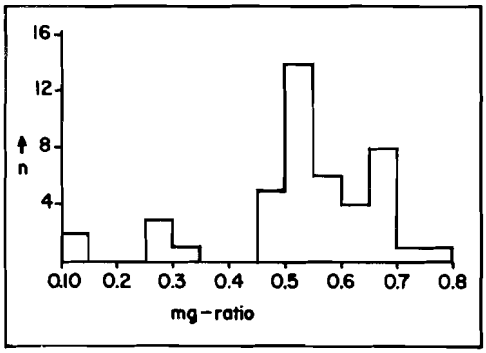

Figure IV.13.: Histogram of the mg-ratio of the samples with FeO (Fe_2O_3)-wet chemical analysis.

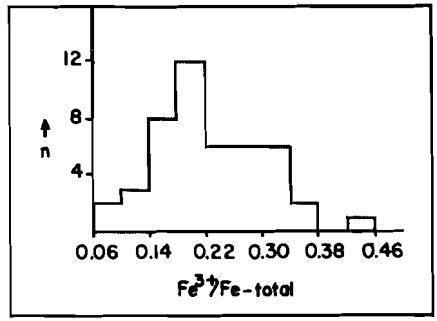

Figure IV.14.: Histogram of the oxidation grade of the samples from fig. IV.13.

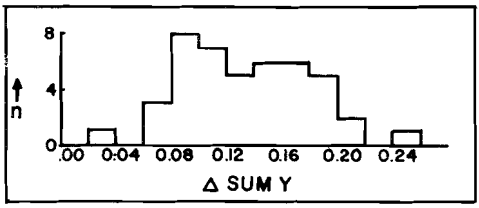

Figure IV.15.: Histogram of the ΔSUM Y of the samples from fig. IV.13.

SUM Y_{cal} and the mg-ratio are known from the microprobe, and the SUM Y_{mea} and the oxidation grade are unknown. C is a constant. The equation can be written as follows :

$$\Delta\text{SUM Y} = C.\ \frac{Fe^{3+}/\text{Fe-total}}{\text{mg-ratio}} \qquad (2)$$

All parameters are known for the measured group, so the constant C can be determined, and the formula can be checked, see fig. IV.16. C appears to be 0.30 for samples with an mg-ratio greater than 0.20. This , however, does not help very much in solving the equation. There remain two unknown values in equation (1), so it can not be solved.

Brown (1974) found a good correlation between calculated (Z+Y+X=15 instead of Z+Y=13) and measured values for Na-amphiboles and some sub-calcic actinolites with, very likely, vacant A-sites ($X \leqslant 2.00$ and therefore Z+Y+X=$\pm$15.00). This is the same case as SUM Y_{mea}=$\pm$5.00 which resulted also in a good correlation. All cations should be incorporated in a calculation of the Fe^{3+} content and this is not possible if the A-site is partly used by Na and K as is the case for

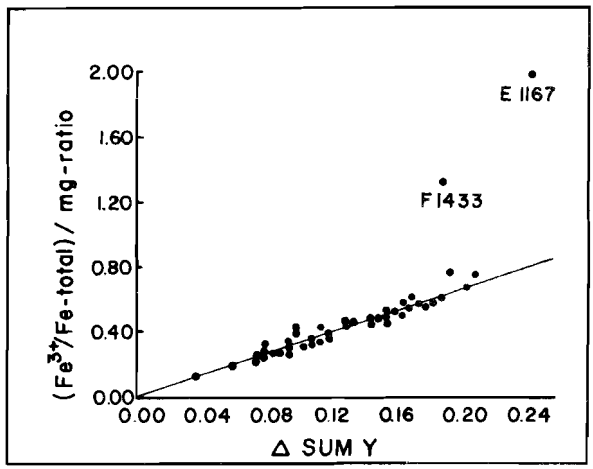

Figure IV.16.: Relation between the ΔSUM Y and the oxidation grade and mg-ratio. The line function is : $\Delta SUM\ Y = 0.30\ \frac{(Fe^{3+}/Fe\text{-total})}{mg\text{-ratio}}$. F1433 and E1167 are the samples with the lowest mg-ratio.

common hornblendes.
For this reason the Fe^{3+}-values for the non Ca-amphiboles A 168, B2016, L2143 and R3229, which are calculated on Z+Y+X=15 basis, may yet be approximately correct.

IV.2.6. : Final remarks concerning the calculation of the structural formulae

1 : Influence of the oxidation ratio : $Fe^{3+}/(Fe^{2+} + Fe^{3+})$ and the mg-ratio on the 23(0) half-unit cell contents.

If only microprobe information is used to calculate the structural formula, Fe^{3+} is unknown and influences the values of several ions and positions. The influence will be greater for amphiboles with higher Fe-total contents, i.e. with lower mg-ratio, and higher oxidation ratio. For the Rogaland amphiboles several good 24(O,OH,F) formulae are available with (OH + F) = 1.75 - 2.25. These are used to determine the influence of the above mentioned ratio's on the 23(O) formula. The amphiboles are all hornblendes with Si = 6.00 - 6.75.

Because the "magmatic" amphiboles have lower mg-values, they are influenced stronger than the metamorphic amphiboles. The relation is shown in fig. IV.17.

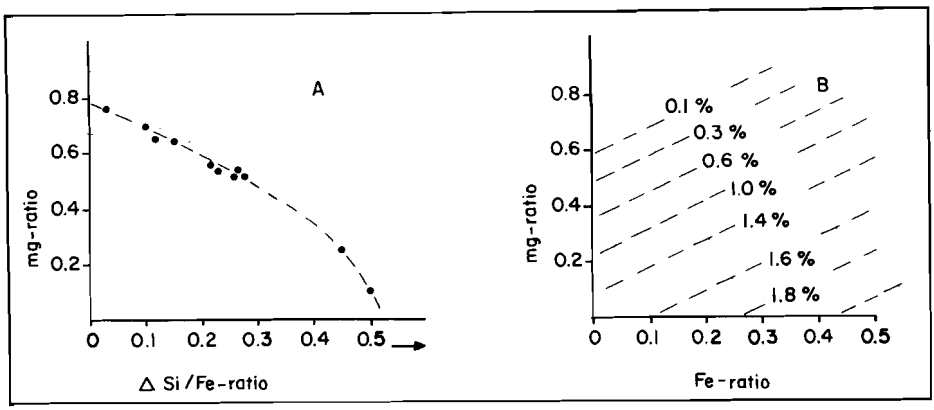

Figure IV.17.: Influence of mg-ratio and oxidation-ratio on the absolute (A) and relative (B) difference between 23(O) and 24(O,OH,F) Si-value.

The figures are only indicative because not enough measurements are available to draw exact curves and zones.

For most elements the influence may be neglected. The differences for Ti, Fe-total, Mn, Mg, Ca, Na, K and Al-tot. are for the highest values of 3-4 ions per half-unit cell 0.065 ions. This absolute value for an amphibole from the lopolith corresponds to 1.6%. The maximum for metamorphic amphiboles is 0.035 (=1.4%). If for these elements, characteristic curves for variation are to be accepted, the differences between lowest and highest values should exceed these maxima. For Si the values may be higher because of the greater amount of ions in the formula. Absolute maxima for metamorphic and magmatic rocks are 0.08 and 0.135 resp. (=1.3 and 2.0%). This causes a possible crossing of the name transition lines in the Leake diagrams towards the Si-poor side. Therefore the name transition zones in fig. IV.8 are partly drawn in a sloping way, in accordance with the above mentioned Si-differences. It should be clear that the presence of a sample in the name transi-

tion zone on the basis of 23(O) does not automatically mean a crossing of the name transition line on the basis of 24(O,OH,F). It simply is not known. For amphiboles with a higher Si-content the relations are not available (no wet-chemical data) and a zone of 0.05 is accepted, not only for Si but also for Ca+Na+K and the mg-ratio. The last two values do not differ very much, Ca+Na+K has a maximum difference of 0.04 ions for both kinds of amphibole (=±1.5%) and the mg-value does not differ at all, only instrumental errors may cause a transition to another name group. The trouble starts mainly with the two Al-positions. For Al^{IV} the maximum differences are the same as for Si, which causes a much greater relative percentage : 4.7 and 9.0% resp. for metamorphic and magmatic. This might not be that important because the Al^{IV}- value is only seldom used, but the error is accumulated in the Al^{VI}-value. The Al-sum is approximately stable and therefore the relatively small Al^{VI}-value becomes totally unreliable. It will always be too high, up to 50% for metamorphic amphiboles and 100% for the magmatic (if there are between .00 and .15 ions in the 24(O,OH,F) structural formula). In diagrams, the Al^{VI}-values from 23(O) will always represent the highest possible values. The use of SUM Y is, because of the same reason, also totally rejectable. The value bears all errors in the above mentioned elements in it. Absolute difference maxima are 0.165 and 0.21 (=3.3 and 4.2%) for metamorphic and magmatic samples. If these restrictions are realised, the easy to get 23(O) formula will be a reasonably reliable tool to determine trends in colour changes etc.

2 : Influence of the fluid determination on the 24(O,OH,F) half-unit cell contents.

The 24(O,OH,F) formula depends too much on an accurate fluid determination. If less than 1.75 fluid ions are measured one can not be sure if this is due to a dry amphibole or an incomplete analysis. The influence of an incomplete fluid analysis can be determined by calcu-

lating the formulae on 24(O,OH) basis for an analysis with ± 98 wt% non fluid oxides and, in this case, 2.25% H_2O, by varying the fluid content. Fig. IV.18 shows the result.

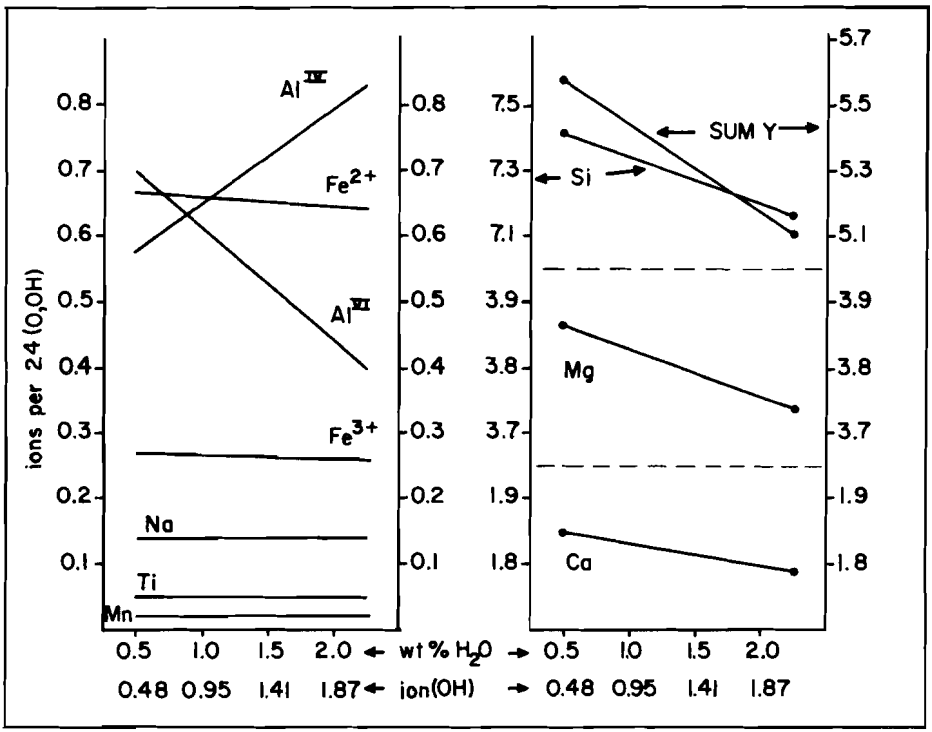

Figure IV.18.: Influence of incomplete H_2O analysis on the 24(O,OH) structural formula positions.

The damage is not too great for elements less than 1 ion, except for both Al-positions; the elements with levels above 1 ion (Ca, Mg and Si) show strong changes. This makes the reliability of 24(O,OH,F) formulae with less than 1.75 fluid positions rather dubious. In this thesis 38 out of 54 24(O,OH,F) formulae have less than 1.75 (OH+F), which in itself does not have to imply that the analyses are bad. Some of these low fluid analyses do have some Cl as can be seen from table IV.6, but this is obviously not enough for most of the analyses to be completed. Therefore most of the analyses can not be used for variation diagrams, contrary to the 23(O) formulae which show less disastrous

variation in the critical elements Si, Mg and Ca. The change of sum Y with H_2O content in Leake (1968, fig. 29) may be explained by poor fluid analysis rather than anything else.

3 : Statistical comparison of the three calculation methods.

Starting from the principle that crystal structures are logic frameworks, where the various compounds and positions are interdependant, one can calculate the correlation coëfficients between all available ions and the sum totals for the Y and Z position. In section IV.2.6. part 1 it is shown that sum Y and Al^{VI} from 23(0) are, as external parameters, totally unreliable. This does not mean that they are to be rejected for internal comparison. The amount of ions in these positions is the result of other ion-amounts in the structural formula, and the calculation method does not influence the individual analyses, but the total system of analyses and ions in all their positions. Therefore, the coherence inside the formulae for a certain method of calculation is not affected, with the exception of Al^{VI} possibly because it is an overflow position of the Si-value.
The Fe-total is not used because it is compiled in too different ways for the three methods and therefore it might influence the result (if it is used, it favours the 23(0) method).
The following relations greater than or equal to .50 are found (if the value is less, it is considered not significant) : table IV.11.

The obvious relation Mg versus mg-ratio is not mentioned. It is clear that the 23(0) structural formulae are, on the average, better of than the other two methods.

From this chapter it may be concluded that the 23(0) system, knowing its restrictions, is the best to use, certainly in this study. Furthermore it might be advisable to use the Fe_2O_3 determinations in the 23(0) formula and omit the fluid analyses. This does not influence

	23(0)	23(0), ideal	24(0,OH,F)
Si vs.* Al^{VI}	-.75	-.85	
Si vs. Ti	-.52		-.54
Si vs. Mn	.50		
Ti vs. sum Y	-.68		
Ca vs. Na	-.65	-.55	-.60
Ca vs. K	.65	.67	.58
Na vs. K	-.57	-.54	-.56
K vs. sum X	.54	.56	.52
Al^{VI} vs. sum Y			.67
Mn vs. mg-ratio		.52	
Sum X vs. sum Y	-.67		
Relation total	9	6	6

Table IV.11.: Significant correlation coëfficients between ions and positions for three calculation methods. vs.* = versus.

the Fe-ratio but takes away the problem of too high 23(0) values (section IV.2.6.-1/2). See table IV.12.

Leake (op.cit) gives 8 criteria by which to discriminate between superior and inferior analyses on the basis of 24(0,OH,F).
If these 8 criteria are applied to the table IV.10 formulae, 32 out of 57 formulae are superior, the other 25 mostly show incorrect sum totals, too high SUM Y or too low fluid sum. All three are, in most cases, the effect of a too low fluid determination. If more fluid is analysed, the sum total goes up, SUM Y goes down and the (OH+F) rises.

It is important to realise the restrictions of ones information.

	A 037 B	A 128	F 118 L	B 254	B 302	D 307	D 442	D 444	E 067	E 145	E1167	E 170
Si	6.035	6.18	6.50	6.04	6.31	6.42	6.485	6.33	6.48	6.08	6.47	6.355
Al	1.965	1.82	1.50	1.96	1.69	1.58	1.515	1.67	1.52	1.92	1.53	1.645
Al	.055	.595	.155	.38	.395	.345	.42	.40	.185	.43	.11	.355
Ti	.165	.19	.205	.245	.21	.205	.14	.225	.20	.425	.24	.235
Fe^{3+}	.405	.375	.445	.36	.42	.275	.50	.53	.645	.325	.84	.795
Fe^{2+}	.935	1.24	1.77	1.63	1.515	1.155	1.065	1.145	2.22	1.525	1.22	1.79
Mn	.025	.025	.035	.04	.015	.015	.04	.04	.00	.025	.07	.03
Mg	2.805	2.645	2.44	2.075	2.48	2.835	2.845	2.83	2.175	2.29	.47	2.315
Ca	1.91	1.84	1.73	1.765	1.775	1.835	1.775	1.67	1.84	1.745	1.65	1.785
Na	.39	.455	.58	.68	.605	.525	.515	.655	.61	.68	.62	.65
K	.38	.28	.305	.295	.21	.28	.25	.175	.25	.30	.27	.22
Z	8.00	8.00	8.00	8.00	8.00	8.00	8.00	8.00	8.00	8.00	8.00	8.00
Y	4.99	5.03	5.085	4.93	5.035	4.93	5.01	5.07	5.035	4.935	4.95	5.035
X	2.68	2.575	2.615	2.74	2.59	2.64	2.54	2.56	2.50	2.725	2.54	2.655
mg	.675	.615	.57	.505	.56	.66	.505	.455	.255	.54	.10	.52
Cr										.005		015

	F 005	F1043	F1052 D	F3u52 L	F 070	F1107 D	F1126	F1252	F1433	H1047 R	H1050	H 307
Si	6.55	6.49	6.56	6.565	6.49	6.445	6.47	6.58	6.50	6.62	6.545	6.22
Al	1.45	1.51	1.44	1.435	1.51	1.555	1.53	1.42	1.50	1.38	1.455	1.78
Al	.17	.215	.16	.135	.21	.255	.255	.16	.225	.18	.15	.305
Ti	.185	.115	.18	.20	.165	.225	.22	.17	.105	.18	.21	.225
Fe^{3+}	.625	.745	.545	.525	.505	.505	.63	.66	.655	.55	.545	.61
Fe^{2+}	1.21	1.455	1.385	1.38	1.705	1.64	1.56	1.175	1.325	1.05	.97	1.345
Mn	.05	.095	.055	.065	.05	.03	.045	.045	.09	.04	.03	.055
Mg	2.70	2.32	2.625	2.66	2.36	2.355	2.25	2.72	.545	2.95	3.055	2.385
Ca	1.81	1.84	1.795	1.775	1.82	1.765	1.785	1.815	1.745	1.79	1.78	1.845
Na	.515	.485	.615	.62	.515	.48	.415	.515	.70	.555	.55	.475
K	.26	.27	.28	.275	.30	.315	.295	.255	.315	.25	.285	.395
Z	8.00	8.00	8.00	8.00	8.00	8.00	8.00	8.00	8.00	8.00	8.00	8.00
Y	4.94	4.945	4.95	4.965	4.995	5.01	4.96	4.93	4.945	4.95	4.96	4.925
X	2.585	2.595	2.69	2.67	2.635	2.56	2.485	2.585	2.76	2.595	2.615	2.715
mg	.59	.505	.57	.575	.51	.52	.50	.59	.17	.64	.665	.545

	H 325	H 415	J 119	M 101	N1041-1	N1041-2	N1041-3	N2041-1	N2041-2	N2041-3	N1264	N 317
Si	6.20	6.46	6.295	6.495	6.935	6.88	7.02	7.04	7.15	7.29	6.575	6.145
Al	1.80	1.54	1.705	1.505	1.065	1.12	.98	.96	.85	.71	1.425	1.855
Al	.47	.13	.245	.12	.345	.30	.34	.37	.325	.23	.145	.35
Ti	.255	.245	.27	.205	.08	.085	.03	.015	.00	.00	.17	.31
Fe^{3+}	.455	.57	.655	.585	.345	.265	.23	.275	.30	.32	.60	.475
Fe^{2+}	1.19	1.52	1.31	.75	1.13	1.225	1.055	1.015	.88	.71	1.145	1.50
Mn	.02	.04	.02	.025	.04	.04	.035	.035	.03	.03	.035	.025
Mg	2.68	2.48	2.45	3.255	3.145	3.235	3.45	3.42	3.605	3.85	2.885	2.315
Ca	1.69	1.76	1.81	1.785	1.77	1.755	1.76	1.75	1.75	1.735	1.79	1.775
Na	.75	.56	.48	.535	.355	.40	.42	.385	.34	.305	.55	.615
K	.09	.305	.345	.35	.145	.165	.145	.13	.115	.10	.245	.31
Z	8.00	8.00	8.00	8.00	8.00	8.00	8.00	8.00	8.00	8.00	8.00	8.00
Y	5.07	4.985	4.95	4.96	5.085	5.15	5.14	5.13	5.14	5.14	4.98	4.975
X	2.53	2.625	2.635	2.67	2.27	2.32	2.325	2.265	2.205	2.14	2.595	2.70
mg	.615	.54	.55	.705	.675	.68	.725	.72	.75	.785	.62	.535

	N 337	N1402-1	N1402-2	N1572 R	N1572 K	N 809	N1827-1	N1827-2	N1827-3	N1827-4	Q 100	P 303-1
Si	6.49	6.46	6.475	6.075	6.125	6.40	6.41	7.025	6.55	6.345	6.48	6.57
Al	1.51	1.54	1.525	1.925	1.875	1.60	1.39	.975	1.45	1.655	1.52	1.43
Al	.25	.135	.12	.63	.67	.225	.455	.245	.385	.42	.31	.245
Ti	.20	.24	.265	.205	.21	.285	.04	.04	.05	.07	.275	.195
Fe^{3+}	.30	.705	.65	.195	.185	.295	.565	.49	.52	.545	.17	.315
Fe^{2+}	1.57	2.615	2.615	.795	.79	1.10	2.375	2.075	2.195	2.285	1.19	1.655
Mn	.03	.05	.055	.01	.01	.015	.055	.05	.055	.05	.01	.05
Mg	3.695	3.295	3.32	3.28	3.28	3.07	1.58	2.145	1.865	1.735	3.025	2.56
Ca	1.79	1.615	1.625	1.745	1.715	1.825	1.885	1.88	1.875	1.865	1.86	1.80
Na	.55	.645	.655	.835	.80	.64	.315	.175	.305	.33	.525	.555
K	.34	.26	.27	.10	.10	.24	.275	.13	.245	.28	.27	.27
Z	8.00	8.00	8.00	8.00	8.00	8.00	8.00	8.00	8.00	8.00	8.00	8.00
Y	5.045	5.04	5.025	5.115	5.145	4.98	5.07	5.045	5.07	5.105	4.98	5.02
X	2.68	2.52	2.55	2.68	2.615	2.705	2.475	2.185	2.425	2.475	2.655	2.625
mg	.585	.28	.285	.765	.77	.685	.345	.45	.405	.375	.69	.56

Table IV.12.: Amphibole analyses : half-unit cell contents; 23 O, microprobe + $Fe^{2+}(Fe^{3+})$-measurement.

	P 303-2	P1580 D	P2580 L	R1666	V1187	V 363	W 012 D	W 017	W 196 B	W1226 D
Si	6.52	6.29	6.285	6.555	6.415	6.615	6.635	6.51	6.45	6.64
Al	1.48	1.71	1.715	1.445	1.585	1.385	1.365	1.49	1.55	1.36
Al	.28	.45	.47	.195	.27	.295	.33	.33	.37	.425
Ti	.205	.10	.10	.175	.24	.14	.12	.22	.195	.08
Fe^{3+}	.325	.41	.43	.215	.255	.16	.38	.373	.37	.305
Fe^{2+}	1.69	1.075	1.155	3.085	2.025	2.095	1.815	1.765	1.955	1.23
Mn	.05	.015	.02	.055	.02	.07	.055	.04	.03	.025
Mg	2.485	3.015	2.87	1.35	2.175	2.395	2.415	2.31	2.19	3.055
Ca	1.785	1.84	1.82	1.77	1.89	1.795	1.74	1.795	1.765	1.775
Na	.575	.54	.55	.635	.385	.51	.465	.435	.47	.465
K	.27	.31	.33	.305	.445	.26	.235	.235	.195	.19
Z	8.00	8.00	8.00	8.00	8.00	8.00	8.00	8.00	8.00	8.00
Y	5.035	5.065	5.045	5.075	4.985	5.155	5.115	5.04	5.11	5.12
X	2.63	2.69	2.70	2.71	2.72	2.565	2.44	2.465	2.43	2.43
mg	.545	.67	.64	.285	.485	.505	.52	.515	.48	.66

Table IV.12.: continued

IV.3. : Microscopic description of the amphiboles.

IV.3.1. : Introduction.

Most physical parameters determined with the microscope can be communicated in a fairly exact way, except one : the colour. Pleochroic colours of minerals are normally described rather subjectively and are therefore difficult to handle. If one wants to learn something about the influence of chemistry on the pleochroic colours of amphiboles, one needs more information than just : green - brownish green - brown. One needs a better classification system, a system everyone can use and everyone can interpret.
The descriptions of all amphiboles studied can be found in the Appendix.

IV.3.2. : A numerical colour system.

"When you can measure what you
are speaking about and express
it in numbers, you know something
about it."

Lord Kelvin

Specific features of the amphiboles were studied with the Leitz Ortholux. Colours are determined with the 3.5X or 10X objective and the 10X ocular, using a 6 volt 30 watt lamp, with 5 ampère on the transformer. The upper condensor is not used, and for the determinations normal petrographic thin sections (± 30 μm) are preferred, because a polished or double-polished thin section gives too bright colours.
No spectrometer with the desired qualities (λ-range, universal stage adaption, etc.) could be found in Holland (as for instance the Gary-14 Spectrometer, Burns (1966)). Therefore it was decided to create a colour chart, containing the "normal" colours of the Rogaland amphiboles, i.e. from greenish blue, via green, to reddish brown. A total of 13 colours was chosen. See fig. IV.19.

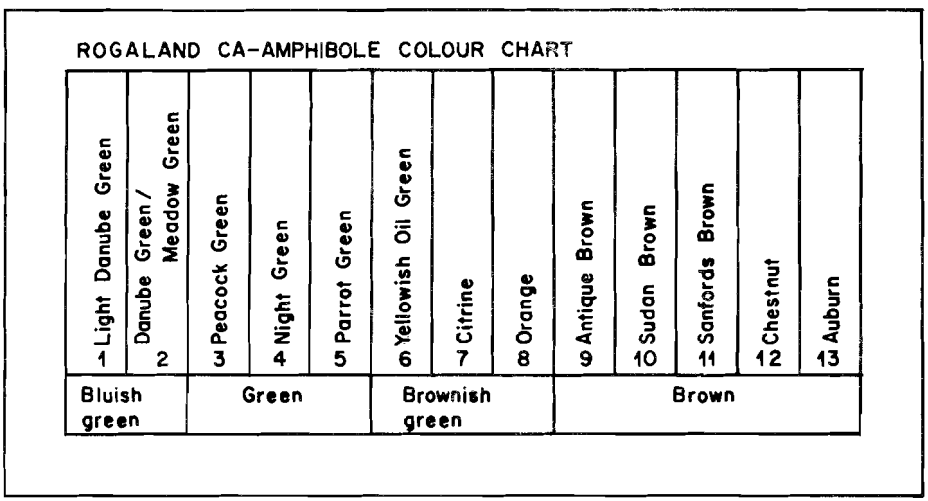

Figure IV.19. : Colour chart. Names after Ridgway (1912); 1-2 : Plate XXXII, 3-5 : Plate VI, 6 : Plate V, 7-8 : Plate IV, 9-10 : Plate III, 11-13 : Plate II.
Colour recipe to make your own chart : Use Ecoline no 411 (reddish), 416 (dark brown), 548 (violet), 601 (grassgreen), 602 (bluish green) and 657 (dark green).
No 4 = pure 601, No 3 = 601 + 657, No 2 = 657 + 602, No 1 = 602 + 657. From No 5 till No 8, 601 is mixed with more and more 416, but 601 is the main constituent. From No 9 till No 11, 411 is added and 601 disappears. No 12 = 411 + 416, No 13 = 411 + 416 + 548. It is not possible to give exact quantities of each colour, so the result may not be identical with the authors copy.

Numbers were given to each colour in order to use them as a parameter. It should be clear that this chart was designed for the Rogaland amphiboles. In other areas the tints may differ, but everyone should be able to make his own chart, and I think that they will have a lot in common.

The numbers 1 to 13 were used for normal colours; if the sample colour was lighter, 100 was added to the number, for darker colours 200 and for greyish 300. So a greyish blue-green amphibole section may receive the number 301 or 302. This procedure makes the colour description easier and more objective : each indicatrix axis gets its number, and different persons may describe the same amphibole colour in the same way without using subjective terms.

A test in our department learned that the descriptive terminology of several members of our team differed quite a lot, and that one could not always reproduce the colour from the description. Using the colour chart, however, the variation was small, only one number up or down, and mostly there was even complete agreement. The difficult parts of the colour chart lie between the numbers 3 to 5 and 9 to 11, where the colours resemble each other very much.

Special numbers have been added for less frequent "colours" e.g. colourless cummingtonite, violet riebeckite etc. See table IV.13.

No	Colour
20	colourless
21	yellow
22	yellowish brown/brownish yellow
23	orange
24	orange brown
25	brown (if deviating from the chart)
26	violet
27	violet blue
28	indigo
29	bluish green/greenish blue (if deviating from the chart)
30	green (if deviating from the chart)
31	yellowish green/greenish yellow

Table IV.13.: Special colours outside the colour chart range. N_x-colours are mostly 20, 121,122 and 131. Number 23 is never found, but is remained in the colour system because it was part of the original computer storage pack. 24 is found once as the n_y of a pargasite (E 128). The numbers 25, 29 and 30 are used whenever the microscopic colour cannot be fitted in the amphibole chart. 26 and 27 are riebeckite-arfvedsonite colours as well as 28 which is also the n_y- and n_z-colour for actinolite and magnesio-hornblende (= 128). See further table IV.14 and fig.IV.20-D.

There is no connection between number and gradual colour change, as with the numbers 1 - 13. All colours for the various indicatrix axes are assembled in table IV.14.

The normal series becomes a rough parameter which can be used for all kinds of calculations. The scale is of course arbitrary : the step from 2 to 3 may not be of the same size as the step from 10 to 11. The steps are created by the painter of the chart, and therefore it is possible that one has to adjust the scale, according to the results one finds.

A check on the colour scale is represented by fig. IV.20. In A and C all colour numbers for n_x, n_y and n_z are brought together : the colour numbers also include the corresponding lighter (+100), darker (+200) and greyish (+300) hues.

This should give an indication on the precision of the colour choice.

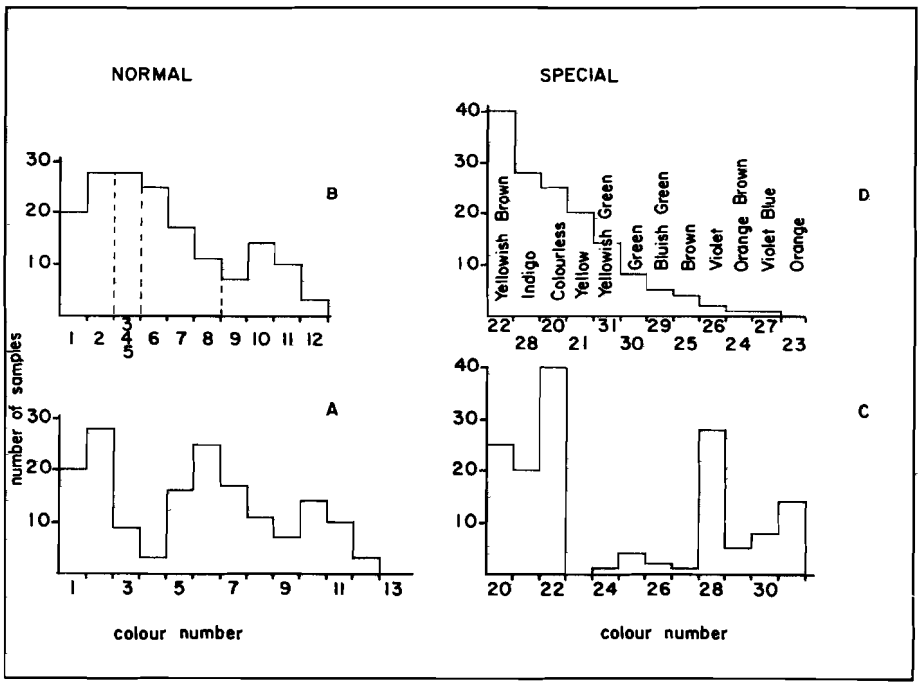

Figure IV.20. : Enumeration of all colour indices for n_x, n_y and n_z.

If in a histogram of slowly changing colours a certain colour is only rarely found, there could be something wrong.
In part A, there is a minimum at no 4, even though there are a lot of samples with more or less green axes. If no 4 is covered on the colour chart, the difference between no 3 and no 5 is very small. This seems to indicate that the choice was wrong in the green area.
Therefore, no 3, 4 and 5 (=c) are taken together in graphs with colour numbers as a parameter. The result is shown in fig. IV.20-B, a rather nice histogram. There is a second peak on the brown side (numbers 9-12) which represents the granulitic amphiboles. No 13 is never found, and may therefore be omitted. In fig. IV.20-C, there is of course no gradual change : the connection of colour and number is completely arbitrary, so one can never expect a normal histogram. The only thing one can do is find out which colours are mentioned most, and which least or not at all. In part D the order of frequency of occurrence is used as basis. In fig. IV.21 all colour possibilities are taken as abscissa for light, normal, dark and greyish tints. The ordinate is the number of samples with the specific number for each main axis. Fe-rich and Mg-rich samples are separated.

Subdivision in Mg-rich and Fe-rich Ca-amphiboles.

The Ca-amphiboles found in the migmatitic rocks are rich in Mg and have been grouped as Mg-rich amphiboles with a mg-ratio generally between 0.45 and 0.80. Fe-rich amphiboles are found in the igneous complexes (: the lopolith of Bjerkreim-Sokndal, the syenite massifs of Gloppurdi and Botnavatnet, and the anorthosites), their mg-ratio is generally less than 0.45, except for the secondary amphiboles which may be present beside the main hornblendes.
Some of the samples from the igneous complexes, however, were assigned to the Mg-rich group, because they did not fit in the Fe-rich (= more or less igneous) trends. These are samples from the leuconoritic phase of the lopolith and some xenoliths in various parts of the lopolith

Sample	2V	Δ	ZAc	Colour n_x	n_y	n_z	Twins	Name	T
A 037 B	-80°	.019	17°	122	8	6		Ferroan pargasite	F
A 128	-88	.019	16	122	10	7		Ferroan pargasite	F
A 168		.008	5x	28	26	27		Magnesioriebeckite	-
B1016	-50x	.020	18	129	2	1	s	Ferro-hornblende	M
B2016	90x	.023	16	20	20	20	l	Grunerite-59	-
B 118 L	-74	.023	18	122	10	8	s	Edenitic hornblende	M
B 254	-76	.035	10	121	11	10	s,l	Ti-ferroan pargasite	M
B 322	-75	.025	10	131	8	7		Ferroan pargasitic hbl.	M
D 172 D	-71	.020	14	122	8	7		Edenitic hornblende	M
D 307	-85	.035	15	121	12	11		Ti-ferroan pargas.hbl.	M
D 442	-81	.040	15	121	6	2	s	Edenitic hornblende	M
D 444	-72	.045	16	121	8	6	s	Mg-hastingsitic hbl.	M
E 067	-60	.025	17	122	7	3	s	Ferro-edenitic hbl.	F
E 125	-82	.040	10	121	12	10		Ti-ferroan pargasite	M
E 128	-86	.022	13	20	24	310	s	Titaniferous pargasite	M
E 131	+77	.016	19	20	110	121		Ferroan pargasite	M
E1167	-49	.020	10	122	7	2		Ferro-edenitic hbl.	F
E2167		.010		122	128	128		Ferro-actinolite	F
E 170	-75	.022	15	122	11	10	s	Ferroan pargasitic hbl.	M
E1232 R	-46	.010	16	131	2	1	s	Ferro-hornblende	F
E1232 K	-53	.015		131	102	101		Ferro-hornblende	F
E2232 N	-80	.030	15	20	130	129	l	Actinolite	F
E3232 N	-50	.030	13	22	5	1		Ferro-hornblende	F
F 005	-63x	.020	18	131	205	2	s,l	Edenitic hornblende	M
F1043	-60	.013	20	122	5	1	s	Edenitic hornblende	M
F2043	-70		16	20	128	128		Actinolite	M
F1052 D	-62	.022	20	122	206	2	s	Edenitic hornblende	M
F2052 D	-80	.025	20	20	128	128		Actinolitic hbl?(N.A.)	M
F3052 L	-62	.022	20	122	206	2	s	Edenitic hornblende	M
F4052 L	-80	.025	20	20	128	128		Actinolitic hornblende	M
F 070	-64	.022	8	321	7	2	s	Edenitic hornblende	M
F 074	-71	.020	18	122	6	1	s	Edenitic hornblende	M
F1107 D	-74	.023	17	122	7	6	s	Edenitic hornblende	M
F2107 D		.023		20	103	101		Edenitic hornblende	M
F1126	-58	.020	19	131	6	5	s	Edenitic hornblende	M
F2126	-74		16		106	2		Variety of F1126 (N.A.)	M
F1252	-74	.023	15	121	6	3	s	Edenitic hornblende	M
F2252	-78		16	20	128	128		Actinolite	M
F1433				125	3	206		Ferro-edenitic hbl.	F
F2433				125	2	3		Ferro-edenitic hbl.	F
H1047 B	-74x	.021	18	131	7	6	s	Edenitic hornblende	M
H2047 B				20	128	128		Actinolite?(N.A.)	M
H1050	-76	.023	16	122	7	6	s	Edenitic hornblende	M
H2050		.022	16	20	128	128		Actinolite?(N.A.)	M
H 307	-77	.024	15	122	9	7		Ferroan pargasitic hbl.	M
H 325	-81	.026	13	131	9	7	s	Ti-ferroan parg.hbl.	M
H 415	-76	.035	15	122	210	208	s	Ti-edenitic hbl.	M
J 119	-76	.030	13	122	209	7	s	Ti-ferroan pargasite	M
L1143	-80	.022	17	121	130	129		Actinolitic hbl.	F
L2143	+70	.025		20	20	20		Cummingtonite-69	-
M 101	-89	.012	18	122	110	108	s,l	Edenitic hornblende	M
N1041 B	-88	.020	20	122	104	101		Magnesio-hornblende	M
N2041 B	-87	.020	20	20	130	129		Actinolitic hbl.	M

Table IV.14. : Amphibole parameters determined under the microscope. For several amphiboles it was not possible to measure all parameters because of scarcity. See section IV.3.3. for information about 2V, Δ, ZAc and twins. See section IV.3.2. for colour informations.

Twins : l=lamellar, s=simple; in all cases were it could be determined the twinplane was (100).

Sample	2V	Δ	Z∧c	Colour n_x	n_y	n_z	Twins	Name	T
N1264	-68	.020	18	122	6	3	s	Edenitic hornblende	M
N2264	-78	.022	18	20	128	128		Actinolite	M
N 317	-76	.025	9	121	12	8	s	Ti-ferroan pargasite	M
N 337	-85*	.020	19	121	10	110	s	Edenitic hornblende	M
N1402	-62		10	122	7	4		Ti-ferro-edenitic hbl.	F
N2402				122	5	1		Ferro-hornblende	F
N1528 B	-55*	.025	10	122	8	6	s	Ti-hastingsitic hbl.	F
N2528 B		.008		28	26	22		Arfvedsonite?(N.A.)	-
N3528 B		.023		125	5	3		Mg-hastingsitic hbl.	F
N4528 B		.020		20	128	128		(N.A.)	-
N1572 L	-88	.025	16	121	111	111		Pargasite	M
N2572 D	-88	.025	16	121	111	111	s	Pargasite?(N.A.)	M
N 809	-82	.035	16	121	11	11		Ti-ferroan pargas.hbl.	M
N1827 F	-45	.015	12	131	5	2		Mg-hastingsitic hbl.	F
N2827 F	-66	.020		131	105	102		Actinolite	F
O 100	-82	.025	16	121	10	9	s,1	Ti-edenitic hbl.	M
P1097	-80	.015	20	122	9	325	s	Ferro-edenitic hbl.	F
P2097				122	3	301		Ferro-edenitic hbl.	F
P 248	-70	.023	17	121	6	5	s	Edenitic hornblende	M
P 303	-77	.028	16	122	9	6	s	Edenitic hornblende	M
P1580 D	-81	.025	20	131	5	102		Ferroan pargasitic hbl.	M
P2580 L	-81	.027	20	121	5	102		Ferroan pargasitic hbl.	M
R 227	-61	.024	12	122	7	205	s	Ferro-edenitic hbl.	F
R1229	-42	.022	16	122	6	2		Ferro-edenitic hbl.	F
R2229	-58	.018		130	2	1		Ferro-hornblende	F
R3229				20	128	128		Grunerite-75	-
R1269	-40	.020	13	121	202	201	1	Ferro-hornblende	F
R2269		.026		20	130	129	1	Ferro-actinolite	F
R 356	-56	.022	12	122	206	2	s	Ferro-edenitic hbl.	F
R1668	-68	.024	18	122	10	7	s	Ferro-edenitic hbl.	F
R2668	-73	.018		131	330	102	s	Ferro-edenitic hbl.	F
V 147	-60	.020	18	121	2	1	s	Mg-hastingsitic hbl.	F
V1187	-73	.023	15	122	11	10	s	Mg-hastingsitic hbl.	M
V2187		.023		20	104	101		Actinolite	M
V 276		.020		131	2	1		Hastingsitic hornblende	F
V 277	-69	.020	13	121	305	302	s	Ferro-edenitic hbl.	F
V 363	-69	.023	14	122	8	6	s	Edenitic hornblende	M
W 012 D	-72	.025	15	122	6	2	s	Magnesio-hornblende	M
W 017 B	-66	.021	14	122	6	5		Magnesio-hornblende	M
W 162 D	-62	.012	16	122	2	1		Edenitic hornblende	M
W 196 B	-72	.022	15	122	7	5	s	Ferro-hornblende	M
W 217	-57	.022	11	122	205	202		Mg-hastingsitic hbl.	M
W1226 D	-80	.030	18	131	6	3	s	Magnesio-hornblende	M
W2226 L	-72	.030	15	131	209	207	s	Edenitic hornblende	M
Y1055	-71	.023	14	122	8	6		Ferroan pargasitic hbl.	M
Y2055				121	102	101		Ferro-hornblende	M
Y1128	-50	.015	4	125	2	1		Hastingsitic hornblende	F
Y2128				20	128	128		Ferro-actinolite	F
Y1131 B		.010		130	3	1		Hastingsite	F
Y2131 B		.012		130	6	302		Hastingsite	F
Y3131 K				20	128	128		Ferro-tschermakite	F
Y3131 R				20	128	128		Hastingsite	F

Table IV.14. : continued.

Exsolution of another amphibole phase was found in B1016, B2016, L1143, L2143, N1041 and N2041. For E1167 exsolution was not clear. See section IV.3.4. If necessary, more information about these parameters is given with the sample description, see Appendix. x : X∧c, (N.A.) : not analyzed. Names are simplified after table I.1. T : trend analysis group; M = Mg-rich, F = Fe-rich, see text; * = measured with the aid of twins.

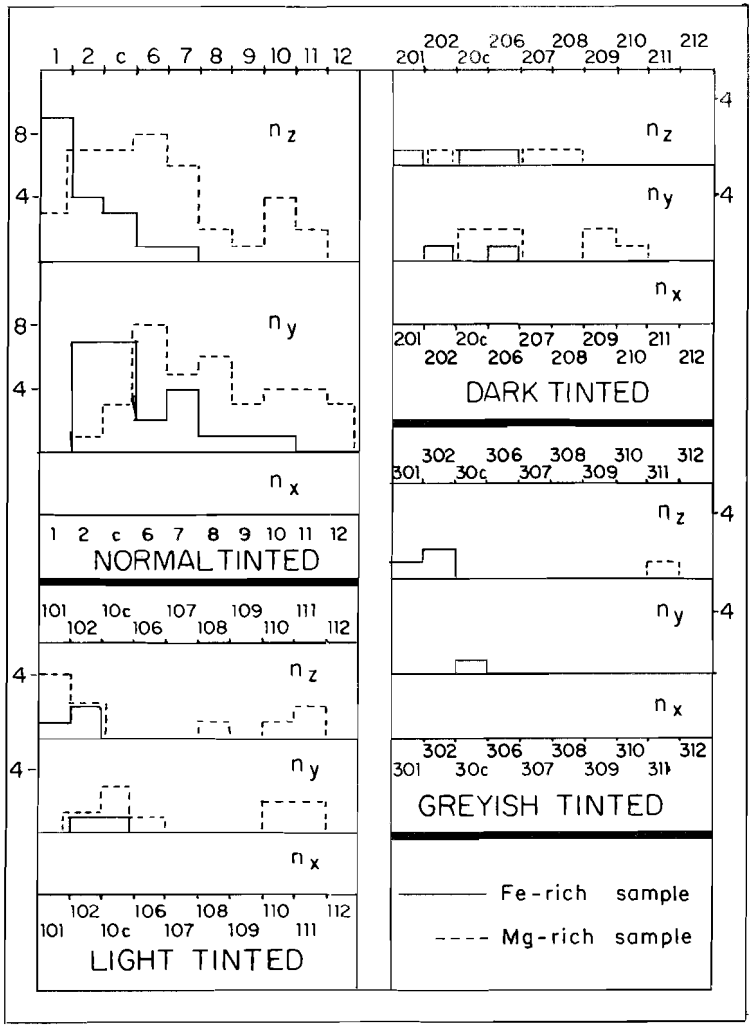

Figure IV.21. : Differentiation of the "normal" colours into separate tints, and their coupling to the various indicatrix axes, for the Fe-rich and the Mg-rich amphibole group.

(B 322, E 125, E 128, E 131, E 170, P 248), and one sample from the Egersund-Ogna anorthosite (L 143). On the other hand, a sample from the migmatitic environment of Gloppurdi followed the Fe-rich trend (V 147). More extensive information for the separate samples is given in the Appendix.

The non-Ca-amphiboles were not used for chemical trend analyses. In table IV.14 the division is indicated (M and F). Chapter VI deals with trend analyses for the Mg-rich-, Fe-rich- and combined Ca-amphibole groups.
The division of the whole rocks in a migmatitic- and an igneous group is mainly independant of the amphibole chemistry (see section VI.1.1).

On an average the normal-tinted Fe-rich amphiboles have lower colour numbers than the Mg-rich amphiboles. Fig. IV.22 shows that the n_z-values are on the whole one to two classes lower than the n_y-values. This means that the n_z is, normally, greener (or less brown) than the n_y.

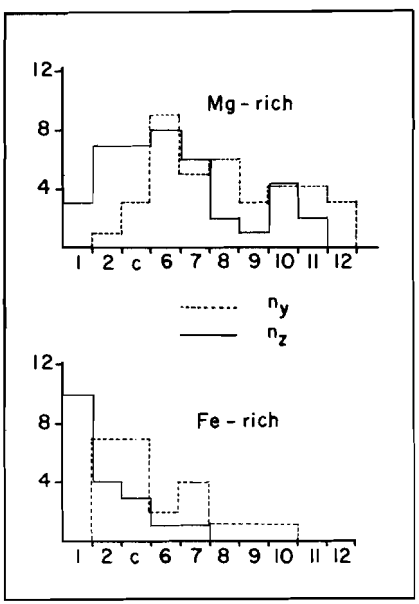

Figure IV.22. : Difference between the n_y- and n_z-colours, for Mg-rich and Fe-rich samples. Only the normal tinted colours are used for these histograms.

IV.3.3. : General remarks on other microscopic parameters.

2V measurements were done with a Leitz 4-axial Universal Stage. This method also gives information concerning Z∧c and the twinning- and exsolution planes. For all samples, at least three grains were measured, after which the mean was calculated. If the spread was greater than 4 degrees, more measurements were performed to see if the variation was due to zoning or erroneous measuring. If one value is given for 2V, a spread of 3^o up and down should be taken into account as error range. When the measurements were performed with the aid of twins, the accuracy may even be better, see table IV.14. All amphiboles with distinct optical zoning also are chemically zoned.

In that case both rim and core composition are given (e.g. E1232 R and K).

The ZΛc values are assumed to have an accuracy of 2^{o} up and down.

The birefringence is determined with the aid of a known mineral as thin section thickness indicator (normally quartz or plagioclase, taking the An % into account), and the colour chart of Michel-Lévy.

As can be seen from fig. IV.23, the 2V values show an average of about -60^{o} for the Fe-rich samples, and about -76^{o} for the Mg-rich amphiboles. The 3 high Fe-rich values are for cummingtonite (B2016), actinolite (E2232) and a ferro-edenitic hornblende (P1097).

The 2 positive Mg-rich values are for cummingtonite (L2143) and a ferroan pargasite (E 131).

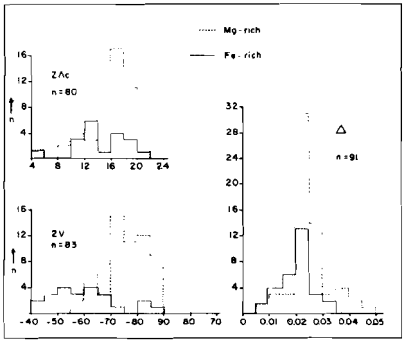

Figure IV.23. : 2V-, ZΛc- and Δ-histograms for the Fe-rich and Mg-rich amphibole group. Values from table IV.14.

The average ZΛc for Fe-rich samples is about 2^{o} less than the angle for the Mg-rich amphiboles, resp. 14^{o} and 16^{o}.

The modes for the birefringence coincide, with means of 0.019 for the Fe-rich and 0.024 for the Mg-rich amphiboles.

The total result of these measurements is : lower average values for all three characteristics for the Fe-rich amphiboles presumably as a response to the lower mg-ratio values.

Fig. IV.24 shows this clearly for the 2V-mg relation. The ZΛc and Δ versus the mg-ratio show no linear relationship.

Three groups can be discerned in the relation 2V versus mg-ratio:

1 : Mg-rich samples, $2V = -(67 \times mg + 36) \pm 15$, $r = -.62$. The width of the zone is caused mainly by the influence of the Si-content. Low Si-contents favour high 2V-values. A second factor is the Ca+Na+K-content, low values sooner show a high 2V for a certain

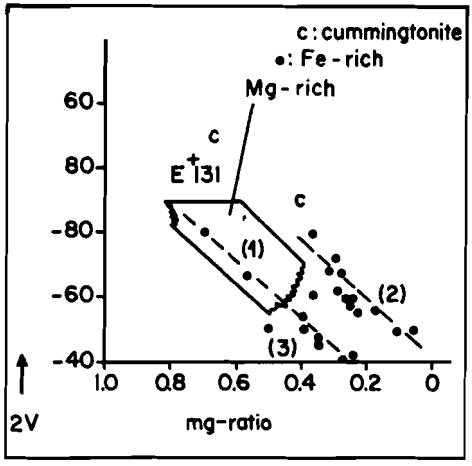

Figure IV.24. : Relationship between the 2V-value and the mg-ratio.

mg-ratio than high ones.

2 : Fe-rich samples, 2V = -(91 x mg + 40) $\pm$ 7, r = -.89. This trend lies above the Mg-trend, the 2V-values are higher for a certain mg-ratio.

3 : the transition group of Fe-rich samples (mainly coinciding with the low Ti (= lower T) group in section I.4). They form the extension of the lower part of the Mg-rich group. The Si-contents are low with respect to the mg-ratio for Fe-rich samples; in fig. IV.8 they form the transition between the Mg-rich samples and the lower part of the Fe-rich samples (E 232 - N 827, cores and rims; B1016, R 227, R1229, R1269). 2V = -(81 x mg + 20) $\pm$ 11, r = -.90. The two points in the Mg-rich field of fig. IV.24 are actinolite cores.

Résumé : 2V is influenced positively by the mg-ratio and, in the Mg-rich group, negatively by the Si- and Ca+Na+K-content.

Twins are divided into lamellar (more than 4 twin elements per crystal) and simple. The latter appear more often than the former. Only 8 amphiboles out of the 105 in table IV.14 display lamellar twinning, whilst 45 exhibit simple twins. Because all measured twin planes, lamellar as well as simple, are (100), it seems acceptable to presume that the unknown planes are also (100).

The elongation is normal for most amphiboles : positive; the only negative values are for A 168, a riebeckite, and for N2528, a presumed riebeckite/arfvedsonite.

r>v	r<v
B2016, B 322, F1043, F1433, F2433, F1252, L1143, N1528, N1827, O 100, R 356, R1668, V 277, W 012, W 196, Y1055.	B 254 E 128 N1402 V 363 W 018

Table IV.15. : Dispersion around n_x.

Dispersion : the Rogaland amphiboles only rarely show a distinct dispersion. Samples showing dispersion of the optic axes (related to n_x) are assembled in table IV.15.

IV.3.4. : Exsolution and the presence of fine-grained ore in amphiboles.

Exsolution of a former amphibole phase into two new amphibole phases is only rarely observed optically in the Rogaland amphiboles. Only a few samples show two different amphiboles intergrown in a single crystal, for instance N 041 which has a texture very similar to fig. 1B of Ross et al (1969). Recently $(\bar{1}01)$ is indicated as the normal exsolution plane for amphiboles instead of (100), see Robinson et al (1971-b). Universal stage measurements on the Rogaland exolution planes indicated $(\bar{1}01) \pm$ a few degrees.

Some samples possibly containing very fine exsolutions were sent to Dr. Champness in Manchester, England, for T.E.M.-investigations. Further information is mainly in the sample description of B 016 and L 143 which are cummingtonite-hornblende combinations, and N 041, see Appendix.

Small oreinclusions in amphibole may also be due to exsolution. Two types can be distinguished (table IV.16) :

a : ore needles inside the amphibole crystals, sometimes randomly scattered, but mostly in zones;

b : ore specks at amphibole crystal boundaries, mostly at amphibole-amphibole interfaces.

The ore needles of group "a" are thought to be the product of exsolution. They often have no connection with the crystals surface, may change gradually into round, small grains, mostly inside the crystal but sometimes at the amphibole grainboundary, and may influence the

		Much	Little
Needles	Scattered	A 128, F2433	B 118, E2232, N2528, N 809
	Zones	F1433, H1050, H 325, L2143.	A 037, B 254, D 173, D 307, E 067, E 125, E 131, E1167, F1052, F 070, F 074, F1107, F1252, H1047, H 307, J 119, L1143, M 101, N1264, N 317, N 337, N1572, N2572, O 100, P1097, P1580, R1269, R 356, R1668, V 363, W 012, W 017, W 196, W 217, W2226, Y1055, Y2131.
Grains		A 128, B 254, F1107, H1050, H 325, P1580, W 196, W2226, Y1055.	A 037, B 118, B 322, D 172, D 307, D 444, E 067, E 128, E 131, H 307, H 415, J 119, M 101, N 317, N 337, N1572, N2572, N 809, P2580, R 356, R1668, V1187, V 277, W 012, W 017.

Table IV.16. : Ore presence in amphibole divided in needles and grains, and tabulated according to the intensity of occurrence. It is clear that "a little ore in the form of needle zones" often combined with "some fine dispersed grains on crystal boundaries" is the most common form.

colour of the surrounding part of the amphibole, changing it from green to blue, or from brownish to greenish. The colour change indicates a depleted zone, with lowering of the Ti-, Fe- and Na-content (e.g. F1107 = normal amphibole, F2107 = depleted zone).
Because this depletion is not sufficient to explain the amount of exsolved Fe-Ti-ore, we have to assume that the whole amphibole crystal lowers its Ti- and Fe-content (and Na) to form titanomagnetite needles (microprobe measurement by F.J.M. Rietmeijer on H 050, pers.comm.).
The direct surroundings of the needle zone are most depleted.
It is well known that Ti in amphibole is sensitive to changes in temperature (section I.2.1). It has also been shown that high-grade metamorphic amphiboles contain more Fe-total than lower- grade amphiboles in the same kind of host rock (Engel and Engel, 1962-a and -b). This results in an increase of the mg-ratio with decreasing metamorphism

(actinolization). Therefore the nucleation of titanomagnetite needles seems to be the response to a decreasing metamorphic grade, possibly due to denudation of the area, without important mineralogical changes.

Ross et al. (op.cit, fig. 3B) show unmixing of amphibole which may be accompanied by this type of ore exsolution (also possible for pyroxene). The ore is determined as magnetite (or ulvöspinel; Ross, pers.comm.) and thought to be the result of a coupled unmixing reaction caused by a fall in temperature and perhaps also by an increase in oxygen fugacity. In Rogaland the unmixing of amphibole is not always coupled with the generation of ore needles, both are separately possible. Unmixing occurs if the original amphibole was rich in the cummingtonite (or tremolite) component, whereas the ore inclusions are found if the original amphibole was rich in Ti.

Our group b was described by Sen and Ray (1971-a) as: "granules of ilmenite along borders (and cracks) of hornblende", in two pyroxene basic granulites as indicators of the prograde reaction :

amphibole + quartz $\longrightarrow$ opx + cpx + plagioclase + opaques + water.

In Rogaland the granules are not restricted to basic granulites, nor to two-pyroxene assemblages.

It even may appear in pyroxene-free rocks. They display no colour change in the immediate surroundings.

To checke the hypothesis of Sen and Ray (op.cit.), our samples are divided in four groups :

1: no pyroxene in the sample

2: only clinopyroxene

3: ortho- and clinopyroxene

4: only orthopyroxene

In group 1 (19 samples) only 16% contains ore granules of type b (D 444, V 277 and W 012). In group 2 (14 samples) 50% has ore specks and in group 3 (35 samples) 57%. The fourth group contains 5 samples of which only N 041 has no ore granules. The last sample shows unmixing of the amphibole.

This indicates that there is a positive relationship between the presence of ore granules on amphibole grain boundaries and the presence of pyroxene. However, in a high-grade polymetamorphic environment it is difficult, if not impossible, to recognize reaction relationships like the amphibole-pyroxene transition. The only thing that can be concluded here is the fact that the higher-grade rocks (opx-present) contain type b ore granules more frequently than the medium-grade (opx-absent) rocks. This may be due to the above mentioned prograde reaction, or to the fact that these amphiboles contained originally more Ti (higher T) and had to exsolve more titanomagnetite during denudation of the area. The grains on the crystal boundaries formed in that case by the process of impurity segregation.
Therefore it is not possible in the plurimetamorphic terrain to come to a conclusion about the hypothesis of Sen and Ray.
The presence of ore needles in amphibole is, in contradistinction to the granules, not mainly restricted to the pyroxene-carrying rocks. It seems to depend on the Ti-content of the original amphibole and of the whole rock. A Ti-poor whole rock may contain Ti-poor amphiboles, depending on the quantities of other mafics, and the amount of amphibole present. Therefore the amphibole may have less Ti than the maximum amount allowed for the former metamorphic grade. If the temperature goes down, there is no reason for these crystals to decrease their already low Ti-content (for example D 442 : it contains no free ore at all, the Ti-content of the amphibole as well as the Ti-content of the whole rock are lower than those from comparable samples in the surroundings which do contain ore needles).

V : Additional mineral investigations

V.1. : Introduction .

Some additional analyses were made to complete or extend the picture for a certain sample or environment. It was not possible to insert this additional information in former investigation chapters and in the computer runs, because of time. All minerals are analysed by microprobe, and hence all Fe is given as FeO and Fe^{2+}.

V.2. : Analyses and other information

A : Amphibole, see table V.1.

BA 92 : Biotite hornblendite with pargasitic hornblende, 3473-64824, near the top of the Stokkafjellet, at ca the same location as B 254 and N 572. Equal amounts of light greenish-blue amphibole ($2V_z$= 80-85°, $Z\wedge c$ = ca 20°, colours : n_x= 122, n_y= 104, n_z= 101) and soft-green biotite. A few percent plagioclase is almost completely altered. The biotite transects amphibole, which has crystals upto 5 mm. This causes an irregular outline of the amphibole.
R 179 : Amphibole-apatite-ilmenite diorite with titaniferous ferroan pargasite, 3465-64772, phase A.
R 313 : Apatite-ilmenite-amphibole diorite with titaniferous ferroan pargasitic hornblende, 3500-64762, phase A.
R 385 : Amphibole-apatite-ilmenite hypersthenite with titaniferous ferroan pargasite, 3431-64744, phase A.
Modal analyses of the former 3 samples are :

	R 179	R 313	R 385
Pyroxene*	32	30	45
Amphibole	7	29	7
Ore	13	12	37

* Orthopyroxene is much more abundant than clinopyroxene

	R 179	R 313	R 385
Plagioclase	33	23	2
Apatite	12	6	7
Biotite	3	0	2

See further B 322 for mineral descriptions and structures of R 179, R 313 and R 385.

W 175 : Biotite-amphibole gneiss with ferro-tschermakitic hornblende, 3703-65056, E of Tonstad. It is one of the few migmatite samples with extreme poikiloblasts of amphibole, as described by Rietmeijer and Dekker (1978). Therefore, this amphibole was analysed and found to be very low in mg-ratio, lower than any other amphibole from the migmatitic environment. This result supports the suggestion that there is a relation between the Fe/(Fe+Mg)-ratio and the nucleation energy. See further Rietmeijer and Dekker, and chapter II.

	BA 92	R 179	R 313	R 385	W 175
SiO_2	43.65	41.8	42.8	41.95	42.55
Al_2O_3	14.75	12.45	11.15	12.3	14.75
TiO_2	0.1	3.15	2.35	3.7	2.2
FeO	8.0	15.45	17.35	12.45	19.9
MnO	trace*	trace*	trace*	---	.4
MgO	16.05	10.85	10.3	12.25	8.85
CaO	11.8	11.3	11.2	11.3	11.5
Na_2O	2.5	2.3	1.95	2.6	1.4
K_2O	1.5	1.7	1.55	1.65	.95
Sum	98.35	99.0	98.65	98.2	98.15
Si	6.27	6.21	6.405	6.205	6.47
Al	1.73	1.79	1.595	1.795	1.53
Al	.765	.39	.375	.35	.33
Ti	.01	.35	.265	.41	.25
Fe	.96	1.92	2.175	1.54	2.53
Mn	---	---	---	---	.05
Mg	3.435	2.40	2.30	2.695	2.005
Ca	1.82	1.795	1.795	1.79	1.875
Na	.695	.665	.575	.75	.42
K	.28	.32	.295	.315	.185
Z	8.00	8.00	8.00	8.00	8.00
Y	5.17	5.06	5.115	4.995	5.165
X	2.795	2.78	2.665	2.855	2.48
mg	.78	.555	.515	.635	.435

Table V.1. : Additional amphibole analyses. Oxides and 23(O) structural formulae, microprobe information only. Analyst : Dr.C.Kieft, Free University, Amsterdam. Trace : less than 0.10 wt %.

B : Pyroxene, see table V.2. Only clinopyroxenes have been measured.

A 037 : Salite in a banded spinel-bearing gabbro.

A 128 : Augite in an amphibole xenocryst in A 037.

H 050 : Mean value of four spots on clinopyroxene fragments in amphibole.

For further descriptions of these samples, see Appendix. The Al_2O_3-content of the $A\ 037_{cpx}$ varied somewhat.

The A 128-analysis is a mean. There are some chemical changes from core (with only fine ore exsolution), via the main exsolution zone (with ore and plagioclase exsolution) to the exsolution-free rim. SiO_2, CaO, and Al_2O_3 increase; FeO and TiO_2 decrease (titanomagnetite exsolution); and MgO, MnO, and Na_2O are more or less stable. The relatively low amount of Si-Ca-Al in the centre may explain the plagioclase-free core. This indicates a rather strong original zonation.

	A 037	A 128	H 050
SiO_2	48.8	48.5	52.5
Al_2O_3	5.2	4.35	1.5
TiO_2	.6	.25	.2
FeO	7.95	11.8	9.4
MnO	.25	.3	.4
MgO	12.75	12.5	13.8
CaO	23.1	21.4	21.5
Na_2O	NA	.15	.55
K_2O	NA	NA	.00
Sum	98.65	99.25	99.85
Si	1.85	1.85	1.965
Al	.15	.15	.035
Al	.08	.05	.03
Ti	.02	.01	.005
Fe	.25	.38	.29
Mn	.01	.01	.01
Mg	.72	.71	.77
Ca	.94	.88	.86
Na	NA	.01	.04
K	NA	NA	.06
En	37.7	36.0	40.0
Fs	13.1	19.3	15.3
Wo	49.2	44.7	44.7

Table V.2. : Some clinopyroxene analyses. Oxides and 6(O) structural formulae, microprobe information only. Analysts : A 037 Dr.R.P.E.Poorter, Utrecht; A 128 Dr.C.Kieft, Amsterdam and A.G.C.Dekker; H 050 A.G.C.Dekker. NA : not analyzed.

	A 037	A 128
SiO_2	43.05	44.65
Al_2O_3	36.4	35.45
CaO	20.0	19.5
Na_2O	.13	.43
K_2O	.01	.02
Sum	99.59	100.05
Si	6.01	6.18
Al	5.99	5.79
Na	.035	.115
Ca	2.985	2.895
K	.00	.005
Ab	.01	.04
An	.99	.96
Or	.00	.00

An = Ca/(Ca+Na+K)
Or = K /(Ca+Na+K)
Ab = Na/(Ca+Na+K)

Table V.3. : Some plagioclase analyses. Oxides and 24(O) structural formulae, microprobe information only. Analyst : Dr.R.P.E.Poorter, Utrecht.

C : Plagioclase, see table V.3.

A 037 : Anorthite in a banded spinel-bearing gabbro.

A 128 : Anorthite in an amphibole xenocryst in A 037.

For further descriptions of these samples, see Appendix.

$A\ 128_{plag}$ is an average of measurements on plagioclase crystals in amphibole, in clinopyroxene and in the contactzone between amphibole and pyroxene. No clear variation could be established.

D : Spinel, see table V.4.

E 128 : Intermediate composition in the spinel-hercynite-chromite-magnesiochromite system; in amphibole mela-troctolite.

E 131 : $Hercynite_{55}/Spinel_{45}$ in an ore-rich amphibole-bearing norite.

For further descriptions of these samples, see Appendix.

	E 128	E 131
SiO_2	.14	NA
TiO_2	.15	.05
Al_2O_3	45.35	62.27
Cr_2O_3	24.73	.17
FeO	23.85	25.11
MnO	.33	.37
MgO	10.39	11.76
CaO	.03	NA
Sum	104.96	99.73
Si	.005	NA
Al	1.465	1.97
Cr	.535	.005
Ti	.005	.00
Fe	.55	.565
Mg	.425	.47
Mn	.01	.01
Ca	.00	NA
Al/(Al+Cr)	.73	.995
Fe/(Fe+Mg)	.565	.545

Table V.4. : Some spinel analyses. Oxides and 4(O) structural formulae, microprobe information only. Analyst : A.G.C.Dekker. NA : not analyzed.

E : Opaque ore

A qualitative microprobe analysis was performed on ore needles in A 128 and H 050. A 128 appears to contain an ilmenite-magnetite exsolution, and H 050 titanomagnetite.

For information on analysis techniques, see chapter III and IV.

VI. : Correlations between the chemical parameters

VI.1. : Rock parameters

VI.1.1. : Introduction

Correlation coefficients were calculated to investigate the correlations between the various chemical elements in the bulk composition of the analyzed samples, and to find possible differences between trends in the igneous complexes and the migmatitic environment. When the whole rock correlations are known, it becomes easier to interpret the amphibole-whole rock correlations.

The samples were divided into the following rock groups :

--igneous group : lopolith of B-S (except xenolith E 128 and chemically extreme B 322) + anorthosites + Gloppurdi (with related sample V 147) + Botnavatnet.

--migmatitic group : migmatites + metamorphosed minor intrusions + xenolith E 128 - V 147.

Sample A 168 from the Faurefjell formation and B 322 from phase A were left out because of their extreme chemistry; N 041 was omitted because its location is not sure. Neither were the analyses of the banded samples D 172 and F 107 used, only the analyses of their dark bands. The groups are given in table VI.1.

Migmatitic group :

A 037, A 128, B 118 L, B 254, D 172 D, D 307, D 442, D 444, E 128, F 005, F 043, F 052 D and -L, F 070, F 074, F 107 D, F 126, F 252, H 047 B, H 050, H 307, H 325, H 415, J 119, M 101, N 264, N 317, N 337, N 572 D and -L, N 809, O 100, P 248, P 303, P 580 B, V 187, V 363, W 012 D, W 017 B, W 162 D, W 196 B, W 217, W 226 D and -L, Y 055.

Igneous group :

B 016, E 067, E 125, F 131, E 167, E 170, E 232 B, F 501, F 502, F 503, L 143, N 402, N 528 B, N 827, P 097, R 227, R 229, R 269, R 356, R 668, V 147, V 276, V 277, Y 128, Y 131.

Table VI.1. : Subdivision in migmatitic and igneous samples for the calculation of the rock correlation coefficients. Number of samples is 45 and 25 resp.

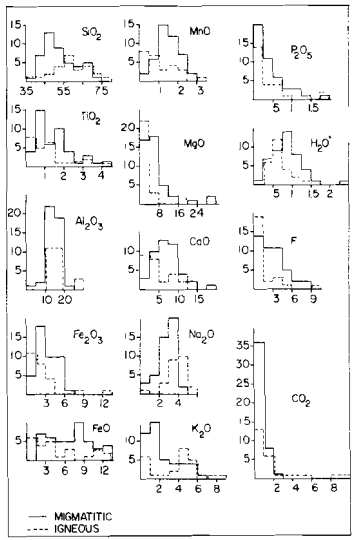

Figure VI.1. : Composition histograms for the two rock groups from table VI.1.

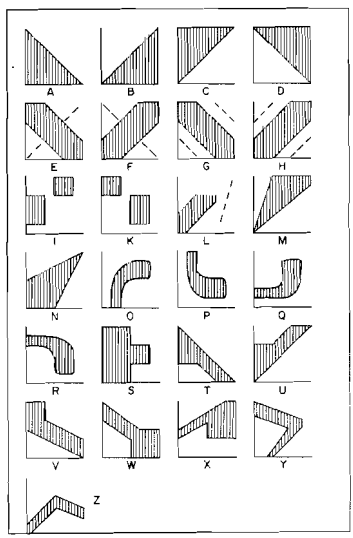

Figure VI.2. : 25 types of non-linear correlations. These types were encountered from bulk composition plots and from amphibole plots.

The chemical characteristics of both groups can be seen from fig. VI.1. The main differences are :

--higher SiO_2, Na_2O, K_2O, and CO_2 for the igneous group,

--higher TiO_2, Fe_2O_3, FeO, MnO, MgO, CaO, P_2O_5, H_2O, and F for the migmatitic group,

--equal Al_2O_3.

These differences may influence the correlation coefficients.

The correlation between two oxides (elements) is not always either a straight line or a cloud of scattered points. There are many reasons why a correlation coefficient may be insignificant (in this study $\geq |.50|$ is accepted as significant), while the diagram shows a clear relation which is not linear. Therefore, it is not sufficient to mention only the r-values greater than or equal to $|.50|$. Fig. VI.2 shows the various possibilities for non-linear relations met during this study.

VI.1.2. : Results

All graphs were drawn by computor in square diagrams, using automatic scaling of the axes. Only the correlations with r-values $\geq |.75|$ are tabulated in table VI.2, while a graphical representation of all significant correlations is shown in fig. VI.3. Correlations with r-values between $|.50|$ and $|.75|$ are not tabulated here for

editorial reasons, but information can be obtained from the author. The results are given for the migmatitic-, igneous- and combined group.

Relation		Mig	Ign	Com
CaO	$-K_2O$	-.66	<u>-.93</u>	-.78
TiO_2	-FeO	.36C	<u>.92</u>	.61C
FeO	-MnO	.81	<u>.87</u>	.85
SiO_2	-CaO	-.73	<u>-.85</u>	-.79
SiO_2	-FeO	<u>-.84</u>	-.71	-.80
SiO_2	-MgO	-.61A	<u>-.80</u>	-.63A
TiO_2	$-P_2O_5$	.69	<u>.80</u>	.73
FeO	$-K_2O$	<u>-.79</u>	-.42E	-.65A
SiO_2	$-K_2O$	.74	.76	<u>.77</u>
TiO_2	$-Fe_2O_3$	<u>.77</u>	.57M	.66F
TiO_2	-MnO	.30C	<u>.76M</u>	.53C
SiO_2	$-TiO_2$	-.37A	<u>-.75</u>	-.54A

Table VI.2. : Strongest whole rock oxide correlations in order of decreasing absolute r-value. Underlined are the "highest r-values per correlation". Letters refer to types in fig. VI.2. Mig : migmatitic; Ign : igneous; Com : all rocks together.

The igneous group contains most correlations $\geq |.50|$ and also most "best fits" (highest r-value per correlation, underlined in the table) :

	N	B
migmatitic group	20	10
igneous group	28	23
combination	23	4

N : number of correlations $\geq |.50|$

B : number of best fits.

It should go too far in the frame of this study to treat every separate correlation. There are, however, some remarkable points :

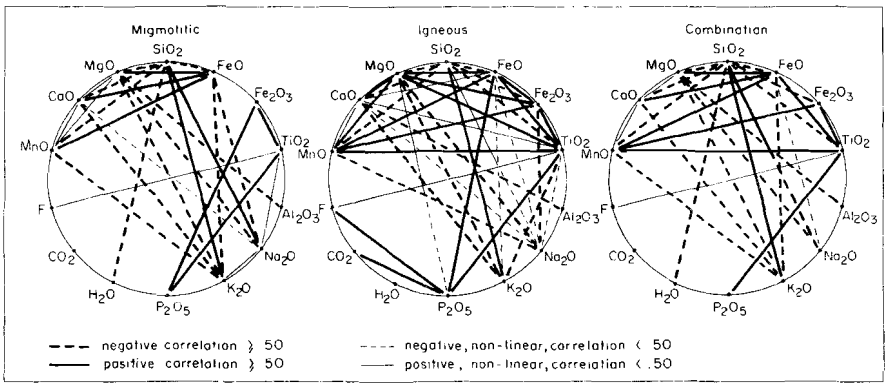

Figure VI.3. : Overall picture of all significant linear- or zone correlations in the migmatitic-, igneous- and combined group.

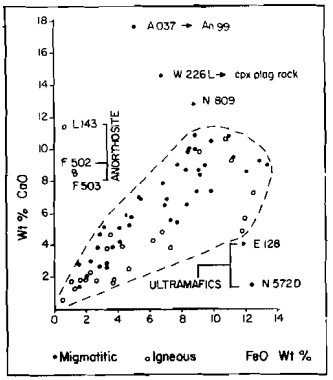

Figure VI.4. : FeO vs CaO bulk composition, F-type (see fig. VI.2). Similar graphs can be drawn for CaO vs MnO and MgO.

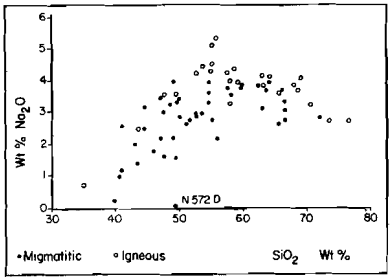

Figure VI.5. : SiO_2 vs Na_2O bulk composition. The igneous trend shows a clearly bent curve; the migmatitic trend only reaches a maximum for Na_2O.

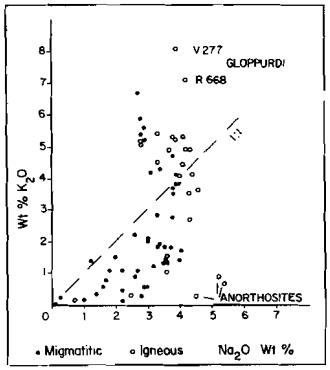

Figure VI.6. : Na_2O vs K_2O bulk composition. Both migmatitic- and igneous group show a bent curve.

--TiO_2 is highly correlated with FeO in the igneous group and with Fe_2O_3 in the migmatitic group (resp. ilmenite and Ti-magnetite preference).

--TiO_2 and P_2O_5 have a high positive correlation in the igneous group, indicating a positive correlation between ilmenite and apatite (this is also shown by the high FeO-P_2O_5 correlation (= .74)).

--The only r-values$\geq|.50|$ for F and for CO_2 are found in relation to P_2O_5 in the igneous group (.50 and .56 resp.).

--All correlations between CaO and FeO, MnO and MgO are positive and disturbed by a less important negative correlation (fig. VI.4). This negative trend is caused by the relatively CaO-rich anorthosites for the igneous group, and by CaO-poor ultramafics and CaO-rich mafics for the migmatitic group.

--Na_2O first increases and later decreases with increasing SiO_2 in the igneous group (fig. VI.5). The turning point for the igneous group lies at 55% SiO_2; the migmatitic trend curves somewhat, caused by the maximum value of 4% Na_2O for migmatitic samples and a possible decrease at higher SiO_2 values.

--K_2O shows a positive correlation with SiO_2 over the whole concentration range. This results in a curved Na_2O-K_2O diagram (fig. VI.6). If the anorthosites are left out, both rock groups show the

same curve from $Na_2O > K_2O$ for the mafic rocks, to $K_2O > Na_2O$ for the leucocratic samples. The most K_2O-rich samples are from Gloppurdi.

The overall picture of significant correlations (fig. VI.3), includes all r-values $\geq |.50|$ and several types from fig. VI.2, excluding A-D and S because these types do not show significant decreasing or increasing zones. It is obvious that there are various differences between the migmatitic- and igneous group. These differences may influence the correlations between the amphibole- and bulk composition.

The seemingly intricate set of correlations is mainly the result of a decrease of most elements with increasing SiO_2-content, except for K_2O (steady increase), Na_2O (fig. VI.5) and Al_2O_3 (stable in the migmatites). Therefore, SiO_2 has a negative correlation with most elements, which have mutual positive correlations; Na_2O and K_2O react mainly the same as SiO_2. The fluid phase (H_2O, F and CO_2) shows only weak correlations if any.

A few rock characteristics deduced from the chemical analyses will be treated briefly :

I : If the samples are plotted in the (Na_2O+K_2O) - $(FeO+Fe_2O_3)$ - MgO triangle (fig. VI.7), it can be seen that the igneous group follows approximately the tholeiitic trend, except for the anorthosites and phase A. Some analyses from Van Riel (1973-a) from phase A were added in the graph because the meager data in the author's collection would not permit any firm statement on the behaviour of phase A. Together with the anorthosites they seem to form a trend in the calc-alkali field, which is opposite to the tholeiitic trend. The migmatitic group forms a broad mixed trend. Both igneous trends are in good agreement with, for instance, the trends found in the Marcy massif (Buddington, 1972).

II : Various bulk composition indexes have been used in literature (e.g. Fiala et al, 1976) to show the characteristics of various complexes and petrographic provinces, for instance the

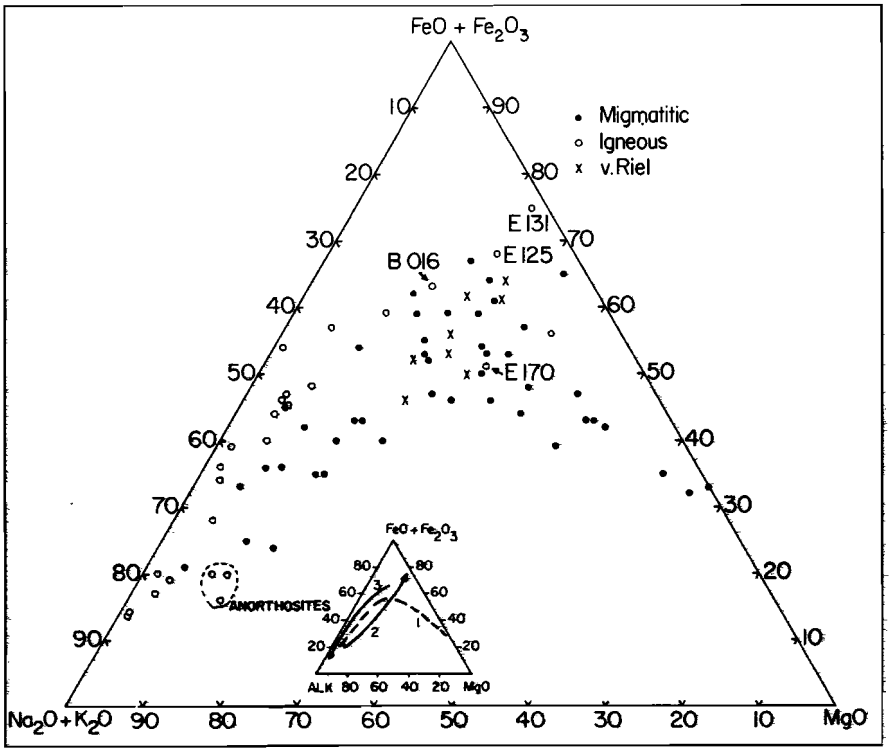

Figure VI.7. : Alkali-iron-magnesia triangle for the migmatitic- and igneous group, with some additional analyses from Van Riel (1973-a). The inset shows the generalized trends for : migmatites (1), anorthosites and phase A (2), and other igneous rocks (3).

--Larsen variation index : $1/3SiO_2+K_2O-FeO-MnO-MgO-CaO$ (total Fe as FeO)
--mafic index : $(Fe^{2+}+Fe^{3+})/(Fe^{2+}+Fe^{3+}+Mg)$ (it may include Mn)
--felsic index : (Na + K)/(Na + K + Ca)
--alkali index : K/(Na + K)
--differentiation index : CaO + MgO

The highest correlation coefficients for the various groups (Mig-Ign-Com) were found for the Larsen variation index. In the migmatitic group SiO_2, FeO, MnO, MgO, CaO, Na_2O, and K_2O all have r-values $\geq |.50|$. F, H_2O, P_2O_5 and TiO_2 show a decrease of the maximum amount possible with increasing Larsen index (fig. VI.8). The results in the igneous group are equally good. If the curves from the igneous group are compared with the petrographic provinces given by Larsen (1938), it becomes immediately clear that the igneous group is notably rich in FeO

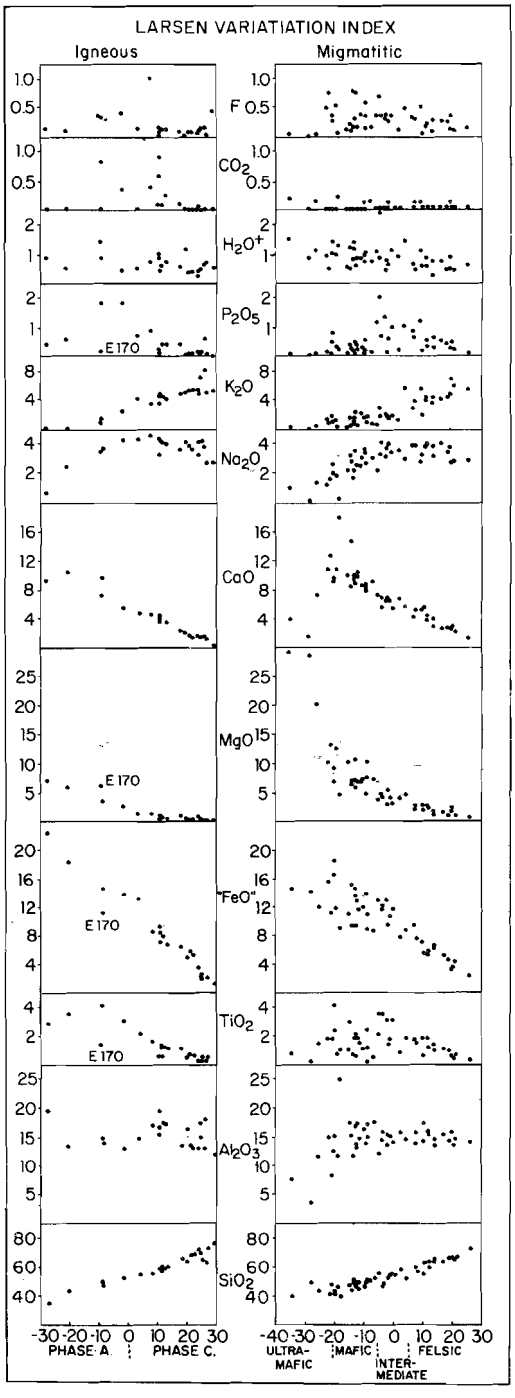

and poor in MgO and CaO.

The main differences between the igneous- and migmatitic rock group are :

--slightly higher "FeO" (=FeO+ MnO+0.9Fe_2O_3)-values for the igneous group, and lower MgO-values,

--and a greater variation in CO_2-values for the igneous rocks.

Further remarks : E 170 deviates from some of the igneous trends, fitting better in the migmatitic graphs (E 170 is an amphibolite in the top of the lopolith; Al_2O_3 is almost completely indifferent with regard to changing chemistry;

because of the good correlations in fig. VI.8 for the igneous

Figure VI.8. : Larsen variation index vs bulk composition parameters for the igneous- and migmatitic group.
Larsen index : 1/3SiO_2+ K_2O - CaO - MgO - "FeO"; "FeO = FeO + MnO + 0.9Fe_2O_3 (Larsen, 1938).
The main phases of the lopolith can be divided by means of the Larsen index :
--phase A : index mostly less than 0.
--phase C : index mostly greater than 0.
There is only 1 sample from the intermediate phase (R 269, index = 8).
Gloppurdi- and Botnavatnet samples are in agreement with the higher values of phase C. The anorthosites (+5 - +9) are completely out of line, and therefore not plotted. There is a strong resemblance with a comparable rock suite in the Lac Rouvray area, Quebec (Kehlenbeck, 1974).

group (narrower zones than for the migmatitic group), it is possible to estimate roughly the chemical composition of a sample if only one oxide, for instance CaO, is known. Phase A is less reliable than phase C, because only few samples are used for the left-side of the graphs; comparable Larsen indexes for several samples indicate comparable chemistry, e.g. V 363 and W 162 D (resp. 17.9 and 15.8). The bulk compositions and the amphibole chemistry are very much alike. The only difference is the colour. It is more brownish for V 363 which lies close to the hypersthene line, and green for W 162 which is situated in the amphibolite facies area. The colour-difference is not caused by different Ti-contents, but probably by strong differences in oxidation ratio.

Several authors have used modified versions of Larsens variation index, e.g. : Carmichael et al (1974) : 1/3Si + K - Ca - Mg; and Fiala et al (1976) : 1/3(Si + K) - (Ca + Mg).

III : the K_2O/Na_2O-ratio is mainly a function of the alkalifeldspar/plagioclase-ratio (fig. VI.9 and fig. VI.6). Alkalifeldspar-free rocks have a K_2O/Na_2O-ratio less than 1.0 (except for amphibole xenocryst A 128), and all K_2O will be contained in amphibole and biotite. In general, K_2O/Na_2O is greater than 1.0 if plagioclase is less abundant than alkalifeldspar. The An-percentage of the plagioclase will influence the position in the zone.

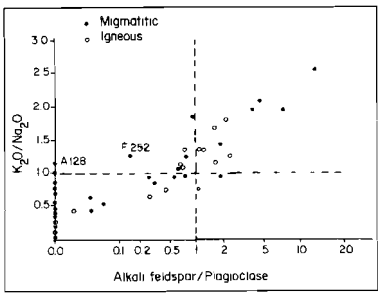

Figure VI.9. : Bulk composition K_2O/Na_2O versus the feldspar ratio (resp. normal scale and logarithmic). Rocks rich in mesoperthite are not plotted. F 252 contains too little alkalifeldspar in the modal analysis (fig. III.8).

IV : the Kuno diagram (fig. VI.10) is an extension of fig. 10 in Hermans et al (1975). The igneous group covers the alkali-basalt field, mainly according to Hermans et al but there are more extremes, e.g. at the SiO_2-rich side of the graph, the samples (V 147 and V 276 from Gloppurdi) plot in the high-alumina field because Na_2O decreases stronger than

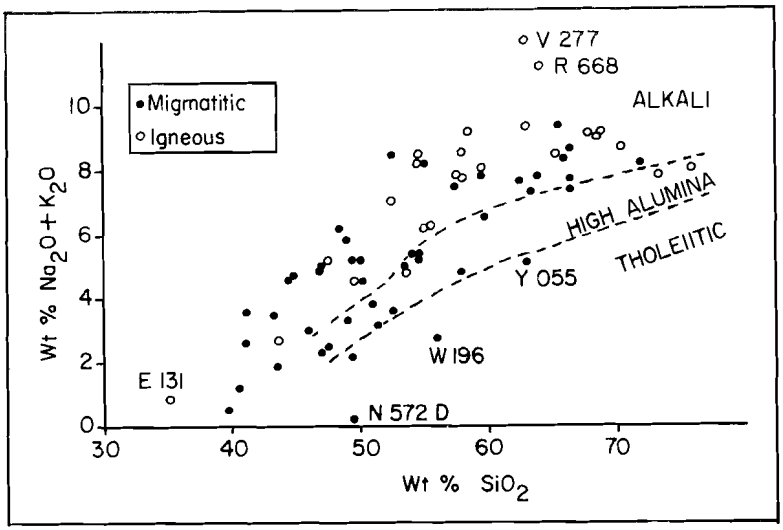

Figure VI.10. : SiO_2 vs $(Na_2O + K_2O)$ for the migmatitic- and igneous bulk compositions. The dashed lines are from Kuno (1968).

K_2O increases (see fig. VI.5 and VI.6). The migmatitic groups shows a greater spread.

VI.2. : Amphibole oxide and fluorine parameters

VI.2.1. : Introduction.

This section is the amphibole equivalent of section VI.1. The Ca-amphiboles are not only divided in Mg-rich (generally migmatitic) and Fe-rich (generally from the igneous complexes) samples, but also in main and secondary (table VI.3). Phase A samples are now placed in the Mg-rich group except for the Fe-rich B1016 (see further sections VI.3.2. and VI.1.1.). The secondary group contains all amphiboles which occur as rims or spots besides a main amphibole; their compositions are more actinolitic than those of the main amphiboles and, therefore, they would influence the graphs too much if no distinction were made.

In cases were more than one analysis is tabulated for a single amphibole (e.g. B1016), only one of these is used if the differences are rather small. The chemical characteristics of the four groups can be

Mg-rich group :

Main : A 037, A 128, B 118, B 254, B 322, D 172, D 307, D 442, D 444, E 125, E 128 1, E 131, E 170, F 005, F1043, F1052, F3052, F 070, F 074, F1107, F1126, F1252, H1047, H1050, H 307, H 325, H 415, J 119, (L1143 M), M 101, (N1041 2), N1264, N 317, N 337, N1572 R, N 809, O 100, P 248, P 303 2, P1580, P2580, V1187, V 363, W 012, W 017, W 162, W 196, W 217, W1226, W2226, Y1055.

Secondary : F2043, F4052, F2252 1-3, L1143 1-3, N1041 1-3, N2041 1-3, N2264 M and 1, V2187.

Fe-rich group :

Main : B1016 1, E 067, E1167, E1232 K and R, E3232 N, F1433, N1402 1, N1528, N3528, N1827 4, P1097, R 227, R1229, R1269 1, R 356 1, R1668, V 147, V 276, V 277, Y1128 1, (Y1131 1, Y2131, Y3131 K and R).

Secondary : E2167, E2232 N, N1827 2, N2827 1-3, R2229 1 and 3, R2269 1-3, Y2128.

Table VI.3. : Subdivision of the Ca-amphiboles in Mg-rich and Fe-rich, main and secondary amphiboles. Samples between brackets are problematic : L1143 is a magnesio-hornblende in anorthosite, N1041 is a loose sample with strange mineralogy and an extreme amphibole composition. Both samples may be used for amphibole-amphibole correlations, but not for amphibole-whole rock relations. Because of their position at the transition from main to secondary amphiboles in the Leake diagram (fig. IV.8) both samples are also present in the secondary group. Different microprobe spots on Y 131-amphiboles showed great variation (see Appendix) they are omitted because they fit poorly in the graphs.

seen from fig. VI.11.

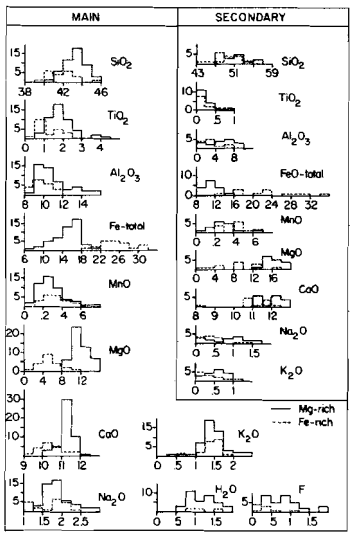

Figure VI.11. : Oxide- and fluorine histograms for the four amphibole groups from table VI.3. From the secondary groups too little is known about the fluid contents to draw histograms. L 143, N 041 and Y 131 are left out.

VI.2.2. : Results for the main amphibole groups.

Table VI.4 has four sections i.e.: oxides determined by microprobe; additional Fe^{2+}, Fe^{3+}, H_2O and F; and some important ratios and sums. General information is found in section VI.1.2.

The Fe-rich group contains most correlations $\geq |.50|$ and also most "best fits" in the microprobe information table (table VI.4).

	N	B
Mg-rich	8	3
Fe-rich	16	14
Combination	6	3

A graphical representation of all significant correlations between

Relation	Mg	Fe	Com	Relation	Mg
FeO-t -MgO	-.91	-.99	-.98	FeO-t -FeO	.90
SiO_2 -MgO	.30C	.86	.64C	MgO -FeO	-.87
SiO_2 $-Al_2O_3$	-.81		-.44A	CaO -FeO	-.52G
SiO_2 -FeO-t		-.81		K_2O -F	.51
CaO $-Na_2O$		-.80		Al_2O_3 -F	-.50A
FeO-t -CaO	-.56	-.78	-.79	---	
MgO -CaO	.54	.74	.79	FeO -II	.89
---				Fe_2O_3 -III	.87
MgO -I	-.95	-1.00	-.98	F -IV	.74N
FeO-t -I	.99	.99	.99	FeO -III	-.66
microprobe only				add. Fe, H_2O and F	

Table VI.4. : Strongest main amphibole oxide and fluorine correlations in order of decreasing absolute r-value. Underlined are the "highest r-values per relation". Fe : Fe-rich; Mg : Mg-rich; Com : all main amphiboles together. FeO-t : All Fe as FeO. I : (Fe+Mn)/(Fe+Mn+Mg); II : (as I but with separate Fe^{2+} and Fe^{3+}); III : $Fe_2O_3/(Fe_2O_3+FeO)$; IV : (H_2O+F). Mg-rich : 49 samples, Fe-rich : 21 samples. L1143 M, N1041 2 and all Y 131 amphiboles are left out. Additional laboratory measurements were performed on 39 amphiboles from the Mg-rich group. Too little is known about the Fe-rich.

microprobe determined amphibole oxides is shown in fig. VI.12.

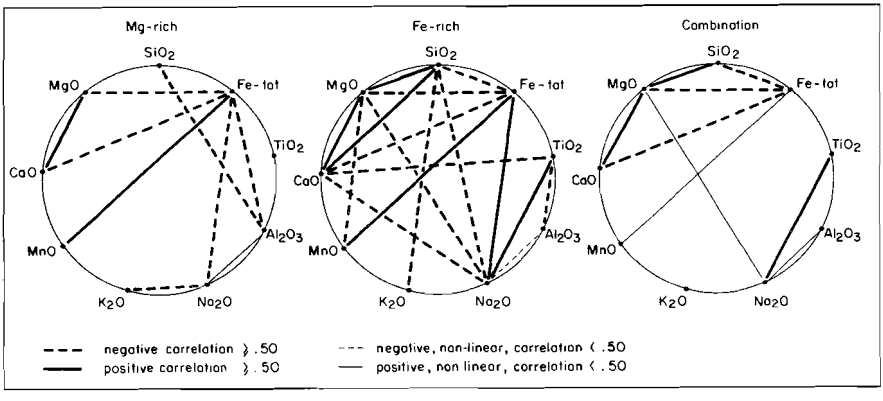

Figure VI.12. : Overall picture of all significant linear- or zone correlations in the Mg-rich, Fe-rich and combined group of main amphiboles.

Some remarkable points are :

--The only good correlations for the Mg-rich group are Fe-Mg and Si-Al, the rest is very weak.

--The only good correlations for the Combination are Fe-Mg and Fe-Ca (and thus Mg-Ca).

--Na_2O vs Al_2O_3 is positive for the Mg-rich and negative for the Fe-rich group (resp. .47F and -.40E), see fig. VI.13.

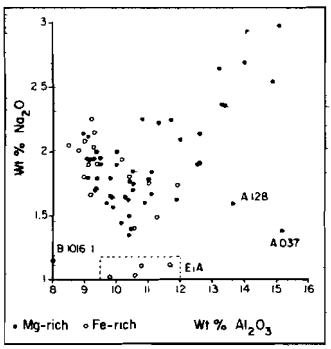

Figure VI.13. : Na_2O vs Al_2O_3 for the main amphiboles of table VI.3. The Mg-rich trend can be divided in two parts:
-a negative correlated low Al_2O_3-part, coincident with the Fe-rich trend,
-a positive correlated high Al_2O_3-part, mainly pargasites, ferroan pargasites, and ferroan pargasitic hornblendes.

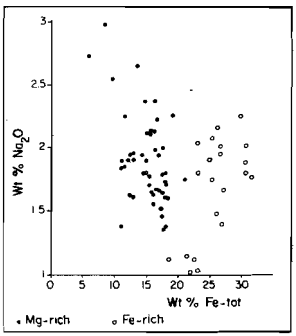

Figure VI.14. : Na_2O vs FeO-t for the main amphibole groups of table VI.3. The Mg-rich trend is negative, the Fe-rich trend is positive.

--Na_2O vs FeO-total also shows different trends for the Mg- and Fe-rich group (fig. VI.14). The graph shows that Na_2O is high in MgO- and FeO-rich amphiboles and low in intermediate amphiboles.

--Na_2O and Al_2O_3 have the same sort of correlations with H_2O, F, Fe_2O_3 and FeO for the Mg-rich amphiboles (resp. N- and 3A-types, fig. VI.2). This may be caused by the positive correlation between Na_2O and Al_2O_3, especially for the higher values (fig. VI.13). Al_2O_3-rich (and thus Na_2O-rich) amphiboles in the Mg-rich group contain more H_2O and less F than the Al_2O_3-poor amphiboles. Because the Al_2O_3-rich amphiboles from the Mg-rich group are more or less pargasitic in composition, their FeO- and Fe_2O_3-contents are relatively low.

--The oxidation ratio of the main amphiboles is not related to other chemical characteristics.

--The sum of fluids is not influenced by other chemical parameters.

It is interesting to see in fig. VI.12 that in the Mg-rich group there is a correlation between SiO_2 and Al_2O_3, which is absent in the Fe-rich group, while the SiO_2-MgO (and FeO-t) correlation from the

Fe-rich group is absent in the Mg-rich group.

Camerons (1971) finding that Fe avoids bonds with F (in his case in synthetic, Fe-Mg, Fluororichterites) is possibly supported by the findings for the amphiboles from this study. Most fluor analyses were performed on hornblendes containing much more Al_2O_3 than richterite. If only the Mg-rich amphiboles are considered, no relation between FeO-t and F can be seen, but if the Fe-rich amphiboles are plotted too, these contain rather low F (fig. VI.15). There is no linear relation, only the maximum amount of F seems to be restricted. It should be kept in mind that there are only 6 Fe-rich points versus 37 Mg-rich. One might also conclude that F is not restricted by the Fe-content of the amphibole but that the igneous complexes contained less F available for amphibole.

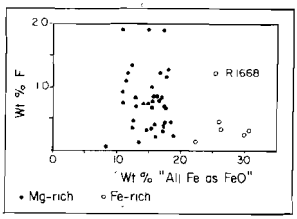

Figure VI.15. : F vs FeO for the main amphibole group.

VI.2.3. : Results for the secondary amphibole groups.

The strongest correlations are given in table VI.5, and all significant correlations in fig. VI.16.

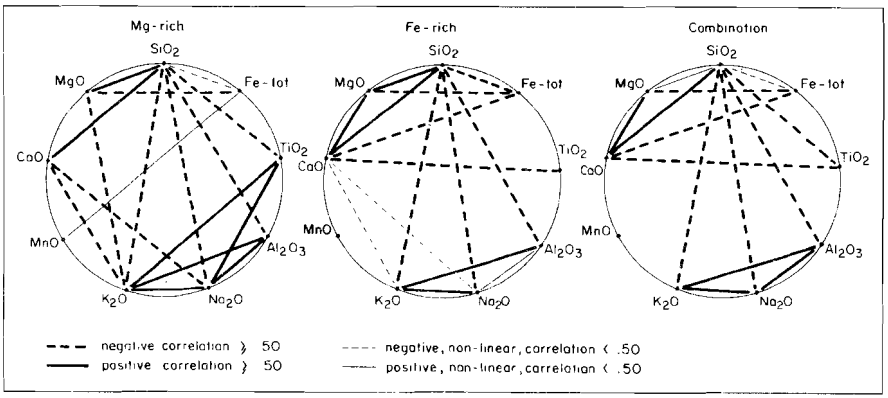

Figure VI.16. : Overall picture of all significant linear- and zone correlations in the Mg-rich, Fe-rich and combined group of secondary amphiboles.

Relation	Mg	Fe	Com
FeO-t -MgO	-.89	-.99	-.99
SiO_2 -Al_2O_3	-.97	-.75W	-.77W
SiO_2 -K_2O	-.97	-.66	-.77G
Al_2O_3 -K_2O	.94	.51H	.76H
Na_2O -K_2O	.90	.92	.88
SiO_2 -Na_2O	-.85	-.66	-.63
Al_2O_3 -Na_2O	.84	.43H	.75H
CaO -Na_2O	-.84	-.29G	
FeO-t -I	.98	.99	.99
MgO -I	-.96	-.99	-.99

Table VI.5. ± Strongest secondary amphibole oxide correlations in order of decreasing absolute r-value. See further table VI.4 subscript.

The Mg-rich group contains most correlations $\geq |.50|$ and also most "best fits".

	N	B
Mg-rich	16	13
Fe-rich	12	5
Combination	12	3

(correlations with the Fe-ratio (=I) are not included).

The result is quite different from the main group where the Fe-rich amphiboles had the highest N- and B-values. The ferro-actinolites E2167 and Y2128, and a subcalcic ferro-hornblende (R2229 3) seem to disturbe the picture.

Some remarkable points are :

--There are more high r-values for the secondary group than for the main group. This is a result of the lesser degree of substitution of Al_2O_3 for SiO_2, demanding a decrease of other charge compensating elements (Na_2O, K_2O and TiO_2).

--Besides the earlier found Fe-Mg and Si-Al correlations, the alkalies play an important role. K_2O and Na_2O are much stronger correlated with SiO_2 than TiO_2 (SiO_2-TiO_2 : -.58A -.49A -.56A).

--K_2O in the Mg-rich group is much better correlated with SiO_2 than Na_2O. This is caused by the fact that the influence of CaO on Na_2O is stronger than on K_2O. A deficiency of CaO must be compensated by alkalies, mainly Na_2O.

--Fig. VI.16 is dominated by the charge compensating points SiO_2-Al_2O_3-K_2O-Na_2O.

VI.3. : Rock parameters versus main amphibole oxides and fluorine.

VI.3.1. : Introduction

Before the influence of the metamorphic grade on the amphibole composition can be assessed one must know the influence of the rock composition. And in order to understand the interrelations of the various rock- and amphibole parameters on one another, one has to know the individual correlations in the rock and amphibole systems (sections VI.1 and VI.2.).

In this section the interest is focussed on the main amphiboles. The secondary amphiboles are left out because they are the result of retrograde metamorphism. The samples are again divided into a Mg-rich, Fe-rich and combined group, mainly in accordance with table VI.3. B 322, L 143 and N 041 were left out of the Mg-rich group (n=48) : B 322 because of the extreme rock composition; L 143 and N 041 see table VI.3 subscript. Y 131 and F 433 were omitted in the Fe-rich group (n=20) : Y 131 amphiboles usually show a poor fit, on account of their hastingsitic composition; of F 433 there is no bulk analysis. E1232 is combined with F 501, E3232 with F 502 because the E 232 specimen is partly quartzmonzonite and partly anorthosite (see Appendix). The combined group contains 68 samples.

For an understanding of the different correlation patterns for the Mg- and Fe-rich group, one has to bear in mind that :
--the Mg-rich (mainly migmatitic) rock group is more mafic than the Fe-rich group (fig. VI.1) which results in a relatively high Fe/(Fe+Mg) (=mafic index) for the Fe-rich group.
--the Mg-rich amphibole group is richer in SiO_2, Al_2O_3, TiO_2, MgO and CaO than the Fe-rich group (fig. VI.11).

VI.3.2. : Results

A complete scheme of the strongest correlations is given in table VI.6.

AMPHIBOLE PARAMETERS	Mg-rich		Fe-rich		Combination	
SiO_2	π	(-.59)	MAF	(-.69)	P_2O_5	(-.27 A)
TiO_2	FeO	(.52 Q)	H_2O^+	(-.66)	L	(-.53 G)
					fm	(.53)
Al_2O_3	π	(.85)	no relation		π	(.79)
Fe_2O_3	w	(.60)	no info		no info	
FeO ss.	LARS	(.52)	no info		no info	
FeO-Total	MgO	(.70)	mg	(-.75)	mg	(-.84)
	μ	(-.70)				
MnO	alk	(.71)	w	(.58)	alk	(.58)
MgO	MAF	(-.59)	mg	(.76)	mg	(.81)
	μ	(.59)				
CaO	Na_2O	(-.31 D)	π	(.74)	mg	(.64)
Na_2O	MgO	(.56)	π	(.79)	MgO	(.51)
K_2O	K_2O	(.08 S)	MgO	(-.75)	FeO	(-.15 R)
H_2O	F	(-.31 A)	no info		no info	
F	μ	(-.41 A)	no info		no info	
Ratio I	MgO	(.68)	mg	(-.78)	mg	(-.84)
	MAF	(.68)				
	μ	(-.68)				
Ratio II	MgO	(-.46 K)	MgO	(-.37 K)	MgO	(-.45 K)
Ratio III	F	(.45 C)	no info		no info	
F + H_2O	mg	(-.40 G)	no info		no info	
Oxid. rat.	w	(.60)	no info		no info	

Table VI.6. : Scheme of the strongest correlations between bulk- and amphibole chemical parameters. Rock parameters consist of oxides, niggli-values and indexes : LARS : Larsen variation index; MAF : Mafic index; π, μ, mg, fm, L, w and alk are niggli values. Special amphibole parameters are : Ratio I : (Fe+Mn)/(Fe+Mn+Mg); Ratio II : K/(K+Na); Ratio III : F/(F+H_2O); Oxid. Rat. : $Fe_2O_3/(Fe_2O_3+FeO)$.

For rock parameters the oxides, niggli values and indexes were used. From this table one can see if the relation counts for the more mafic rocks (Mg-rich group), the felsic rocks (Fe-rich group), or if it is a

general rule for the Rogaland/Vest-Agder area (Combination).

The only amphibole parameter which shows no relation with the bulk composition is Al_2O_3 in the Fe-rich group.

Niggli-π and -mg are the rock parameters which control the amphibole composition most strongly (π = Ca-part of the leucocratic minerals, = comparable to the An% of plagioclase, see fig. VI.17).

The 10 strongest influenced amphibole parameters are :

1 :	Al_2O_3	(Mg-rich)	versus niggli π :	.85
2 :	FeO-total	(Combination)	niggli mg:	-.84
3 :	(Fe+Mn)/(Fe+Mn+Mg)	(Combination)	niggli mg:	-.84
4 :	MgO	(Combination)	niggli mg:	.81
5 :	Al_2O_3	(Combination)	niggli π :	.79
6 :	Na_2O	(Fe-rich)	niggli π :	.79
7 :	(Fe+Mn)/(Fe+Mn+Mg)	(Fe-rich)	niggli mg:	-.78
8 :	MgO	(Fe-rich)	niggli mg:	.76
9 :	FeO-total	(Fe-rich)	niggli mg:	-.75
10 :	K_2O	(Fe-rich)	MgO :	-.75

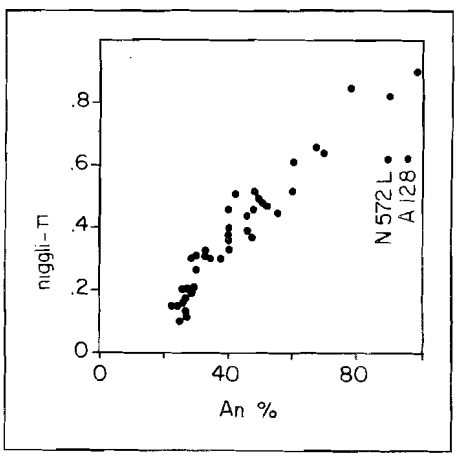

Figure VI.17. : Correlation between niggli-π values and the An-percentages of plagioclase. Values from table III.4 and III.1.

In fig. VI.18 the influence of the bulk composition oxides on the amphibole composition is graphically presented, and directly interpretable. The differences between the more mafic group of rocks with Mg-rich amphiboles and the more felsic rock group with Fe-rich amphiboles are clear. All r-values in this fig. VI.18 are generally less than |.70|. Only the following correlations are stronger :

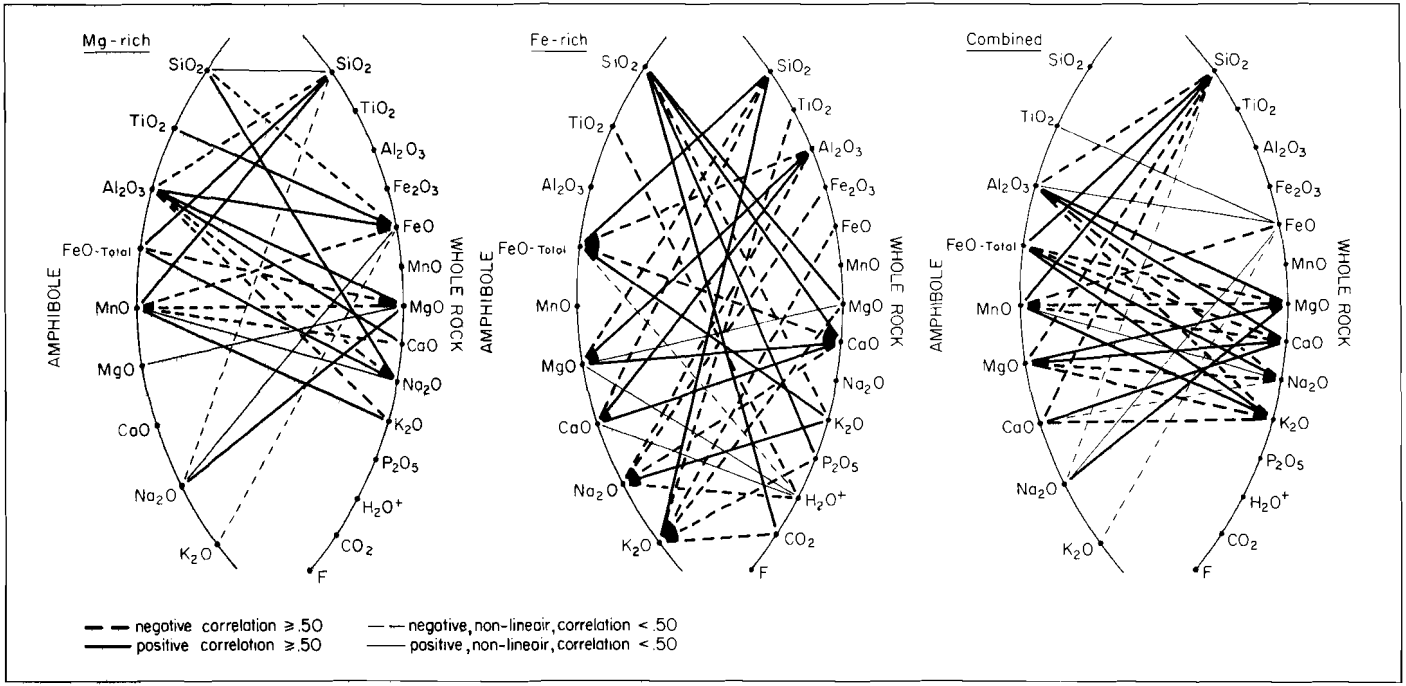

Figure VI.18. : Overall picture of all significant linear- or zone correlations in the Mg-rich, Fe-rich and combined group between bulk- and amphibole composition.

Relation	Mg	Fe	Com
Na_2O -Al_2O_3	-.77		-.68
MgO -K_2O		-.75	
SiO_2 -Al_2O_3	-.73P		-.63P
TiO_2 -K_2O		-.71	
Rock -Amph.			

Signatures, see table VI.4 and fig. VI.2.

Further remarkable points are :

--SiO_2-amphibole first increases with SiO_2-bulk and decreases at higher bulk values.

--The highest TiO_2-amphibole values are found in the most mafic rocks.

--Na_2O-amphibole first decreases and than increases with increasing SiO_2-bulk.

--MnO-amphibole is higher in felsic rocks.

--Most Al_2O_3-bulk correlations are mainly determined by the anorthosite samples. The only reasonable Al_2O_3-bulk trend is vs CaO-amphibole in the Fe-rich group.

--Water-rich rocks prefer MgO- and CaO-rich, Na_2O- and FeO- (and TiO_2-) poor amphiboles in the Fe-rich group.

--The oxidation ratio of the amphiboles does not show any correlation with the bulk composition or its indexes, only with the niggli-w (bulk oxidation ratio).

--MnO and FeO-t (amphibole) in the Mg-rich group are about equally strongly correlated with the bulk composition (resp. .71 vs niggli-alk and -.70 vs MgO).

(Fe+Mn)/(Fe+Mn+Mg)-ratio : bulk composition versus main amphibole.

One of the strongest correlations between bulk- and amphibole composition is the (Fe+Mn)/(Fe+Mn+Mg)-ratio (amphibole) vs niggli mg for the Combination (-.84). Niggli-mg is approximately the reciprocal of the (Fe+Mn)/(Fe+Mn+Mg)-ratio (rock) which is the same as the Mafic index. Therefore, we may use the Mafic index to analyse the strong above mentioned correlation.

The diagram for this function (fig. VI.19-a) shows a tendency for the 1:1 ratio but many samples lie on the more Fe-rich bulk side. These deviations are mainly caused by the presence of free Fe-oxides (ore) in the sample.

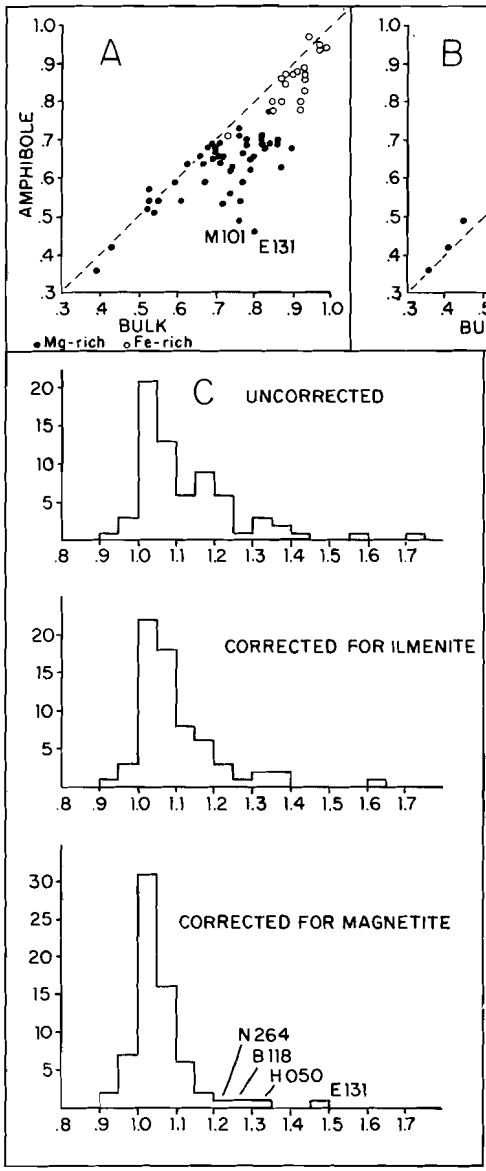

Figure VI.19. : (Fe+Mn)/(Fe+Mn+Mg) ratio bulk versus amphibole. A : uncorrected, B : corrected for ilmenite and magnetite, C : histograms for the K_D-values.

From the ratios for the bulk and amphibole one can calculate a K_D-value ($=\frac{\text{bulk ratio}}{\text{amph ratio}}$). These K_D-values are compiled in a histogram for the uncorrected bulk composition (fig. VI.19-C), the mode of the histogram lies between 1.00 and 1.05 but there is a strong skewness to higher K_D-values.

If the ore in the samples is thought to consist of ilmenite, and the modal percentages (table III.1) are roughly taken as weight percentages (this results in slightly too low wt%, depending on the density of the rock), then the bulk Fe-oxides can be decreased by half the ore modal % as FeO (ilmenite consist approximately of 50% FeO). This results in a new bulk ratio and K_D for every ore-bearing sample. The histogram now is less irregular.

The second step is done by considering the ore as magnetite. An extra amount of Fe_2O_3 (equal to the already subtracted amount of FeO) is subtracted from the bulk

Fe-oxides. The final histogram is much better than the uncorrected. Most bulk- and amphibole ratios are now about equal (fig. VI.19-B). Ore percentages less than 1% are not corrected for.

Some samples do not need (or only partially need) the magnetite correction. From ore microscopical investigation it was found that most Rogaland rocks contain magnetite and ilmenite, which means that a complete magnetite correction is a bit too extreme. This, however, is counteracted by the fact that the modal percentages are taken as weight percentages.

In general it may be said that the K_D-value in the corrected form is approximately 1.00. This is not surprising for rocks with only amphibole as mafic phase, but it is interesting for the more mafic rocks with larger amounts of pyroxene and olivine.
The metamorphic zoning in Rogaland seems to have no influence : Fe-oxides and MgO in the main amphibole is almost completely determined by the composition of the silicate part of the host rock.

Most interesting are the deviating samples, of which only the extremes are treated here :

N 264 : K_D= 1.20. The sample is retrograde, the large quantity of biotite may be more Fe-rich than the amphibole.

B 118 : K_D= 1.28. The amphibole is present at the contact between an amphibolite band and a charnockite. The bulk composition of the light band has been used. This deviating K_D-value indicates that the amphibole does not belong to the light band but to the amphibolite band (see also Chapter II).

H 050 : K_D= 1.31. Strong exsolution of titano-magnetite needles, due to retrogressive metamorphism (see section IV.3.4.).

E 131 : K_D= 1.46. This sample contains 12% ore, mainly magnetite. The (Fe+Mn)/(Fe+Mn+Mg)-ratio in amphibole is 0.46, in spinel 0.73; the corrected rock ratio is 0.67. In this case the modal % as wt% calculation causes a great difference : magnetite has a density of ca 5.2 and the remaining part of the rock ca 2.9

(plagioclase and pyroxene). 12 Modal % ore result in ca 20 wt% Fe-oxides. If, considering this, the bulk ratio is recalculated, it is $\pm$ 0.45, which is in complete agreement with the amphibole ratio. Orthopyroxenes with this ratio occur at the base of phase C of the lopolith of Bjerkreim-Sokndal (Duchesne, 1972; Rietmeijer, 1973). This sample belongs, possibly, to phase A, see Chapter II.

If the other correlations between an amphibole parameter and niggli-mg (FeO-total, MgO, SiO_2) are plotted with recalculated bulk ratios as described above, the scatter of the points is much reduced. Both FeO-total and MgO are about the same as fig. VI.19-B, MgO of course the opposite of FeO-total.

Influence of the plagioclase composition on amphibole chemistry

Niggli-π is strongly correlated with amphibole Al_2O_3. This indicates an influence of the An-percentage of the plagioclase (fig. VI.17).

If the rocks of similar chemical composition from various metamorphic grades are compared, one can often see a change in An% of the plagioclase. In Rogaland, however, such a change is not clear. Granitic- and charnockitic rocks all over the area have An-contents between 15 and 30%, while amphibolites vary from An_{30} to An_{70}.

The differences in An% are mainly caused by differences in bulk composition and not by differences in metamorphic grade. From one and the same location one can collect leucocratic samples with An_{25} and mafic samples with An_{70}. The An% increases with, for instance, decreasing Na_2O-bulk, Larsen index, and Mafic index, and with increasing niggli-π, CaO-bulk and Al_2O_3/SiO_2-bulk ratio.

Because amphibole has several relations with the bulk composition, it may also have these relations with the An% of the plagioclase. It appears that with increasing An%, the main Mg-rich amphiboles become richer in : Al_2O_3, MgO, CaO, Na_2O, Al_2O_3/SiO_2, and $Na_2O/(Na_2O+CaO)$

(compare with Leake, 1965-a, p. 305-310). A 037 and A 128, the samples with the highest An-percentages, disturb the Na_2O graphs. SiO_2, MnO and FeO-total decrease, and TiO_2 and K_2O do not change markedly. The changes for the Fe-rich group are less clear to see, because of the small spread in An-percentages (14-35).

The correlation between Al_2O_3-amphibole and the An%-plagioclase has an r-value of 0.83, it completely determines the Al_2O_3/SiO_2-amphibole versus An% (=Al_2O_3/SiO_2-plagioclase) graph with r = 0.82, see fig. VI.20.

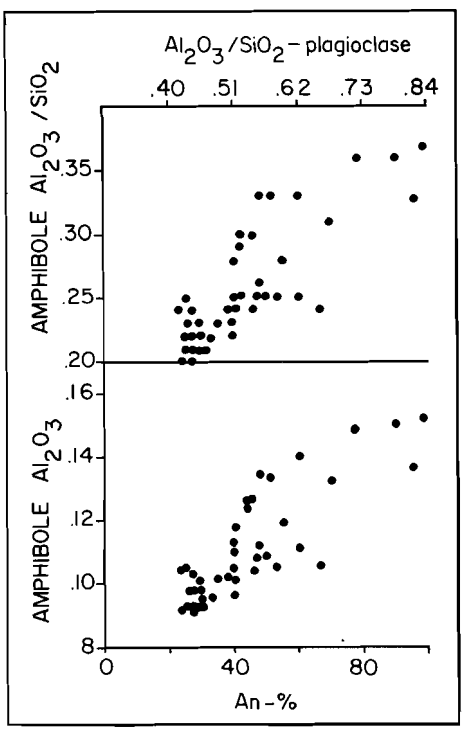

Figure VI.20. : An% plagioclase (=Al_2O_3/SiO_2) vs Al_2O_3 and the Al-Si ratio of the amphibole in the Mg-rich group.

The K_D-value for the last relation is $\pm$ 2 (K_D= Al_2O_3/SiO_2-plag : Al_2O_3/SiO_2-amph).

The SiO_2-content of the amphibole is much less important for the ratio than Al_2O_3. If the correlation between the Al_2O_3/SiO_2-amphibole vs the same ratio for the bulk composition is drawn, no significant result is found.

VI.4. : Secondary amphiboles and the influence of the bulk composition

The secondary amphiboles all moved from the original composition of the main amphibole to a (ferro-)actinolitic composition. There is no direct correlation between the chemistry of these amphiboles and the bulk composition. All correlations are inherited via the line : bulk composition-main amphibole composition-secondary amphibole composition.

There is only one restriction : actinolitic amphiboles are never found in the most mafic rocks of Rogaland/Vest-Agder. West of the hypersthene

line (granulite facies) they only occur in rocks with a mafic index > .67 (mafic index = $(Fe^{3+} + Fe^{2+} + Mn)/(Fe^{2+} + Fe^{3+} + Mn + Mg)$). East of the hypersthene line (amphibolite facies) they are found in slightly more mafic rocks : > .58.

The fact that the most mafic rocks do not allow the forming of actinolite may be caused by a lack of SiO_2 in the system. Actinolite needs much more SiO_2 than common hornblende.

VI.5. : Amphibole structural formula correlations

VI.5.1. : Introduction

As shown in section IV.2.6-3, the 23(0) structural formula gave better results for ion- and position correlations than the other calculation methods. Therefore, it is the only formula type used to investigate the correlations for the various groups, and for all samples. In the above mentioned section only Mg-rich amphiboles with a complete analysis were considered. The samples used here are the same as those used in section VI.2.

VI.5.2. : Results for the main amphibole groups

Some correlations found in section VI.2.2. for the oxides are completely missing or strongly changed when the ion relations are calculated. Most important is the change in SiO_2-correlations. Former SiO_2-MgO (or FeO) correlations (table VI.4) are completely lacking here. This is caused by the fact that there is no linear relationship between SiO_2 and Si for groups of amphiboles with varying Fe/Mg-ratio. For Fe-rich amphiboles a certain amount of SiO_2 results in more Si in the structural formula than for Mg-rich amphiboles. MgO has a much lower molecular weight than FeO, hence it increases the amount of mol. proportions (and atom. proportions of oxygen) stronger than the same weight % of FeO (see calculation method in Deer, Howie and Zussman, 1974). This results in a

Relation	Mg	Fe	Com
Fe -Mg	-.90	-.99	-.98
Si -Al-t	-.96	-.84	-.94
Al^{VI}-Al-t	.90	.82	.86
Al^{VI}-Ti		-.80	
Si -K		-.77	
Si -Al^{VI}	-.75		-.64
Mg -I	.99	1.00	.99
Fe -I	-.99	-.99	-1.00
Na -Alk	.72	.96	.83
X -A	.67	.92	.73
Alk -A	.64L	.90	.78L
Si -ComY	-.89	-.52	-.85
Ti -CaY	-.88	-.86	-.87
X -Alk	.85	.88	.84
Na -CaY	-.59	-.87	-.70
K -A		.87	
Al-t-ComY	.84		.78
K -X		-.83	.51
Al^{VI}-CaY		.79	
Ca -CaY		.79	
Ti -ComY	.79		.76
Na -A		.77	.53
Na -X		.76	.55
Alk -CaY	-.61	-.76	-.67
SumY-OH+F	-.90		
OH -OH+F	.77C		
SUMY-OH	-.73		
Al^{VI}-F	-.60A		
Al^{VI}-OH+F	-.59D		

smaller multiplication factor, and less ions in the formula for all elements, in the case of Mg-rich amphibole. The correlation SiO_2 vs MgO (or FeO) disappears, but the correlation SiO_2 vs Al_2O_3 becomes stronger.

The correlations involving Al^{VI} and other charge compensating ions in the Fe-rich group are new, as well as Al^{VI} vs Si in the more Mg-rich group. See table VI.7 and fig. VI.21, compare with table VI.4 and fig. VI.12.

Again the Fe-rich group contains most correlations $\geq |.50|$ and most "best fits" (see section VI.2.2.), caused by the correlations between the charge compensating ions and -positions in the Fe-rich group.

Only a few correlations have high r-values in all three groups, suggesting that they are of general validity :

Table VI.7. : Strongest main amphibole ion and position correlations in order of decreasing |r|-value. The table is divided in four sections i.e. element vs element, element vs mg-ratio (I), element and combinations vs combinations, and some additional correlations in the Mg-rich group for the additional OH and F. Al-t= Al^{IV}+ Al^{VI}; Alk= Na+K; X= Sum X; A= A-site = Sum Y + Sum X - 7; ComY= known charge compensators in the Y-position = Al^{VI}+ 2Ti; CaY= Ca + Sum Y. See further section IV.2.2. for the general formula.

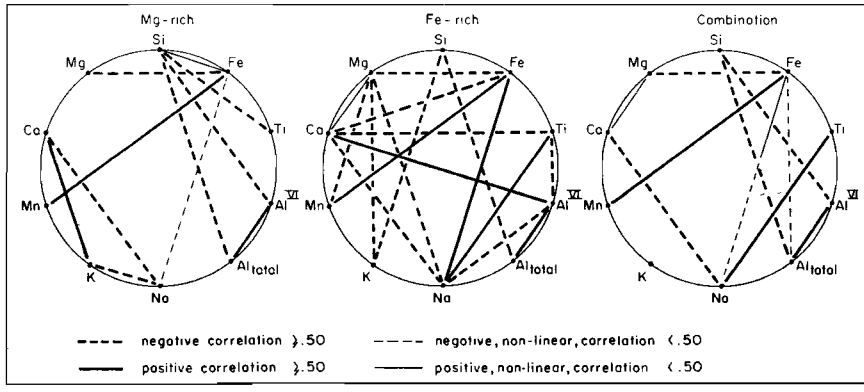

Figure VI.21. : Overall picture of all significant linear- and zone correlations in the Mg-rich, Fe-rich and combined group of main amphiboles.

--Fe vs Mg (and thus vs mg-ratio)

--Si vs Al-total

--Al^{VI} vs Al-total

--Ti vs Ca + Sum Y

--Sum X vs Na + K

The first two correlations are well known. The strong correlation between Al^{VI} and Al-total indicates that Al^{VI}-differences in the Rogaland/Vest-Agder area are not the result of varying P-conditions but are caused by internal differences in amphibole chemistry, which are determined by the An% of the coexisting plagioclase (section VI.3.2. and fig. VI.20). It is, however, possible to discriminate between two groups of Al^{VI} versus An% correlations (section I.5.). The fourth correlation is caused by the substitution of Ti^{4+} for 2 (Mg,Ca). In the last relation Na + K is an important part of Sum X (=Ca+Na+K), and as the variation in Ca is rather small, this makes Na + K the main value-determining group.

Further remarkable points are :

--The antipathetic relationship between Al^{VI} and Ti in the Fe-rich group, and K as most important charge compensator. In the Mg-rich group the charge is mainly compensated by ComY (Al^{VI} + 2Ti).

--Na and K are antipathetic in the Mg-rich group (r= -.58), but show no correlation in the Fe-rich group.

In section IV.2.6-1 it is shown that Al^{VI} and Sum Y are unreliable, however, this counts for the absolute values. Variations in the mg-ratio and the oxidation ratio are the most important causes of the unreliability of the parameters. In the groups used here there is already a separation in amphiboles with a low and high mg-ratio, while the oxidation ratio (Fe-ratio in fig.IV.17), on an average, does not differ too much. This causes a change (increase) in Al^{VI}- and Sum Y values which is more or less equal for all samples in a certain group, except in the Combination. Therefore, the correlations found between Al^{VI} or Sum Y and other parameters are not a result of the calculation method, but really do exist. The line-functions (x= Ay+B) will have correct angle constants (A) but wrong intercept values (B).

The correlations involving specially determined parameters (Fe^{3+}, Fe^{2+}, OH and F), are essentially the same as found in section VI.2.2., therefore, only the new correlations are mentioned in table VI.7. All correlations with Sum Y and Al^{VI} result from calculations with insufficient amounts of (OH+F) (as shown in section IV.2.6.-2). OH is more important than F for the sum of fluids.

If Fe^{3+} is plotted against other charge compensators or combined parameters, it is shown that an increase of Fe^{3+} is compensated by a decrease in the maximum amount of Al^{VI} and Na. Therefore, Fe-rich amphiboles with the same oxidation ratio as a Mg-rich amphibole usually have lower contents in Al^{VI} and Na. Ti and K have no direct relation with Fe^{3+} (they appear to be influenced by the metamorphic grade, Chapter I). The oxidation ratio itself is not correlated with any of the above mentioned elements or combined parameters. The actual amount of Fe^{3+} determines the correlations.

Other remarkable points have already been mentioned with the oxides, section VI.2.2.

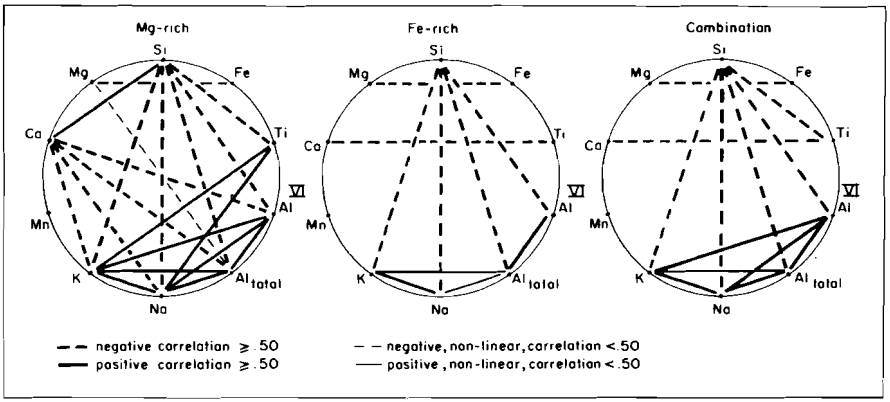

Figure VI.22. : Overall picture of all significant linear- or zone correlations in the Mg-rich, Fe-rich and combined group of secondary amphiboles.

VI.5.3. : Results for the secondary amphibole groups

The correlations which are weakened or even disappeared in the ion table (table VI.8) as compared to the oxide table (VI.5) mainly involve CaO and the mg-ratio (and thus FeO and MgO), see also fig. VI.22 and VI.16.

The correlation between SiO_2 and Si for the Mg-rich group is very high, unlike the Fe-rich group. Therefore, SiO_2-correlations in the Fe-rich group change, while they are stable in the Mg-rich group. The Al^{VI}-correlations with other charge compensating ions are rather different from the relations found for the main group.

The Mg-rich group has most correlations $\geq |.50|$ and most "best fits". The disturbing samples are again Y2128, R2229 3 and E2167, see section VI.2.3. The remaining samples from the Fe-rich group follow more or less the same trends as the samples from the Mg-rich group, though Na is lower and Sum Y somewhat higher (Fe-rich amphiboles have larger calculation errors than the Mg-rich, section VI.2.3.). Disturbing samples in the Mg-rich group are : V2187 and F2043 (high Fe-content), and F2252 1 (high N, K and Ca).

Relation		Mg	Fe	Com
Si	-Al-t	-.99	-1.00	-.99
Fe	-Mg	-.93	-.99	-.99
Al^{VI}	-Al-t	.96	.96	.96
Si	-K	-.95	-.58	-.78
Si	-Al^{VI}	-.92	-.93	-.93
Na	-K	.91	.93	.89
K	-Al-t	.93	.53H	.75H
Si	-Na	-.85	-.51	-.76
Na	-Al-t	.84	.45H	.74
Al^{VI}	-K	.84		.63
Al^{VI}	-Na	.77		.65
Ca	-Na	-.75		
Mg	-I	.97	1.00	1.00
Fe	-I	-.99	-1.00	-1.00

Relation		Mg	Fe	Com
Na	-Alk	.99	.99	.99
K	-Alk	.95	.97	.95
Alk	-A	.97	.90	.94
Si	-A	-.96	-.84	-.93
Al^{VI}	-ComY	.96	.93	.95
Si	-ComY	-.95	-.91	-.94
X	-A	.94	.65H	.79H
Al^{VI}	-Y	.91	.66	.56
K	-X	.91	.72	.77
K	-ComY	.90	.38H	.67H
Na	-X	.88	.76	.82
A	-ComY	.88	.61	.80
Si	-X	-.87		
Ca	-Y	-.82	-.87	-.85
Y	-ComY	.87	.77	.65
Si	-Y	-.85	-.58	-.53
Al^{VI}	-A	.84	.63	.79
Na	-ComY	.82	.29H	.66
Y	-A	.81		
K	-Y	.79		
Na	-Y	.78		

Table VI.8. : Strongest secondary amphibole ion and position correlations, see further table VI.7 subscript.

The correlation between Al^{VI} and Sum Y is a result of the calculation method.

The correlations between the charge compensating ions are approximately :

Mg-rich group	Fe-rich group
Al^{VI} vs Na : 1:1	Na vs K : 2:1
Al^{VI} vs K : 2:1	Na vs Ti: 4:1 (with 4 measurements
Na vs K : 2:1	deviating strongly)

The other correlations are irregular.

High r-values in all three groups are much more frequent than in the main amphibole groups because of a few strong correlations : Si vs Al-total, Al^{VI} vs Al-total, Na vs K, Na+K vs A-site (Ca+Sum Y = $\pm$ 7.00), and Si vs A-site. These five correlations are responsible for a large set of combinations. Therefore, many correlations with high r-values were left out of the lower part of table VI.8 : (Al-total, some Alk and A) to prevent doubling,

Further remarkable points are commented in section VI.2.3.

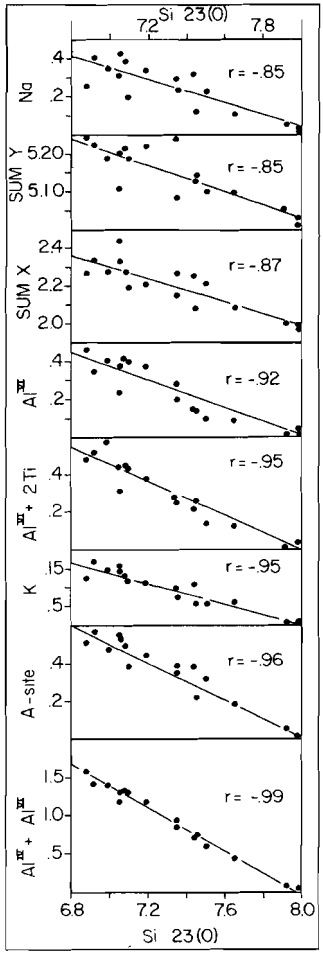

The transition from hornblende to actinolite for the Mg-rich group is illustrated in fig. VI.23. The formulae belonging to the various graphs are :

--Al^{VI} + Al^{IV} = -1.45 Si + 11.54
--A-site = -0.49 Si + 3.94
--K = -0.137Si + 1.10
--Al^{VI}+2Ti = -0.46 Si + 3.68
--Al^{VI} = -0.388Si + 3.09
--Sum X = -0.314Si + 4.51
--Sum Y = -0.175Si + 6.43
--Na = -0.30 Si + 2.45

Error ranges can be seen from the graphs.

The strong correlation between Al^{VI} and Al-total, which was also found for the main amphibole groups, leaves no room for P-differences in the investigated area during retrograde metamorphism.

There is no linear correlation between Si

Figure VI.23. : Transition from magnesio-hornblende to actinolite for the Mg-rich group. Only strong correlations are given. Various parameters are interrelated.

and Ti, in most actinolitization reactions Ti decreases very fast (Chapter II).

The differences between the main and secondary amphibole groups are evident from fig. VI.21 and VI.22.

VI.5.4. : Coupled substitutions

Various schemes of coupled substitutions which involve charge balancing, leading to idealized endmembers in the amphibole groups, have been recognized in the various amphibole groups in the investigated area.

Substitutions described by Czamanske and Wones (1973) are :

Substitution			Identifying relations
1 Edenite	: A TET A TET		
	$Na,K + Al$ for $\square + Si$		Si vs A-site, K,Na+K and Na
2 Tschermakite	$:M_{1-3}$ TET M_{1-3} TET		
a)	$Al + Al$ for $Mg + Si$		Si vs Al^{VI}, Mg vs Al^{VI}
b)	$Fe^{3+} + Al$ for $Mg + Si$		Si vs Fe^{3+}, Mg vs Fe^{3+}
3 Glaucophane	: M_4 M_{1-3} M_4 M_{1-3}		
a)	$Na + Al$ for $Ca + Mg$		Ca vs Al^{VI}, Mg vs Al^{VI}
Riebeckite b)	$Na + Fe^{3+}$ for $Ca + Mg$		Ca vs Fe^{3+}, Mg vs Fe^{3+}
4 Richterite	: A M_4 A M_4		
	$Na + Na$ for $\square + Ca$		Na vs Ca
5 Ti-Tschermakite	$:M_{1-3}$ TET M_{1-3} TET		
	$Ti + 2Al$ for $Mg + 2Si$		Si vs Ti
6 Nameless	: M_4 M_{1-3} M_4 M_{1-3}		
a)	$2Na + Ti$ for $2Ca + Mg$		Ti vs Ca, Ti vs Mg
b)	$Na + Ti$ for $Ca + Al$		Ti vs Ca, Ti vs Al^{VI}

The results for the main amphibole groups are :

Mg-rich group : the only important substitution is no 2 ($Si-Al^{VI} = -.75$). No 1, 4 and 5 are of minor importance (r-values of -.58, -.59 and -.55 resp.)

Fe-rich group : three substitutions of more or less equal importance : no 1, 4 and 6 (r-values of -.77, -.72 and for no 6 : -.68 (Ti-Ca) and -.80 ($Ti-Al^{VI}$) indicating substitution 6b).
Combined group : only two rather weak substitutions : no 2a and 4 (r-values of -.64 and -.55 resp.).

In the main amphibole groups there are no very strong separate substitutions. The Richterite substitution is the only general one.

The results for the secondary amphibole groups are :
Mg-rich group : two important substitutions : no 1 and 2a with r-values $\geq |.90|$, see also fig. VI.23. No 3a and 4 are of lesser importance (r-values of -.68 and -.75 resp.). No 5 is very weak (-.54).
Fe-rich group : the same important substitutions as for the Mg-rich group : no 1 and 2; no 5 (-.50) and 6 (Ti-Ca= -.72) are less important.
Combined group : strong relations no 1 and 2a, weak no 6.

In the secondary amphibole groups there are two strong substitutions, which are found in all groups : the Edenite and Tschermakite (a) substitution. It is interesting to see that the Glaucophane substitution can be recognised in the Mg-rich group, indicating a higher pressure for the formation of the secondary amphiboles.

VI.6. : Niggli values versus amphibole structural formula parameters

VI.6.1. : Introduction

The possibility of stronger correlations between bulk- and amphibole-ion parameters than between bulk- and amphibole-oxide parameters, has been investigated with the strongest amphibole determining niggli values : π, μ, mg, fm, L, T and alk (see table VI.6). Main amphibole parameters, see section VI.5.2.

Secondary amphiboles were not investigated (see section IV.4.). Fe^{3+} and the fluid parameters were neither reinvestigated, because Fe^{3+} is

not determined by the rock composition, and the fluid parameters do not show clear correlations with rock parameters.

VI.6.2. : Results

The only increasing r-values were found for Si (Mg-rich and Combination). Mg-rich : SiO_2 vs π was -.59, Si vs π = -.79.
Combination : SiO_2 vs P_2O_5 was -.27 (A-type), Si vs π = -.67.
See table VI.6. The differences in SiO_2- and Si correlations are explained in section VI.5.2.

The extra correlations, which could not be calculated for the oxides, are given in table VI.9. With the exception of Si, table VI.6 with the strongest correlations between amphibole- and bulk parameters, is still valid, only Al^{VI} should be added.

	Mg-rich		Fe-rich		Combined		
Al^{VI}	π	(.82)	T	(.57)	π	(.62)	1
Al^{VI} + 2Ti	π	(.72)			π	(.70)	2
Na + K	alk	(-.19S)	π	(-.77)			3
A-site	alk	(-.01S)	alk	(.70)			4
Ca + Sum Y			T	(.63)			5
Sum Y					μ	(-.60)	6a
					mg	(-.57)	6b
Sum X			alk	(.61)			7a
			ti,p	(-.55)			7b

Table VI.9. : Niggli values versus additional amphibole parameters. S : see fig. VI.2.
1-2 : resulted from the Si and Al-t vs π correlation and Si and Al-t vs Al^{VI}.
3-4 : from Na_2O and K_2O correlations; 5 : from T vs Ca; 6a/b : from the calculation method; 7a/b : from the ti and p vs K relations.

VI.7. : Summary

The strongest correlations found in this chapter are summarized below.

Mutual rock correlations :

Migmatitic		Igneous		Combination	
SiO_2 - FeO	: -.84	CaO - K_2O	: -.93	FeO - MnO	: .85
FeO - MnO	: .81	TiO_2 - FeO	: .92	SiO_2 - FeO	: -.80
FeO - K_2O	: -.79	FeO - MnO	: .87	SiO_2 - CaO	: -.79
TiO_2 - Fe_2O_3	: .77	SiO_2 - C[illegible]	: -.85	CaO - K_2O	: -.78
		SiO_2 - MgO	: -.80	SiO_2 - K_2O	: .77
		TiO_2 - P_2O_5	: .80		
		SiO_2 - K_2O	: .76		
		TiO_2 - MnO	: .76		
		SiO_2 - TiO_2	: -.75		

Neither Al_2O_3 nor the fluid components show any strong correlation. Most conspicuous is the TiO_2 behaviour with respect to the Fe-oxides: in the Migmatitic group magnetite is favoured, in the igneous group ilmenite.

Mutual amphibole oxide parameters : main amphibole groups

Mg-rich		Fe-rich		Combination	
FeO - MgO	: -.91	FeO - MgO	: -.99	FeO - MgO	: -.98
SiO_2 - Al_2O_3	: -.81	SiO_2 - MgO	: .86	FeO - CaO	: -.79
		SiO_2 - FeO	: -.81	MgO - CaO	: .79
		CaO - Na_2O	: -.80		
		FeO - CaO	: -.78		

The number of correlations is very small, the Fe-rich group indicates that with rising SiO_2 content, MgO and CaO increase, and that FeO and Na_2O decrease (change from hornblende to actinolite). The SiO_2-Al_2O_3 relation is missing for the Fe-rich group.

: secondary amphibole groups

Mg-rich		Fe-rich		Combination	
SiO_2 - Al_2O_3	: -.97	FeO - MgO	: -.99	FeO - MgO	: -.99
SiO_2 - K_2O	: -.97	Na_2O - K_2O	: .92	Na_2O - K_2O	: .88
Al_2O_3 - K_2O	: .94	SiO_2 - Al_2O_3	: -.75	SiO_2 - Al_2O_3	: -.77

Mg-rich	Fe-rich	Combination
Na_2O - K_2O : .90		SiO_2 - K_2O : -.77
FeO - MgO : -.89		Al_2O_3 - K_2O : .76
SiO_2 - Na_2O : -.85		Al_2O_3 - Na_2O : .75
Al_2O_3 - Na_2O : .84		
CaO - Na_2O : -.84		

The Mg-rich group clearly demonstrates the actinolitization proces. In the Fe-rich group it is disturbed by some relatively Fe-rich actinolites.

Mutual amphibole structural formula correlations : main amphibole groups

Mg-rich	Fe-rich	Combination
Si - Al-t : -.96	Fe - Mg : -.99	Fe - Mg : -.98
Al^{VI} - Al-t : .90	Na - Na+K : .96	Si - Al-t : -.94
Fe - Mg : -.90	SumX - A.site: .92	Ti - CaY : -.87
Si - ComY : -.89	Na - CaY : -.87	Al^{VI} - Al-t : .86
Ti - CaY : -.88	K - A.site: .87	Si - ComY : -.85
SumX - Na+K : .85	Ti - CaY : -.86	

An explanation of the various terms is given in table VI.7. Only correlations with r-values $\geq |.85|$ are given. The differences between the oxide correlations and these tables are :

Mg-rich group : much stronger Si-Al correlation, and information on the charge compensation. On the other hand the oxide tables and figures are much easier to handle, because no disturbing calculation methods have been used.

Fe-rich group : disappearance of the Si vs Mg (and Fe) correlation, Ca correlations weakened. New correlations are found between all alkali containing parameters.

Combination : about the same as the Mg-rich group.

Mutual amphibole structural formula correlations : secondary amphibole groups

As was the case with the oxides, the Mg-rich group has much more correlations than the Fe-rich group. The number of correlations greater than |.85| is 23 (Mg) 11(Fe) and 12(Com), see table VI.8. Actinolitization determines the correlations.

The structural formula parameters describe the interrelations inside the amphibole system much better than the oxides, but on the other hand the oxides are much easier to handle.

Bulk versus amphibole correlations, only the main amphibole groups

Mg-rich		Fe-rich		Combination	
π - Al-t	: .85	π - Na	: -.80	mg - mg	: .85
π - Al^{VI}	: .82	mg - mg	: .77	mg - Fe-t	: -.85
π - Si	: -.79	mg - mg	: .77	mg - MgO	: .81
π - ComY	: .72	mg - Fe-t	: -.75	π - Al_2O_3	: .79
alk - MnO	: .71	MgO - K_2O	: -.75		
μ - Fe-t	: -.70	π - CaO	: .74		
		ti - K	: -.71		
		alk - Na+K	: .70		

The correlations in the tables above are collected from table VI.6 and VI.9. There are many more correlations between r-values of |.50| and |.70|.

The most important rock parameters are : niggli- π (Ca-part of the leucocratic components, comparable with the An-percentage of the plagioclase, see section VI.3.2.), niggli-mg (Mg-part of the ferro-magnesia elements) niggli- μ (Mg-part of the mafic components), and niggli-alk (sum of alkalies).

This leads to the conclusion that the main amphiboles are partly

restricted in their chemical composition by the host rock chemistry. These restrictions, however, leave a lot of room for metamorphic influences.

The secondary amphibole groups have no direct relation with the bulk composition of the rock. The whole range from hornblende to actinolite can be found in one handspecimen.

VII. : K-Ar-dating of hornblendes from the lopolith of Bjerkreim-Sokndal and the metamorphic environment.

VII.1. : Introduction

In addition to the analyses performed by Versteeve (1975, table 5) on three hornblendes from the SE corner of the investigated area, eleven hornblende samples from the present collection were dated by the Z.W.O. Laboratorium voor Isotopen Geologie, Amsterdam. Three other samples were kindly supplied by the same laboratory. For the experimental procedures : see Versteeve.

The main conclusions of Versteeve, which are of interest here, are : Regional metamorphism around 1200 Ma and between 850 and 1000 Ma. Intrusion of the upper part of the lopolith : around 950 Ma, final solidification around 850 Ma ago.

VII.2. : Results

The analytical data and calculated ages are listed in table VII.2. Versteeve's hornblende dates were recalculated with the constants used in this paper (see table VII.2).

Sample information for A 037 to W1226 D, see Appendix and table I.1. For the Rog samples see table VII.1.

Sample No.	Rock name	Coordinates
Rog 242	clinopyroxene quartz amphibolite	3683 - 65090
Rog 244	amphibole biotite gneiss	3683 - 65090
Rog 252	biotite quartz amphibolite	3732 - 65314
Rog 43	biotite amphibolite	3626 - 64772
Rog 129	quartz hornblende norite	3637 - 64703
Rog 175	dehydrated amphibolite	3726 - 64719

Table VII.1.: Sample names and localities.

The regional distribution of the dated hornblendes is shown in fig. VII.1.

Sample no.	K (% wt)	radiogenic ^{40}Ar (ppm Wt)	atmospheric ^{40}Ar (% total ^{40}Ar)	Calculated age (Ma)*
A 037	1.714	0.150	18	949 ± 30
	1.710	0.146	13	
A 128	1.445	0.128	23	971 ± 30
	1.446	0.130	12	
B 118 D	1.254	0.107	25	941 ± 30
	1.250	0.108	13	
B 254	1.234	0.108	24	948 ± 30
	1.241	0.107	16	
B 322	1.013	0.0871	20	959 ± 50
	1.009	0.0901	13	
D 444	0.722	0.0639	14	964 ± 50
	0.701	0.0618	21	
E 167	0.986	0.0867	14	951 ± 30
	1.004	0.0858	23	
F 126	1.211	0.105	20	937 ± 50
	1.207	0.101	13	
N 572 L	0.495	0.0439	20	963 ± 30
	0.501	0.0439	13	
W 196	0.903	0.0767	14	937 ± 30
	0.908	0.0774	25	
W1226 D	0.796	0.0701	15	956 ± 30
	0.800	0.0693	20	
Rog 242	1.13	0.0984	2	956 ± 30
	1.13	0.0990	2	
	1.14			
Rog 244	1.10	0.0947	2	963 ± 30
	1.06	0.0956	2	
	1.08			
Rog 252	1.31	0.118	2	972 ± 30
	1.31	0.115	3	
Recalculated with new constants :				
Rog 43				1171 ± 35
Rog 129				942 ± 30
Rog 175				939 ± 30

Table VII.2. : K-Ar data of hornblendes. Samples from this collection : A 037 to W1226 D. Samples from Z.W.O. Laboratory : Rog 242 to Rog 252. Samples from Versteeve (op.cit.) : Rog 43 to Rog 175.

* Constants used : $\lambda_e = 0.581 \times 10^{-10} a^{-1}$, $\lambda_\beta = 4.962 \times 10^{-10} a^{-1}$, abundance $^{40}K = 0.01167$ atom % total K.

Errors based upon estimated accuracies of 2% for the K analyses and 3% for the Ar analyses.

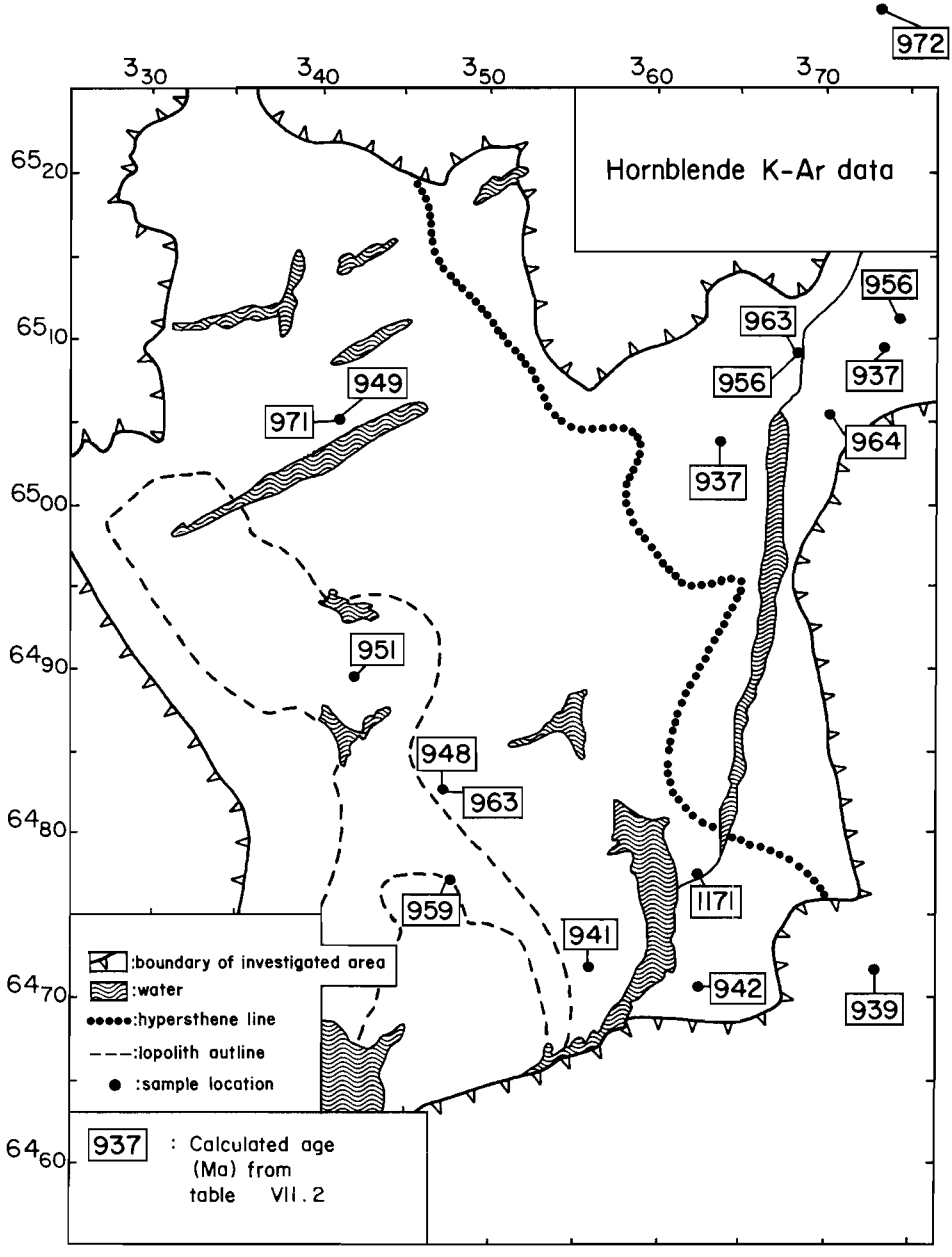

Figure VII.1. : Regional distribution of hornblende K-Ar ages. The one sample outside the figure outline (Rog 252), is located east of Gravatnet, near Fjörhom.

VII.3. : Conclusions

Except for sample Rog 43, all hornblende data lie between about 940 and 970 Ma, averaging 953 ± 10 Ma. This indicates that the temperature of the crystal block during the cooling stage after the last event of high-grade metamorphism passed the blocking temperature of hornblende (550 ± 50°C, Hanson and Gast, 1967) at about the same time over the whole area. Also, since about 950 Ma ago the temperature in this part of the crust has always remained below the blocking temperature.

There is one hornblende K-Ar age significantly higher than about 940 to 970 Ma, Rog 43 (1171 ± 35 Ma). Versteeve has explained this date as a relict age of an older amphibolite facies metamorphism at about 1200 Ma. However, the new hornblende data make this explanation highly implausible. It is postulated by Versteeve that this crustal block underwent metamorphism in the granulite and amphibolite facies about 1000 Ma ago. Anyhow, from the regional pattern of K-Ar dates it is evident that the temperature during this event rose above 550 ± 50°C and it is difficult to understand why only hornblende Rog 43 would have escaped the general resetting. Possibly, we are dealing with a case of excess radiogenic Ar due to local conditions of high partial Ar pressure during the metamorphism.

The fact that hornblendes from the base (B 322) and the top (E 167) of the lopolith give the same K-Ar age of about 950 Ma indicates that the crystallization of the lopolith cannot have continued until 842 Ma* as assumed by Versteeve. The lopolith as well as the migmatitic environment cooled at the same time through the 550 ± 50°C level. The biotite Rb-Sr and K-Ar systems closed between about 840 and 900 Ma*, averaging about 870 Ma*, corresponding to a temperature of 300 ± 50°C (Wagner et al, 1977). Thus, in about 80 Ma the temperature in the whole

* Rb-Sr dates recalculated with $\lambda^{87}_{Rb} = 1.42 \times 10^{-11} a^{-1}$.

area decreased between about 150 and 350°C, approximately 3 (±1)°C/Ma.

The geothermal gradient cannot have been 30-35°C/km as assumed by Versteeve for his calculation of the rise of the area. In that case granulite facies metamorphism should have taken place at depths of 25-30 km (800-1000°C and 7-10 kb). The hornblende, however, indicates pressures of 3-4 kb, anyway, no higher than 5 kb (section I.5.).

For the amphibolite facies area around Tonstad this implies a geothermal gradient of 50-70°C/km (originally higher part of the amphibolite facies metamorphism, near the hypersthene line : about 700°C and 3-4 kb, 10-12 km; the forming of retrogressive actinolite is bound to certain zones, and of later age : transition of amphibolite to greenschist facies, see Chapter I). Even if the amphibolite facies metamorphism is thought to have taken place at lower temperatures (about 600°C) the geothermal gradient would still be rather high (50-60°C/km). Thus the geothermal gradient in the granulite facies is even higher (between 50 and 100°C/km), and the calculation by Versteeve for the rise of the area cannot be correct.

The lopolith of Bjerkreim-Sokndal intruded in the area between 1000 and 950 Ma ago. 1000 Ma stands for the granulite facies metamorphism, and the top of the lopolith is not metamorphosed. At about 950 Ma the hornblende blocking temperature was reached. This means that the top of the lopolith cooled during 50 Ma at most from about 1000°C (Rietmeijer, 1978) to 550 ± 50°C. During the same time the granulitic envelope decreased from 800 - 1000°C to 550 ± 50°C, and the amphibolite facies terrain from ca 700°C to 550 ± 50°C. The Rb-Sr and K-Ar biotite clocks started between 900 and 840 Ma ago, see fig. VII.2.

This model implies a cooling rate of at least 9°C/Ma for the first stage of cooling of the lopolith, before 950 Ma ago. In that time the metamorphic envelope had cooling rates between 9 and 3°C/Ma (from granulite facies rocks near the contact to amphibolite facies rocks near Tonstad). The cooling rate of 3 (±1)°C is also found between about 950 and 870 Ma ago. After that time the cooling may have slowly continued

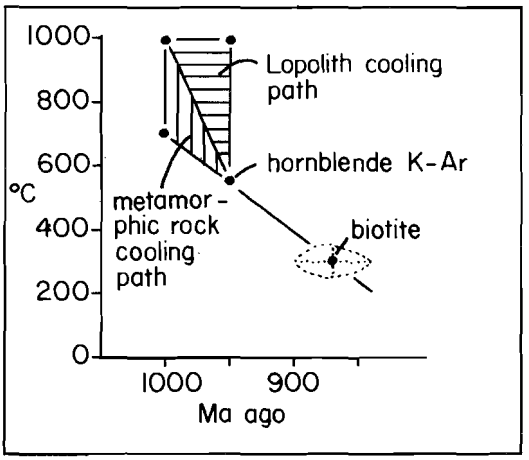

Figure VII.2. : Schematic interpretation of isotope ages of the Rogaland/Vest-Agder area. Error bars around biotite indicate that the angle of the line may vary some, but that does not influence the general picture of a high cooling rate.

untill denudation was complete, or there may have been some unrecorded fluctuations.

AMPHIBOLES AND THEIR HOST ROCKS IN THE HIGH-GRADE METAMORPHIC PRECAMBRIAN OF ROGALAND/VEST-AGDER, SW. NORWAY.

Part III

Appendix

A : Description and analysis characteristics of the samples

A.1. : Introduction

This extensive Appendix holds information on the field occurrence, macroscopic appearance, rock- and amphibole microscopy, and analysis characteristics of the investigated collection, with some sidesteps to other samples containing additional information about a certain locality or sample.
For general information concerning the formations in the Rogaland/Vest-Agder area the reader is referred to Hermans et al (1975). Only some additional information, needed for a better understanding of certain samples is given in this Appendix.
Localities can be found in fig. I.1; names, grid references and formations in table I.1; whole rock chemistry information in chapter III; amphibole parametera in chapter IV, and some additional analyses in chapter V.

A.2. : Subdivision of the descriptions

The following headings are used :

--FO : field occurrence; this information is obtained from the fieldnotes of the various collectors;
--MAD : macroscopic description of the hand specimen;
--Texture : according to Moore (1970);
--MID : microscopic description;
--AC : analyses characteristics; here all remarkable values for bulk chemistry, modal analysis, niggli values, amphibole chemistry and -optics are mentioned. All the values are judged relative to the total of the collection;
--Further remarks : special information on analysis spots, calculation methods, chemical differences between the various amphiboles present in one sample, etc. This heading may be absent.

A.3. : Descriptions

A 037 : Banded spinel-bearing amphibole gabbro with ferroan pargasite.

FO : Interlayer of about 1 m thick in garnetiferous migmatites, containing fist-size amphibole crystals (sample A 128). Concordancy and extent could not be observed. The immediate surroundings consist of various rock types in thicknesses of several cm to meters.
MAD : Bands of 0.5 to 2.0 cm, caused by changing amounts of amphibole in a pyroxene- and euhedral plagioclase-rich rock of medium grainsize. One side of the sample is a layer consisting exclusively of relatively coarse amphibole.
Texture : Hypidiomorphic, equigranular with polygonal contact; partly straight grainboundaries, partly slightly curved. Clinopyroxene crystalboundaries are sometimes irregular because of resorption. A later event produced cracks with alteration products in its surroundings. Amphibole determines the banding.
MID : The amphibole is anhedral, often enclosing other minerals. Circular cracks may develop around pyroxene- and ore-inclusions. Many strings of angular (carbonate?) inclusions are present. The amphibole is relatively fresh and coarse in comparison with pyroxene and plagioclase. Subgrain boundaries can be seen without exsolution phenomena on the contacts between the subgrains. Plagioclase is pure anorthite (99%, see table V.3.); $2V_x$= ca 80°. Rather irregular crystals with albite-, carlsbad- and acline-pericline twins. Zoning is sparse and weak; apatite, green spinel and ore may be enclosed as well as two-phase inclusion strings. Zoisite formes in plagioclase, mainly along cracks with serpentine and around some metamict grains with radiating cracks. The zoisite displays anomalous blue interference colours (dispersion of the birefringence), +2V=30-40°, r>v, n_v=h, colourless, n=1.65-1.70, birefringence = ca 0.007. The radioactive crystals are colourless to light brown, isotropic. They are probably allanite (orthite), a common accessory in Rogaland/Vest-Agder. The pyroxene is a salite (see table V.2.) : $Z\wedge c$= 48°, $2V_z$= 56°, birefringence = 0.022, r>>v, pinkish, often anomalous blue interference colours. Some crystals contain systems of very fine, green spinel flakes in $(010)_{cpx}$ elongated along the c-axis$_{cpx}$. Enclosed plagioclase may be euhedral or vermicular. The latter texture indicates a reaction relationship or co-precipitation, and is accompanied by resorbed crystalboundaries of the clinopyroxene. Many strings of 3-phase inclusions are present. Each inclusion contains, in ratio 1:20:100, a dark brown crystal (possibly ore), some light-green crystals (possibly salt) and an enclosing crystal (possibly carbonate) which is colourless. They can be seen as fine, coloured strings in the extinction position, see fig. A.1. The constant ratio indicates a former fluid inclusion.

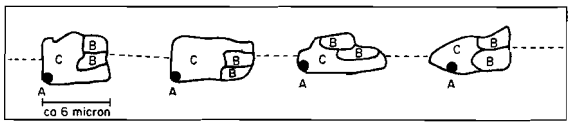

Figure A.1.: Inclusion string in A 037-clinopyroxene. A = dark brown; B = light green; C = colourless.

Green spinel is present as schiller in pyroxene, grains in pyroxene and plagioclase, and, most frequently, interstitial. Dark green, almost opaque. The interstitial spinel is commonly associated with opaque ore grains of larger size. The rounded spinel in plagioclase and pyroxene may represent the first crystallized phase, the interstitial spinel together with the opaque ore the last phase. Spinel alters to diaspora. The opaque ore consists mainly of ilmenite, and some magnetite, pyrite and pyrrhotite. It occurs within the main phases and interstitially. Very small grains of light yellowish-brown biotite are accompanied by secondary minerals : chlorite, muscovite and calcite. Some pinkish, rounded zircon crystals are present.

AC : Modal analysis : highest in spinel, zoisite and diaspore.
Bulk composition : highest CaO; high Al_2O_3; low Na_2O.
Niggli values : highest c and π; high T and γ; low alk.
Amphibole oxides : highest CaO; high Al_2O_3 and K_2O.
23(O) formula : high Al^{VI} and Ca.
Plagioclase : highest An-percentage. Pyroxene : high in CaO and Al_2O_3.

Further remarks : see section V.2.B and -C.

A 128 : Plagioclase-bearing 2-pyroxene hornblendite xenocryst with farroan pargasite.

FO : see A 037.

MAD : One big black crystal (8x6x5 cm) with several distinct crystalfaces, containing a few smaller randomly oriented crystals of amphibole and yellow apatite.

Texture : The large amphibole encloses some smaller amphiboles, apatites and clinopyroxenes. These may reach 1.5 (amphibole and clinopyroxene) and 1.0 cm (apatite). Apart from these inclusions the large amphibole contains numerous homogeneously distributed aggregates consisting of plagioclase + orthopyroxene + ore, elongated along the c-axis of the amphibole, with a minor extension along the a-axis.

Inside the amphiboles abundant ore needles with straight boundaries occur either dispersed or in groups. There are also many inclusion strings (as in A 037) all more or less in the same direction, although they may form flowing curves in some of the enclosed amphibole crystals. At amphibole-amphibole contacts some strings or groups of strings cross the contact, while others do not. They also may continue in adjacent grains of plagioclase or orthopyroxene. There is no obvious system.

Enclosed clinopyroxene and amphibole crystals are frequently enveloped by a rim of plagioclase + orthopyroxene + ore. Apatite inclusions are in direct contact with the host.

MID : The large amphibole crystal shows undulatory extinction. Zoning is not visible. The smaller amphiboles do not show undulatory extinction. The ore needles are abundant in some enclosed amphibole grains (1), numerous in the large crystal (2), and absent in some smaller amphiboles (3) at the contact between (1) and (2). This may indicate the order of crystallization.

The ore naedles are interpreted as an exsolution phenomenon due to falling temperature (see section IV.3.4). The more exsolution present, the greater the T-gap was, the higher the original temperature, the earlier in the sequence it crystallized.

Ore is present in two main ways in the amphibole : I : needles and laths, II : irregular and rounded larger crystals. The ore consists mainly of titanomagnetite with ilmenite lamellae.

I : The first group can be divided according to size and orientation in various subgroups. The main point however is their orientation as laths parallel $(010)_{amph}$ with their elongation 1 : // c-axis, 2 : roughly // n_z, 3 : roughly // n_x (frequency in this order for the medium sized sheets = 0.1 - 3.0 mm long, 15 - 150 micron in width and 3 - 15 micron thick)[2]. Coarser columns are only elongated along the $c\text{-axis}_{amph}$ and are not so frequent. Part of these coarser columns may belong to group II, because orientation of the thin section may influence the grain outline. The finest needles are mostly found near contacts with orthopyroxene-plagioclase-ore assemblages (fig. A.2), curiously elongated // n_z and n_x of the amphibole. At the contact they form clouds of needles with rounded edges mostly parallel to the contact, but away from the contact they may be arranged in curved rows.

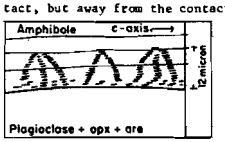

Figure A.2.: Ore needles at the contact between amphibole and the plagioclase-orthopyroxene-ore assemblage in A 128.

II : The second type seems to be restricted to the plagioclase-orthopyroxene-ore assemblage, even though several isolated ore grains may be found in the amphibole, see 1. Because this assemblage is elongated along the $c\text{-axis}_{amph}$ a section perpendicular to this plane may show ssparate ore, plagioclase, plagioclase + orthopyroxene and plagioclase + ore apots. Separate orthopyroxene is only seldom found because of the greater amount of plagioclase. Ore and plagioclase may sometimes grow out of the assemblage spots and stretch along the $c\text{-axis}_{amph}$. Green spinel and diaspore are rarely present in the assemblage.

An oblique cut through an ore-lath, -needle or -column may reveal a lamellar or crossed exolution pattern in the thinnest parts. Some fine ore grains may be present at amphibole-amphibole contacts (see section IV.3.4). A few red hydroxide specks are accompanied by serpentine. Plagioclase develops plates // $(010)_{amph}$, elongated along the $c\text{-axis}_{amph}$.

1 : Plate III, figure 3.
2 : Plate VII, figures 1 and 2.

A minority of the plates is extended //(110) and $(1\bar{1}0)_{amph}$. They are presumably part of the plagioclase-orthopyroxene-ore assemblages. Several sections may show simultaneous extinction. The An-content is very high : 96% (see table V.3). The plagioclase displays very small lamellae which are lensshaped and peter out near the crystal boundaries and near inclusions of ore and orthopyroxene. They represent at the utmost 5-10% of the plagioclase crystal area.

The orthopyroxene in the aggregates is often coaxial with the amphibole; several sections showing equal optical orientation may float like an archipelago in a sea of plagioclase and ore. Some crystals show very thin lamellae of clinopyroxene on $(010)_{opx}$. They occupy up to 5% of the orthopyroxene crystal. $2V_x$ = 55-60°, the pleochroism of the orthopyroxene is weak. At some places in the sample the orthopyroxene is partly altered into serpentine and a few small flakes of light- to dark-brown biotite.

Plagioclase, orthopyroxene and ore may all be in contact with amphibole. Plagioclase : orthopyroxene : ore = ca 75 : 20 : 5.

The subhedral to rounded crystals of apatite enclosed by the large amphibole may show very fine coaxial ore needles : homogeneously dispersed, or in dendritic patterns with one sharp boundary. The last are 2-dimensional and appear in groups. Both groups are only visible with a very high magnification. Fluid inclusion stringlets are also present.

The most intriguing inclusions in the amphibole are the subhedral clinopyroxenes (augite, see table V.2) up to 1.5 cm in size! $Z \wedge c$ = ca 40°, greyish, no pleochroism. The largest crystals can be divided in several zones :

-- I : the core, which displays a very fine needle-like ore exsolution //c

-- II: the largest, middle, part which is crowded with plagioclase and ore exsolutions

-- III: the exsolution-free outer rim.

Both plagioclase and ore exsolutions are elongated laths in the $(010)_{cpx}$ plane like in the amphibole. Some fishhooks can be seen in section $\perp c$. The ore and plagioclase are not associated; they have their own regular distribution pattern within the clinopyroxene. With higher magnifications it is possible to see a small subhedral orthophyroxene grain in each plagioclase drop in certain areas of the clinopyroxene. All orthopyroxene grains show the same optical orientation. The ore system is comparable to group I in the amphibole. The regular pattern is disturbed near cracks and inclusion stringlets, the plagioclase and ore-drops and-sheets become smaller and more rounded. The cracks may be filled with the plagioclase-orthopyroxene-ore assemblage, known from the amphibole. The exsolution phenomena in the clinopyroxene show a stronger epitaxial relation than those in the amphibole. Some very fine lamellae (possibly orthopyroxene), 1-3 micron wide, occur $//(100)_{cpx}$. Coarse plagioclase and ore crystals are rare; they are possibly related to the cracks with plagioclase-orthopyroxene-ore assemblages.

The contact between enclosed clinopyroxene or amphibole and the large amphibole consists mainly of the plagioclase-orthopyroxene-ore aggregate. In some places the contact is direct and undisturbed. Via this contact zone the aggregates are in direct contact with similar groups in the amphibole and in the clinopyroxene cracks.

Quartz is found in a few spots on the outermost side of the sample. It appears as a late crack-filling phase, with undulatory extinction and fluid inclusions. One atol-shaped pyrrhotite grain is present.

The largest enclosed amphibole contains beautiful pleochroic haloes (30-35 micron Ø).

AC : High An-percentage, apatite content, and amphibole 23(O) Al^{VI}.

Further remarks : The chemistry of the amphibole does not change markedly for most elements from central parts to contact zones. Only K increases 14% from centre to rim (the tabulated value is a mean). K could not be incorporated in the prograde plagioclase-orthopyroxene-ore assemblage and was left behind in the neighbouring amphibole. All other elements could be divided between plagioclase (Ca, Na, Al and Si), orthopyroxene (Fe, Mg, Mn and Si) and ore (Fe and Ti). See further section V.2.B and -C.

A 168 : Alkalifeldspar granite with magnesioriebeckite.

FO : Centre of the Faurefjell formation, just above the marble.

MAD : Fine-grained, leucocratic, greenish-grey rock.

Texture : Granoblastic, equigranular, polygonal-interlobate. Grainsize less than 1 mm. Amphibole forms very small, radiating fibres around ore grains and barite crystals, and, to a lesser extent, forms clouds of needles in quartz[2]. The fibres are 1 to 3 micron in width and up to 150 micron in length. Ore grains are mainly arranged in two thin levels. A sample from nearby shows a distinct layering : the greenish-grey material of A 168 contains parallel, bluish layers several mm thick, which can be intensely folded. These layers are coarser and consist mainly of alkalifeldspar, which is more cloudy than in A 168 and contains numerous needles of the same amphibole, plus the beginning of microcline texture.

MID : The violet-blue amphibole is often accompanied by stilpnomelane. If the size of the amphibole fragment increases, a more or less prismatic habit can be seen. The amphibole prefers quartz crystals above alkalifeldspar as a host.

Barite occurs as an accessory (<1%), $2V_z$ = ca 40°, v>r. The small rounded crystals are mostly surrounded by stilpnomelane. The alkalifeldspar is sanidine-like, $2V_x$ = ca 20°. The cores are clear, the rims cloudy. They envelop rounded quartz crystals with undulatory extinction. The ilmenite grains may have very thin titanite rims, around which the amphibole formed. Rounded zircon and euhedral apatite are rare.

1 : Plate III, figure 4.

2 : Plate III, figure 1.

AC : Modal analysis : highest quartz content, no plagioclase.

Bulk composition : highest SiO_2; high K_2O; low Na_2O and MgO; lowest MnO, Fe_2O_3, FeO and CaO.

Niggli values : highest si, alk, k and O; high al and γ; lowest fm, c and T.

Amphibole oxides : highest SiO_2 and Na_2O; lowest MnO and CaO.

Further remarks : The microprobe analysis is the mean of several slightly differing analyses, depending on the nucleation centre and neighbouring crystals.

B 016 : Biotite amphibole diorite with ferro-hornblende and grunerite.

FO : Sample from the E-side of the Mydland tunnel. According to Rietmeijer (1973) it belongs to the top of the leuconoritic phase. Surrounding samples often show carbonate veins and strong retrograde metamorphism.

MAD : Mesocratic, fine-grained, schistose (parallel arrangement of biotite).

Texture : Granoblastic, seriate, polygonal. Amphibole and biotite form the largest crystal aggregates, the other minerals build up an irregular, finer-greined matrix with mainly Y-contacts. There are two amphiboles present :

--1 : colourless grunerite/cummingtonite (B2016) and

--2 : green ferro-hornblende (B1016).

Most of the amphibole crystals are zoned, with a colourless core and green mantle. The transitions may be sharp. The core/mantle ratio varies from 0.0 till 1.0. Quartz is often present as drops in the hornblende, in a more or less symplectitic way or as interstitial crystals around the hornblende, often accompanied by biotite. The amphibole crystals, especially grunerite, are irregular and bent (kinkbands are found), and interpenetrate randomly. They appear in groups of crystals, together with large, brown, parallelly oriented, biotite crystals. These biotites seem to be old, show kinkbands (with stilpnomelane) and crenulation cleavage. There also are smaller randomly oriented biotite flakes, often symplectitic with quartz and related to the hornblende-quartz symplectites. They seem to represent a younger generation. The amphibole-biotite-ilmenite-quartz groups drift in a sea of plagioclase.

MID : The colourless amphibole shows a strong dispersion of the optical axes. It may contain black (ore) and colourless (apatite or quartz) rods parallel to the c-axis (3-10 micron long and ca 1 micron wide, rounded edges). Besides lamellar twinning (100) it shows very fine lamellae ($\bar{1}01$), less than 1 micron in width. They look colourless, and are not homogeneously distributed through the crystals.[1]

Several green crystals are clearly pseudomorphic after orthopyroxene-clinopyroxene-intergrowths. The so-called "ladder-structure" is not uncommon in the lopolith (Rietmeijer, op.cit.) : the clinopyroxene-host contains elongated blebs of orthopyroxene along $(001)_{cpx}$. The clinopyroxene part is now ferro-hornblende, the orthopyroxene part is altered into amphibole with another orientation (ferro-hornblende or grunerite), or into carbonate blebs.[2] The very fine colourless lamellae described above, persist in the green hornblende. If ilmenite grains are in contact with amphibole the contact is mainly green, the rest may be colourless. Plagioclase (normally 29% An) is sometimes zoned (18-20% An rim). It may contain ore needles and drops, apatite and rounded zircon; the latter minerals are also interstitially present. Alkalifeldspar is found as blebs in plagioclase in some thin (1 mm), coarser-grained, leucocratic levels, accompanied by myrmekite on the contact with the main rock. Some small carbonate crystals are found between the mafics. Pyrite, chalcopyrite and pyrrhotite are accessories.

AC : Modal analysis : high biotite content.

Bulk composition : high TiO_2, P_2O_5 and CO_2.

Amphibole oxides : highest MnO (B2016); high "All Fe as FeO" (B2016); low K_2O (both).

Further remarks : B1016 1 is the mean of 2 crystals, B1016 2 is a deviating crystal. B2016 is determined on three crystals.

B 118 : Banded amphibole-bearing 2-pyroxene charnockite with edenitic hornblende.

FO : Banded sample from the mainly massive charnockitic migmatites.

MAD : Mainly fine- to medium-grained, leucocratic rock, with several darker layers of various thicknesses.

Texture : Leucocratic band : Granoblastic, inequigranular, interlobate. Pyroxene strings and platy quartz determine the lineation. The average grainsize is less than 1 mm. The amphibole is subhedral, sometimes blastic with more or less parallel orientation and varying grainsizes. The leucocratic band only contains amphibole near the contact with the dark band.

Dark band : oriented amphibole in a polygonal amphibole-plagioclase fabric. The contact between both bands is formed by a dehydration zone (Schrijver, 1973).

MID : Leucocratic band : Some apatite, ore and zircon (rounded as well as euhedral) may be enclosed in amphibole. The ore consists of magnetite with ilmenite lamellae, or alternating magnetite and ilmenite as parts of the same grain. Very fine submicroscopic spinel exsolutions may be present in the ilmenite parts (see Ramdohr 1975, fig. 566). Quartz may form large crystals, up to 3 mm, with wavy extinction. Orthoclase and plagioclase (27% An) form the other main constituents of the matrix. Orthopyroxene and clinopyroxene form thin bands. Serpentinization of the orthopyroxene is present, mainly near the contact with the dark band.

1 : Plate IV, figure 2.

2 : Plate IV, figure 1.

Some orange-brown biotite around ore grains, Fe-hydroxides near serpentine, carbonate in amphibole and pyrite and pyrrhotite in irregular grains and thin veins complete the mineralogy.
The dark, amphibolite band, contains only little pyroxene, quartz and microperthitic alkalifeldspar beside amphibole, plagioclase, apatite, zircon, biotite and ore.
AC : Highest amphibole F (together with N 337 and M 101).
Further remarks : Measurements have only been performed on the leucocratic band.

B 254 : Olivine amphibolite with titaniferous ferroan pargasite.

FO : An amphibolite layer in the banded migmatites east of the lopolith.
MAD : Melanocratic, medium- to fine-grained, strongly lineated amphibolite.
Texture : Granoblastic, inequigranular, polygonal-interlobate. Grainsize mainly less than 1 mm, some amphibole crystals are larger. They determine the schistosity. The olivine crystals are rounded and often enclosed by groups of amphibole crystals.
MID : Anhedral amphibole with some clinopyroxene, ore and apatite enclosed, without a special poikiloblastic appearance. Ore specks at amphibole crystal margins are abundant. Thin ore dendrites are present in several directions in the crystals. The ore consists mainly of magnetite with ilmenite lamellae and some ilmenite grains. The plagioclase is partly altered to saussurite. Deformation features are scarce. Ortho- and clinopyroxene occur mainly as small intercrystalline fragments. Olivine with Fa_{40} has ore along its cleavage planes. All other minerals, including plagioclase, are also speckled with ore. Reddish-brown biotite, serpentine with olivine and some Fe-hydroxide are rarely present.
AC : High olivine content, high bulk- and amphibole TiO_2; low amphibole F.

B 322 : Apatite amphibole ilmenite bypersthenite with ferroan pargasitic hornblende.

FO : Mainly leuconoritic, fine-grained rocks, with fragments of coarse-grained anorthosite and some banded, ultramafic, ore-rich lenses. The sample is from one of these lenses in the leuconoritic phase (A) of the lopolith.
MAD : Fine-grained, black and glittering, heavy rock with rusty weathering.
Texture : Granoblastic, seriate, polygonal. Orthopyroxene forms large crystals up to 4 mm. They are sometimes bent. Most of the "groundmass" is smaller than 1 mm. The amphibole is not homogeneously distributed through the rock, it occurs mainly in pockets and zones. The ore is a main phase and forms interstitial groups of crystals-in-polygonal-contact, which consist of homogeneous magnetite and ilmenite.
MID : The amphibole contains no ore needles. The subhedral crystals often enclose apatite and some opaque ore. Orthopyroxene may contain clinopyroxene lamellae, and encloses a lot of apatite, ore needles and smaller orthopyroxene crystals. They show a strong pleochroism. A few crystals of orange-brown biotite, associated with amphibole, are also bent. Plagioclase displays only few deformation features. The ilmenite and magnetite contain extremely fine spinel exsolutions. Some fine-grained pyrite is also present.
AC : Modal analysis : highest ore and apatite content.
Bulk composition : highest TiO_2, FeO, Fe_2O_3 and MnO; high F; lowest SiO_2.
Niggli values : highest M; high fm and ti; low alk and L; lowest si and Q.
Amphibole oxides : high H_2O.

D 172 : Amphibole biotite quartz gabbronorite gneiss with edenitic hornblende.

FO : Transition from granitic migmatites (amphibolites, gneisses and granites) to Sirdalen augengneisses.
MAD : Banded, medium-grained, biotite gneiss.
Texture : The dark band is granoblastic, seriate, interlobate; the mafic minerals are smaller than 1 mm. Plagioclase is sometimes larger. Biotite is oriented and transects all other minerals, cutting them into several pieces with equal orientation. Amphibole is mainly concentrated along the contact between the dark and light band. It may be intimately intergrown with pyroxene, suggesting a reaction relationship (pyroxene → amphibole), but mostly the contacts are sharp.
The light band is coarser grained, seriate, interlobate.
MID : The amphibole is subhedral, sometimes a bluish discolouring appears against ore grains. The pyroxene is mainly clinopyroxene with orthopyroxene exsolution lamellae. The orthopyroxene grains are strongly serpentinized. Biotite is reddish brown and partly associated with quartz. The quartz is partly present as interstitial undulatory grains, and partly as small irregular crystals near biotite-amphibole-pyroxene concentrations. This might point to two generations. Besides magnetite with ilmenite lamellae, some ilmenite, pyrite and Fe-hydroxide are present, as well as apatite and rounded zircon. Plagioclase contains ilmenite schiller and deformation twins. The An-percentage does not change between dark and light band : An_{29-30}.
The light band consists of equal amounts of quartz and plagioclase. Alkalifeldspar is rare. The plagioclase is some-

times antiperthitic, quartz is strongly undulatory. Biotite, ore and apatite are present as accessories.
AC : no remarks.

D 307 : Amphibole gabbronorite with titaniferous ferroan pargasitic hornblende.

FO : Charnockitic migmatites, mainly banded, close to garnetiferous migmatites.
MAD : Mesocratic, medium- to fine-grained sample, with amphibole crystals of several mm causing a lineation. A plagioclase-rich zone 1 cm in width cuts straight through the lineation.
Texture : Granoblastic, seriate, polygonal-interlobate. Anhedral amphibole crystals are present in two grainsizes. Fine-grained, interstitial amphibole of the same size as the rest of the minerals, and coarse-grained crystals up to 3 mm.[1] Around some amphibole crystals, pyroxene may look altered, partly serpentinized, but most of the amphibole-pyroxene contacts are sharp. The plagioclase displays Y-contacts, the outlines of the mafic minerals may vary from straight or curved to irregular for some of the large amphiboles. The grainsize is mainly less than 1 mm. There is a vague lineation caused by pyroxene and amphibole. Biotite grew athwart the other mafics.
MID : Optically there are no important differences between the two kinds of amphibole. The crystals are rather clean and not poikiloblastic.
Ore plates, oriented in three directions, are present in some of the larger crystals; needles are rare. The largest crystals show undulatory extinction. Orthopyroxene is less frequent than clinopyroxene. Some orthopyroxenes contain very fine exsolution lamellae of clinopyroxene. Ore needle systems occur in the pyroxenes next to ore grains. The reddish-brown biotite shows the same feature; it is sometimes more or less symplectitic with quartz. The plagioclase (An_{60}) shows deformed twins, and contains inclusions of apatite and some flakes of colourless mica. Magnetite grains are very fine and strikingly rare. The plagioclase-rich zone contains some large orthopyroxene crystals, and is coarser-grained than the main part of the sample. Interstitial orthopyroxene, clinopyroxene and biotite are present in small quantities. At the contact with the main rock, orthopyroxene is serpentinized and carbonate crystals may be found.
AC : High amphibole TiO_2 and 23(O) Ti; the amphibole colour is extremely brown.
Further remarks : microprobe analyses are from the large crystals.

D 442 : Biotite amphibolite with edenitic hornblende.

FO : Banded alternation of amphibolites and granitic and some charnockitic rocks.
MAD : Melanocratic, fine-grained, strongly lineated, amphibole-rich rock.
Texture : Granoblastic, seriate, polygonal. The grainsize is mainly under 1 mm, except for amphibole poikiloblasts which may reach 3 mm. Most crystals are anhedral, but amphibole forms generally subhedral crystals. Straight, uncurved crystals of biotite occur at crystal boundaries. They rarely transect other minerals as in many other rocks of this collection (e.g. D 172 and D 307). Amphibole and biotite delineate the schistosity.
MID : Amphibole poikiloblasts, which are less abundant than the small subhedral crystals, enclose some plagioclase and apatite. Plagioclase contains deformation twins and displays some undulatory extinction; apatite inclusions, colourless and green, occur only in the centre of the crystals. Small zircons cause pleochroic haloes in the reddish-brown biotite. Some quartz crystals are probably present.

D 444 : Biotite amphibolite with magnesian hastingsitic hornblende.

FO : Same location as D 442.
Only differences with D 442 are described.
MID : The amphibole colour is more brownish than in D 442, small rounded ilmenite grains are present in plagioclase, amphibole and at their contacts. In some cases the amphibole-colour may become more greenish around ore grains, indicating an interaction with the ore (see B 322). Serpentine patches may indicate the former presence of pyroxene. Pyrrhotite, pyrite and chalcopyrite are rare.
AC : Low amphibole F and K_2O.

E 067 : Amphibole 2-pyroxene quartzmonzonite with ferro-edenitic hornblende.

FO : Lower levels of the quartz-monzonitic phase.
MAD : Leucocratic, coarse-grained, greenish-grey rock with large, equally oriented, amphibole fragments.
Texture : Granoblastic, seriate, interlobate-amoeboid. The amphibole forms very extensive crystals (several cm) with a more or less intercumulus character. It contains all other mafic minerals and is intimately intergrown with quartz. The amphibole is very irregularly distributed through the rock; therefore, the pointcounter analysis is highly unreliable. Ortho- and clinopyroxene are frequently enclosed by amphibole, but they also occur independenrly between

Plate I, figure 2.

felsic minerals. Opaque ore and rounded apatite are mainly associated with the mafic minerals. Biotite forms small symplectites on the contact between dark minerals and microperthite. Zircon varies from euhedral to slightly rounded, and is rather coarse : up to 1 mm. Plagioclase is the most euhedral mineral after zircon. It is often continuously zoned, from an oligoclase core (An_{16}) to a thin outer rim of albite, and shows deformation twins. Quartz has a strong wavy extinction. Alkalifeldspar forms large crystals with coarse microperthite texture, including patch perthite (Spry, 1974, fig. 52).

MID : Around ore grains the amphibole colour may become more greenish. Clinopyroxene shows fine exsolution lamellae (100), has a greenish colour and $2'c = 48^{\circ}$. Orthopyroxene may also contain very fine lamellae. Both pyroxenes are partly altered to one or more of the following minerals : serpentine, carbonate, chlorite and muscovite. Biotite is very dark brown. Zircon may contain various inclusions, even fluid inclusions. Quartz is partly connected with amphibole, partly a matrix constituent. It contains abundant strings of fluid inclusions. The microperthite becomes more plagioclase-rich towards the rim, which may be pure plagioclase with ore inclusions. Very fine myrmekite is rarely present. The ore consists of magnetite with ilmenite lamellae (and extremely fine spinel at the lamella boundaries), and ilmenite. Magnetite and ilmenite may occur together as irregular parts of the same crystal. Pyrrhotite is rare.

AC : The amphibole is high in FeO and H_2O; its density is greater than 3.3.

Further remarks : see Riermeijer and Dekker (1978) : the gronp 2 amphiboles; and E 167, N 402, R 229 and R 356. The chemistry of the amphibole is rather irregular.

E 125 : Ore-rich amphibole gabbronorite with titaniferous ferroan pargasite.

FO : In the field it looks like a xenolith in the leuconoritic phase of the lopolith, this may be caused by the bad exposure (swamps).

MAD : Fine-grained, mesocratic rock without lineation or banding.

Texture : Granoblastic, equigranular, polygonal-interlobate. Grainsize much smaller than 1 mm. All minerals show deformation features. Pyroxene sometimes forms larger crystals. The amphibole is concentrated in small groups of more or less equally oriented crystals (the extinction positions vary a few degrees) which appear beside ore and pyroxene. The amphibole seems to be the last magmatic crystallization product, filling the last open spaces. Sometimes it encloses the pyroxene. A reaction relationship between amphibole and pyroxene can not be established. The crystals are anhedral. Magnetite and ilmenite grains are interstitial. Biotite occurs only rarely, around ore.

MID : The amphibole colour is extremely brown. Clinopyroxene is more abundant than orthopyroxene. Both may contain some apatite and ore needles. Orthopyroxene may show very fine lamellae. Biotite is reddish-brown; apatite is very fine; zircon is rounded, and serpentine is only locally present.

AC : Highest amphibole H_2O; high ore content and bulk Fe_2O_3, high amphibole TiO_2.

E 128 : Amphibole mela-troctolite with titaniferous pargasite.

FO : Disturbed appearance of the monzonitic phase, almost a migmatitic impression.

MAD : Fine-grained, melanocratic rock without a clear lineation or banding.

Texture : Granoblastic, equigranular, polygonal. The grainsize is less than 1 mm. The minerals are irregularly distributed. A real banding can not be seen, but a vague alternation of amphibole-rich and olivine-rich layers is present. Olivine forms an adcumulate in the most olivine-rich parts. The amphibole is subhedral and is often accompanied by clinopyroxene. Clinopyroxene never occurs without amphibole. Olivine and spinel are absent in the clinopyroxene-amphibole aggregates. Amphibole may also be accompanied by plagioclase, in that case it may contain anhedral spinel grains. Olivine and plagioclase also carry spinel. The distribution of the spinel through the rock is irregular. In olivine the spinel is very fine and rounded (10-20 micron), in plagioclase coarser crystals are present, but the largest (up to ca 0.25 mm) are interstitial or enclosed in amphibole. Opaque ore is mainly dispersed in serpentine-filled cracks, on crystal faces of amphibole and olivine, and sometimes as interstitial grains.

The plagioclase as well as the amphibole and amphibole-clinopyroxene aggregates are intercumulus.

MID : The colour of the amphibole differs from other mafic and ultramafic samples. It is softer and brighter, and more orange brown. The extinction is undulatory. Olivine is the main constituent, $2V_x = 80\text{-}90^{\circ}$ (= ca Fa_{20}), along some major cracks in the rock the olivine is serpentinized. Plagioclase may show gradual zoning, deformed twins and alteration to sericite "flowers". The spinel is reddish-brown. Magnetite forms elongated crystals parallel with the shearzones. In the main part of the sample only pyrrhotite and chalcopyrite are found as opaque ore. Ilmenite is absent.

AC : Modal analysis : highest olivine content; high spinel; no phyllosilicates.

Bulk composition : highest MgO.

Niggli values : highest mg and u; high fm and M; low alk, Q and L.

Amphibole oxides : highest TiO_2; high Al_2O_3, MgO and Na_2O; low MnO; lowest "All Fe as FeO".

23(0) formula : highest mg-ratio.

Further remarks : The spinel is analysed by microprobe (table V.4). It represents an intermediate composition in the spinel-hercynite-chromite-magnesiochromite system (fig. A.3). Microprobe analyses of several amphibole crystals showed some variation; E 128 1 : average of 2 crystals, E 128 2 : average of 3 crystals.

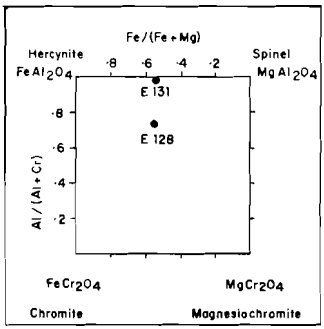

Figure A.3.: Position of E 128- and E 131-spinel in the Fe-Mg/Al-Cr spinel diagram.

E 131 : Ore-rich amphibole-bearing norite with ferroan pargasite.

FO : Badly exposed, probably phase A sample.
MAD : Mesocratic, fine-grained, lineated rock.
Texture : Equigranular, fine-grained. The plagioclase fabric is polygonal, and the intercrystalline phase varies from polygonal to amoeboid. Lineation is caused by the plagioclase. The anhedral amphibole is concentrated in groups as is typical for the leuconoritic phase; it fills the last interstices and may show epitaxial intergrowth with orthopyroxene. These aggregates are irregularly distributed in the rock and all crystals of a certain aggregate have a more or less equal orientation (like E 125). Each fragment may exhibit undulatory extinction. Orthopyroxene forms irregular crystal-aggregates with opaque ore, spinel and some apatite. Some orthopyroxene crystals contain symplectitic intergrowths of ore (ilmenite/magnetite) as described by Gierth and Krause (1973) for the ilmenite-norite ore body of Tellnes, some 20 km SSE of this location. The most beautiful examples are found if the orthopyroxene is completely enclosed by amphibole. Randomly oriented flakes of biotite cut through orthopyroxene and amphibole. Against plagioclase the biotite boundaries may be irregular. Spinel, opaque ore and apatite are mainly associated with orthopyroxene, but they are also interstitially present. Clinozoisite forms secondary "flowers" in some plagioclase crystals, which dispay undulatory extinction.
MID : The amphibole has a very light colour. Orthopyroxene is strongly pleochroic. Spinel is green, in contrast to E 128-spinel. The opaque ore consists mainly of magnetite with thin lamellae of ilmenite and extremely fine spinel. Ilmenite also occurs as separate crystals associated with magnetite. The symplectites in orthopyroxene consist of magnetite + ilmenite. The biotite colour is orange.
AC : Modal analysis : high ore and spinel.
Bulk composition : high Fe_2O_3, Fe-total and MnO; low SiO_2.
Niggli values : high r; low alk.
Amphibole oxides : high Al_2O_3, MgO and Na_2O; low Fe-total; no Cr_2O_3 (see E 128-amphibole).
23(O) formula : high Al^{VI} and mg-ratio.
The An-content is rather high.
Further remarks : The spinel is analysed by microprobe (table V.4). It lies halfway between spinel s.s. and hercynite (fig. A.3). The Fe/(Fe+Mg)-ratio is about equal to the E 128-spinel.

E 167 : Clinopyroxene-olivine-bearing amphibole granite with ferro-edenitic hornblende and ferro-actinolite.

(Compare with E 067, which belongs to a lower level of this phase).
FO : Top levels of the quartz-monzonitic phase of the lopolith. Very homogeneous formation with strong joint system. It contains in a few places some xenoliths, probably from the migmatitic roof (e.g. E 170).
MAD : Leucocratic, coarse-grained, yellowish-grey rock with large equally oriented amphibole fragments.
Texture : see E 067.
MID : The amphibole is more or less the same as in E 067, it exhibits pleochroic haloes around apatite, and zircon. Stilpnomelane often forms rims around the amphibole. Remarkable are the almost euhedral plagioclase crystals which may be enclosed by amphibole. The main amphibole E1167 contains some very fine colourless zones, possibly //($\bar{1}$01). They are only found in one crystal, and may be actinolitic exsolution lamellae. They were too thin to analyse with the microprobe. E2167 is a light bluish, fibrous ferro-actinolite. It is only found once in this sample; together with some small ore grains, at the contact of E1167 and quartz. Clinopyroxene is, in contradistinction to E 067, only present as an accessory, partly altered to reddish-brown stilpnomelane. Olivine is mainly enclosed by amphibole; it is altered into serpentine, chlorite, ore and iddingsite. Quartz, alkalifeldspar and plagioclase are the same as in E 067. Zircon is sometimes zoned, with a metamict core. Like in E 067 it may contain many inclusions, form great crystals and it is euhedral to slightly rounded. The ore consists of reddish brown components, ilmenite and magnetite, (see E 067) enclosed in amphibole. Biotite is rare.
AC : Amphibole oxides : E1167 : highest Fe_2O_3; high H_2O^-, FeO and total Fe; low MgO and CaO.
E2167 : high total Fe; lowest MgO.
Niggli values : low mg.
23(O) formula : lowest mg-ratio for E2167.
Density for E1167 is greater than 3.30.
E2167 : 1 microprobe spot.

1 : Plate IV, figure 3.

E 170 : Amphibolite with thin diorite zones and ferroan pargasitic hornblende.

FO : Lens of 5 meter long in the quartzmonzonitic phase of the lopolith.
MAD : Fine-grained, melanocratic, strongly lineated, amphibole-rich rock.
Texture : The sample consists of two rocktypes : the main part is an amphibolite which contains several diorite bands of a few mm width.
The amphibolite is granoblastic, equigranular, interlobate with a grainsize less than 1 mm, mainly much smaller. The amphibole forms subhedral poikiloblastst up to 1 mm.
The diorite is granoblastic, inequigranular, interlobate. The thickness of these bands may vary somewhat. In the centre of the bands the clinopyroxene is relatively coarse (>1 mm). The crystals are anhedral and the crystal boundaries display resorption. On the contact with the amphibolite there is a fine mixture of plagioclase and orthopyroxene. These small orthopyroxene crystals are long prismatic (c:a= 4:1). The transition between both rock types is gradual but thin, and the amphibolite lineation is parallel with the, local undulatory, contact. In some of the diorite layers the clinopyroxene forms skeletal crystals which are not bounded by the very fine-grained orthopyroxene-plagioclase mixture. These skeletal crystals (c:a= 5:1) have very irregular crystal boundaries (resorption or the granophyric texture of Rosenbusch?), and in the centre plagioclase grains are present. Small rounded ilmenite grains are approximately homogeneously dispersed throughout the amphibolite.
MIN : -the amphibolite-
The brown hornblende contains some apatite and rounded zircon, the latter enveloped by pleochroic haloes. A second amphibole was found only much later and therefore was not analysed and tabulated. It has a light bluish-green pleochroism, and occurs partly fibrous and partly as homogeneous zones or pieces at pyroxene-amphibole and pyroxene-plagioclase (+ hornblende) contacts. It is only present in the transition zone between the amphibolite and the diorite bands. The birefringence is about the same as for the main hornblende. Extinction angle unknown, sometimes it appears to be zero, other crystals show an angle of 10-20°. Possibly this description covers a combination of several light coloured, fine-grained minerals (actinolite, muscovite, a third amphibole?) which can not be distinguished in this sample. The best name seems to be uralite, it is locally accompanied by some biotite specks. The plagioclase is so strongly clouded and altered to sericite that the An-content can not be established anymore.

-the diorite-

The coarse clinopyroxene is zoned and has a clear diallage-cleavage. It is colourless, sometimes twinned and contains some serpentine. In several of the coarse clinopyroxene crystals a possible epitaxial relation between normal clinopyroxene with medium to large $2V_z$, and a pyroxene with a very small $2V_z$ (Pigeonite?) can be seen. Very fine exsolution lamellae are omnipresent. The small orthopyroxene crystals are slightly pleochroic. The plagioclase is, in contrast to the plagioclase in the amphibolite, more or less clear, very small and strongly zoned. A bent crystal is present.
AC : The hornblende is high in H_2O^+ and low in Fe^{3+}/Fe-total.

E 232 : Quartzmonzonite in mela-anorthosite (leuconorite) with ferro-hornblende and actinolite.
(together with F 501, F 502, F 503 and N 827)

FO : At the contact between the intermediate monzonoritic phase of the lopolith and the Haaland-Helleren anorthosite body (described by J. Michot, 1961), many irregular features can be seen (section II.7.2).
MAD : The quartzmonzonitic xenolith (E 232 F, F 501, N 827) has remarkably white light constituents. The mafic minerals are up to several mm in size. The anorthosite (E 232 N, F 502, F 503) contains vaguely oriented mafic minerals up to several cm.

-the quartzmonzonitic xenolith-

Texture : Granoblastic, seriate, amoeboid, without orientation. The mafic minerals (amphibole and biotite) are generally larger than the felsic ones. Mafics upto 5 mm, felsic less than 1 mm. There is a vague banding. Amphibole and quartz form symplectitic intergrowths, which are anhedral and sometimes elongated; several symplectites may grow through one another. Biotite may grow straight through the amphibole, but is than mainly restricted to the outermost rim. It too forms symplectites with quartz, and great irregular aggregates of crystals which grow in all directions through each other. Very fine symplectites may be present at the crystal boundaries. Some of the biotites are curved. The opaque ore is mainly anhedral, but a few crystals have distinct crystal faces. The ore is not homogeneously distributed, certain levels being richer in ore than others. The felsic minerals are intimately intergrown.
MIN : In many cases the amphibole-quartz symplectites are enveloped by a homogeneous amphibole rim. These may be compared with Beach (1974)[1]. The colour of the amphiboles is rather variable. It seems to depend partly on the presence of retrograde minerals in the immediate surroundings, which create a brownish tint in the green amphibole; also, the centre of many crystals displays a lighter greenish tint than the rim (E1232 K and N2827 F versus E1232 R and N1827 F, table I.1). Other optical parameters also change from core to rim (see table IV.14). The change is gradual. However, several crystals, especially the small ones, contain no actinolite in the core. They consist completely of ferro-hornblende. The (001) cleavage of the amphibole is strongly developed. The brown biotite aggregates often contain opaque

1 : Beach, plate 1-c; this thesis plate VI, figure 2.

ore and titanite. The opaque ore consists of magnetite, magnetite with ilmenite lamellae, magnetite and ilmenite as irregular parts of the same crystal (mosaic texture), and some separate crystals of ilmenite and pyrite. Some of the ore-rich levels contain titanite, surrounding the opaque ore. In some cases the titanite forms great irregular crystals with lamellar twins, and oriented biotite flakes.
Great anhedral zircons (up to 2 mm), brownish pleochroic allanite, and large apatite needles are accessories. Muscovite in plagioclase, serpentine in amphibole centres, chlorite and epidote are present in small quantities.
Alkalifeldspar displays microcline twinning and microperthite in many forms. Plagioclase is often zoned with an average An-content of 27% (core somewhat higher than the rim). It contains deformated twins. Quartz is mainly restricted to amphibole- and biotite symplectites. Some quartz is found between the feldspars, and another part forms beautiful myrmekites with plagioclase.

-the anorthosite-

Texture : Granoblastic, seriate, polygonal-interlobate. The mafic aggregates (amphibole and biotite) are sometimes bent and appear irregularly distributed through the rock. Alteration products are common on plagioclase-plagioclase contacts. Small green hornblende crystals formed along some cracks which break straight through plagioclase crystals and some coarse, dark brown, biotites. If these cracks cross an amphibole aggregate, they disappear and continue on the other side. There seems to be a clear relation between the cracks and at least part of the amphibole formation. It also shows that part of the biotite is older than the green hornblende.
Amphibole forms aggregates of crystals, mainly with soft coloured centre of the aggregate (E2232 N = actinolite) and a greenish mantle (E3232 N = ferro-hornblende). Small crystals which are not part of an aggregate often do not show any zoning, except for the symplectitic intergrowth in the centre, as described under the quartzmonzonite. Both amphibole and biotite form symplectites with quartz. These intergrowths sometimes appear as fine-grained, granoblastic, polygonal aggregates between large hornblende or biotite crystals, and the actinolite core. They seem to from a stable phase, and are much less irregular than the symplectites; however, the mafic fragments all have the same orientation as the homogeneous rim. Biotite is often formed on hornblende-plagioclase contacts, but large isolated crystals are also present. Plagioclase varies in grainsize from 1-5 mm, and the crystal boundaries are irregular, but the contacts tend to be polygonal.
MID : The actinolite core of the amphibole aggregates is sometimes very irregular, with crystals growing in various directions through one another[1]. In other cases the actinolite consists of a group of parallel, bent crystals. It may contain some ore needles and plates, especially in the folds. Lamellar twins are omnipresent. Quartz is usually absent in the actinolite cores of large crystals, but increases near the contact with green hornblende. The transition to ferro-hornblende/ferro-tschermakitic hornblende is mostly gradual, but sometimes very sharp. In the last case the actinolite core contains a lot of quartz drops while the green hornblende forms a homogeneous mantle. Double pleochroic haloes occur rarely. The optical parameters differ slightly from those of the quartzmonzonitic amphiboles. The colour of biotite varies from dark brown for the coarse crystals, to green for some of the finer crystals connected with hornblende. Opaque ore is mainly connected with the mafic aggregates and consists of magnetite, ilmenite with haematite exsolution, and some ilmenite and pyrite grains. The ore grains are irregular and often rimmed by titanite. In amphibole it always causes a broad zone of green hornblende. Finer-grained ore and sagenite systems are found in plagioclase. Titanite also forms individual grains, mainly in biotite. Plagioclase displays some normal zoning. Deformed twins are found. The An-content (35-39) is lower than the average of 45% An for the Haaland-Helleren anorthosite. The plagioclase contains, beside ore and sagenite, also apatite, some sericite flowers, and muscovite. Remnants of colourless clinopyroxene coated by carbonate and partly overgrown by amphibole are rarely present. Accessories are a few large (3 mm) apatite crystals, serpentine in some amphibole cores and cracks, chlorite in biotite, yellow epidote in biotite and interstitially, and some small rounded crystals of monozite or zircon in the symplectitic quartz. Finally there are some extremely fine, myrmekite-like spots of unknown composition.

-Vein in F 502-anorthosite-

This sample is taken just outside the xenolith. The vein is about 2 mm thick and curs razorsharp through the anorthosite. It seems to disappear into the quartzmonzonitic xenolith. The mineralogy coincides very well with the quartzmonzonite, but there is more serpentine, amphibole and apatite, and less plagioclase. Clinopyroxene remnants are sometimes present, surrounded by serpentine and with an outer rim of amphibole.
AC : N1827 is high in FeO, and low in F, Na_2O and $2V_x$.
F 503 : highest Na_2O; high niggli al, L, T and t; low niggli fm.
Further remarks : The universal stage measurements for N 827 are only indicative and not too precise.
Wet chemical analysis was possible for N1827 only. The FeO_{wet} is subtracted from the FeO_{probe}, this results in a Fe_2O_3-value which makes it possible to determine the oxidation ratio. This ratio is used to determine the FeO and Fe_2O_3-values for each microprobe spot (N1827 1/4).

F 005 : Quartzmonzonite with edenitic hornblende.

FO : Alternation of augen gneisses and quartzmonzonitic-granitic bands at the contact between the Sirdalen augen gneiss and granitic migmatites. The environment is rather retrograde (faults and epidote bands).

1 : Plate VI, figure 3.

MAD : Medium-grained, leucocratic rock with an amphibole-biotite lineation. The leucocratic minerals are white in contrast to the greenish-grey colours of the charnockitic migmatites and the lopolith.
Texture : Granoblastic, seriate, interlobate. The leucocratic minerals form the largest crystals. They seem to press the mafic minerals aside. The amphibole is anhedral, very irregular in shape and size, and mostly occurs with fine-grained leucocratic minerals between the larger quartz and feldspar crystals. Sometimes quartz seems to replace (dissolute) the amphibole, resulting in a few equally oriented amphibole fragments around a large quartz crystal. Biotite may grow straight through the amphibole.
MID : Dark brown biotite in many places is altered into chlorite. Plagioclase displays myrmekite, ilmenite-schiller, sericitization and deformed twins; alkalifeldspar shows swopped boundaries, a vague microcline grid and some saussuritization. The undulatory quartz contains numerous two-phase inclusions.
Magnetite, ilmenite with haematite exsolutions, some pyrite, hydroxides partly pseudomorphous after pyrite, rounded zircon, apatite and allanite are minor phases. Retrograde minerals are chlorite, muscovite, epidote and titanite.
AC : Amphibole Fe^{3+}/Fe-total is very high (0.34).

F 043 : Biotite-bearing amphibole gneiss with edenitic hornblende and actinolite.

FO : Banded granitic migmatites, with many folds and pegmatites (or leucosomes). An outcrop of folded basic intrusions is nearby. Only a dark band was sampled.
MAD : Mesocratic, fine-medium grained, lineated rock.
--The mineralogy and texture resemble F 005 very much. Only the differences are given here--
Texture : Granoblastic, seriate, interlobate. Biotite determines the lineation. The leucocratic minerals are less blastic than in F 005, while the main mafic minerals are more (poikilo-)blastic. This creates a more homogeneous mineral distribution in the rock. The mafic constituents are all more or less subhedral. The grainsize is finer than in F 005. The relation between amphibole and fine-grained leucocratic minerals is absent.
MID : Besides the sometimes poikiloblastic hornblende (F1043), actinolite (F2043) is found, always in combination with biotite, titanite and epidote. It is never found in the centre of a hornblende grain, like in E 232, but on the rims. The contacts with the hornblende are sharp! Cleavage planes continue over the contact. Universal stage measurements indicated a very small angle (5^{o}) between the planes of optical axes for the two phases in one crystal. There are no separate grains of actinolite. Biotite is more yellowish brown than in F 005, and forms extreme poikiloblasts as described by Rietmeijer and Dekker (1978). Incidentally it alters to chlorite. Plagioclase contains no ilmenite-schiller but fine cubes of opaque ore. Zoning is found in a few crystals. Alkalifeldspar is locally perthitic. Quartz is relatively fine-grained, but here too it seems to replace some of the hornblende.
AC : Modal analysis : highest in titanite.
Amphibole oxides : high Fe_2O_3 (F1043) and MnO (both amphiboles).
Fe^{3+}/Fe-total for F1043 equals the high value (0.34) of F 005 hornblende.
Further remarks : The amphiboles are rather inhomogeneous; however, there is a large chemical distance between the hornblende and the actinolite.

F 052 : Amphibole mela-syenite and amphibole mela-alkalifeldspar quartzsyenite with edenitic- and actinolitic hornblende.

FO : A vertical zone of a few meters wide in a gneissose environment at the northside of the Björnestadvatn. On the eastside of this zone, a very coarse-grained quartz-feldspar band of ca 50 cm wide is present, which is strongly tectonized. On the westside a coarse-grained, leucocratic alkalifeldspar rock with amphibole crystals up to 1 cm (F 052 L). It seems to invade an amphibole-rich, strongly lineated layer (F 052 D). The environment of the Björnestadvatn, where this sample as well as F 070 and F 107 comes from, is very complex. Many rocktypes form thin bands and zones in the mainly massive granitic migmatite. Faults and slipplanes are common. Felsic (pegmatites) and mafic (folded basic intrusions, e.g. F 107) intrusions cut through the migmatites. Several gneiss bands of 50-100 meters thick can be traced over long distances through the leucogranites. Contacts are often very sharp oand covered with chlorite. The sample under discussion comes from a subvertical band at the contact with the more coarse-grained amphibole-carrying rock.
MAD : Mesocratic, medium-grained, amphibole-rich, lineated rock (F 052 D), transected by veins of various sizes (F 052 L : 1 cm to several decimeters). These are partly parallel (mainly thin veins), and partly unrelated to the lineation. The veins consist of coarse amphibole and pinkish alkalifeldspar, up to 2 cm in size. Some sulfide is also recognisable. It resembles Mehnert (1968), fig. 1.10 : stictolith (fleck) structure and fig. 98 : mobilizate veins in their paleosome.
--medium-grained main phase : F 052--
Texture : Granoblastic, equigranular, interlobate, Retrograde zones and spots are finer grained than the rest. Amphibole and bent phyllosilicates (biotite and chlorite) determine the lineation. The amphibole (F1052 D) is anhedral, partly poikiloblastic, with varying grainsize. The crystals may be cut to pieces by biotite and chlorite. Pyroxene remnants are mostly rimmed or replaced by serpentine and enveloped by amphibole. Small microcline blasts press the

1 : Plate 1, figure 1.

amphibole crystals aside. The transition to the coarse-grained veins is sometimes sharp, sometimes gradual, with slightly increasing grainsize. The pre-retrogression minerals are more or less homogeneously distributed through the melasyenite.

MID : The extinction of the main amphibole (F1052 D) is often undulatory. Along fractures, crystal boundaries and sometimes as patches inside the green edenitic hornblende (F1052 D), light blue actinolitic hornblende (F2052 D) has formed. It is optically continuous with the original hornblende. The contacts may be sharp. The edenitic hornblende is locally overgrown with quartz, especially once, in contact with a long prismatic pyroxene, which has strongly developed cleavage planes and a yellowish pleochroism. Another pyroxene displays light bluish pleochroism, $2V_x = 70\text{-}80^o$, $Z\wedge c = 45\text{-}50^o$ (Hedenbergite?). It alters to green hornblende on one side of the crystal. Reddishbrown biotite is strongly altered to chlorite, frequently only the crystalcentres are biotite. The ratio c:a (or b) for both phyllosilicates is extremely small with respect to other rocks in the migmatites. Fine-grained quartz with undulatory extinction accompanies the phyllosilicates and, less frequent, amphibole. In addition to the quartz, retrograde minerals like titanite, epidote, carbonate and fine dispersed ore grains are related to the chlorite/biotite. The epidote is yellow or purple (Piemontite). Perthitic microcline full of inclusion strings is the main felsic mineral. Plagioclase (presumably oligoclase) is sericitisized and often myrmekiticly intergrown with quartz. The myrmekite varies from coarse to very fine. Apatite is rather coarse, zircon fine and rounded. The opaque ore consists of magnetite, ilmenite with haematite exsolution lamellae, and large pyrite crystals.

AC : Modal analysis : high alkalifeldspar

Bulk composition : high K_2O (and niggli k).

--the coarse-grained veins : F 052 L--

Texture : Amphibole and microcline form a cumulate-like fabric with quartz as the main intercumulus phase. The grainsize may reach 2 cm. The distribution of amphibole is not homogeneous, therefore the modal analysis of this part of the sample is highly unreliable. The cumulate crystals are more or less euhedral. The other minerals (the same as in F 052 D) are intergranular, or derived from retrogression of the amphibole. Especially quartz forms a strongly undulatory to granulated intercumulus phase, with numerous rutile needles.

MID : The mineralogy is almost the same as in F 052 D, only the differences are described here. The amphibole has the same characteristics as in the finer-grained part : actinolitization along boundaries and cracks, and some pyroxene remnants enclosed. Remarkable is a large, zoned allanite crystal, intergrown with an amphibole. The ore is mainly sulfide. Plagioclase is only present as myrmekite, it forms flower-like on microcline-microcline and microcline-quartz contacts.

AC : same as for F 052 D.

Further remarks : The difference in chemistry between the two parts (table A.1) indicates that the modal analysis of the vein (F 052 L, table III.1), which is almost equal to that of the dark part, is dubious. As stated before, this is caused by the inhomogeneity and the large grainsize. Amphibole is estimated too high, alkalifeldspar too low.

Oxide	F 052 D 1	F 052 L 2	Δ_{abs} 3	Δ_{rel} 4
SiO_2	52.49	65.39	+12.90	+24.6%
TiO_2	1.89	0.50	- 1.39	-73.5%
Al_2O_3	14.51	13.62	- 0.89	- 6.2%
Fe_2O_3	3.97	1.34	- 2.63	-66.2%
FeO	4.93	2.32	- 2.61	-52.9%
MnO	0.19	0.08	- 0.11	-57.0%
MgO	4.70	2.28	- 2.42	-51.5%
CaO	5.80	3.02	- 2.78	-47.9%
Na_2O	2.89	2.70	- 0.19	- 6.6%
K_2O	5.60	6.68	+ 1.08	+19.3%
P_2O_5	1.01	0.45	- 0.56	-55.4%
$H_2O^?$	1.39	0.83	- 0.56	-40.3%
F	0.48	0.33	- 0.15	-31.3%

Table A.1.: Rock analyses of both parts of F 052, with the absolute and relative differences. All elements except Si and K decrease from the dark to the light part. 3=2-1; 4=3:2.

The difference in bulk chemistry indicates an increase in microcline and quartz, and a decrease in all other minerals. Measurements in the green hornblende at the contact with the light blue actinolitic hornblende revealed that the composition did not differ markedly from homogeneous green to the transition zone. The chemical discontinuity is sharp. There is no significant difference between the green hornblende from the dark or light zone. The actinolitic hornblende is only measured chemically in the light band, but optical resemblance indicates a similar composition for F2052 D. There is some variation in chemistry between various crystals of both kinds of amphibole, but not significant.

The pegmatite bordering F 052 on the eastside consists mainly of plagioclase and quartz, and is strongly deformed. Quartz is undulatory and in many places granulated, plagioclase displays a wavy twin pattern, sometimes with kinkbands. Mafic minerals are replaced by a combination of chlorite, epidote and titanite. The leucocratic zone on the westside was not sampled separately but will be of the same mineralogical composition as F 052 L.

F 070 : Biotite amphibole augen gneis with edenitic hornblende.

FO : The Espetveit augen gneiss seems to intrude the granitic environment. From east to west the amount of granitic bands, with platy quartz up to 10 cm, increases until they form the main rock. The contact between the augen gneiss and the granitic migmatite is strongly tectonized and retrograde metamorphic (see F 052 for Björnestadvatn area description).

MAD : Mesocratic, fine layered rock, with leucocratic lenses of ca 1 cm long and ca 0.5 cm diameter, elongated in one direction.
Texture : The "eyes" consist mainly of several crystals of microcline and some small quartz grains. In a few eyes, plagioclase and some mafic minerals may be incorporated. The microcline forms the coarsest constituents, up to 2 mm. The matrix is mainly rather fine-grained, with granulated and strongly lineated quartz,which together with biotite determines the lineation. The matrix is bent around the equigranular, polygonal, interlobate eyes. The grainsize of the amphibole varies from fine near the leucocratic lenses, to intermediate. Thin quartz rims are locally present in contact with amphibole and biotite. Biotite is partly bent, it may grow through amphibole.
MID : The anhedral amphibole displays frequently undulatory extinction. Biotite is yellowish-btown. Plagioclase is strongly sericitisized, partly myrmekitic and displays deformed twins. Microperthitic alkalifeldspar has a microcline grid and contains numerous inclusion strings. Quartz is granulated around the eyes, and shows sttong undulatory extinction in the non-granulated crystals. Homogeneous magnetite, ilmenite and pyrite, composite crystals of magnetite + ilmenite (mosaic texture) rather coarse apatite, rounded and zonary zircon, rare allanite, and retrograde chlorite, carbonate and epidote are minor phases.
AC : The hornblende has a rather small extinction angle (8^{o}), see fig. IV.23.
Further remarks : There was only enough amphibole mineral separate for Fe-analysis.

F 074 : Retrograde ortho-amphibolite with edenitic hornblende.

FO : See section 11.4.3.
MAD : Mesocratic, black to greenish, very fine-grained rock.
Dolerite petrology : The average mineralogy of non retrograde dolerites is described by Hermans et al (1975, p.64). In this case the dolerite is completely recrystallized and altered. There is a clear difference between margin and centre. In the centre (additional sample F 075, not treated in the tables) there are long, zoned plagioclase laths, in a very fine matrix of plagioclase-ore-actinolite-chlorite-epidote-carbonate-apatite, creating some sort of flow texture. At the margins no laths are present, and the average grainsize is somewhat greater than in the centre. Green hornblende instead of actinolite is the main mafic phase, and some quartz is present. Pyroxene occurs only as completely altered pseudomorphs. All biotite is altered to chlorite and epidote.
Margin F 074 : Texture : Granoblastic, equigranular, polygonal-interlobate. Grainsize less than 1 mm. The amphibole is poikiloblastic, and often accompanied by very small quartz grains with undulatory extinction. Quartz is also present in a thin vein.
MID : Plagioclase is strongly sericitisized and deformed, it contains a lot of apatite and opaque ore, illustrating the zoned character of the plagioclase. Microcline is a minor phase, while apatite, ilmenite, magnetite, and composite crystals of magnetite + ilmenite (mosaic texture) are omnipresent. Pyrite occurs less frequent. Zircon forms some small rounded crystals. Chlorite and epidote not only replaced the biotite but also some of the green edenitic hornblende.
AC : Modal analysis : highest chlorite content.
Bulk composition : highest H_2O-content.

F 107 D : Apatite amphibole 2-pyroxene quartzmonzonorite with edenitic hornblende.

FO : Mafic rock with a planar system of leucocratic lenses (discs) of 10-20 cm, in the irregular migmatitic environment of the Björnestadvatn (see F 052 FO). The outcrop is about 200 meters long. The real width of this "folded basic intrusion" (see Hermans et al, 1975, p.61; their fig. 6 is from this location) is about 50 meters.
MAD : Mesocratic, fine-medium grained rock in which the medium-coarse grained leucocratic lenses are parallel with the lineation indicated by the dark minerals.
--Only the mafic part is under discussion here--
Texture : Granoblastic, seriate, polygonal-interlobate. The amphibole forms the largest and most irregular mafic crystals (poikiloblasts). All main minerals are anhedral. The grainsize is mainly less than 1 mm. lineation is not clear. The transition to the leucocratic lenses is sharp.
MID : Myrmekite like patterns of ore are common in amphibole at contacts with mafic minerals. In the immediate surroundings of such an ore-rich zone, the edenitic hornblende (F1107 D) is often discoloured to a soft bluish-green tint (F2107 D), which also forms very small fragments at the crystal boundaries of pyroxenes and ore. The transition from F1107 D to F2107 D inside an amphibole crystal is gradual. It is not the same as the hornblende-actinolite transition found in, for instance, F 252, but comparable to the change in B 322, expressed in table II.4. Clinopyroxene is greenish $2V_z = 55\text{-}60^{o}$, $Z\wedge c = \pm 43^{o}$, strong diallage-cleavage, exsolution lamellae //(100) which are 0.5 micron wide. Some crystals appear to be zoned, but closer inspection on the universal stage shows no zoning at all. Presumably augite. Orthopyroxene occurs less frequently than clinopyroxene; it shows strong pleochroism from pink to greenish-blue, $2V_x = 60^{o}$; rims are altered to serpentine, chlorite, carbonate and muscovite. A few crystals contain some exsolution lamellae. Plagioclase with wavy deformed twins, some antiperthite, schiller, small ore crystal clouds, and locally sericite is the dominant leucocratic mineral. Microperthitic microcline; quartz with numerous inclusions and undulatory extinction;

opaque ore as intergranular phase and as small rounded inclusions in the main minerals; apatite enclosed in all minerals and omnipresent, often euhedral; reddish-brown biotite with colourchange to green in the same crystal, it grows through amphibole crystals or lies adjacent to opaque ore; and rounded zircons which group together, complete the picture. The opaque ore consists of magnetite, ilmenite, composite crystals of magnetite + ilmenite (mosaic texture), magnetite with ilmenite exsolution lamellae and very fine spinel at the contact between magnetite and ilmenite, some pyrrhotite and pyrite.

The leucocratic lenses consist of equal amounts of quartz, microcline and plagioclase. The An-content is the same as in the dark part (An_{38}). Orthopyroxene with alteration rims, biotite, chlorite, muscovite, epidote, serpentine, carbonate, apatite and zircon form together 10 percent of the modal analysis : charnockite.
AC : Dark part : Modal analysis : very high in apatite (same as B 322).
Further remarks : Besides the bulk composition of the dark part (F 107 D), the composition of the combination dark and leucocratic is given (F 107 B) in table III.3. The chemical differences between F1107 D and F2107 D are small (see table II.3).

F 126 : Retrograde amphibole biotite enderbite with edenitic hornblende.

FO : Dark zone of 100 m width, enclosed in leucogranite. Thin leucocratic bands are intercalated in the dark rock. The contacts between this "folded basic intrusion" (see also F 107) and the mainly massive migmatite are sharp and retrograde. The dark zone forms a valley.
MAD : Mesocratic, fine-medium grained rock, with some lineation of biotite. Several feldspar crystals up to 1 cm long are visible.
Texture : Plagioclase can be divided into three groups : large, completely sericitisized crystals (up to 1 cm); laths with deformed twins, but rather fresh (up to 3 mm); and, mainly, subhedral crystals up to 1 mm, with straight twins.[1]
Apart from the few large plagioclase crystals, the sample is granoblastic, equigranular, polygonal-interlobate. Biotite, which may be bent, determines a weak lineation; in most cases it grows in various directions. Amphibole is concentrated in a few, biotite-poor, spots. Clinopyroxene is very irregularly formed, like an intercumulus phase, enveloping plagioclase and quartz, and with alteration products at crystal boundaries. There is no reaction relationship visible between amphibole and pyroxene. Quartz is frequently associated with biotite and clinopyroxene.
MID : The main amphibole is stubby prismatic with rounded crystal corners, and only contains some apatite and opaque ore. The second amphibole (F2126) is a light coloured variety, comparable with F2107. It formes a separate crystal, and is not found as rims, or near ore in amphibole. Clinopyroxene shows (001)-lamellae. Dark brown biotite is the main mafic constituent, partly consisting of large poikiloblasts with quartz; it may be altered to chlorite. Quartz is remarkably fresh, it displays some undulatory extinction, but much less than the other samples from this region, described above. Apatite is omnipresent. Zircon is rounded. Opaque ore is sometimes surrounded by hydroxide and an outer rim of stilpnomelane and serpentine. The ore consists of homogeneous grains of magnetite, ilmenite and some pyrite; composite crystals of magnetite + ilmenite (mosaic texture) are also present. Yellow epidote and chlorite are the main alteration products of biotite and pyroxene.
AC : Modal analysis : highest biotite content.
Further remarks : The amphibole is rather homogeneous, and about equal to the other amphiboles described from this region. The second amphibole was too rare to analyse.

F 252 : Biotite-bearing amphibole augen gneiss with edenitic hornblende and actinolite.

FO : Sirdalen augen gneiss formation, near the contact with a leucogranitic interlayer.
MAD : Mesocratic, medium-coarse grained gneiss with feldspar crystals up to 3 cm long.
Texture : Granoblastic, seriate, interlobate. The augen consist of several large alkalifeldspar crystals, and some smaller plagioclase and quartz crystals. They press the mafic minerals aside, into thin bands, which often display granulation. Biotite determines the lineation in these bands. The great leucocratic crystals all show undulatory extinction. Quartz consists, besides of the large partly granulated plates, of small fragments in contact with amphibole and biotite. Most of the amphibole crystals are irregularly shaped due to overgrowth of biotite, and the late formation of large quartz plates which replace part of the amphibole (as in F 005).
MID : Around ore inclusions the main green amphibole (F1252) is more bluish, as described by F 107 and B 322. Some crystals are zoned ($2V_x = 66^{o}_{core} - 72^{o}_{rim}$, $Z\wedge c = 14^{o}_{core} - 16^{o}_{rim}$), others may exhibit undulatory extinction. A twin lath in the centre of a large amphibole crystal does not reach the outer rim. The second amphibole is a magnesio-hornblende to actinolite (F2252). It appears at crystal margins as spots and sometimes replaces half a crystal of edenitic hornblende (same as F2043 and F2052/F4052). Clinopyroxene is partly rimmed by green hornblende; this amphibole also forms laths along the c-axis of the light green clinopyroxene. Reddish-brown biotite is partly replaced by chlorite. Apatite

1 : Plate III, figure 2.

consists of rather coarse crystals, between the mafic minerals. It is never enclosed in other crystals. Rounded zircon forms pleochroic haloes in biotite and amphibole. Opaque ore, which consists of magnetite, haematite-ilmenite exsolutions, and some pyrite and pyrrhotite, mainly forms an interstitial phase between the mafic minerals, often surrounded by titanite. The ore is partly present as a schiller system in plagioclase. Epidote and allanite are rare. Large quartz crystals contain numerous 2-phase-, carbonate-, rutile- and other inclusions. Beside schiller, the plagioclase contains deformed twins, antiperthite, and myrmekitic rims. The An-content will be between An_{20} and An_{30}. Alkalifeldspar is a minor phase between the above mentioned minerals, and the main component of the augen.

AC : F1252 has a high Fe^{3+}/Fe-total ratio : 0.36.

Further remarks : The modal analysis is low in alkalifeldspar because no "eye" was present in the counted slide (see fig. III.8). Amphibole chemistry, see section II.2.3.

F 433 : Amphibole pegmatite with ferro-edenitic hornblende.

FO : Pegmatites of about 30 cm wide cut subhorizontal through the base of phase C at the southside of the Orrestadvatn in the Bjerkreim-Sokndal lopolith. Amphiboles range up to 30 cm long, sometimes they form groups of smaller crystals. The wallrock displays strong amphibolization near the contact, the feldspar is yellow, but at a distance of 1 meter the influence is already neglectable. The wallrock amphibole consists of groups of sections with the same optic orientation (extreme poikiloblasts, group 2 amphiboles : see Rietmeijer and Dekker, 1978, and section II.5.3).

MAD : Leucocratic, coarse-grained quartz-feldspar rock with subhedral, very coarse-grained, black amphibole crystals, which may contain equidimensional inclusions up to 1 cm and plates of a leucocratic mineral along cleavage planes. Large biotite crystals form an additional phase in the pegmatite.

Texture : The pegmatite is inequigranular. The crystal contacts are mainly interlobate. Amphibole is subhedral.

MID : --the amphibole--

The amphibole is very remarkable. Not only does it (F1433) contain bluish zones (F2433), but is also devoid of a clear extinction position. Instead, the amphibole shows dark brown and purple colours with an undulatory character over a range of 10-15°. The $2V_x$ seems to be zero. Examination on a universal stage showed very strong dispersion of the optic axes with r>>v (related to n_x). $2V_x$= 18-23° for F1433 with the optic axial plane ⊥ c-axis (like crossite) and $2V_x$= 15-19° for F2433 with optic axial plane //(010). F2433 forms, irregularly distributed, thin zones, mainly along the c-axis of F1433, and partly along cracks and as patches in the main amphibole. These are all accompanied by parallel magnetite needles. Another part of F2433 amphibole is found along enclosed biotite, quartz, carbonate, titanite and magnetite as irregular broad zones. Albite plates along cleavage planes of F1433 are not rimmed by F2433. In a small pocket (±0.3 mm Ø) with frayed outline in one of the main amphibole crystals, some clinopyroxene is present, together with plagioclase. Additional phases in this pocket are biotite, magnetite, and at a short distance from the pocket (16 micron) some carbonate. The contact between clinopyroxene and amphibole is sharp. Amphibole seems to replace clinopyroxene + plagioclase. Quartz in the amphibole forms irregular crystals and streaks with undulatory extinction; it fills cracks and is often accompanied by yellowish brown biotite. In that case they may be symplectitically intergrown. Biotite consists of several sections with equal orientation, mainly with axes parallel to the cleavage planes of the host. This creates a skeletal appearance. Twinned carbonate also fills cracks; titanite and allanite are once found enclosed. The allanite is polyzoned. Stilpnomelane may be found along cracks.

--the pegmatite--

Outside the amphibole and biotite, the pegmatite is completely leucocratic : quartz full of 3-phase inclusions, microcline with intricate perthite systems (e.g. braid perthite, Spry 1974, p.182); and albite (An_8), which forms some large crystals with a sagenite system, and which mainly appears as equally oriented sections in microcline. These sections (patches) may contain bent twins.

AC : Amphibole oxides : wet chemical analyses on F1433 showed highest FeO-content; high Cl, and low F.
Total Fe as FeO, and MnO are high for both amphiboles.

23(O) structural formula : high Na (both amphiboles).

Density : greater than 3.30 for F1433.

Further remarks : The microprobe measurements already revealed some chemical inhomogeneity in both amphiboles, and the table values are means; therefore, the difference between the presented values for each element between F1433 and F2433 is already rather meaningless. The pegmatite was not analysed.

--the wallrock--

The non-influenced rock consists of olivine-2 pyroxene-syenite. The wallrock in direct contact with the pegmatite contains no olivine and orthopyroxene, only some clinopyroxene remnants enclosed by amphibole and biotite in exactly the same way as in E 167. More quartz is present, often intergrown with amphibole. The An-content changes from An_{16} at 1.5 meters from the contact, via An_{12} at 1 meter to An_8 at the contact. The alkalifeldspar is mainly microcline with an intricate perthite system. The grainsize increases towards the contact. The leucocratic minerals are almost the same as in the pegmatite itself.

F 501 -- F 502 -- F 503 : see E 232.

H 047 : Biotite-bearing amphibole gneiss with edenitic hornblende and actinolite.

FO : Dark band from the Sirdalen augen gneisses near the contact with the migmatites.
MAD : Fine-grained, mesocratic, lineated rock with several thin, coarser grained, leucocratic bands.
This sample resembles F 005 and F 043 very much, even though it contains more mafic constituents, some clinopyroxene and actinolite.
Texture : Granoblastic, seriate, interlobate. Inclusions strings transect all minerals. The hydrous minerals are lineated. Retrograde spots are found throughout the rock. The blastic character of the leucocratic components found in F 005, is absent.
MID : Actinolite is accompanied by epidote and stilpnomelane, and forms on the outside of H1047 (see also F 043, F 052, F 252). Light bluish-green clinopyroxene is partly altered to amphibole and biotite, and surrounded by secondary mineral aggregates of very fine grainsize. The original clinopyroxene has a very irregular outline, in between the extreme poikiloblasts (Rietmeijer and Dekker, 1978) and an intercumulus texture. Alkalifeldspar does not display a microcline grid. Apatite contains many inclusions.
AC : H1047 : high Fe^{3+}/Fe-total (0.34)
Further remarks : H2047 was not analysed because of scarcity.

H 050 : Amphibole gneiss with edenitic hornblende and actinolite.

FO : Dark band of a migmatite intercalation in tectonized Sirdalen augen gneisses.
MAD : Medium-grained, mesocratic, irregularly lineated rock with greyish feldspar. It looks less fresh and lass firmly lineated than H 047. There is a strong similarity with H 047 and F 043.
Texture : Granoblastic, seriate, interlobate. The mafic minerals are lineated. The leucocratic minerals are partly blastic, as in F 005.
MID : The main amphibole(H1050) contains very much ore exsolution without discoloured depletion zones. Actinolite behaves as in H 047/F 043. Light bluish-green clinopyroxene forms strongly serpentinized relics. Carbonate-serpentine-chlorite-opaque ore aggregates are pseudomorphic after clinopyroxene. Biotite is less frequent. The ore consists of haematite-ilmenite exsolutions, some magnetite and pyrite. The sulfide mainly belongs to retrograde aggregates.
AC : Niggli values : high w
H1050 : high MgO and Fe^{3+}/Fe-total (0.36)
Further remarks : H2050 was not analysed because of scarcity. A clinopyroxene analysis is given in table V.2.

H 307 : Clinopyroxene biotite amphibolite with ferroan pargasitic hornblende.

FO : Amphibole-rich bands in strongly folded charnockitic migmatites.
MAD : Melanocratic, fine-grained, strongly lineated amphibole-rich rock; vaguely banded on mm-scale.
General resemblance with D 444.
Texture : Granoblastic, mainly equigranular, polygonal. Inside the amphibolite several thin clinopyroxene- and biotite-rich layers (= biotite hornblende gabbro) are present. The lineation is strong, and determined by amphibole and biotite. The biotite cuts straight through amphibole and pyroxene. Clinopyroxene may be enclosed in amphibole, without showing a reaction relationship. It is finer grained than amphibole, which is anhedral, medium-grained. Plagioclase formed prior to amphibole, in view of the crystalboundaries.
MID : The ligh bluish clinopyroxene contains some alteration products, presumably carbonate and muscovite. Biotite is reddish brown. The plagioclase, which contains bent twins and some sericite, is rather Ca-rich for this environment (An_{55}). Inclusions in plagioclase are rare. Rounded zircon, some apatite, magnetite with ilmenite lamellae mainly near clinopyroxene, and the alteration products, are minor phases.
AC : Amphibole : high K_2O and Fe^{3+}/Fe-total (0.31). It is rather Si-poor as compared with other samples from the Tonstad-Sirdalen area.

H 325 : Orthopyroxene amphibolite with titaniferous ferroan pargasitic hornblende.

FO : Large amphibolite bank in a massive part of the charnockitic migmatites.
MAD : Melanocratic, fine-grained, amphibole-rich rock, without clear lineation.
Texture : Granoblastic, equigranular, polygonal. Grainsize ca 1 mm.The amphibole is slightly lineated. Plagioclase, amphibole and orthopyroxene form a fresh, anhedral mineral aggregate. There is no reaction relationship visible between amphibole and orthopyroxene. Everything seems to be in perfect equilibrium, with only some deuteric alteration.

MID : Amphibole contains many ore exsolution zones, sometimes with needles perpendicular to each other in one zone.[1] The crystal contacts between mafic minerals are characterized by the frequent occurrence of ore drops (see section IV.3.4). Contacts with plagioclase are sometimes very irregular and fine symplectite-like, but mostly sharp. The plagioclase contains deformed twins, some sericite and enclosed apatite, and it displays fine Huttenlocher intergrowths. Orthopyroxene is pleochroic : pink to bluish, $2V_x = 60\text{-}70^o$, r>v (n_x). It shows the same ore exsolution zones as the amphibole. Several crystals have fine lamellae. The pyroxene rims are in some places altered to a serpentine-like material. Magnetite with ilmenite lamellae, pyrite, carbonate, epidote and apatite are accessories. The main minerals almost contain no inclusions of other minerals.

AC : Modal analysis : phyllosilicates other than sericite are absent.

Bulk analysis : high An-content (An_{70}).

Amphibole oxides : high Na_2O; low F; lowest K_2O.

Structural formula : high Ti.

Niggli values : lowest k.

H 415 : Biotite-bearing amphibolite with titaniferous edenitic hornblende.

FO : Banded migmatite zone around a massive charnockite core. The migmatite displays agmatitic structures in some places.

MAD : Mesocratic, fine-grained, amphibole-rich rock with slight lineation. It is rather weathered.

Texture : see D 442.

This sample is about the same as D 444; only differences are described.

MID : The amphibole colours are darker, and more brownish. Biotite is less important and partly transects amphibole. Some fine-grained clinopyroxene remnants are present, which are strongly altered to serpentine. Apatite is enclosed in great quantities in all minerals. The ore consists of magnetite with ilmenite lamellae, ilmenite and some pyrite. The sample has a dirty appearance under the mieroscope, due to weathering.

J 119 : Amphibole gabbronorite with titaniferous ferroan pargasitic hornblende.

FO : Amphibole carrying bands of varying sizes in mainly massif charnockitic migmatites, east of the Ørsdalsvatn (see Hermans et al. 1975, p.56).

MAD : Melanocratic, very fine-grained rock without lineation.

Texture : Granoblastic, equigranular, polygonal. Lineation is absent. The grainsize is smaller than 1 mm. The mafic minerals are not completely homogeneously distributed through the rock. Anhedral amphibole forms stubby crystals, which partly envelop pyroxene. The contacts are sharp. It always forms independant grains, and never appears as thin rims around pyroxene, as is found in the igneous complexes. Some orthopyroxeue crystals seem to be partly rounded, resorbed. Biotite transects amphibole and pyroxene.

MID : Amphibole contains some apatite inclusions. Clinopyroxene displays diallage cleavage, and a few crystals have exsolution lamellae of orthopyroxene. Orthopyroxene is less frequent; it is pleochroic : pink to bluish-green. Serpentinization occurs along cracks in the crystals. Very thin exsolution lamellae of clinopyroxene are found. Plagioclase with some bent twins is partly sericitisized. It contains only few inclusions. Biotite is reddish-brown. Opaque ore forms small, rounded, mainly interstitial grains; it consists of ilmenite, some magnetite, and composite grains of magnetite + ilmenite in polygonal contact (mosaic texture). Pyrite is a late omnipresent phase, chalcopyrite is rare. Apatite is included in all minerals, often euhedral. Chlorite + ore aggregates are found in a few small spots, rounded zircon is rare.

AC : Structural formula : high Ti and Fe^{3+}/Fe-total (resp. 0.27 and 0.33).

L 143 : Amphibole-bearing anorthosite with magnesio-hornblende and cummingtonite.

FO : Lineated anorthosite of Egersund-Ogna near the septum.

MAD : Leucocratic, medium-grained, beige coloured rock with a few thin strings of mafic minerals.

Texture : Plagioclase forms irregular, anhedral crystals of varying sizes with polygonal-interlobate contacts. The main mafic minerals are aligned in thin zones which lie 0.5 to several cm apart. The pyroxene beads of these strings are mostly separated by plagioclase, but sometimes they group together. The amphiboles form in that case an enveloping medium, which separates the pyroxenes. The beads always have rounded outlines.

MID : Plagioclase contains many fine schiller, antiperthite (blebs as well as myrmekite-like patterns), and deformed twins. Alteration products mainly appear near antiperthite : epidote, muscovite and clinozoisite. There are also extremely fine symplectites at plagioclase-plagioclase contacts, with rather high refractive indices (1.70-1.75), colourless and with varying birefringence; they possibly consist of the same alteration products as described above. The plagioclase may be zoned (outer albite rim) near alteration spots. Orthopyroxene is clearly pleochroic, it alters to

1 : Plate II, figure 1.

serpentine aloug cracks aud along the outer rim; some crystals are completely serpentinized. Thin red schiller may be present, homogeneously distributed through the crystal. Light bluish-green clinopyroxene is less frequent and smaller. Very fine exsolution lamellae are rare, $2V_z = 60^o$, $Z\wedge c = 41^o$, $\Delta = 0.026$. In one case clinopyroxene partly envelopes orthopyroxene. Little opaque ore grains (ilmenite-haematite exsolutions) are mainly enclosed in plagioclase.
Most remarkable in this anorthosite, however, are the amphiboles. L1143 is a soft-coloured greenish magnesio-hornblende, L2143 a colourless Fe-Mg-amphibole. Amphibole always forms rims around pyroxene or pyroxene remnants. Orthopyroxene may have three rims : an inner rim of serpentine, an outer rim of L1143, and in between a complete or partial zone of L2143.[1] The outer hornblende rim is always present. Clinopyroxene crystals only have a rim of hornblende, mostly complete, sometimes partial. In a few cases it even is absent. The contacts between L1143 and L2143 are sharp (see fig. 11.15).
--L1143 : The hornblende may be slightly zoned, universal stage measurements give a maximum of 4^o difference between the most inward optical angle (-78^o) and the most outward value (-82^o). There is also some variation in colour intensity. Wavy extinction is common, the rims appear as a patchwork of crystals with slightly different orientation, sometimes looking like twins. Very fine exsolution lamellae (ca 0.5 micron wide) can be seen in some crystals, possibly along the $(\bar{1}01)$ plane. Universal stage measurements indicate the (001) plane (see Robinson et al, 1971-b). They are colourless, and seem to contiuue into the cummingtonite in a few cases, but that is not sure because of the small size and optical resemblance of L2143 and the exsolved phase. The presumed continuation possibly is the (001)-cleavage of the cummingtonite. However, exsolution lamellae have their main appearance in L1143. The extinction is simultaneous with the host amphibole(s). The hornblende contains a few ore grains (ilmenite-haematite exsolution, lamellar), and some ilmenite needle zones.
--L2143 : The Z∧c could not be measured because of the weak cleavage, and the thin zones this mineral forms (average width : 20-30 micron, maximum 70 micron). It is in complete, or almost complete, optical continuity with L1143, but not with the orthopyroxene. Ilmenite needles and drops are omnipresent, starting at the contact with the serpentine, and growing into the cummingtonite. They are very fine, irregular and abundant.
Quartz accompanies the amphiboles as contiguous fragments in only a few cases.
AC : Modal analysis : highest plagioclase; no apatite.
Bulk composition : highest Al_2O_3; low MnO.
Niggli values : highest L and T; high al and c; low fm; lowest k.
Amphibole oxides : L1143 : high MnO, SiO_2, CaO; low Na_2O and TiO_2.
L2143 : highest MgO; high SiO_2; low Na_2O, K_2O, CaO and TiO_2.
23(O) formulae : L1143 : high Mg and mg; low Mn and Ti.
L2143 : highest Mg; low Al^{VI}, Ti, Ca, Na and K.
Optics : L2143 has a positive 2V of 70^o.
Further remarks : Because of the variation in chemistry between the various microprobe spots, the analyses are divided :
L1143 1 : 1 spot between an ore grain and clinopyroxene.
L1143 2 : 2 spots in two separate grains.
L1143 3 : 3 spots in three separate rims.
L1143 M : the average of all six spots.
L2143 : mean of two spots in various crystals which are in good agreement.

M 101 : Apatite amphibole quartzmonzonorite with edenitic hornblende.

FO : Amphibole-bearing dark layer in mainly banded charnockitic migmatite. Other dark layers consist mainly of (leuco-) norites. The sample is one of the few amphibole-bearing rocks in this region. Amphibolites are absent.
MAD : Fine-medium grained, mesocratic, weakly lineated rock.
Texture : Granoblastic, equigranular, polygonal-interlobate. The grainsize is less than 1 mm; plagioclase crystals are somewhat larger than the other minerals. The pyroxenes are concentrated in amphibole-poor layers with fine amphibole, the remaining part of the rock contains less pyroxene and coarser blastic amphibole. The alternating layers are a few mm wide. Biotite rransects amphibole and pyroxene. Some quartz accompanies part of the biotite and amphibole. Biotite-quartz symplectites are also present. Amphibole partly envelopes plagioclase.
MID : The amphibole has an unusual light brown colour. Pleochroic orthopyroxene is strongly altered to serpentine + muscovite + stilpnomelane + ore. Light bluish-green clinopyroxene is less frequent, and less altered. Biotite is orange-brown. Opaque ore, consisting of ilmenite-haematite exsolutions, is partly interstitial, and partly fine-grained near pyroxene remnants. Pyrite is a minor phase. Coarse apatite crystals may contain many lineated, long prismatic, colourless inclusions. The plagioclase displays bent twins, some antiperthite and myrmekite, and contains fine euhedral apatite. A little microperthite is present in alkalifeldspar; quartz occurs between the feldspars. Reddish iddingsite sometimes accompanies amphibole in a few disrinct layers.
AC : Modal aualysis : highest serpentine; high ore and apatite.
Bulk composition : highest P_2O_5; high Fe_2O_3.

1 : Plate VI, figure 4.

Amphibole oxides : highest F (together with N 337 and ß 118), high MnO.

24(O) formula : highest Fe^{3+}/Fe-total (0.44).

Further remarks : The amphibole is rather inhomogeneous.

N 041 : Hypersthene biotite amphibole vein with magnesio-hornblende.

FO : A loose sample near the beginning of one of the tunnels SE of Tonstad, in the NW-flank of the Raudtoknuten. It has not been found in situ. Some macroscopically similar rocks (F 404-F 407,not in this collection), consisting mainly of biotite and hypersthene, occur as discordant veins of 10-20 cm width and ± 50 cm long, with mafic rim and leucocratic core. The plagioclase in these rocks is labradorizing, the quartz smoky. However, no similar amphibole was present in these rocks, only a little bit hornblende. Therefore, it is not clear whether N 041 belongs to these veins, found in front of one of the tunnels, or if it comes from somewhere in a tunnel.

MAD : Medium-coarse grained, glittering greenish, mica-rich, melanocratic sample. Leucocratic minerals are not visible.

In thin section it is not possible to distinguish between N1041 and N2041. All amphibole crystals are soft greenish coloured, with variations due to orientation. During mineral separation two fractions were found : a lightgreen part with s.g. = 3.10-3.14 (N2041), and a dark-green coloured sample with s.g. = 3.14-3.22 (N1041). The quantities were different : N1041/N2041 = 1/2. Grains from these two fractions were used for microprobe analysis.

Texture : The sample can be divided in three zones; the main part consists of a biotite hornblendite, changing into orthopyroxene hornblendite and rimmed by biotite gneiss on one side.

The biotite hornblendite is more or less equigranular, interlobate, with subhedral amphibole and biotite. The amphibole is rather coarse-grained, and forms various long-prismatic crystals and intergranular anhedral grains. The biotite mainly occurs at amphibole crystal boundaries, but a few biotites transect amphibole. Some fine irregular quartz crystals are scarcely present.

At one side of the sample some pyroxene fragments appear in amphibole. Further to that side, orthopyroxene becomes more abundant, forming extensive skeletal crystals, interfingered with equally oriented amphibole fragments and some plagioclase. Pyroxene fragments in amphibole are irregular shaped, and groups of sections have the same optic orientation. Biotite is rare in this zone and the transition from biotite- to orthopyroxene hornblendite is gradual. The contact with the biotite gneiss is sharp. The gneiss consists of strongly lineated biotite, quartz (some symplectitic intergrowths with biotite) and some plagioclase. The lineation is parallel to the contact with the orthopyroxene hornblendite.

MID : Some amphibole crystals are zoned, with a maximum 2V difference of 12° (core $2V_x$ = 86°, rim $2V_z$ = 82°, no difference in $Z\wedge c$: universal stage measurement), and no colour change. The amphibole looks fresh and clean in the biotite hornblendite, and only contains some apatite, very fine rounded zircon surrounded by pleochroic haloes, and fine inclusions of, presumably, carbonate which are elongated parallel to the c-axis of the amphibole. With a large magnification (200 x) one can see very fine exsolution lamellae of ca 0.5 micron width in the amphibole in both hornblendite zones. The lamellae seem to be colourless. The angle between the pole of the exsolution plane and the c-axis of the host is ca 22°($Z\wedge c$= 20°). This small angle is also mentioned by Robinson et al (1971-b) between exsolution plane and $(\bar{1}01)$.[1]

The pleochroic orthopyroxene is partly altered to serpentine and fine opaque ore along the crystal boundaries. The colour of the biotite changes from light brownish-green in the biotite hornblendite, to brown in the biotite gneiss. In the orthopyroxene hornblendite, only some very fine brown biotite crystals are present. The An-content of the plagioclase could not be determined optically, some crystals contain many fine ore inclusions. Quartz in the hornblendite parts shows two-phase incluaions.

AC : The bulk composition is determined on a rock slice with the complete above described sequence : 1.5-2.0 cm biotite hornblendite,0.5-1.0 cm pyroxene hornblendite,and ca 0.2 cm biotite gneiss. The biotite-rich rim is not incorporated in the modal analysis.

Bulk analysis : high MgO and F.

Niggli values : high fm, k, mg and u; low L.

Amphibole oxides : high SiO_2 (N2041), MgO (both) and H_2O (N2041); low Fe_2O_3, total Fe and K_2O.

The density is low due to the high MgO content.

Universal stage measurements indicated a constant $2V_x$ = ±86° for unzoned crystals. Zoning from $2V_x$ = 86° to $2V_z$ = 82° and from $2V_x$ = 90° to $2V_x$ = 86° from core to rim. Measurements on loose grains gave a greater variation between the grains : N1041 : $2V_x$ = 76-88°, N2041 : $2V_x$ = 77-87°; so there is no great difference between the light (N2041) and dark (N1041) fractions, but both show a certain spread. Three exsolutionplane measurements resulted in a constant angle of 3° between the exsolution plane and $(\bar{1}01)_{host}$. $Z\wedge c$ varied from 18-23°.

Further remarks : The colourdifference between N1041 and N2041 appears to be caused by the amount of exsolution lamellae.

1 : Plate VII, figure 3.

The light coloured grain fraction contains up to 25% lamellae, the darker fraction less and also unexsolved crystals. There is no constant percentage lamellae and therefore no constant chemical composition. The microprobe spot is greater than 0.5 micron (1-2 micron), which results in the possibility that host as well as lamellae have been measured together, especially for N2041. This could not be seen because the grains were embedded in an amorphous pellet. It is clear from table IV.7 that the composition of the various crystals differs a lot.
N1041 1/2 and N2041 2/3 : 2 spots on one grain, good agreement between the spots. N1041 3 and N2041 1 : 1 spot on a grain, close resemblance between these grains. Intracrystalline spots are in good agreement, intercrystalline measurements may differ rather much.

The additional analyses for FeO, H_2O and F have been performed on the two grain fractions, resulting in mean values for both groups. To be able to relate these values to the various analysed grains, graphs were drawn on basis of the Si-content in the 23(0) formula. First the microprobe measured "Total Fe as FeO" was plotted, resulting in a more or less straight line with deviations for N1041 1 and 3 (fig. A.4-A). N1041 1 and N2041 2 are taken as arbitrary means for both fractions in view of their central position in the graph. The distribution of the various compositions in the grain fractions is not known, the analysed grains are considered representative of the whole chemical range. If the measured FeO-values are plotted for N1041 1 and N2041 2, one can draw a connecting line. From this line the values for the other points can be read (or calculated if the line function is determined via linear regression). The difference between both FeO lines stands for Fe_2O_3 ($Fe_2O_3 = 1.111 \times (FeO_{probe} - FeO_{wet})$), from which we can calculate the oxidation ratio. This ratio increases with increasing Si-content, i.e. with increasing actinolite component. The same procedure was followed for H_2O and F (fig. A.4-B). The percantages found in this way are given in table A.2 and they are used

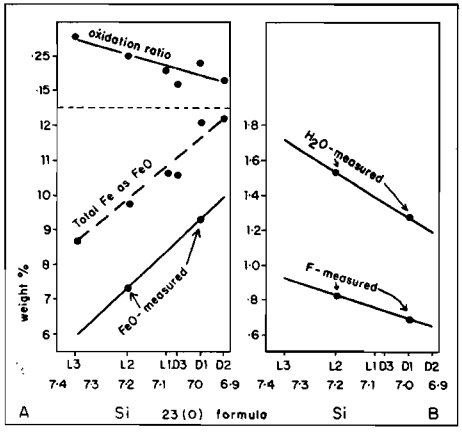

Figure A.4. : Calculation of the FeO-, H_2O- and F-content of various microprobe analysed grains of N 041. N1041=D, N2041=L. All values are given in table A.2.

To determine the chemical composition of the exsolved phase, fig. A.5 was drawn. Ions in the 23(0) structural formulae (table IV.8) are plotted versus Si. It was concluded above that the lighter fraction contained more lamellae. This results in a higher Si-value, so the lamellar composition lies on the Si-rich side of the graph. However, we do not know the percentage of lamellae included in the various analyses. Therefore, we have to make two assumptions :
1 : the lowest Si-containing analysis (N1041 2) is lamellae free,
2 : the lamellae are more or less pure endmember.
In that case, the lamellae-free matrix has a Si-content of 6.92. The lamellae consist of tremolite, of approximately the following composition : $Na_{.17}Ca_{1.73}Mg_{4.77}Mn_{.02}Fe^{2+}_{.35}Al^{VI}_{.27}Si_{8.00}O_{22}(OH,F)_{2.9}$. Al^{VI} is possibly too high, the mg-ratio is 0.93. Oxidation ratio will be high; according to fig. A.4-A it may be 0.48. The sum of fluids as determined from fig. A.4-B should be 2.5 wt% H_2O + 1.35 wt% F, resulting in $(OH,F)_{2.8-2.9}$ which is high but not impossible (Leake, 1968).

	D1 N1041-1	D2 N1041-2	D3 N1041-3	L1 N2041-1	L2 N2041-2	L3 N2041-3
FeO-probe	12.12	12.21	10.56	10.69	9.79	8.70
FeO-wet	9.28	10.02	8.67	8.40	7.31	6.00
Fe_2O_3	3.16	2.43	2.10	2.54	2.76	3.00
ox.ratio	.23	.10	.17	.21	.25	.31
H_2O	1.29	1.19	1.37	1.40	1.55	1.72
F	.70	.65	.74	.76	.84	.93
Fluid sum	1.99	1.84	2.11	2.16	2.39	2.65

Table A.2. : Measured and calculated Wt% of FeO, Fe_2O_3, $Fe^{3+}/(Fe^{3+} + Fe^{2+})$, H_2O and F, for the various microprobe anslysed grains. The values are derived from grain fraction analyses and linear regression, combined in fig. A.4.

The average light-coloured amphibole N2041 2 contains 25% lamellae according to the above mentioned assumptions and results :

$(1-x)Si_{hbl} + xSi_{lam} = Si_{N2041\ 2}$

$(1-x)6.92 + 8.00x = 7.195$

$x = 0.25$

100x = percentage lamellae

hbl : hornblende, lam : lamella

This is in perfect agreement with the microscopic observation about the lamellar percentage of the N2041-fraction, if the conclusion is accepted that N2041 2 contains the maximum amount of lamellae, and that the microprobe measurement was carried out on a section perpendicular to the exsolution plane. If the analysis is performed on an inclined cut, all lamellae are wider than 0.5 micron in the plane of the section. This allows the lamellar percentage of the small microprobe spot to increase, as may have been the case with N2041 3.

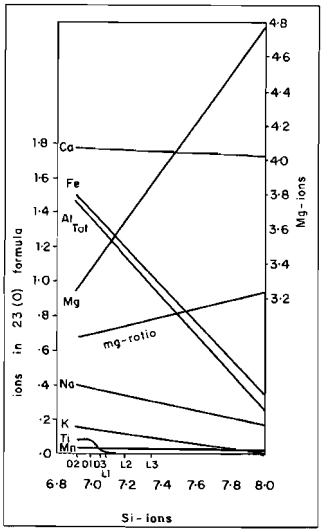

Figure A.5. : Extrapolation of the N1041-N2041 analyses to determine the composition of the exsolved phase. All elements, except Mg, are referred to on the left ordinate. N1041=D, N2041=L. Values derived from table IV.8.

If assumption 1 is wrong, the matrix hornblende will have a lower Si-content which makes it necessary to introduce a higher percentage lamellae. Other amphiboles in this region have Si-contents of 6.5 to 6.7, but as mentioned before, the location of this sample is not known. If assumption 2 is wrong, the lamellae may consist of tremolite with a certain percentage hornblende in solid solution. It that case the percentage lamellae can be suppressed, and the hornblende matrix composition may lie at a lower Si-content.

Conclusion : It is possible to construct various models, with a small variation in matrix and lamellar composition. The most important fact is that the lamellae are more or less tremolitic/actinolitic in composition and that the matrix is a magnesio-hornblende. The amount of lamellae (present as well as analysed) creates a spread in the analyses.

This implies that the original composition of the amphiboles was variable, and that the decrease of the metamorphic grade caused the amphibole to exsolve, supporting the existence of a miscibility gap between tremolite and hornblende (Misch and Rice, 1975; see also section II.7.2). It is possible that the same effect blurred the L1143 analyses, however, exsolution lamellae do not seem to be very important there.

Conclusions about the origin of this rock are omitted because of the lack of knowledge on the field occurrence, the small size of the sample and the variation in mineralogy. It is not known if this variation is complete, or part of a larger series.

N 264 : Biotite amphibole quartzsyenite with edenitic hornblende and actinolite.

FO : Gneissic intercalation in massive granitic migmatites.

MAD : Medium-grained, mesocratic, lineated rock.

Texture : Granoblastic, seriate, interlobate. The mafic constituents are concentrated in irregular zones which create the gneissic appearance. Only some biotite is lineated and grows partly through amphibole. Alkalifeldspar is the main leucocratic mineral and forms the largest crystals of the rock. Amphibole is anhedral, fine-medium grained. Quartz is partly connected with amphibole and biotite.

MID : Light coloured actinolite (N2264) is present at some crystal margins of the hornblende (N1264), and as small spots inside the main amphibole. Contacts between the two amphiboles are sharp and may contain very fine ore spicks. The actinolite is also found in aggregates of alteration products of amphibole and biotite : epidote, titanite, carbonate and chlorite. Dark brown biotite is partly accompanied by titanite. Alkalifeldspar contains some very fine microperthite and some saussurite. Wavy extinction and an indistinct microcline texture may be found. Possibly partly orthoclase and partly microcline. Plagioclase is zoned against alkalifeldspar (An_{24}-An_7). The albite rim is thin. Deformed twins, sericitization, and fine myrmekite are present. Quartz shows undulatory extinction. Rather coarse, rounded apatite is omnipresent; zircon is less frequent, also rather coarse and rounded, and sometimes appearing in clusters. Ilmenite-haematite exsolutions, some magnetite and pyrite are partly interstitial, partly related to alteration aggregates.

AC : Bulk composition : high K_2O and P_2O_5.

Amphibole oxides : highest SiO_2 (N2264); high MgO (N2264).

24(O) formula : high Fe^{3+}/Fe-total (N1264).

Further remarks : N1264 is very homogeneous. N2264 M is the average of 4 microprobe spots on two grains, one grain near alteration products, and one in the centre of an N1264 crystal. Both grains are in good agreement. N2264 I is a deviating spot on a light coloured rim.

The relatively high alkalifeldspar content is not common in this region, see also F 052.

N 317 : Two-pyroxene amphibolite with titaniferous ferroan pargasite and uralite.

FO : Gneisses with darker amphibolites, sometimes thin layered, in the banded migmatites between the Outlier (=anorthosite) and the lopolith, within 100 m from the lopolith.

MAD : Melanocratic, fine-medium grained, strongly lineated rock. Greyish lenses between the dominating dark parts seem to be squeezed out. They are several mm long and ca 1 mm high. There is a strong macroscopic resemblance with B 254, an olivine amphibolite, from the same formation.

Texture : The sample consists of an irregular alternation of fine-grained amphibole-(leuco)gabbronorite (the lenses) and medium-grained hornblendite. The thicknesses vary (mm-scale), the transitions are vague. Therefore, everything is

taken together as a two-pyroxene amphibolite. The anhedral amphibole is in a few cases, in the transition zones, poikiloblastic, containing fragments of ortho- and clinopyroxene.[1] These pyroxene fragments may be in optical continuity. Plagioclase is sometimes present in the transition zones. In the gabbro-norite part the contacts between amphibole and pyroxene are mainly sharp, amphibole never rims pyroxene, no reaction relationship can be seen. The minerals seem to be in perfect equilibrium (polygonal contacts). In the hornblendite parts the orthopyroxene fragments are mostly serpentinized along the rim, along cleavage planes and cracks, sometimes accompanied by sulfide formation (pyrite) on these surfaces. The sulfide may replace large parts of the orthopyroxene. On the contacts between the brown amphibole and the serpentinized orthopyroxene a light bluish, sometimes fibrous, zone may be present, which is in optical continuity with the host amphibole. These zones are very thin : 5-10 micron, mainly ca 5 micron and thought to consist of uralite. The clinopyroxene fragments have no alteration rims; one large example is formed by many fragments of which a few lie outside the amphibole blast, between other amphibole crystals. It is accompanied by irregular sulfide-serpentine and sulfide-orthopyroxene spots inside and around the amphibole blasts. Biotite transects amphibole and is also present as very fine crystals on some amphibole-plagioclase contacts. A mylonite vein of 150 micron width cuts through the rock. The main minerals are tectonized near the vein.[2] Plagioclase has a broken appearance in several spots of the sample.

MID : The uralite zones display bright interference colours and is in great contrast to the extreme-brown main amphibole. Light greenish-blue clinopyroxene, $2V_z$=ca 60°, is much more frequent than the strong pleochroic orthopyroxene with $2V_x$ = 70-80°. Some completely altered crystals are present in the gabbro-norite part, consisting of serpentine + chlorite + opaque ore (mainly chalcopyrite) + ill-defined quartz. In most cases all these minerals are present, with sulfide and quartz in the centre. These alteration products occupy each time only one former crystal in the furthermore perfectly normal, polygonal gabbronorite. It is dubious what the original mineral was and, if it was pyroxene, why the surrounding pyroxene crystals were not influenced. Reddish-brown biotite is late and rare.

The thin vein contains chlorite, carbonate, serpentine, green biotite, brown amphibole fragments and uralite prisms. The last grow in various directions through the vein material. Uralite also replaces the main amphibole along crystal margins and it fills cracks which resulted from the mylonitization. It is always in optical continuity with the host amphibole, and resembles the actinolite rims in the fonstad area (e.g. N 264). Around the vein, this uralite may replace up to 50 micron of brown amphibole.

The plagioclase is strongly saussuritisized throughout the rock, in the form of flowers in the centres of crystals or crystal fragments. Plagioclase may also contain sulfide along cracks and margins, near some hornblendite concentrations. Apatite is rather coarse and rounded, interstitial and partly enclosed by plagioclase and amphibole. Zircon is very small and rounded. The interstitial opaque ore mainly consists of ilmenite and some magnetite with ilmenite lamellae.

AC : The amphibole is very rich in TiO_2, and extremely brown. Microprobe analyses only show a slight variation in Fe/Mg ratio. The light coloured amphibole was not analysed and tabulated because of its recent discovery.

N 337 : Amphibole gabbronorite with edenitic hornblende.

FO : Banded charnockitic migmatites against the eastern border of the Outlier (= anorthosite). The banding is very distinct with varying thicknesses. It points at strong shearing, stronger than further away from the contact.

MAD : Fine-grained, melanocratic, lineated rock.

Texture : This sample is more or less comparable to J 119, another amphibole gabbronorite. However, N 337 is finer grained, contains less amphibole, more opaque ore, and is clearly lineated. This description is related to J 119. Granoblastic, equigranular, polygonal-interlobate. The grainsize is less than 1 mm. Amphibole is concentrated in thin layers, where it is lineated, coarser and more blastic than in the pyroxene-rich layers. Orthopyroxene is remarkably long prismatic, with c:a= up to 10:1. Resorption of orthopyroxene is not very obvious, even though orthopyroxene enveloped by plagioclase or amphibole seems to be more rounded than orthopyroxene enveloped by clinopyroxene.

MID : Around ore grains the hornblende may be more bluish coloured (as in B 322 and F 107). Light bluish-green clinopyroxene displays, besides diallage-cleavage and orthopyroxene lamellae, also ore needles in the lamellae. Orthopyroxene is partly serpentinized, which may be accompanied by sulfide forming as in N 317, but less abundant. The pleochroism is strong, several orthopyroxene crystals contain kinkbands. Orthopyroxene is less frequent than clinopyroxene. Plagioclase has a lower An-content than in J 119 (An_{29}), and contains euhedral, fine-grained, apatite, some antiperthite and sericite, and bent crystals. Little alkalifeldspar with microperthite is also present, mainly finer grained than plagioclase. Orange-brown biotite and green chlorite form mainly around interstitial ore (magnerite with ilmenite lamellae, some ilmenite and pyrite). Fine, rounded zircon is present in plagioclase and pyroxene.

AC : The amphibole is highest in F (together with B 118 and M 101).

Further remarks : Microprobe analyses revealed a rather inhomogeneous composition of the amphibole.

1 : Plate I, figure 3.

2 : Plate I, figure 4.

N 402 : Amphibole granite with titaniferous ferro-edenitic hornblende and ferro-hornblende.

Compare with E 067 and E 167.

FO : Pegmatite-like veins in the quartzmonzonitic phase of the lopolith, near E 067.

MAD : Leucocratic, coarse-grained, yellowish-grey rock, with large (up to 4 cm), equally oriented, amphibole fragments. Texture : Granoblastic, seriate, interlobate. The minerals are very coarse-grained. The crystal contacts between the leucocratic minerals are less intricate than in E 067/E 167. The amphibole forms extreme poikiloblasts (Rietmeijer and Dekker, 1978, gronp 2 amphiboles). See further E 067. Only plagioclase and zircon show euhedral forms, all other minerals are anhedral. The leucocratic minerals determine the crystal outline of the amphibole.

MID : The main amphibole (N1402) is very fresh and simple : no twins, zoning, exsolution lamellae or ore needles. It only encloses some ilmenite grains, large apatites (up to 0.5 cm Ø) with dark pleochroic haloes, and biotite along cleavage planes and crystal boundaries. This biotite forms some symplectitic intergrowths with quartz. Around ore grains and biotite, the main amphibole may be slightly more greenish (n_y) to bluish (n_z) (=N2402). The remaining part of the rock is almost completely leucocratic. See E 067 for quartz, alkalifeldspar and plagioclase (An_{14}-An_{0-3} in saussurite-rich parts) descriptions. The extinction of the quartz is less undulatory than in E 067. Between the leucocratic minerals some apatite, reddishbrown biotite (which is poikiloblastic), and subhedral zircon are present. Late cracks contain stilpnomelane and serpentine.

AC : Bulk composition : high SiO_2; low H_2O^+.

Amphibole oxides : high Fe_2O_3 and FeO (N1402), high Fe-total (both).

Amphibole fluid content : high Cl (N1402, table IV.6).

The s.g. is greater than 3.30 due to the high Fe-content.

Further remarks : Because of the one-sided orientation of the amphibole in thin section, not all parameters could be measured (table IV.14).

N1402 1 : 2 spots between the more bluish rim and the core of the main amphibole.

N1402 2 : 2 spots on the centre of the main amphibole. N2402 : 4 spots. See section II.5.3 for further information on the colour-change.

N 528 : Olivine-bearing mangerite with a pyroxenite band and four different amphiboles.

FO : Lower part of the (quartz-)monzonitic phase of the lopolith, see section II.5.3-2.

MAD : N 528 (and F 419/F 420) : Mesocratic, medium-grained rock, consisting mainly of greenish-grey feldspar with labradorinzing effects. Fine-grained, partly mafic, mineral aggregates surround the feldspars. A melanocratic fine-grained band of varying thickness (ca 0.5 cm)transects N 528.

F 421 : fine-grained, black rock with greenish-grey crystal fragments on the cleavage plane of the handspecimen.

N 528 and F 419 are mangerites unrelated to the "dike", F 420 was taken within 1 meter from the contact, and F 421 represents the "dike". [1]

Texture : Mesoperthite, microperthitic alkalifeldspar and some clinopyroxene form the largest crystals in a mortar structure. Mesoperthite is the main constituent. In the fine-grained cataclastic mineral aggregates all N 528-minerals are present. Plagioclase and quartz are rare in these zones, and rounded olivine is often enclosed by clinopyroxene crystals, but not in a corona-like texture. Orthopyroxene appears inside and around clinopyroxene crystals. It may grow far out of the clinopyroxene crystal boundary into the leucocratic minerals. Opaque ore is interstitial, and often accompanied by coarse-grained, rounded apatite. Another part of the apatite is pencilshaped, and appears in the fine-grained zones. The recrystallized mafic minerals may develop an extreme poikiloblastic texture, as described by Rietmeijer and Dekker (1978). This is mainly shown by orthopyroxene.

The pyroxenite forms an irregular interlayer in the mangerite. Granoblastic, seriate, polygonal-interlobate. The contacts between both rocktypes do not show any indication for a later intrusion of the pyroxenite. The grainsize is up to 1 mm for the pyroxenite, and up to several mm for the mangerite. Added to the original mineralogy are carbonate, serpentine, iddingsite, sericite, biotite and amphibole. The carbonate consists of relatively large crystals (ca 1 mm) compared to the carbonate formed around Tonstad. It is frequently rimmed by serpentine. Serpentine replaces olivine and orthopyroxene and forms several green crystals with an hourglass structrore. Amphiboles see MID.

Several exsolved pyroxene crystals show a remarkable feature : the clinopyroxene component is replaced by carbonate + ore + orthopyroxene. The orthopyroxene lamellae have broadened in the carbonate, creating a set of equally oriented, long prismatic orthopyroxene fragments in a carbonate + ore aggregate.

MID : The large mesoperthite crystals may contain albite zones with sericite. The microperthite intensity of the alkalifeldspar crystals varies. Clinopyroxene shows diallage cleavage, exsolution lamellae of orthopyroxene, ore needles in various sizes and directions, and a bluish-green pleochroism. Orthopyroxene is only weakly pleochroic. The ore consists of ilmenite with some magnetite and pyrrhotite. A few crystals of brown as well as green biotite are associated with the alteration products.

1 : Plate V, figure 3 and 4; Plate VI, figure 1.

The amphibole can be divided in four groups :

1 : N1528, only in the pyroxenite. It seems to have formed from the clinopyroxene along cracks and crystal boundaries, and is very irregularly divided. The amphibole is a brownishgreen titaniferous hastingsitic hornblende.

2 : N2528, a possible arfvedsonite-riebeckite (Na-amphibole), which appears in both parts of the sample. It occurs mainly fibrous along amphibole- and pyroxene rims, or as fine bushels in pyroxene and alteration products. The mineral is so fine that good optical measurements are difficult, and microprobe measurements impossible.

3 : N3528, a more greenish variety of N1528, which is only found in the mangerite parts, as rims around pyroxene, olivine and ore. It grows from the contact between a mafic mineral and a feldspar with a comb-like texture into the alkalifeldspar component of adjacent mesoperthites. The same comb-like texture can be seen for both pyroxenes, olivine and ore. The amphibole is a magnesian hastingsitic hornblende.

4 : N4528, a thin, almost colourless zone between N2528 and N3528 (or N1528), see fig. A.6. More or less equal zones zones are found in Y 128. Zone b in fig. A.6 is only 2 micron wide, this makes the colour determination rather unreliable, because the colours of the accompanying green and blue amphiboles may influence the N4528 colours.

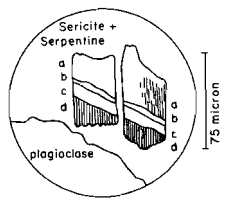

Figure A.6. : Three amphiboles at the contact between the mangerite and the pyroxenite zone of N 528. The sericite + serpentine forms the contact between a plagioclase and a large carbonate crystal.
a : partly massive, partly fibrous N2528; b : N4528;
c : N3528 (or N1528, this could not be established);
d : fibrous N2528.

AC : The modal analysis is performed on the mangerite part of N 528, the bulk composition includes both parts.
Modal analysis : highest carbonate and (together with R 356) mesoperthite.
Niggli values : low w.
Amphibole oxides : N1528 is high in TiO_2.

Further remarks : The carbonate is irregularly distributed through the rock. This follows from the fact that another thin section of the same handspecimen contains almost no carbonate (nor amphibole N2528). The bulk analysis revealed a CO_2 wt% less than 0.10 (table III.3).

N1528 : 5 microprobe spots indicating inhomogeneity; N3528 : 3 spots on an amphibole rim around ilmenite, against clinopyroxene and mesoperthite.

N 572 : Olivine amphibole mela-norite and amphibole olivine hypersthenite with pargasite.

(compare with B 254)

FO : Around the top of the Stokkafjellet, in the banded migmatites between the lopolith and the Outlier, several intercalations of mafic and ultramafic rock are present. These may vary from amphibolites and hornblendites, to pyroxenites with various amounts of olivine. This formation is the subject of a special study at this moment and will therefore not be treated here in any detail.

MAD : Melanocratic rock, partly fine-grained and partly medium- to coarse grained with plagioclase rims around brownish olivine. The rock is very heavy (high density).

The sample is divided in an ultramafic part : N 572 D and a more plagioclase-rich part : N 572 L.

--N 572 D : Texture : large irregular olivine fragments, with equal orientation for several neighbouring parts, are enveloped by a polygonal fabric of fine-grained orthopyroxene, with some intergranular amphibole and plagioclase. Olivine crystal boundaries are partly resorbed and mainly determined by the enveloping pyroxene. The olivine fragments (up to 1 cm) are serpentinized along an intricate, fine, vein system which also transects the pyroxene and connects the various olivine parts.[1]

MID : The Mg-rich olivine (Fa_{6-15}) shows undulatory extinction. Orthopyroxene is strongly pleochroic, and contains some kinks and ore schiller. The amphibole colours are soft brown, some kinks are found with ore needles growing from the kinkplane. Plagioclase is very high in An-content (An_{88-92}), and contains a little zoisite. It may be accompanied by small reddish-brown biotite flakes, which are also present in several olivine fragments. A few small ilmenite grains are interstitial.

AC : Modal analysis : high orthopyroxene; high olivine and An%; no apatite.
Bulk composition : high MgO; lowest Al_2O_3 and Na_2O.
SiO_2+MgO+FeO forms over 90% of the rock composition.

1 : Plate II, figure 3.

Niggli values : highest fm and mg; high M, -, u; low c; lowest al, alk and t.
The amphibole is analysed in N 572 L.

--N 572 L : Texture : the large olivine fragments are in this part of the sample mainly enveloped by plagioclase, and the remaining space is filled with a plagioclase-amphibole-orthopyroxene mixture. Some olivine remnants have partial coronas of orthopyroxene.[1] The plagioclase+amphibole forms an interlobate fabric with irregularly distributed subhedral orthopyroxene. Locally amphibole may concentrate around a larger ilmenite crystal, which may be accompanied by green spinel.
MID : see N 572 D.
AC : Modal analysis : high olivine and An%; no phyllosilicates or apatite.
Bulk composition : high MgO.
Niggli values : high fm, mg and u; low alk.
Amphibole oxides : highest MgO (not counting the actinolitic secondary amphiboles) and Na_2O (excluding Na-amphibole A 168); high Al_2O_3 and H_2O; low Fe_2O_3, total Fe and K_2O; lowest F.
23(O) formula : high Al^{VI} and mg-ratio.
--The transition between N 572 L and D is rather quick, and characterized by a fine-grained zone with quickly decreasing orthopyroxene content and increasing plagioclase and amphibole.
Further remarks : From the AC it is clear that N 572 is a rather exceptional sample in this collection. Optically there seemed to be some zoning in the amphibole, therefore microprobe measurements were performed on cores and rims : N1572 K and R resp. Mineral separation resulted in 2 fractions with densities between 3.14 and 3.18, and between 3.18 and 3.22. Both fractions were analysed for FeO, H_2O and F. The highest density was assigned to the microprobe analysis with the lowest mg-ratio : N1572 R, because decreasing mg-ratio increases the density (fig. IV.1). However, this division is in this case rather dubious, because of the very small difference between core and rim analyses. FeO and F are about the same for both mineral separates, but H_2O has a higher value for the high density fraction. The conclusion is that there is no real zoning, only some inhomogeneity. The H_2O contents are divided arbitrary.
The 23(O) formula for additional sample BA 92 results in a pargasitic hornblende (table V.1), but including the unknown oxidation ratio it will certainly be a pargasite. The most resembling composition in Rogaland is N1572 R, however, there are some remarkable differences : BA 92 contains almost no TiO_2, less Na_2O and much more K_2O than N1572 R, and the mg-ratio and $Si/(Si+Al^{IV})$-ratio are slightly higher. These differences must have caused the lightgreen colour for BA 92 which is in strong contrast to the brown colour of N1572 R.

N 809 : Plagioclase-bearing 2-pyroxene hornblendite with titaniferous ferroan pargasitic hornblende.

FO : The contact between the augen gneisses and the charnockitic migmatites is wildly folded and contains numerous hornblendite intercalations.
MAD : Melanocratic, medium-grained, amphibole-rich rock.
Texture : The sample consists of fine-grained amphibole norite/pyroxenite (granoblastic, equigranular, polygonal-interlobare) with irregular distributed, medium-coarse grained, amphibole blasts which are sometimes grouped together. They form the lineation.
MID : The amphibole resembles D 307-amphibole optically as well as mineralogically and chemically. Some crystals contain ore needles in zones and randomly distributed. Another type of needles is rutile-like : very long, thin colourless, high birefringence, sagenite texture. Orthopyroxene is strongly pleochroic, showing kinkbands; it is serpentinized along rims and cracks. Colourless clinopyroxene is much more frequent. Plagioclase contains deformed twins. Reddish-brown biotite forms locally short, amphibole-transecting, crystals. Apatite, fine-grained ilmenite and pyrite are rare.
AC : Niggli values : high y; low L and t.
Amphibole oxides : high MgO; low H_2O.
23(O) formula : high Ti.

N 827 : see E 232.

O 100 : Amphibole norite with titaniferous edenitic hornblende.

FO : Mainly noritic rocks with a vague banding and a few charnockitic intercalations. The environment is strongly tectonized. It belongs to the Folded Basic Intrusions.
MAD : Mesocratic, fine-medium grained, lineated rock.
Texture : Granoblastic, equigranular, polygonal-interlobate. There are a few larger orthopyroxene crystals, more or less rounded. Amphibole formed partly around and partly inside pyroxene, as poikiloblastic crystals. Clinopyroxene

1 : Plate II, figure 4.

is less frequent than orthopyroxene. biotite transects all other minerals, it may be rimmed by a very thin serpentine-like zone. Amphibole and biotite determine the lineation. Many plagioclase crystals are broken.
MID : The amphibole is slightly zoned (section ⊥c-axis) : $2V_x$= 80°_{core}- 84°_{rim}, $Z\wedge c$= 17°_{core}- 15°_{rim}. Chemical differences were not found. Orthopyroxene is weakly pleochroic, slightly zoned and contains kinkbands and very thin (100)- exsolution lamellae of clinopyroxene. Alteration to serpentine in thin zones. The creme-coloured clinopyroxene also shows fine exsolution lamellae. Biotite is reddish-brown. The An-content of the plagioclase is bigh (An_{65-70}). Various fragments of the broken crystals are saussuritisized. Twins are deformed, Huttenlocher intergrowths are common. Apatite, rounded zircon and muscovite are rare.
AC : Modal analysis : no ore.
Niggli values : high μ; lowest w.
Amphibole oxides : high CaO; low Fe_2O_3 and MnO.
24(O) formula : high Ti; low Fe^{3+}/Fe-total.
Further remarks : Microprobe results did not indicate inhomogeneity or chemical zoning. The Al_2O_3-content of the amphibole is relatively low in view of the rock characteristics, e.g. An% (see section VI.3).

P 097 : Amphibole-m-granite with ferro-edenitic hornblende.

FO : A granitic part of the mainly massive pyroxene-syenite body of Bornavatnet.
MAD : Leucocratic, fine-grained rock with well-foliated dark minerals.
Texture : Granoblastic, ca equigranuler, interlobate-amoeboid. Amphibole-quartz symplectites appear in thin zones in the perthitic feldspar fabric. The grainsize is mainly less than 1 mm, except for part of the feldspar.
MID : The amphibole is divided in a brownish- (P1097) and bluish (P2097) part. The n_z-colours are exceptionally greyish. The amphibole-quartz symplectites may consist of various equally oriented amphibole fragments, more or less comparable with the extreme poikiloblasts described in E 067/E 167/N 402. However, the grainsize in this case is much finer and the texture more vermicular. The only enclosed mineral is quartz. P2097 is a minor phase and several optical parametera could not be determined. This bluish amphibole may be part of the brownish crystals (sometimes near enclosed ilmenite grains or along the rim) or form individual symplectites, which are not obviously connected with ore grains. The feldspar is partly mesoperthite, partly microperthite, and has very irregular rims. Plagioclase occurs rarely, as sericitisized crystals. Quartz shows a faint undulatory extinction and contains many fluid inclusions; it forms irregular crystals between the feldspar or is associated with the amphibole. Yellowish-green biotite, stilpnomelane (around amphibole), chlorite, muscovite and serpentine are found near the amphibole zones. Rounded zircon, partly euhedral apatite and interatitial ilmenite grains are rarely present.
AC : High mesoperthite content and niggli alk.
Further remarks : The microprobe analyses show some variation between the various spots for each colour, which is not remarkable in the view of the gradual change between P1097 and P2097. There is, however, a clear difference for several elements between both amphiboles, see table II.7.

P 248 : Amphibole-bearing granite with edenitic hornblende.

FO : Granitic xenolith in the leuconoritic phase of the lopolith near the contact with the charnockitic migmatites. The contact shows tectonization and retrograde metamorphism.
MAD : Leucocratic, very fine-grained rock with well-foliated dark minerals.
Texture : Granoblastic, aquigranuler, interlobate. The grainsize is less than 1 mm. Aggregates of alteration products (biotite-chlorite-epidote-titanite-allanite-ore-quartz and serpentine + ore) are omnipresent. Amphibole is a more or less interstitial phase.
MID : The anhedral, fine-grained amphibole contains some zircon, and alters to chlorite. The crystals are randomly distributed. The green colours are remarkable in these surroundings. Most reddish-brown biotite forms symplectitic intergrowths with quartz, this quartz may contain vermicular ilmenite. Chlorite, epidote, titanite and allanite may accompany the biotite-quartz-ilmenite aggregates. Serpentine + ilmenite forms independant alteration aggregates. Alkalifeldspar is the main leucocratic mineral; microcline grid and microperthite are present. Several plagioclase crystals are strongly sericitisized; a faint zoning may be seen. Some myrmekite is found. Quartz contains numerous inclusions of, among others, apatite, zircon and amphibole; the extinction is slightly wavy. The opaque ore consists mainly of small ilmenite grains, enclosed in other minerals, with very fine haematite- and spinel exsolutions; magnetite, with in some cases ilmenite lamellae, is a minor phase.
AC : The modal analysis is highest in alkalifeldspar.

P 303 : Biotite amphibolite with edenitic hornblende.

FO : Amphibolite band in the mainly massive charnockitic migmatites, just north of the contact with the lopolith. The

migmatites are folded and intruded by pegmatites.
MAD : Meso-melanocratic, medium-grained, foliated, amphibole- and biotite-rich rock.
Texture : Granoblastic, inequigranular, interlobate. Amphibole occurs as roughly lineated poikiloblasts up to 2 mm long; the other minerals, together with the amphibole, form the fine-grained matrix.
MID : The poikiloblastic amphibole is completely anhedral and may envelop all other minerals. The extinction is irregular, in patches, indicating subgrains. Reddish-brown biotite transects the amphibole. Plagioclase displays strong sericitization in flower-like patterns; zoning is clear with rim-An_{30} and core-An_{40}. Soft-green clinopyroxene may contain diallage cleavage; $2V_z$ = ca 60°.
Beside these main constituents, some chlorite (near biotite), carbonate, muscovite (in plagioclase) and serpentine are present, representing retrograde metamorphism. Ilmenite, rounded zircon and partly coarse/partly fine apatite are accessories.
AC : The amphibole contains little H_2O and rather high F.
Further remarks : P 303 1 : 2 spots in one poikiloblast; P 303 2 : 3 spots in 2 crystals.
The differences are small, only Al_2O_3, MgO and FeO vary more than one standard deviation (fig. IV.5).

P 580 : Biotite amphibole norite with a diorite layer and ferroan pargasitic hornblende.

FO : No information.
MAD : Mainly mesocratic, fine-grained, foliated and slightly banded rock with a leucocratic, medium-grained band or vein.
Texture : The norite is granoblastic, equigranular, polygonal, with a thin layering due to the presence of either amphibole or biotite. The biotite is lineated, the whole rock is folded. The diorite part is granoblastic, seriate, polygonal-interlobate, with large clinopyroxene crystals, varying plagioclase grainsizes and fine-grained minor phases. The transition is abrupt but not completely discontinuous.
MID : --the norite--
The amphibole shows undulatory extinction, indicating subgrains. The green colours are, as for P 248 and additional sample BA 92, remarkable in these surroundings. The crystals look very fresh. Orthopyroxene is slightly zoned, alters to to serpentine along cracks and rims and contains some very fine exsolution lamellae. Plagioclase displays deformed twins, and is partly sericitisized. Light brownish-green biotite transects other minerals. Chlorite, muscovite, serpentine and clinopyroxene are minor phases. Ore is only present on crystal boundaries of amphibole, pyroxene and biotite, partly opaque, partly with a red internal reflex. No free ore grains are found.
--the diorite--
The plagioclase is broken up in sharply bounded subgrains. Some of these subgrains are intensely sericitisized, as in N 317. This seritization is more extensive than in the noritic part of the sample. The An-contents for both rock parts are equal. Soft green clinopyroxene, with fine exsolution lamellae, ore schiller and colourless-inclusion strings, forms irregular crystals; at the rims and between pyroxene grains, some fine amphibole and biotite formed. These hydrous minerals have about the same optical characteristics as in the norite part. A few grains are found between the plagioclase. Orthopyroxene, quartz (near biotite), muscovite, serpentine (in a thin vein), carbonate and chlorite are accessories. A few small irregular opaque ore concentrations appear with the clino-pyroxene.
AC : Modal analysis : high clinopyroxene content (diorite); no apatite.
Niggli values : high μ.
Amphibole oxides : low H_2O.
Further remarks : For the wet-chemical Fe^{2+} determination a mineral separate was used, containing amphiboles from both layers. Therefore, the measured Fe-content had to be recalculated :
Separate : 90% P1580 D and 10% P2580 L (estimation from the used rock sample). The total Fe as FeO, measured by probe for this separate is :

$$0.9 \times FeO_{P1580\ D} + 0.1 \times FeO_{P2580\ L} = 12.16$$

$FeO_{wet} = 8.80$
$FeO_{wet}/FeO_{probe} = 0.72$. Accepting equal oxidation ratios for both amphiboles, one can determine the FeO and Fe_2O_3 content from both :
$FeO_{wet} = 0.72 \times FeO_{probe}$ and $Fe_2O_3 = 1.111 \times FeO_{probe} - FeO_{wet}$.
The dioritic amphibole, P2580 L, contains more MnO and FeO_{total} and less MgO than the noritic amphibole P1580 D. The mineralogical difference between the two parts is remarkable : clinopyroxene in the diorite and orthopyroxene in the norite.

R 227 : Amphibole 2-pyroxene monzonorite with ferro-edenitic hornblende.

FO : The southern margin of the Orrestadvatn, at the SW-tip of the lake, is characterized by an irregular alternation

of zones of fine-grained monzonorites and coarse-grained olivine-2 pyroxene-(Q-)syenites. The contact between these rock groups is sharp and vertical with a 20 cm wide, fine-grained, mesocratic zone, which shows a vertical macroscopic lineation, due to the parallel arrangement of amphibole prisms. Further away from the contact, the lineation seems to disappear; the amphiboles occur here in a pattern of scattered spots without specific orientation (R 227). In the coarse-grained, leucocratic syenite some amphibole pegmatites are present (F 433).

MAD : Fine-grained, mesocratic rock with scattered spots of amphibole.

Texture : Granoblastic, inequigranular, polygonal. Amphibole and biotite are coarser than the very fine-grained groundmass. All minerals are lineated, the direction is clearly indicated by the abundant apatite needles. All feldspar crystals are elongated in more or less the same direction. Amphibole as well as orthopyroxene display groups of sections with equal orientation. The sections are separated by the fabric of other minerals. Pyroxenes are omnipresent, amphibole and biotite are concentrated in spots. The last two minerals may grow athwart the lineation.

MID : The outline of each group of amphibole sections tends to a euhedral form. Inside each amphibole group no pyroxene is present, only some grains in the rim fragments. Near enclosed ore grains the colour may be more bluish (see also B 322, F 107 etc.). Orthopyroxene ($2V_x = 72^o$) contains few exsolution lamellae and alters partly to serpentine. Pleochroism is weak. Clinopyroxene ($2V_z = 64^o$, $Z \wedge c = 34^o$) shows lamellae //(001). Reddish-brown biotite forms symplectites with quartz. Plagioclase is jammed with lineated apatite. If the gypsum plate is inserted, all plagioclase crystals show addition in the same direction. Alkalifeldspar is microperthitic. Apatite and ilmenite are omnipresent in all phases, except pyroxene which contains only incidentally apatite. Rounded zircon, fine muscovite, carbonate, pyrite and phyrrothite are rare.

AC : Bulk composition is high in P_2O_5 and CO_2.

R 229 : 2-pyroxene monzonite with ferro-edenitic hornblende/ferro-hornblende/grunerite$_{75}$.

FO : Several decameters NE of the above described R 227 locality, an alternation of medium-grained, mesocratic rock (R 229) and coarse-grained leucocratic syenite is found. Thicknesses of both rock groups are unknown.

MAD : Medium-grained, dark grey, unfoliated rock with some coarser grained feldspars.

Texture : Granoblastic, seriate, interlobate. Groups of medium-grained feldspar crystals, with polygonal contacts, are enveloped by a fine-grained fabric which occupies the largest part of the sample. Pyroxenes determine a lineation. Part of the pyroxene is rather coarse-grained, but the majority is fine-grained. Amphibole and biotite developed locally and are accompanied by quartz and alteration products.

The first amphibole (R1229) forms extreme poikiloblasts (as described for E 067/E 167/N 402 and the wallrock of F 433) of rather small size. The second amphibole (R2229) is contiguous to pyroxene, frequently replacing part of a pyroxene crystal, or it forms rims around R1229. The third amphibole (R3229) lies in the centre of a R1229 poikiloblast, together with some biotite.

MID : Amphibole : R1229 is subhedral, fine-grained and often associated with quartz. Pyroxene is frequently enclosed. R2229 is anhedral, and more bluish, more irregular and finer than R1229. R3229 is light bluish with bright interference colours, and is found only once as several thin laths and at the crystal margin of a R1229 amphibole. All amphibole seems to result from the alteration of pyroxene. Ortho- and clinopyroxene contain various systems of exsolution lamellae and intricate intergrowth patterns (e.g. the so-called "ladder structure", see B 016). Rietmeijer (1978) deals further with the Fe-rich pyroxenes in the magmatic complexes in Rogaland. Both pyroxenes show strong alteration, mainly to amphibole, reddish-brown biotite, quartz, carbonate and muscovite. Alkalifeldspar is microperthitic; plagioclase contains deformed twins and some sericitization. Quartz is mainly connected to amphibole and biotite. Myrmekite is rare. Apatite and zircon are both long prismatic and rounded. Opaque ore consists mainly of magnetite, and some ilmenite, pyrrhotite and pyrite.

AC : Bulk composition : highest in CO_2.

Amphibole oxides : highest Fe as FeO (R3229); high MnO (R3229); and low CaO (R2229 3).

Amphibole optics : The $2V_x$-value for R1229 is very low.

Further remarks : R1229 : 5 microprobe spots in various fragments of one extreme poikiloblast. R2229 1 : 1 spot near pyroxene; R2229 2 : 2 spots near pyroxene; R2229 3 : 1 spot near ore; R3229 : 2 spots which are in good agreement. R2229 shows an increase in FeO and MgO, and a decrease in TiO_2, Na_2O and K_2O with respect to R1229. CaO is very low in R2229 3. This last analysis has a very high Y-value and a low X-value. The reliability is dubious. The oxide changes are in agreement with former measured discoloured zones (B 322, F 107 etc.).

R 269 : Biotite amphibole monzonorite with ferro-hornblende(rims) and ferro-actinolite (cores).

FO : Sample form the Mydland tunnel. Surrounding samples often show carbonate veins and strong retrograde metamorphism. See also B 016.

MAD : Medium- coarse-grained, mesocratic, greyish rock, with black spots of ca 5 mm Ø.

Texture : Granoblastic, seriate, interlobate. The mafic minerals form aggregates in a felsic environment. The grainsize varies strongly; several coarse feldspar crystals are present, but most of it is very fine-grained. The mafic aggregates may consist of a pyroxene core (mainly orthopyroxene) with rims of green hornblende. The core may be replaced by a soft coloured ferro-actinolite, the rim may consist partly of biotite. The pyroxene is almost completely altered, resulting in a ferro-actinolite core, which may be bent, and which consists of many interpenetrating crystals. The rim of ferro-hornblende may be homogeneous, but is frequently built up of various crystals. The transition from actinolite to hornblende is gradual but quick. Instead of actinolite, the core may also consist of a fine-grained quartz-hornblende aggregate, or a more or less symplectitic intergrowth of fine, irregular quartz drops in a large hornblende.[1] Biotite forms coarse crystals near ore grains, and finer-grained lathes in the hornblende. The biotite may interpenetrate randomly, some crystals are bent. Opaque ore and large apatite crystals are additional phases in the mafic aggregates. Around ore grains the amphibole is always hornblende, even in ferro-actinolitic cores. The leucocratic part seems to be granulated, this is indicated by the medium-coarse grained macroscopic appearance and the division of light and dark parts in thin section.

MID : The 2-amphibole/ reddish-brown biotite/ pyroxene/ ore/ quartz aggregates are comparable with similar groups in E 232/N 827. An additional phenomenon is the difference between the reaction products of former orthopyroxene or clinopyroxene. The few pyroxene remnants are composed of an clinopyroxene host with orthopyroxene lamellae, mainly // (001). The rims and rungs are altered to green hornblende, but inside the rim the orthopyroxene alters to a hornblende-quartz aggregate and in the centre to the light-coloured ferro-actinolite. This results in an equivalent of the so-called "ladder-structure", (see B 016) : rims and rungs are now hornblende, the remaining space consists of hornblende + quartz, or ferro-actinolite.[2]

Inside the pyroxene remnants, ore needle systems are present. The apatite is partly coarse-grained and euhedral, containing various inclusions; and partly very fine-grained and anhedral in quartz. The quartz is commonly related to amphibole and biotite. Plagioclase is the main leucocratic mineral with a clear zoning (core : An_{26} - rim : An_{16}); schiller are omnipresent. Antiperthite and myrmekite are rare. Alkalifeldspar is microperthitic. The ore is mainly homogeneous ilmenite; magnetite and pyrite are less abundant. Titanite is found only once as a rim around a small biotite-quartz aggregate inside a large ilmenite grain. Carbonate occurs near the alteration aggregates. See further the sample description of E 232.

AC : Bulk composition : highest F; high NaO and CO_2.

Amphibole optics : R1269 has a very small $2V_x$-angle.

Further remarks : The microprobe analyses are divided in 6 tabulated analyses :

R1269 1 : 2 spots; R1269 2 : 1 spot; R1269 3 : 2 spots;

R2269 1 : 2 spots in the core of a small crystal; R2269 2 : 2 spots on long-prismatic, light-coloured amphiboles in the middle of a coarse-grained amphibole assemblage; R2269 3 : 1 spot in the same group as R2269 2.

The chemical trend is in complete agreement with E 232/N 827. The only difference is the mg-ratio.

R 356 : Olivine-clinopyroxene-bearing m-granite with ferro-hornblende.

FO : Massive sample from the quartz-rich phase of the lopolith.

MAD : Medium-grained, leucocratic, greyish-brown rock with a slight orientation of the mafic constituents in thin zones.

Texture : Granoblastic, inequigranular, interlobate-amoeboid. Mesoperthite is the main constituent and forms, together with quartz, medium-grained crystals with irregular rims. Between these anhedral crystals, all other minerals are present, including plagioclase (which often forms an irregular rim around the mesoperthite) and fine-grained quartz. The mafic constituents are arranged in zones. Amphibole is commonly accompanied by quartz, as in E 067/E 167 etc., but forms less extensive "extreme poikiloblasts-group 2". It also forms thin rim fragments around pyroxene and ore, and sometimes around olivine.

MID : Amphibole, see E 067; a more bluish tint as in B 322, F 107 etc. is sometimes present. The amphibole may show a comb-like outer rim on contacts with mesoperthite crystals. The alkalifeldspar component is replaced preferent to the plagioclase component (see also N3528), which may contain ore needles. Light greenish-blue clinopyroxene ($2V_z$ = 50°-60°, Δ= 0.018, $Z\wedge c$= 42°) contains thin exsolution lamellae in various directions with very fine ore needles. Fayalitic olivine ($2V_x$= ca 50°, Δ = 0.040, r>v (n_x)) is mainly rounded and alters to iddingsite, and rarely to serpentine. Pyroxene and olivine only seldom show the comb texture. Dark-brown symplectitic biotite, very fine anhedral apatite, and euhedral zircon are accessories. The opaque ore consists of ilmenite, and some magnetite and pyrrhotite. Fe-hydroxide is rare. Mesoperthite has a bluish haze, plagioclase is slightly zoned, and quartz displays a wavy extinction.

AC : Modal analysis : high mesoperthite-content (almost equal to N 528).

Niggli values : low mg.

Amphibole oxides : high "total Fe as FeO"; low CaO.

Further remarks : There is some variation in amphibole composition;

R 356 1 : 2 spots on a large grain; R 356 2 and -4 : 1 spot on a small grain near clinopyroxene; R 356 3 : 1 spot on a small grain near ore and clinopyroxene.

1 : Plate V, figure 1.

2 : Plate IV, figure 4.

R 668 : Amphibole monzonire with ferro-edenitic hornblende.

FO : Massive syenitic occurrence with a pock-marked surface. Groups of amphibole crystals are macroscopically recognisable, which is a rather uncommon feature in the Gloppurdi massif.
MAD : Medium-grained, leucocratic, yellowish-grey rock, with groups of amphibole crystals connected to quartz. Lineation is present without banding.
Texture : Granoblastic, seriate, interlobate. Amphibole + quartz forms isolated aggregates. The amphibole part consists of medium-grained brownish crystals (R1668) which are only partly accompanied by quartz, and finer-grained bluish-green crystals (R2668) which form always symplectitic intergrowths with quartz.
R2668 appears often on the outer rim of R1668 crystals and aggregates, much more extensive than the thin bluish zones around some other amphibole samples (e.g. F 107, N 402), or around ore grains; R2668 also may form small independant aggregates with quartz. This quartz is sometimes part of a myrmekite. The amphibole fragments are not all equally oriented as in the top of the lopolith (E 067/E 167); only a few neighbouring fragments may have the same orientation. R2668 shows this phenomenon more frequently than R1668. Many amphibole sections tend to a euhedral form. In the centres of amphibole-quartz aggregates a few altering clinopyroxenes may still be present, mostly they are completely altered. Amphibole often has a colourless fibrous rim (uralite) with an outer rim of stilpnomelane. Alkalifeldspar, plagioclase and mesoperthite form the matrix with varying grainsizes and irregular crystal outlines. Albite rims are omnipresent.
MID : The amphiboles very much resemble P 097 from the Botnavatnet massif :
--some of the indicatrix colours have a greyish tint,
--both samples have a bluish and brownish amphibole,
--the compositions are very much alike,
--amphibole forms, at least partly, symplectitic intergrowths with quartz.
The extinction is often undulatory, indicating subgrains. The transition from R1668 to R2668 is gradual. Quartz is only present near amphibole. Alkalifeldspar is microperthitic and may display a microcline texture. Plagioclase is slightly sericitisized and contains long ore needles. Myrmekite is fine and rare. Mesoperthite forms a few large crystals with a blue haze. Serpentine, chlorite and stilpnomelane aggregates may represent former pyroxenes, in one such aggregate a former exsolution lamella is still recognisable. Anhedral apatite; euhedral till rounded, zoned zircon, and interstitial ilmenite are minor phases.
AC : Bulk composition : high K_2O.
Niggli values : high alk.
Amphibole oxides : high FeO (R1668) and density; low Fe_2O_3 (R1668).
24(O) formula : lowest Fe^{3+}/Fe-total (R1668).
Further remarks : R2668 was not measured wet-chemical. There is a certain spread in the measurements for both groups. The difference between R1668 and R2668 is rather small. The bluish amphibole contains less TiO_2, and more FeO and MgO. One deviating analysis-spot gave larger differences: decrease in Na_2O, K_2O and TiO_2, increase in MgO and SiO_2. This is in good accordance with the findings for P 097 (see table II.7), except for the fact that the alkalies did not change markedly in P 097.

V 147 : Charnockite with magnesian hastingsitic hornblende.

FO : Exposure in a brook, approximately 2 km W of the Gloppurdi massif. The macroscopic appearance slightly resembles the Gloppurdi rocks : some pock-marks are present but the weathering is mainly smooth. The sample lies in the charnockitic migmatites.
MAD : Fine- medium-grained, firmly lineated, leucocratic rock without banding.
Texture : Granoblastic, seriate, interlobate. The quartz is platy, the mafic minerals are aligned in very thin zones. These zones consist of alteration products. Amphibole forms rim fragments around former pyroxenes; it consists partly of symplectitic intergrowths with quartz.
MID : The amphibole is very fine, anhedral and rare, and is accompanied by various alterstion products : stilpnomelane, chlorite, epidote, titanite and serpentine. These often appear pseudomorphous after pyroxene, former exsolution lamellae are in a few cases texturally preserved. Around these pseudomorphs the amphibole is present. Between the pseudomorphs more alteration products are present, forming the lineation. Quartz has a very undulatory extinction, and contains ore needles and many fluid inclusion strings. Alkalifeldspar shows a microcline grid and microperthite. Plagioclase has deformed twins and is partly sericitisized. It also contains zones which are altered to stilpnomelane. Some coarse myrmekite is present. Biotite, coarse apatite, euhedral and subhedral zircon, fine-grained ilmenite and some yellowish-brown zoned and rounded allanite are minor phases.
AC : High bulk SiO_2, and niggli alk. Highest niggli t (together with V 276), however no spinel is present.
Further remarks : There is some variation between the various grains. The amphibole plots in the Fe-rich part of fig. IV.8, between the igneous rocks, near amphiboles from Gloppurdi, Botnavatnet and the lopolith, and far away from migmatitic samples. It is therefore grouped with the igneous samples, and thought to be an offshoot of the Gloppurdi massif. The alteration products may represent former orthopyroxene, clinopyroxene or olivine.

V 187 : Amphibole norite with magnesian hastingsitic hornblende and actinolite.

FO : Dark band in mainly massive charnockitic migmatites which are rich in garnet. This band occurs above a quartz- and garnet-rich zone. The area is transected by discordant pegmatitic veins.
MAD : Fine-grained, mesocratic rock with phyllosilicate concentrations.
Texture : Granoblastic, equigranular, polygonal-interlobate. Grainsize ca 1 mm. Amphibole, biotite, and part of the pyroxene determine a weak lineation. The sample is tectonized and various minerals are partly altered.
MID : The amphibole consists of subhedral brown crystals (V1187) with in a very few cases a light bluish-green rim or zone (V2187). The last amphibole is only found together with alteration products : serpentine from orthopyroxene, chlorite and sericite. In most cases V2187 is a rim or a crack alteration of V1187, with a sharp contact between both amphiboles; rarely it is found as a rim-fragment outside orthopyroxene. V2187 is much finer than V1187 and always completely anhedral. Pyroxene is made up of equal amounts of :
--orthopyroxene, $2V_x$ = ca 70°, weak pleochroism, strong alteration to serpentine, undulatory extinction, thin exsolution lamellae, ore along cleavage planes and cracks, and
--clinopyroxene : light green, no alteration, thin exsolution lamellae, extra cleavage //(100), $2V_z$ = ca 60°.
Reddish-brown biotite forms several rather large symplectitic crystals which transect all other minerals. Plagioclase is strongly sericitisized and many crystals are broken up as in O 100. Muscovite has replaced about half of the original plagioclase content. Minor phases are : quartz, in biotite symplectites and as a few loose grains in the fabric; rather fine apatite; rounded zircon; fine dispersed ilmenite, and some pyrite which is mainly connected to alteration products.
AC : Highest muscovite content ; high amphibole K_2O (V1187); low amphibole Fe_2O_3 and oxidation ratio (V1187).
Further remarks : There is a rather large spread in composition for the V2187-amphibole, resulting in two tabulated values : V2187 1 and -2, which represent both one spot on different crystals. The bluish amphibole represents the actinolitization product, due to retrograde metamorphism. The change is the same as found in many other samples in the Tonstad area, even though there is a colour difference; near Tonstad the actinolitic amphibole is almost colourless, while in this region a light bluish-green colour is frequently found. See section II.2.3.

V 276 : Leucogranite with hastingsitic hornblende.

FO : A relatively fine-grained intercalation in the pock-marked syenites of the Gloppurdi massif. It contains more quartz than the syenites. The extend of the intercalations is unknown, but presumed to be rather large.
MAD : Medium-grained, leucocratic sample with platy quartz and dark streaks of several cm.
Texture : Granoblastic, seriate, interlobate. The mafic minerals (alteration products) are concentrated in thin zones, the quartz is platy. Amphibole is present as extremely rare, very fine fragments near alteration products and once as a fine symplectitic intergrowth with quartz.
MID : There is a strong resemblance to V 147. It was hardly possible to determine the optical amphibole properties, because of amphibole scarcity and the fine grainsize. The bluish colours are in good accordance with surrounding samples (V 147, V 187, R 668). There is possibly some alteration to actinolite, as indicated by weaker pleochroic colours and brighter interference colours along a contact between a bluish amphibole symplectite and a serpentine cluster. Quartz and feldspars as in V 147. Some mesoperthite is present as in R 668. Serpentine, chlorite, stilpnomelane and part of the opaque ore form aggregates of alteration products. Euhedral and subhedral, zoned zircon; some ilmenite and brown biotite are rare.
AC : Modal analysis : high quartz; no apatite.
Bulk composition : high SiO_2; low CaO.
Niggli values : highest al, w, t; high si, alk, f; low fm, c and mg.
Amphibole : high "Total Fe as FeO".
Further remarks : Microprobe analyses were performed on 4 separate fragments. The results were in good accordance. It is not clear whether the alteration products are pseudomorphs after olivine or pyroxene or both.

V 277 : Amphibole-bearing leuco-quartzmonzonite with ferro-edenitic hornblende.

FO : Another rock which slightly deviates from the "normal" Gloppurdi rocks. The weathering, however, is almost the same. Further field information is missing.
MAD : Medium-grained, leucocratic, brownish-grey rock, with a weak lineation caused by platy quartz and strings of mafic minerals. Microscopically it resembles R 668 as well as V 276, it is somewhere in between.
Texture : Granoblastic, seriate, interlobate. The mafic minerals are aligned in thin zones. Amphibole forms some poikiloblasts and occurs mainly as symplectitic intergrowths with quartz. It may form rims around alteration products. The amphibole shows great structural resemblance with R2668. The grainsize is about 1 mm.

MID : The amphibole looks very dirty and is frequently contaminated with various alteration products : serpentine, stilpnomelane, muscovite, epidote and some opaque ore. The amphibole pleochroic colours show the same greyish hues as in P 097 and R 668. The extinction may be irregular. Alkalifeldspar, plagioclase and mesoperthite are in good accordance with R 668. The plagioclase may be zoned with core An_{35} and rim An_{8}, it also contains deformed twins. Quartz is more frequent than in R 668, and has a strong undulatory extinction. It is partly connected with amphibole and partly independently present in the fabric. Minor phases are reddish-brown symplectitic biotite; coarse and rounded apatite which may contain numerous inclusions; zoned and euhedral, or rounded, zircon, and small grains of ilmenite.
AC : Highest bulk K_2O; high niggli al and alk; low niggli fm and low An-content.
Further remarks : The amphibole composition varies slightly between the grains. V 277 in table IV.7 is the mean of 3 spots on 2 different grains. The average composition is in very good agreement with R1668 - R2668.

V 363 : Biotite-amphibole-bearing granite with edenitic hornblende.

FO : Common sample from the mainly massive granitic migmatites NE of the Gloppurdi massif. To the west, more biotite is present.
MAD : Medium-grained, leucocratic rock, with an amphibole-biotite lineation. It looks identical to F 005.
Texture : Granoblastic, seriate, interlobate. A few larger alkalifeldspar "augen" are surrounded by a fabric of irregular grainsize. Amphibole and biotite are folded around these augen. Quartz also seems to press the mafic minerals aside, and seems to dissolute them as in F 005 and F 252. There are too few "augen" to justify the name "augen gneiss". The amphibole is anhedral, poikiloblastic, and is transected by biotite. The feldspars are rimmed by irregular, thin zones of albite.
MID : Great resemblance to F 005/F 252.
Amphibole : irregular poikiloblasts which, in contradistinction to F 005 and F 252, do not show a more bluish colour near ore grains, and which are not altered to actinolite. Biotite : dark brown, sometimes folded. Quartz : strong undulatory extinction, abundant inclusions of many kinds. Alkalifeldspar : mainly fine-microperthite, some saussuritization. Plagioclase : fine ore grains and needles (sagenite) enclosed, deformed twins and some sericitization. Myrmekites are fine and coarse. Apatite : randomly distributed, interstitial and enclosed. Zircon : rounded and zoned, sometimes concentrated. Epidote and chlorite are rare, they may appear around ore grains. Much less than in F 005/F 252.
Ore : partly interstitial, partly enveloped by amphibole and partly very fine in plagioclase and quartz. Mainly magnetite, with some ilmenite lamellae and very fine spinel on the magnetite-ilmenite contact, pyrite is a minor phase.
AC : The amphibole contains the least Fe_2O_3, which results in the lowest 24(O) Fe^{3+}/Fe-total value. This is in great contrast to the high oxidation ratios of F 005/F 252.

W 012 D : Biotite quartz amphibolite with magnesio-hornblende.

FO : Dark band in the mainly banded granitic migmatites E of Tonstad. Thickness of the bands varies from several mm to a few dm.
MAD : Mesocratic, fine-grained, lineated and banded, amphibole-rich rock. The light band is not considered here.
Texture : Granoblastic, equigranular, polygonal-interlobate. Grainsize mainly less than 1 mm. Amphibole and biotite determine the lineation. Biotite transects all other minerals.
MID : There is a strong resemblance with D 442. Only the differences are described here.
Besides plagioclase and apatite, the amphibole contains some quartz and biotite inclusions. The plagioclase only contains colourless apatite. Quartz is abundant. The extinction is wavy, some crystals are almost broken up. The quartz is mainly concentrated near amphibole and biotite as small crystals, but there is no clear textural relation. Alkalifeldspar is rarely present. Dark-brown biotite is relatively fine-grained. Minor phases are : apatite : long prisms; rounded zircon; magnetite : only very few, small grains; epidote and Fe-hydroxide : they form rare alteration spots. The presence of allanite is not quite sure : several zoned, reddish-brown/yellowish-brown crystals are found which cause pleochroic haloes in amphibole.
AC : No special features.
Further remarks : The difference in bulk composition between D 442 and W 012 is characterized by a higher content in SiO_2 and Na_2O for W 012 D, and a small decrease in the contents of all other elements. This is clear from the presence of 9% quartz in W 012 D and the lower An-content. The amphibole chemistry is more or less similar : W 012 D-amphibole contains more SiO_2, and a bit more MnO and F; it contains less TiO_2, Al_2O_3 and H_2O. The oxidation-ratio is rather low.

W 017 : Schistose biotite-amphibole enderbite with magnesio-hornblende.

FO : Mainly banded migmatite with abundant amphibolites. The formation is wildly folded. Garnet is present at various places, but never accompanied by amphibole. At the top of this zone, leucocratic bands are rare. Some pegmatite-like bands may be found.

MAD : Mesocratic, fine-medium grained, lineated and banded rock. The bands are several mm to cm wide.
Texture : Granoblastic, seriate, interlobate. Amphibole and biotite determine the lineation. Biotite transects other minerals, and formed fine crystals on the outer rim of amphibole. Amphibole partly formed on the outer rim of pyroxene.
MID : The sample may be divided in three rock types which occur in the following order : I : amphibole enderbite 1 cm; II : tonalite 1-2 mm; III : biotite diorite 5 mm; I : amphibole enderbite 0.5-3 cm. Modal compositions, see table A.3.

	I	II	III	Average front	Average back
Amphibole	23	A	A	11	18
Pyroxene	6		A	3	5
Biotite	3		19	8	4
Plagioclase	40	55	80	56	46
Quartz	25	45	A	20	24
Apatite	A		A	A	A
Zircon	A		A	A	A
Ore	A		A	A	A
P.P.C.	2.3	4.0	2.1	2.5	2.4
An%	40	45	36		

Front : I:II:III= 47:18:35
Back : I:II:III= 82:06:12

Table A.3. : Modal compositions of the three rock types in W 017, and the average model composition for two sections through the sample perpendicular to the banding. Alteration products are not mentioned.

Description of the layers :
1 : Poikiloblastic orthopyroxene is partly altered to serpentine, and rimmed by amphibole. Clinopyroxene poikiloblasts contain a few thin exsolution lamellae. The contacts between pyroxene and amphibole are dubious, a reaction relationship seems possible, also in view of the fact that the amphibole-pyroxene aggregates may have some fine-grained quartz as an additional phase. The amphibole crystals are anhedral and they vary from homogeneous to poikiloblastic, fine-grained to medium-grained. Inside the amphibole, ore needle systems are present with several orientations; biotite flakes are arranged $//(001)_{amph}$. Serpentine inclusions are also found. Plagioclase contains bent twins and is partly altered to sericite. Quartz has a strong undulatory extinction, only a small part is connected to amphibole and biotite. The apatite prisms are relatively long, zircon is rounded. Magnetite with ilmenite lamellae, some ilmenite grains, and pyrite mainly with alteration products (epidote and serpentine) form the ore phase.
The contact with layer II is undulatory.
II : Both plagioclase and quartz are relatively coarse-grained. Plagioclase contains subgrains and kinked twins, quartz has a strong wavy extinction. Crystal contacts are irregular.
The contact with layer III is again undulatory.
III : Reddish-brown biotite is partly altered to muscovite. The crystals are lineated parallel with the banding but form rows of crystals perpendicular to the banding. Plagioclase and other minerals, see I. A few small amphibole and pyroxene fragments may be present at the contact between II and III.
After this layer, there is a sharp alteration to another layer of I. There is difference between these layers in mineralogy, not in texture.
AC : Amphibole is low in H_2O-content.

W 162 D : Biotite quartzmonzodiorite gneiss with edenitic hornblende.

FO : Leucocratic intercalation in the Sirdalen augen gneisses. This formation contains many, more or less granitic parts. Amphibole is rare in the surroundings of this location.
MAD : Mesocratic, fine-grained, biotite-rich rock, with a leucocratic, medium-grained band.
Texture : Granoblastic, seriate, interlobate. Biotite determines the lineation in the dark band. The transition from the dark band to the light one is abrupt with a more coarse grainsize in the leucocratic band. Biotite transects the few amphibole fragments which are only present within 1 cm from the contact between dark and light band.
MID : The dark band.
Small remnants of amphibole lie between larger brown biotite crystals, which sometimes show quartz rims or symplectitic intergrowths with quartz. Little can be determined from the amphibole fragments. Plagioclase contains some antiperthite blebs, and a little sericitization. Myrmekite is partly coarse, partly fine. Alkalifeldspar has a microcline grid and some microperthite. The extinction of quartz is wavy. Apatite is abundant. Titanite surrounds most ore aggregates and is also independantly present. Zircon is rounded, biotite alters to chlorite. The ore consists of ilmenite with haematite exsolutions, and magnetite. Allanite is almost completely metamict, with a golden-yellow colour, causing pleochroic haloes in amphibole. It forms some symplectitic intergrowths with titanite.
The light band is a leucogranite.
Further remarks : Microprobe measurements indicated a slight chemical variation between the various amphibole grains.

W 196 B : Schistose amphibole enderbite with ferro-hornblende.

FO : Migmatite outcrop with alternation of amphibolitic bands and thicker leucocratic bands. The dark bands are less than 1 m thick.
MAD : Melanocratic, fine-medium grained, thin-layered, amphibole-rich, lineated rock.
Texture : In a thin section of ca 3 cm, it is possible to distinguish 7 layers, see fig. A.7.

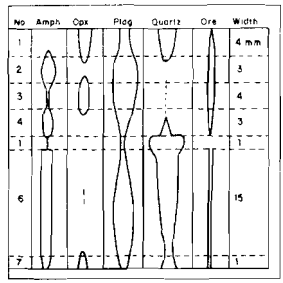

Figure A.7. : Modal variations and widths of seven layers in W 196 B. Amph: amphibole; opx: orthopyroxene; plag: plagioclase.

--1 : enderbite
2 : amphibolite
3 : fleuco-gabbro
4 : quartz-amphibolite
5 : quartzite
6 : amphibole tonalite
7 : amphibole enderbite

Amphibole-bearing layers are granoblastic, equigranular, polygonal; the grainsize is less than 1 mm : layer 2-4-6.

Pyroxene-rich layers are granoblastic, equigranular, interlobate, without lineation. Grainsize less than 1 mm : layer 3 and 7. The exception is layer 1, which is seriate, interlobate, with grainsizes up to 2 mm.

The quartzite band contains bent crystals, with strong undulatory extinction. Grains upto 4 mm long. They are lineated parallel to the amphibole direction. In layer 6 the fine-grained quartz is platy.

The transitions between the various layers are rather abrupt. The only really sharp contacts occur around the quartzite band.

At the contacts between amphibole- and orthopyroxene-rich layers the following phenomena can be seen :

layer 1→2 : small amphibole grains appear on the outer rims of-, between-, and inside orthopyroxene crystals. The orthopyroxene looks rather fresh and groups of neighbouring crystals are optically more or less continuous. Quickly the orthopyroxene disappears and larger amphibole crystals form the main mafic phase,

layer 2→3 : the same as 1→2,

layer 3→4 : mainly the same as 1→2. Some aggregates of fine-grained amphibole- and quartz crystals are present. Serpentinization and ore-formation (sulfides) at the expense of orthopyroxene, which is (partly) enveloped by amphibole, is rare,

layer 6→7 : fine-grained, poikiloblast-like, aggregates of amphibole and quartz are abundant, with frequently some partly serpentinized and sulfidized orthopyroxene remnants in the centre. Layer 7 is not extensively enough present in thin section to see what happens further away from the contact.

MID : Amphibole contains a lot of ore-grains between the crystals, needles inside the crystals, and fine grains on the rims. Apatite is also frequently enclosed. Around ore grains the amphibole may display a discoloured, more bluish, zone as described for B 322 etc. The rim of an amphibole crystal occasionally has a very fine-symplectitic appearance. It is, however, not possible to determine the leucocratic phase. Orthopyroxene has a weak pleochroism, and may contain homogeneously dispersed ore schiller. Some crystals of light-bluish clinopyroxene are present in layer 7. Plagioclase is partly sericitisized, resulting in flower-like muscovite aggregates. The An-content varies between An_{45} and An_{56}, there seems to be no trend. Deformed twins are common. Quartz contains numerous inclusions. Magnetite and ilmenite may be surrounded by green serpentine; pyrite and pyrrhotite occur mainly in the serpentinized orthopyroxene. Apatite is an abundant phase with varying grainsizes. Rounded zircon, yellowish allanite, and dark yellowish-brown biotite are rare. The biotite forms very small flakes on the outer rim of amphibole crystals, at places were ore grains are present.

AC : Niggli Q is low, and the H_2O-content of the amphibole is the lowest measured.

Further remarks : Modal analysis in table III.1 represents 1000 counts over all 7 layers. Bulk analysis is performed on a slice perpendicular to the layering, containing all layers present in the handspecimen. Amphibole optics indicated no difference between amphiboles in various layers. Microprobe measurements are from an amphibolite layer, and show no important variation.

W 217 : Amphibole-bearing biotite granite with magnesian hastingsitic hornblende.

FO : Average sample from the mainly massive granitic migmatites NE of Tonstad. Many pegmatite-like zones and some small amphibolites are present. It is the most E-ward sample of this collection.

MAD : Medium-grained, leucocratic, non-lineated, beige coloured rock.

Texture : Granoblastic, seriate, interlobate-amoeboid. Part of the leucocratic minerals form large crystals up to 5 mm (ca 70% of the rock). In between a very irregular fabric of all minerals is present. Deformation is rather strong : undulatory quartz, deformed twins in plagioclase. The amphibole consists partly of groups of sections with about equal orientation, mainly around quartz. As in F 005, it looks resorbed; biotite transects the amphibole. The rest of the amphibole is a common part of the fabric. Biotite near amphibole forms often symplectitic intergrowths with quartz, and is lineated. Other biotite is coarser-grained, not connected to quartz, and randomly oriented. Amphibole is inhomogeneously dispersed through the rock. Sericitization and saussuritization are limited.

It is wrong to speak of "extreme poikiloblasts" for these amphiboles, because the texture is not the result of new amphibole forming but of resorption and alteration.

MID : The colours for the amphibole as well as for the biotite are rather dark, respectively dark green (n_y) and dark brown. Plagioclase contains randomly dispersed schiller and some antiperthite. Myrmekite is abundant, fine and coarse. Alkalifeldspar is microperthitic. Quartz contains numerous inclusions : fluid-inclusion strings, colourless- and black needles, apatite, zircon, strings of brown flakes, etc. Minor phases are : rounded grains of greenish serpentine with homogeneously dispersed, and oriented, ore needles; rather fine apatite; zoned and rounded zircon; magnetite and ilmenite.

AC : High bulk SiO_2 and niggli t. The mg-ratio for the amphibole is the lowest in the migmatites.

W 226 : Plagioclase-bearing hornblendite with magnesio-hornblende, in contact with an amphibole mela-diorite with edenitic hornblende.

FO : Mainly banded migmatites south of a great E-W dolerite in the NE-part of the area.

MAD : Banded sample with a melanocratic, fine-grained, amphibole-rich band, and a mesocratic, fine-grained, lineated band. The contact is formed by a 1 mm thick, leucocratic zone.

Texture : The sample is only 23 mm thick. In a section perpendicular to the banding, the following layering can be seen, fig. A.8.

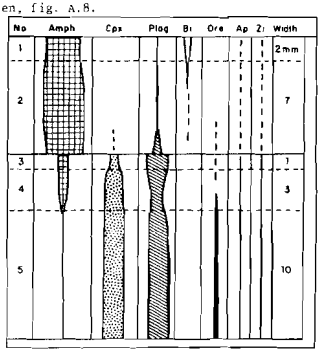

Figure A.8. : Modal variations and widths of 5 layers in W 226. W 226 D : layers 1 and 2; W 226 L : layers 3 - 5. Amph : amphibole; Cpx : clinopyroxene; Plag : plagioclase; Bi : biotite; Ap : apatite; Zi : zircon.

--1 : biotite hornblendite
2 : plagioclase-bearing hornblendite
3 : amphibole diorite
4 : amphibole mela-diorite
5 : mela-diorite

W 226 D : The hornblendite is granoblastic, equigranular, polygonal, lineated. Plagioclase and clinopyroxene are interstitial and mainly present near the contact between layer 2 and 3. Towards layer 1 some biotite appears which quickly becomes more abundant. The biotite is well lineated and transects amphibole. Apatite and zircon are mainly enclosed in amphibole. Some very fine ore grains are rarely present on a few crystal rims.

The contact with layer 3 is sharp and undulatory. The fine- to medium-grained hornblendite (up to 2 mm), abruptly changes into a fine-grained diorite.

W 226 L : The diorite is mainly granoblastic, equigranular, polygonal with an extreme fine grainsize (ca 0.1-0.2 mm). Near the contact between 2 and 3 some larger, strongly sericitisized plagioclase grains (up to 1 mm) are present. Clinopyroxene forms partly poikilohlastic crystals in layers 3 and 4. In layer 5 two thin plagioclase-rich levels with crystals up to 1 mm can be seen parallel to the banding. A more remarkable feature is the presence of a bent band of medium-grained clinopyroxene crystals (up to 1.5 mm) which folds through layer 4 and 5. Amphibole consists of small lineated crystals in layers 3 and 4, and only small fragments connected to pyroxene in layer 5. Ilmenite and magnetite are partly interstitial and partly enclosed in plagioclase, clinopyroxene and amphibole. The enclosed group forms a striking picture, which is very uncommon in the Rogaland rocks. All minerals are jammed with very fine equidimensional, ca cubic ore crystals.[1]

MID : W 226 D.

The amphibole becomes lighter coloured from the contact between hornblendite and diorite, to layer 1. At the contact the colours are of the same iureusity as for the amphibole in the diorite, but more greenish. Zoning is dubious, Universal Stage measurements indicate a difference of a few degrees (2-4) for the $2V_x$ between core and rim (lower values for the rim). Pleochroic haloes are caused by extremely fine, rounded zircons. Along thin cracks the amphibole colours may be completely faded, while the interference colours are brighter. This is possibly actinolitization. The zones are too thin (max. 10 micron) to measure optical properties. A more or less comparable feature was described for N 317. The plagioclase is strongly sericitisized. Biotite is orange-brown, and consists of thin, elongated crystals.

--W 226 L

The larger clinopyroxene crystals may contain numerous ore schiller. Small fragments of amphibole are also frequently enclosed or present on crystal margins. The greenish clinopyroxene has a $2V_z$ of 40 to 50°, Δ =0.030 and ZAc= 44°. The plagioclase is much less sericitisized than in W 226 D. Besides ore it may enclose abundant colourless (apatite) and greenish (at least partly amphibole) crystals. Some coarser apatite crystals are interstitial. Zircon is fine and rounded. The ore consists of magnetite and ilmenite.

AC : W 226 D : high amphibole content, no ore.

W 226 L : highest niggli γ; high pyroxene content, bulk CaO, and niggli c; lowest niggli t.

Further remarks : The amphibole microprobe measurements for WI226 D are performed on grains near the contact between layers 2 and 3, so chemical changes in the hornblendite, as indicated by the changing colour-intensity, are not measured.

1 : Plate II, figure 2.

Y 055 : Enderbite with ferroan pargasitic hornblende / ferro-hornblende.

FO : Mainly massive charnockitic migmatites with some dark bands and pegmatites.
MAD : Leucocratic, medium-grained, greyish rock.
Texture : Granoblastic, seriate, interlobate. The leucocratic minerals form an irregular matrix, with anhedral mafic constituents mainly smaller than 1 mm. Amphbile appears to be independant of pyroxene, except for Y2055 which may be present as very small bluish rims around pyroxene, and also at amphibole-pyroxene and amphibole-ore contacts. Some orthopyroxene crystals seem to be resorbed by quartz in their centres, leaving an atol-like texture. Plagioclase displays deformed twins, quartz has an undulatory extinction.
MID : Amphibole (Y1055) is a rather unimportant phase and shows no direct relationship with quartz. The more bluish variety (Y2055) is extremely rare and, in most cases, clearly an alteration product of orthopyroxene. The orthopyroxene is zoned, contains lamellae //(100), has a weak pleochroism and abundant fine ore grains on crystal rims and in zones inside the crystals, $2V_x$ = 40-50°. It alters mainly to serpentine. Bluish-green clinopyroxene contains some lamellae parallel (001). Antiperthite occurs on twin boundaries in plagioclase, as rows of small specks. It is also found in a sagenite-like texture. Ore schiller are rare. Myrmekite may become extremely fine at plagioclase-alkalifeldspar contacts. Some microperthite is present. Minor phases are : reddish-brown biotite with a greenish rim, the few small crystals may transect amphibole and pyroxene; apatite; rounded, rather coarse zircon; interstitial ilmenite and some magnetite; and chlorite and serpentine as alteration products of orthopyroxene.
AC : High modal plagioclase, niggli t, amphibole K_2O (Y1055 and Y2055 1); low amphibole Na_2O (Y2055 1).
Further remarks : Y1055 : 6 spots on 3 different crystals with a rather irregular chemistry. Y2055 : both table values are 1 spot analyses on thin rims around orthopyroxene. These rims are too rare and fine to perform good optical and chemical measurements.
The difference between Y1055 and Y2055 is mainly the same as for other combinations of brownish and bluish amphiboles, but the trends are far from regular. This may be caused by the fact that both Y2055 analyses are measured on different rims around orthopyroxene, and, therefore, are not related directly to the main amphibole as in most of formerly described combinations (e.g.B 322, F 107 etc.). The only difference from the common trends is the higher Fe-content for the bluish amphibole.

Y 128 : Retrograde 2-pyroxene quartzsyenite with hastingsitic hornblende and ferro-actinolite.

FO : Massive, syenitic series, strongly weathered, with a slightly different appearance from the syenites of the charnockitic migmatites. It is a pyroxene-syenite lobe which is related to the Gloppurdi massif.
MAD : Medium- to coarse-grained, strongly tectonized and chloritisized rock. Various shearzones are present. Formerly it must have been leucocratic, now it is mesocratic.
Texture : Granoblastic, seriate, interlobate-amoeboid. The mafic minerals are smaller than the average leucocratic crystals. Alteration is very strong. The original mafic constituents are partly or completely altered. Quartz has a strong undulatory extinction and plagioclase is sericitisized. Zircon is the only euhedral mineral. Plagioclase is smaller than alkalifeldspar and quartz, and appears as blebs in alkalifeldspar or in an interfingering relation with it. Feldspar rims are albitisized. Apatite and zircon are rather coarse.
MID : The amphibole forms small fragments and rims around pyroxene. The colour may vary some, depending on the neighbouring minerals. Other optical properties vary as well, e.g. $2V_x$ and ZAc. The smaller the fragment, the smaller the $2V_x$, ranging from 18° to 50°. ZAc varies from 0° to 4°. These ranges in optical properties may result from incomplete readjustment of former pyroxene properties. Larger amphibole fragments form symplectitic intergrowths with quartz. Along a few thin cracks the amphibole is discoloured to a very light-bluish tint (Y2128). These cracks may be up to 10 micron wide, mainly ca 3 micron. They resemble the cracks in W 226 D. Some fibrous, uralitic material is also found on the outer rim of an Y1128 amphibole. Ortho- and clinopyroxene are strongly altered, schiller and exsolution lamellae are still recognisable. Alkalifeldspar is all microperthitic.Myrmekite is common, coarse and fine. Zircon is partly euhedral, partly subhedral. Several crystals are zoned, zircon may contain abundant inclusions. Apatite is isotropic and causes pleochroic haloes in amphibole. The colour of the apatite seems to vary from completely colourless to more brownish and yellowish. The yellowish crystals have a low birefringence. It is not quit clear what kind of alteration takes place, and whether it all is (was) apatite. Further recognisable minerals are : stilpnomelane, omnipresent as garlands around pyroxene and alteration products, and dispersed in feldspar; brown serpentine with lathes of ore, possibly representing former olivine; green serpentine forming rows of crystals in strongly altered zones; chlorite; titanite; and allanite. The allanite alters to a fine-grained partly vermicular aggregate with ore along the rim and zoisite on the outside, all very fine. Various aggregates of unrecognisable, fine-grained minerals are scattered through the rock. Magnetite and ilmenite appear partly interstitial and partly as lathes in alteration aggregates.
AC : The amphibole is high in FeO (Y1128 and Y2128) and MnO (Y2128); SiO_2, MgO and mg-ratio are low (Y1128); highest stilpnomelane content; ZAc is extremely low.

Further remarks : There appeared to be a strong variation between the 6 microprobe measurements for Y1128. All spots have been calculated separately, fig. A.9, and for the two groups found in this way, corrected mean values were recalculated, which are tabulated as Y1128 1 and -2, representing resp. 4 and 2 spots on as much crystals. Y2128 is a one-spot measurement on a contact between Y1128 and altered pyroxene.
In fig. A.10 the oxide changes are shown for the transition from hornblende (Y1128) to ferro-actinolite (Y2128). It is clear that the changes from Y1128 1 to -2 are not always consistent with the general trends (e.g. TiO_2).
According to Tröger (1969), the isotropic character of the apatite may be caused by the presence of rare earth elements. The apatite is often enriched in zones.

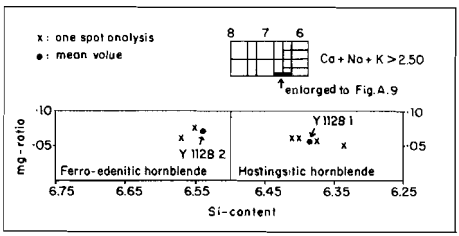

Figure A.9. : Plot of 6 one-spot analyses of Y1128 in the Leake diagram. Only the 2 corrected mean values are given in the tables. Microprobe information only : 23(O).

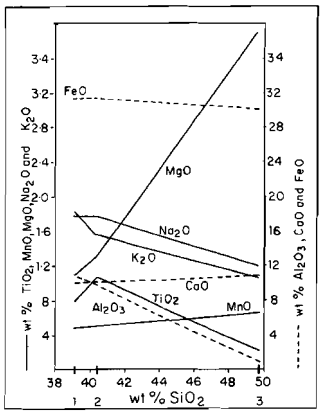

Figure A.10. : Oxide changes due to the transition from hornblende to ferro-actinolite, with respect to SiO_2, for Y 128. Compare with fig. II.2. 1= Y1128 1; 2= Y1128 2; 3= Y2128.

Y 131 : Garnet-bearing clinopyroxene quartzmonzonite with hastingsite and ferro-tschermackite.

FO : Like Y 128, it is from an offshoot of the Gloppurdi massif. Further field information is lacking.
MAD : Mesocratic, medium-grained, lineated or finely banded rock with abundant chloritisized/serpentinized shearzones.
Texture : The sample can be divided in several thin layers of a few mm thick. Alkalifeldspar-rich leucocratic layers which contain only little plagioclase and interstitial quartz alternate with plagioclase-rich zones which carry pyroxene and ore-aggregates. The texture is granoblastic, inequigranular, interlobate for the leucocratic layers and granoblastic, equigranular, polygonal for the more mafic layers. The dark minerals are partly interstitial. Amphibole is only present in the dark layers, as small fragments on the edges of pyroxene crystals, or around ore grains and, rarely, in contact with ore-aggregates. In part of the dark layers these ore-aggregates are surrounded by a rim of garnet (ca 0.1 mm wide), which forms very fine-symplectitic intergrowths. Between this rim and the ore-centre a quartz rim (ca 50 micron) may be present. All ore-aggregates in such a layer are surrounded by garnet, and pyroxene is mainly absent. Amphibole never occurs in contact with garnet.
The only fresh main minerals are alkalifeldspar and quartz; plagioclase is strongly sericitisized, pyroxenes are altered to serpentine. Alteration products dominate the general view.
MID : The amphibole fragments are too small to determine optical parameters other than the colour and birefringence. The bluish variety Y1131 appears mainly in contact with clinopyroxene, the more brownish Y2131 lies against and around opaque ore. Transitions are possible. Quartz may be present as an additional phase, but does not belong especially to amphibole-carrying spots. The quartz frequently forms rims around pyroxene and ore-aggregates, whether amphibole is present or not. The third amphibole Y3131 is only found once as a zoned crystal in plagioclase, not in contact with mafic constituents. The differences between these three amphiboles are small. Greenish clinopyroxene has exsolution lamellae //(001). The degree of alteration varies from spot to spot, but greenish serpentine always rims the pyroxene. Garnet is soft pinkish. Besides as thin rims, the quartz is present as small interstitial crystals (in a thin layer in a plagioclase-rich band), and in myrmekite. Extinction is wavy. Alkalifeldspar displays microcline grid and contains microperthite. Plagioclase is antiperthitic. Myrmekite appears in all sizes. Minor phases are : apatite; euhedral to anhedral, rather coarse zircon, and some interstitial magnetite and ilmenite. Alteration products consist of aggregates up to several mm of magnetite and sulfides, green serpentine, chlorite, muscovite, biotite, carbonate and fine-grained unknown material. Titanite may be present. Allanite has a reddish brown core and a light brown rim, and forms some symplectitic intergrowths with opaque ore.
AC : High bulk CO_2; lowest niggli mg.
Amphibole oxides : highest Al_2O_3 (Y3131 K); high K_2O and "All Fe as FeO"; low MgO and Na_2O; lowest SiO_2 (all Y 131-amphiboles).

23(O) formula : highest Al^{VI} (Y3131 K); high Al^{VI} for all others; high Ca; low mg-ratio.

Further remarks : Y 131 is the only sample in this collection with both amphibole and garnet.

Y1131 1 and -2, and Y2131 are averages of 2 spots. Y3131 K and -R are one-spot analyses on a zoned grain (K=core, R=rim). From fig. A.11 it is clear that from brownish to bluish colour (Y2131 → Y1131), there is an increase in SiO_2, Al_2O_3 and FeO, and a decrease in Na_2O and TiO_2. Some oxides are directly correlated with the SiO_2-content. The zoned amphibole Y3131 shows from core to rim a decrease in Al_2O_3, stable MnO, and an increase in all other elements.

The very low mg-ratio of the amphiboles is in good accordance with the bulk niggli mg. Because of the small size of these amphibole fragments, and the presence of fine alteration products, the microprobe analyses of the Y 131 amphiboles should be handled with care. Their errors will be greater than indicated by fig. IV.5.

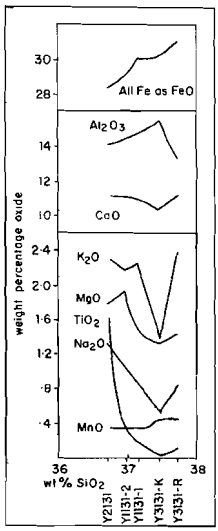

Figure A.11.: Oxide changes with respect to SiO_2 for Y 131 amphiboles.
Y1131 : bluish; Y2131 : brownish: Y3131 : light coloured.

REFERENCES

AHRENS, L.H., 1954, A note on the relationship between the precision of classical methods of rock analyses and the concentration of each constituent. Mineralog. Mag., 30, 467-470.

AKELLA, J., and WINKLER, H.G.F., 1966, Orthorhombic amphibole in some metamorphic reactions. Contr. to Min. Pet., 12, 1-12.

ALBUQUERQUE, C.A.R. De, 1974, Geochemistry of actinolitic hornblendes from tonalitic rocks, northern Portugal. Geochim. et Cosmochim. Acta, 38, 789-803.

BEACH, A., 1974, Amphibolitization of Scourian granulites. Scott. Jour. Geol., 10, 35-45.

BEST, M.G., 1974, Mantle-derived amphibole within inclusions in alkalic-basaltic lavas. Jour. Geophys. Res., 79, 2107-2113.

----------, 1975, Amphibole-bearing cumulate inclusions, Grand Canyon, Arizona and their bearing on silica-undersaturated hydrous magmas in the upper mantle. Jour. Petrology, 16, 212-236.

BINNS, R.A., 1965-a, The mineralogy of metamorphosed basic rocks from the Willyama Complex, Broken Hill district, New South Wales. Part I. Hornblendes. Mineralog. Mag., 35, 306-326.

----------, 1965-b, Hornblendes from some basic hornfelses in the New England region, New South Wales. Mineralog. Mag., 34, 52-65.

BORG, I.Y., 1967, On conventional calculations of amphibole formulas from chemical analyses with inaccurate $H_2O(+)$ and F determinations. Mineralog. Mag., 36, 583-590.

BORNEMAN-STARYNKEVICH, I.D., 1960, The chemical formula of minerals. IV : Amphiboles. All-Union Mineralog. Soc., Mem., 89, 236-247.

BRADY, J.B., 1974, Coexisting actinolite and hornblende from West-Central Hampshire. Am. Mineralogist, 59, 529-535.

BROWN, E.H., 1967, The greenschist facies in part of Eastern Otago, New Zealand. Contr. to Min. Pet., 14, 259-292.

----------, 1974, Comparison of the mineralogy and phase relations of blueschists from the North Cascades, Washington, and greenschists from Otago, New Zealand. Geol. Soc. America, Bull., 85, 333-344.

BUDDINGTON, A.F., 1972, Differentiation trend and parental magmas for anorthosite and Q.-mangerite series, Adirondacks, New York. Geol. Soc. America Mem., 132, 477-488.

BURNS, R.G., 1966, Apparatus for measuring polarized absorption spectra of small crystals. Jour. Sci. Instrum., 43, 58-60.

BURRI, C., 1959, Petrochemische Berechnungsmethoden auf äquivalenter Grundlage. Birkhäuser Verlag Basel und Stuttgart, 334 p.

CAMERON, M.J., 1971, The crystalchemistry of tremolite and richterite : A study of selected anion and cation substitutions. Ph.D.-thesis, Virginia Polytechnic Institute and State University.

CARMICHAEL, I.S.E., TURNER, F.J., and VERHOOGEN, J., 1974, Igneous petrology. McGraw-Hill Book Company, 739 p.

CHOUDHURI, A., 1972, Hornblende-actinolite and hornblende-cummingtonite associations from Cuyuni River, Guyana, South America. Am. Mineralogist, 57, 1540-1546.

----------, 1974, Distribution of Fe and Mg in actinolite, hornblende and biotite in some Precambrian metagraywackes from Guyana, South America. Contr. to Min. Pet., 44, 45-55.

COMPTON, R.R., 1958, Significance of amphibole paragenesis in the Bidwell Bar region, California. Am. Mineralogist, 43, 890-907.

COOPER, A.F., and LOVERING, J.F., 1970, Greenschist amphiboles from Haast River, New Zealand. Contr. to Min. Pet., 27, 11-24.

COOPER, A.F., 1972, Progressive metamorphism of metabasic rocks from the Haast Schist Group of southern New Zealand. Jour. Petrology, 13, 457-492.

CZAMANSKE, G.K., and WONES, D.R., 1973, Oxidation during magmatic differentiation, Finnmarka Complex, Oslo area, Norway. Jour. Petrology, 14, 349-380.

DAVIS, J.C., 1973, Statistics and data analysis in geology. New York, J.Wiley and Sons, 550 p.

De, A., 1969, Anorthosites of the Eastern Ghats, India. In : Origin of anorthosite and related rocks. Y.W. Isachson, Ed., 425-434. New York State Mus. Sci. Serv. Mem., 18.

DEER, W.A., 1938, The composition and paragenesis of the hornblendes of the Glen Tilt complex, Perthshire. Mineralog. Mag., 25, 56-74.

DEER, W.A., HOWIE, R.A., and ZUSSMAN, J., 1963, Rock-forming minerals, 2, Chain silicates. London, Longmans Ltd., 379 p.

----------, 1974, An introduction to rock-forming minerals. London, Longman Group Ltd., 528 p.

DEKKER, A.G.C., 1973, Verslag van een petrografiese kartering in het gebied ten NW. van Tonstad, Zuid Noorwegen. Internal Report, University of Utrecht.

DOWTY, E., KEIL, K., and PRINZ, M., 1974, Lunar pyroxene-phyric basalts : Crystallization under supercooled conditions. Jour. Petrology, 15, 419-453.

DRURY, S.A., 1974, Chemical changes during retrogressive metamorphism of Lewisian granulite facies rocks from Coll and Tiree. Scott. Jour. Geol., 10, 237-256.

DUCHESNE, J.C., 1972, Pyroxène et olivines dans le massif de Bjerkrem-Sogndal (Norvège méridionale). Contribution à l'étude de la série anorthosite-mangérite. 24th IGC, 1972, sec. 2.

EMSLIE, R.F., 1975, Pyroxene megacrysts from anorthositic rocks : new clues to the sources and evolution of the parent magmas. Can. Mineral., 13, 138-145.

ENGEL, A.E.J., and ENGEL, C.G., 1962-a, Progressive metamorphism of amphibolite, northwest Adirondacks, New York. In : Petrologic Studies. A volume in honor of A.F. Buddington. Geol. Soc. America, 37-82.

----------, 1962-b, Hornblendes formed during progressive metamorphism of amphibolites, northwest Adirondack Mountains, New York. Geol. Soc. America,Bull., 73, 1499-1514.

ERNST, W.G., 1966, Synthesis and stability relations of ferro-tremolite. Am. Jour. Sci., 264, 37-65.

----------, 1968, Amphiboles. Minerals, Rocks and Inorganic materials, subseries: Exp. Mineralogy, 1, Berlin, Springer Verlag, 125 p.

----------, 1972, Ca-amphibole paragenesis in the Shiritaki District, Central Shikoku, Japan. Geol. Soc. America, Mem., 135, 73-94.

FAIRBAIRN, H.W., 1953, Precision and accuracy of chemical analysis of silicate rocks. Geochim. et Cosmochim. Acta, 4, 143-156.

FIALA, J., VEJNAR, Z., and KUČEROVÁ, D., 1976, Composition of the biotites and coexisting biotite-hornblende pairs in granitic rocks of the Central Bohemian Pluton. Krystallinikum, 12, 79-111.

FINGER, L.W., 1972, The uncertainty in the calculated ferric iron content of a microprobe analysis. Carnegie Inst. Wash. Yearbook, 71, 600-603.

FLANAGAN, F.J., 1969, U.S. Geological Survey Standards, II : First compilation of data for the new U.S.G.S. rocks. Geochim. et Cosmochim. Acta, 33, 81-120.

FLETCHER, C.J.N., 1971, Local equilibrium in a two-pyroxene amphibolite. Can. Jour. Earth Sci., 8, 1065-1080.

FLORAN, R.J., 1975, Mineralogy and petrology of the sedimentary and contact metamorphosed Gunflint Iron Formation, Ontario-Minnesota. Ph.D.-thesis, State University of New York.

FRANGIPANE, M., and SCHMID, R., 1974, Point-counting and its errors. Schweiz. Min. Pet. Mitt., 54, 21-31.

FRENCH, W.F., and ADAMS, S.J., 1972, A rapid method for the extraction and determination of iron (II) in silicate rocks and minerals. Analyst, 97, 828-831.

FRISCH, T., and SCHMINCKE, H.U., 1969, Petrology of clinopyroxene-amphibole inclusions from the Roque Nublo volcanics, Gran Canaria, Canary Islands(Petrology of Roque Nublo volcanics I). Bull. Volcanol., 33, 1073-1088.

GIERTH, E., and KRAUSE, H., 1973, Die Ilmenitlagerstätte Tellnes (Süd-Norwegen). Norsk geol. Tidsskr., 53, 359-402.

GITTOS, M.F., LORIMER, G.W., and CHAMPNESS, P.E., 1974, An electron-microscope study of precipitation (exsolution) in an amphibole (the hornblende-grunerite series). Jour. Mater. Sci., 9, 184-192.

----------, 1976, The phase distribution in some exsolved amphiboles. In : Electron microscopy in mineralogy, H.R. Wenk, Ed., 238-247. Heidelberg, Springer Verlag.

GOFF, F.E., and CZAMANSKE, G.K., 1972, Calculation of amphibole structural formulae. U.S. Geol. Surv. Computer Contr., 16, 16 p.

GRAHAM, C.M. 1974, Metabasite amphiboles of the Scottish Dalradian. Contr. to Min. Pet., 47, 165-185.

GRAPES, R.H., 1975, Actinolite-hornblende pairs in metamorphosed gabbros, Hidaka mountains, Hokkaido. Contr. to Min. Pet., 49, 125-140.

GREEN, D.H., and RINGWOOD, A.E., 1967, The genesis of basaltic magmas. Contr. to Min. Pet., 15, 103-190.

GREEN, T.H., 1969, High-pressure experimental studies on the origin of anorthosite. Can. Jour. Earth Sci., 6, 427-440.

HANSON, G.N., and GAST, P.W., 1967, Kinetic studies in contact metamorphic zones. Geochim. et Cosmochim. Acta, 31, 1119-1153.

HASELTON, J.D., and NASH, W.P., 1975, Ilmenite-orthopyroxene intergrowths from the moon and the Skaergaard Intrusion. Earth Plan. Sci. Lett., 26, 287-291.

HAWTHORNE, F.C., and GRUNDY, H.D., 1973-a, The crystal chemistry of the amphiboles : I. Refinement of the crysral structure of ferrotschermakite . Mineral. Mag., 39, 36-48.

----------, 1973-b, The crystal chemistry of the amphiboles :II. Refinement of the crystal structure of oxykaersutite. Mineral. Mag., 39, 390-400.

----------, 1975, Resolution of the mössbauer spectrum of oxykaersutite. Can. Mineral., 13, 91-92.

----------, 1976, The crystal chemistry of the amphiboles : IV. X-ray and neutron refinements of the crystal structure of tremolite. Can. Mineral., 14, 334-345.

----------, 1977, The crystal chemistry of the amphiboles :III. Refinement of the crystal structure of a sub-silicic hastingsite. Mineral. Mag., 41, 43-50.

HAWTHORNE, F.C., 1976, The crystal chemistry of the amphiboles : V. The structure and chemistry of arfvedsonite. Can. Mineral., 14, 346-356.

HELLNER, E., and SCHÜRMANN, K., 1966, Stability of metamorphic amphiboles: the tremolite-ferro-actinolite series. Jour. Geol., 74, 322-331.

HELZ, R.T., 1973, Phase relations of basalts in their melting range at P_{H_2O}= 5 kb as a function of oxygen fugacity. Part I : Mafic phases. Jour. Petrology, 14, 249-302.

HENDERSON, C.M.B., 1968, Chemistry of hastingsitic amphiboles from the Marangudzi igneous complex, southern Rhodesia. Pap. Proc. 4th Gen. Meeting, Cambridge (Engl.), 291-304.

HERMANS, G.A.E.M., TOBI, A.C., POORTER, R.P.E., and MAIJER, C., 1975, The high-grade metamorphic Precambrian of the Sirdal-Ørsdal area, Rogaland/Vest-Agder, south-west Norway. Norges geol. Unders., 318, 51-74.

HERZ, N., and BANERJEE, S., 1973, Amphibolites of the Lafaiete, Minas Gerais, and the Sierra Do Navio Manganese Deposits, Brazil. Econ. Geol., 68, 1289-1296.

HESS, H.H., and POLDERVAART, A., (Eds.), 1968, Basalts : The Poldervaart treatise on rocks of basaltic composition. Vol. 2, New York, J. Wiley and Sons.

HIETANEN, A., 1974, Amphibole pairs, epidote minerals, chlorite and plagioclase in metamorphic rocks, northern Sierra Nevada, California. Am. Mineralogist, 59, 22-40.

HIMMELBERG, G.R., and PHINNEY, W.C., 1967, Granulite-facies metamorphism, Granite Falls- Montevideo area, Minnesota. Jour. Petrology, 8, 325-348.

HUANG, W.H., and JOHNS, W.D., 1967, Simultaneous determination of fluorine and chlorine in silicate rocks by rapid spectrophotometric method. Anal. Chim. Acta, 37, 508-515.

IJLST, L., 1973-a, New diluents in heavy liquid mineral separation and an improved method for the recovery of the liquids from the washings. Am. Mineralogist, 58, 1084-1087.

---------, 1973-b, A laboratory overflow-centrifuge for heavy liquid mineral separation. Am. Mineralogist, 58, 1088-1093.

IMMEGA, I.P., and KLEIN, C., 1976, Mineralogy and petrology of some metamorphic Precambrian iron-formations in southwestern Montana. Am. Mineralogist, 61, 1117-1144.

IRVINE, T.N., 1974, Petrology of the Duke Island Complex, southeastern Alaska. Geol. Soc. America, Mem., 138, 240 p.

JASMUND, K., and SCHÄFER, R., 1972, Experimentelle Bestimmung der P-T-Stabilitätsbereiche in der Mischkristallreihe Tremolit- Tschermakit. Contr. to Min. Pet., 34, 101-115.

KALSBEEK, F., 1969, Note on the reliability of point counter analyses. Neues Jb. Min., Mh., 1, 1-6.

KALSBEEK, F., and LEAKE, B.E., 1970, The chemistry and origin of some basement amphibolites between Ivigtut and Fredrikshab, SW-Greenland. Grønlands geol. Unders., Bull. 90, 1-36.

KAMP, P. van der, 1969, Origin of the amphibolites in the Beartooth Mountains, Wyoming and Montana: New data and inrerpretation. Geol. Soc. America, Bull., 80, 1127-1136.

KEHLENBECK, M.M., 1974, Some chemical characterisrics and variations of gneisses, intermediate intrusive rocks, and anorthosite in the Lac Rouvray map area, Quebec. Can. Jour. Earth Sci., 11, 1689-1703.

KIEFT, C., and MAASKANT, P., 1969, Quantitative microprobe-analyses of silicates : a comparison of different correction methods. Abs. Conf. Roy. Micr. Soc. Roy. Min. Soc., Manchester.

KLEIN, C., 1968 , Two-amphibole assemblages in the system actinolite-hornblende-glaucophane. Am. Mineralogist, 54, 212-237.

KOSTYUK, E.A., and SOBOLEV, V.S., 1969, Paragenetic types of calciferous amphiboles of metamorphic rocks. Lithos, 2, 67-81.

KROONENBERG, S.B., 1976, Amphibolite-facies and granulite-facies metamorphism in the Coeroeni-Lucie area, southwestern Surinam. Unpublished Ph.D.-thesis, University of Amsterdam.

KUNO, H., Differentiation of basalt magmas. In : Basalts, H.H. Hess and A. Poldervaart, Eds., 623-688. New York, J. Wiley and Sons.

LARSEN, E.S., 1938, Some new variation diagrams for groups of igneous rocks. Jour. Geol., 46, 505-520.

LARSEN, L.M., 1976, Clinopyroxenes and coexisting mafic minerals from the alkaline Ilimaussaq Intrusion, South Greenland. Jour. Petrology, 17, 158-290.

LEAKE, B.E., 1963, Origin of amphibolites from northwest Adirondacks, New York. Geol. Soc. America, Bull., 74, 1193-1202.

----------, 1964, The chemical distinction between ortho- and para-amphibolites. Jour. Petrology, 5, 238-254.

----------, 1965-a, The relationship between composition of calciferous amphiboles and grade of metamorphism. In : Controls of Metamorphism, W.S. Pitcher and G.W. Flinn, Eds., 299-318. London, Oliver and Boyd.

----------, 1965-b, The relationship between tetrahedral aluminium and the maximum possible octahedral aluminium in natural calciferous and subcalciferous amphiboles. Am. Mineralogist, 50, 843-851.

----------, 1968, A catalog of analyzed calciferous and subcalciferous amphiboles together with their nomenclature and associated minerals. Geol. Soc. America, Spec. Pap., 98, 210 p.

----------, 1969, The discrimination of ortho and para charnockitic rocks, anorthosites and amphibolites. Indian Mineralogist, 10, 89-104.

LEAKE, B.E., JANARDHANAN, A.S., and KEMP, A., 1976, High P_{H_2O} and hornblende in the Sittampundi Complex, India. Mineralog. Mag., 40, 525-526.

LEMAITRE, R.W., 1969, Kaersutite-bearing plutonic xenoliths from Tristan da Cunha, South Atlantic. Mineralog. Mag., 37, 185-197.

LIOU, J.G., KUNIYOSHI, S., and ITO, K., 1974, Experimental studies of phase relations between greenschist and amphibolite in a basaltic system. Am. Jour. Sci., 274, 613-632.

LOFGREN, G., DONALDSON, C.H., WILLIAMS, R.J., MULLINS, O., and USSELMAN, T.M., 1974, Experimentally reproduced textures and mineral chemistry of Apollo 15 quartz normative basalts. Proc. Fifth Lunar Conf., 1, 549-567.

MAASKANT, P., 1970, Chemical petrology of poly-metamorphic ultramafic rocks from Galicia, NW. Spain. Leidse Geol. Mededelingen, 45, 237-325.

MAGETTI, M., and NICKEL, E., 1976, Konvergenzen zwischen Metamorphiten und Magmatiten. Geol. Jhb. Hessen, 104, 147-160.

MARTIGNOLE, J., 1975, Le Précambrien dans le sud de la province tectonique de Grenville (Bouclier Canadien). Edité à l'nniversité de Montréal, 405 p.

MEHNERT, K.R., 1968, Migmatites. Amsterdam, Elsevier Publishing Company, 393 p.

MEHTA, P.K., 1976, Geochemistry and origin of the amphibolite of Kulu, NW. Himalaya, India. Neues Jb. Min., Mh.,8, 365-378.

MERCY, E.L.P., 1956, The accuracy and precision of "rapid methods" of silicate analysis. Geochim. et Cosmochim. Acta,9, 161-173.

MICHOT, J., 1961, Le massif complex anorthosito-lenconoritiquede Haaland-Helleren et le palingenèse basique. Mém.Acad. Roy.Belgique. Cl. Sci. 15 fasc.,1, 95 p.

MICHOT, J., and MICHOT, P., 1969, The problem of anorthosites. The South-Rogaland igneous complex, southwesteru Norway. In : Origin of anorthosite and related rocks, Y.W. Isachsen, Ed., 399-410, New York State Mus. Sci. Serv. Mem. 18.

MICHOT, P., 1969, Geological environments of the anorthosites of South Rogaland, Norway. In : Origiu of anorthosite and related rocks, Y.W. Isachsen, Ed., 411-423. New York State Mus. Sci. Serv. Mem., 18.

MISCH, P., and RIGE, J.M., 1975, Miscibility of tremolite and hornblende in progressive Skagit Metamorphic Suite, North Cascades, Washington. Jour. Petrology, 16, 1-21.

MOORE, A.C., 1970, Descriptive terminology for the textures of rocks in granulite facies terrains. Lithos, 3, 123-127.

MOREY, G.B., PAPIKE, J.J., SMITH, R.W., and WEIBLEN, P.W., 1972, Observations on the contact metamorphism of the Biwabik Iron-Formation, east Mesabi district, Minnesota. Geol. Soc. America,Mem., 135, 225-264.

MORSE, S.A., 1975, Plagioclase lamellae in hypersthene, Tikkoatokhakh Bay, Labrador. Earth Plan. Sci. Lett., 26, 331-336.

MUELLER, R.F., 1960, Compositional characteristics and equilibrium relations in mineral assemblages of a metamorphosed iron formation. Am. Jour. Sci., 258, 449-497.

----------, 1969, Hydration, oxidation, and the origin of the calc-alkali series. Washington D.C., NASA TN D-5400, 27 p.

MYERS, J.S., and PLATT, R.G., 1977, Mineral chemistry of layered Archean anorthosite at Majorqap qâva, near Fiskenaesset, southwest Greenland. Lithos, 10, 59-72.

ORVILLE, P.M., 1969, A model for metamorphic differentiation origin of thin-layered amphibolites. Am. Jour. Sci., 267-I, 64-86.

OXBURGH, E.R., 1964, Petrological evidence for the presence of amphibole in the Upper Mantle and its petrogenetic and geophysical implications. Geol. Mag., 101, 1-19.

PAPIKE, J.J., CAMERON, K.L., and BALDWIN, K., 1974, Amphiboles and pyroxenes : characterization of other than quadrilateral components and estimates of ferric iron from microprobe data. Geol. Soc. America, Abstr. Prog., 6, 1053-1054.

PHILLIPS, R., 1963, The recalculation of amphibole analysis. Mineralog. Mag., 33, 701-711.

PHILPOTTS, A.R., 1966, Origin of the anorthosite-mangerite rocks in southern Quebec. Jour. Petrology, 7, 1-65.

PLIMER, I.R., 1975, The geochemistry of amphibolite retrogression at Broken Hill, Australia. Neues Jb. Min., Mh.,10, 471-481.

POPP, R.K., GILBERT, M.C., and CRAIG, J.R., 1977, Stability of Fe-Mg-amphiboles with respect to sulfur fugacity. Am. Mineralogist, 62, 13-30.

PRETO, V.A.G., 1970, Amphibolites from the Grand Fork Quadrangle of British Columbia, Canada. Geol. Soc. America,Bull., 81, 783-782.

RAASE, P., 1972, Über die Farbung von Hornblenden und die mineralogische Kennzeichnung von Barroisit und Karinthin. Zer Karinthin, 66, 275-280.

----------, 1974, Al and Ti contents of hornbleude, indicators of pressure and temperature of regional metamorphism. Contr. to Min. Pet., 45, 231-236.

RAMDOHR, P., 1975, Die Erzmineralien und ihre Verwachsungen. Berlin, Akademie Verlag, 1277 p.

RIDGWAY, R., 1912, Color standard and color nomenclature. Washington D.C. Published by the author, 44 p.

RIEL, B.J. van, 1973-a, Doktoraal verslag van het veldwerk in het noordelijk deel van de lopoliet van Bjerkreim-Sogndal, tussen Helleland en Eia-Heskestad, Rogaland (SW-Noorwegen). Internal report, University of Utrecht.

----------, 1973-b, "Total-rock" analyses van het intrusief complex in S-Rogaland (Noorwegen). Internal Report, University of Utrecht.

RIETMEIJER, F.J.M., 1973, Verslag van een veldwerk in het zuidelijk en zuidoostelijk deel van de lopoliet van Bjerkreim-Sogndal, Rogaland, SW.-Noorwegen. Internal report, University of Utrecht.

----------, 1978, Pyroxenes from iron-rich igneous rocks in Rogaland, S.W. Norway. Ph.D.-thesis, University of Utrecht, in prep.

RIETMEIJER, F.J.M., and DEKKER, A.G.C., 1978, An extreme form of poikiloblastic texture in Rogaland/Vest-Agder, SW Norway. Norsk Geol. Tidsskr. in press.

RIVALENTI, G., 1970, Genetical problems of banded amphibolites in the Fredrikshab district, S.W. Greenland. Atti Soc. tosc. Sci. nat. Pisa, 77, 342-357.

ROBINS, B., 1975, Ultramafic nodules from Seiland, northern Norway. Lithos, 8, 15-27.

ROBINSON, P., ROSS, M., and JAFFE, H.W., 1971-a, Composition of the anthophyllite-gedrite series, comparisons of gedrite-hornblende, and the anthophyllite-gedrite solvus. Am. Mineralogist, 58, 1005-1041.

ROBINSON, P., JAFFE, H.W., ROSS, M., and KLEIN, C., 1971-b, Orientation of exsolution lamellae in clinopyroxenes and clino-amphiboles: Consideration of optimal phase boundaries. Am. Mineralogist, 56, 909-939.

ROEVER, E.W.F. de, PICCARRETA, G., BEUNK, F.F., and KIEFT, C., 1974, Blue amphiboles from north-western and central Calabria (Italy). Periodico. Mineral. (Rome), 43, 5-37.

ROEVER, E.W.F. de, BEUNK, F.F., and KIEFT, C., 1976, Blue amphibole-albite-chlorite assemblages from Fuscalbo (S Italy) and the role of glaucophane in metamorphism. Contr. to Min. Pet., 58, 221-234.

ROSS, M., PAPIKE, J.J., and SHAW, K.W., 1969, Exsolution textures in amphiboles as indicators of subsolidus thermal histories. Mineral. Soc. America, Spec. Paper,2, 275-299.

ROZENZWEIG, A., and WATSON, E.H., 1954, Some hornblendes from southeastern Pennsylvania and Delaware. Am. Mineralogist, 39, 581-599.

SCHRIJVER, K., 1973, Correlated changes in mineral assemblages and in rock habit and fabric across an orthopyroxene isograd, Grenville Province, Quebec. Am. Jour. Sci., 273, 171-186.

----------, 1975, Deformed root of a composite diapir in granulite facies. Geotekt. Forsch., 49, 1-118.

SEN, S.K.,and RAY, S., 1971-a, Hornblende pyroxene granulites versus pyroxene granulites. A study from the type charnockite area. Neues Jb. Min., Abh.,115, 291-314.

----------, 1971-b, Breakdown reactions for natural hornblendes in granulite facies. Neues Jb. Min., Abh., 114, 301-319.

SHAPIRO, L., and BRANNOCK, W.W., 1962, Rapid rock analysis of silicate, carbonate, and phosphate rocks. U.S. Geol. Surv., Bull., 1144-A, 56 p.

SHAPIRO, L., 1967, Rapid analysis of rocks and minerals by a single solution method. U.S. Geol. Surv., Prof. Paper, 575-B, 187-191.

SHIDO, F., 1958, Plutonic and metamorphic rocks of the Nasoko and Iritono districts in the Central Abukuma plateau. Jour. Fac. Sci., University Tokyo, Sec. II, 11, 131-217.

SMITH, J.V., 1974, Feldspar minerals, 2, Chemical and textural properties. Berlin, Springer Verlag, 690 p.

SPRINGER, G., 1967, Die Berechnung von Korrekturen für die quantitative Elektronenstrahl - Mikroanalyse. Fortschr. Min., 45, 103-124.

SPRY, A., 1969, Metamorphic textures. Oxford, Pergamon Press, 350 p.

STOUT, J.H., 1972, Phase petrology and mineral chemistry of coexisting amphiboles from Telemark, Norway. Jour. Petrology, 13, 99-146.

SUBBARAO, K.V., 1971, The origin of the Kunavaran amphibolites, Khamman district, Andhra Pradesh, India. Geol. Mag. 108, 131-136.

THOMPSON, R.N., 1974, Some high-pressure pyroxenes. Mineralog. Mag., 39, 768-787.

TOBI, A.C., 1963, Plagioclase determination with the aid of the extinction angles in sections normal to (010). A critical comparison of current albite-carlsbad charts. Am. Jour. Sci., 261, 157-167.

TOOMS, J.S., 1959, Field performance of some analytical methods used in geochemical prospecting. Symp. Explor. Geoquimica, (Sec. tomo), 377-388.

TRÖGER, W.E., 1969, Optische Bestimmung der gesteinsbildenden Minerale. Teil 2, Textband. Stuttgart, Schweizerbart'sche Verlagsbuchhandlung, 822 p.

----------, 1971, Optische Bestimmung der gesteinsbildenden Minerale. Teil 1, Bestimmungstabellen. Stuttgart, Schweizerbart'sche Verlagsbuchhandlung, 188 p.

VARNE, R., 1968, The petrology of Moroto Mountain, Eastern Uganda, and the origin of nephelinites. Jour. Petrology, 9, 169-190.

---------, 1970, Hornblende lherzolite and the Upper Mantle. Contr. to Min. Pet., 27, 45-51.

VARNE, R., and GRAHAM, A.C., 1971, Rare earth abundance in hornblende and clinopyroxene of a hornblende lherzolite xenolith. Implications for Upper Mantle fractionation processes. Earth Plan. Sci. Lett., 13, 11-18.

VERSTEEVE, A., 1975, Isotope geochronology in the high-grade metamorphic Precambrian of southwestern Norway. Norges geol. Unders., 318, 1-50.

WAARD, D. de, 1965, A proposed subdivision of the granulite facies. Am. Jour. Sci., 263, 455-461.

WAARD, D. de, and ROMEY, W.D., 1969, Petrogenetic relationships in the anorthosite-charnockite series of Snowy Mountain Dome, south-central Adirondacks. In : Origin of anorthosite and related rocks, Y.W. Isachsen, Ed., 307-316, New York State Mus. Sci. Serv. Mem., 18.

WAGNER, G.A., REIMER, G.M., and JäGER, E., 1977, Cooling ages derived by apatite fission-tracks, mica Rb-Sr and K-Ar dating : the uplift and cooling history of the Central Alps. Mem. Ist. Geol. Min. Univ. Padova, Vol. XXX.

WAKHALOO, S.N., and DAHR, B.L., 1969, Amphibolites of Kishtwar, Jammu and Kashmir State. Indian Mineralogist, 10, 289-297.

WALKER, K.R., JOPLIN, G.A., LOVERING, J.F., and GREEN, R., 1960, Metamorphic and metasomatic convergence of basic igneous rocks and lime-magnesio sediments of the Precambrian of north-western Queensland. Jour. Geol. Soc. Australia, 6, 149-177.

WATTERS, W.A., 1959, An association of hornblende and cummingtonite from Ringaringa, Steward Island, New Zealand. New Zealand Jour. Geol. Geoph., 2, 248-256.

WEBER-DIEFENBACH, K., 1976, Zur Geochemie und Metamorphose von Amphibolieten der Greiner Schiefer-Serie (Zillertaler Alpen/Tirol). Tscher. Min. Pet. Mitt., 23, 1-22.

WENK, E., SCHWANDER, H., and STERN, W., 1974, On calcic amphiboles from the Lepontine Alps. Schweiz. Min. Pet. Mitt., 54, 97-150.

WENK, H.R., Ed., 1976, Electron microscopy in mineralogy. Berlin, Springer Verlag, 564 p.

WERNIMONT, G., 1951, Design and interpretation of interlaboratory studies of test methods. Anal. Chem., 23, 1572-1576.

WETZEL, R., 1974, Hornblenden aus der Albit- bis Albitoligoklaszone zwischen Zermatt und Domodossola. Schweiz. Min. Pet. Mitt., 54, 151-208.

WILSHIRE, H.G., and TRASK, N.J., 1971, Structural and textural relationships of amphibole and phlogopite in peridotite inclusions, Dish Hill, California. Am. Mineralogist, 56, 240-255.

WINDLEY, B.W., HERD, R.K., and BOWDEN, A.A., 1973, The Fiskenaesset Complex, West Greenland. Part I. Bull. Grønlands geol. Unders., 106, 80 p.

WINTER, J., 1974, The origin of a calcareous amphibolite from the Nagssugtoqidian, west Greenland. Lithos, 7, 235-238.

YODER, H.S., 1966, Spilites and serpentinites. Carnegie Inst. Wash. Yearbook, 65, 269-279.

PLATES

P.L. : real length of the longest side of the picture.

Plate I :

Figure 1: Actinolite (act) - hornblende (hbl) assemblage in F 043. The contact between both amphiboles is sharp. Quartz divides some amphibole crystals in various fragments with equal optic orientation, see section II.2.2, and II.2.3. P.L. = 0.94 mm.

Figure 2: Large hornblendes in a finer grained plagioclase-pyroxene-hornblende matrix in D 307, see section II.2.2. P.L. = 3.75 mm.

Figure 3: Amphibole poikiloblasts with equally oriented pyroxene fragments at the contact between a hornblendite- and gabbronorite part in N 317. The black inclusions in the poikiloblast are sulfides. See section II.2.2. P.L. = 3.75 mm.

Figure 4: Fracture with uralite in N 317. The large hornblende crystal is broken up, and light coloured uralite formed along the cracks in the hornblende and as long prismatic needles in the vein, see section II.2.2. P.L. = 0.94 mm.

PLATE I

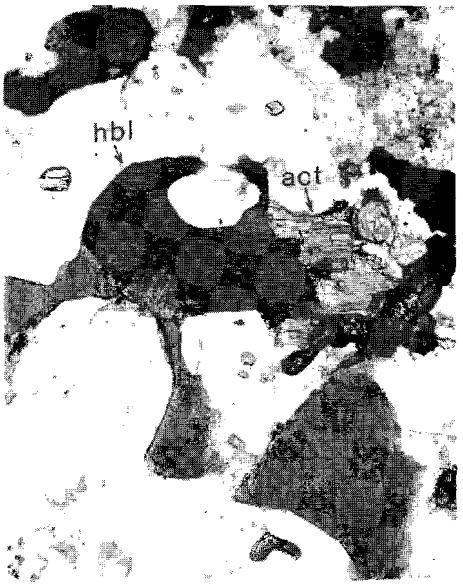

Figure 1 : F 043

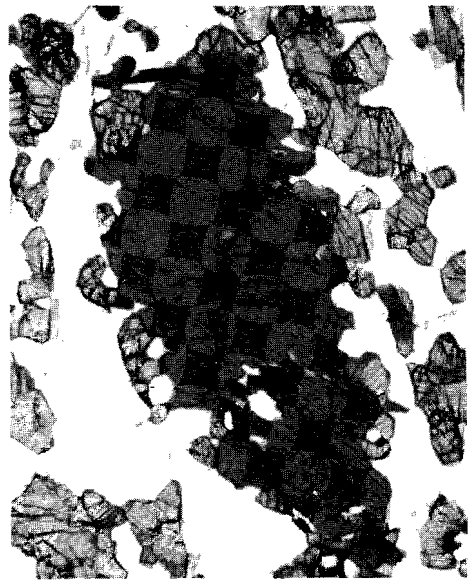

Figure 2 : D 307

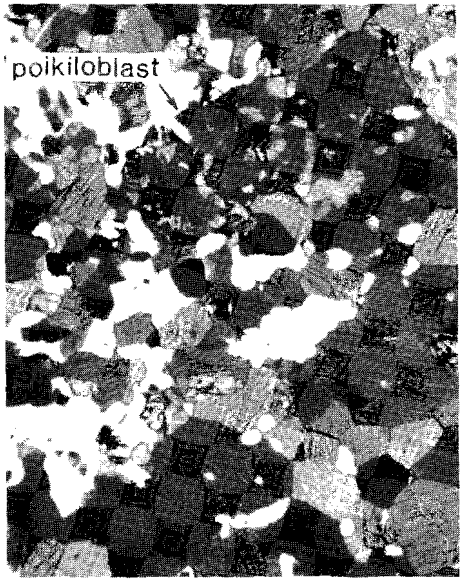

Figure 3 : N 317

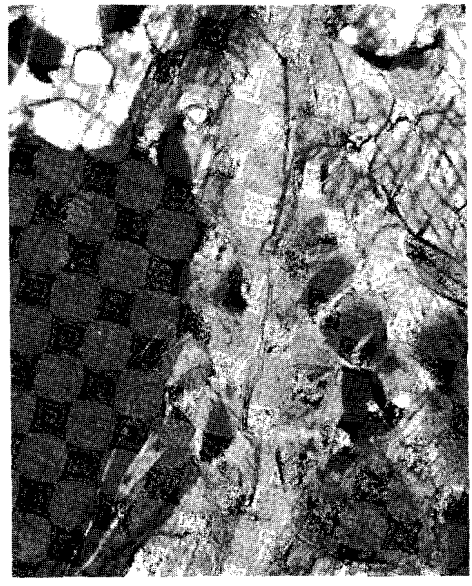

Figure 4 : N 317

Plate II :

Figure 1: Ore needle zones in H 325-amphibole. Beside the main system a finer system, approximately perpendicular to the former, is present. See section II.2.3, and IV.3.4. P.L. = 0.37 mm.

Figure 2: Angular ilmenite and magnetite crystals in plagioclase, clinopyroxene and amphibole, in W 226 L. See section II.2.5. P.L. = 0.94 mm.

Figure 3: Texture of N 572 D (olivine hyperstenite). The left side of the picture shows forsterite with an intricate, fine vein system which also transects the neighbouring orthopyroxene. Plagioclase and amphibole are very fine, intergranular. See section II.2.5. P.L. = 3.75 mm.

Figure 4: Texture of N 572 L (olivine amphibole mela-norite). The large olivine is partly rimmed by orthopyroxene, with an outer rim of plagioclase. Pargasite + orthopyroxene + plagioclase form the fine-grained fabric. See section II.2.5. P.L. = 3.75 mm.

PLATE II

Figure 1 : H 325

Figure 2 : W 226 L

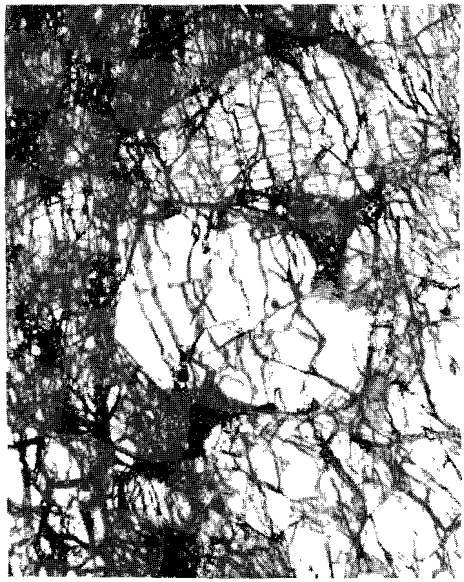

Figure 3 : N 572 D

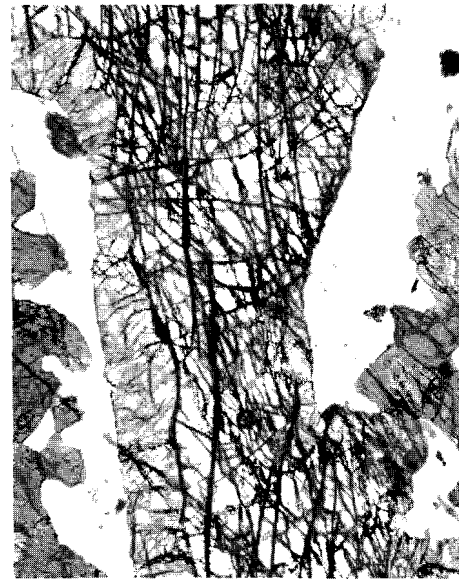

Figure 4 : N 572 L

Plate III :

Figure 1: Magnesioriebeckite in alkalifeldspar granite (A 168). The fibrous amphibole formed in quartz, in contact with ilmenite (ilm). The clouded feldspar is almost riebeckite-free. See section II.3. P.L. = 0.94 mm.

Figure 2: Porphyritic plagioclase crystals in a sample from the Folded basic intrusions (F 126). The largest plagioclase crystal is almost completely sericitisized, the laths and smaller fabric crystals are rather clean. See section II.4.1. Crossed nicols. P.L. = 3.75 mm.

Figure 3: Plagioclase (plag) - orthopyroxene (opx) - ore assemblage in ferroan pargasitic xenocryst A 128 (amph). An enclosed early formed apatite (apa) lies in the plagioclase. The c-axis of the amphibole lies parallel to the long side of the picture. See section II.4.2. P.L. = 3.75 mm.

Figure 4: Contact zone between A 128-amphibole and an enclosed clinopyroxene cumulus crystal. The clinopyroxene contains exsolution patterns of plagioclase and ore. The contact zone consists of plagioclase (An_{96}), ortho- and clinopyroxene, and titanomagnetite. See section II.4.2. P.L. = 3.75 mm.

PLATE III

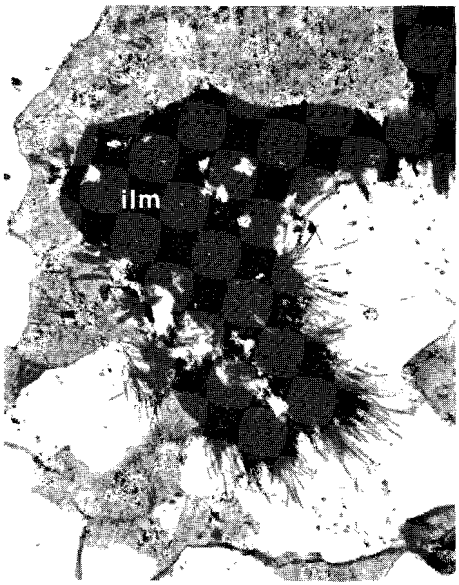

Figure 1 : A 168

Figure 2 : F 126

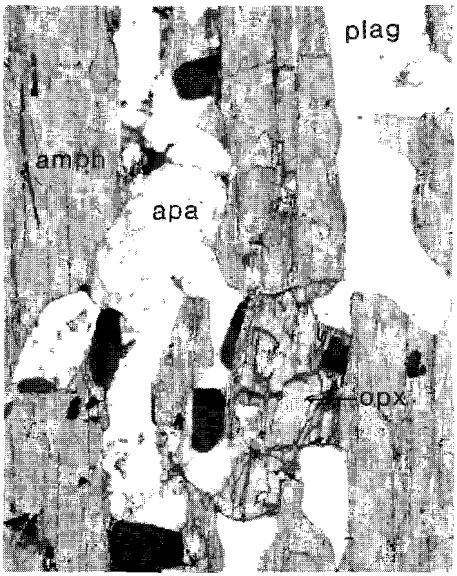

Figure 3 : A 128

Figure 4 : A 128

Plate IV :

Figure 1: Relic pyroxene texture in ferro-hornblende (so-called ladder structure). The darker parts in the upper part of the furthermore light-coloured amphibole (B1016) are former orthopyroxene lamellae. The clinopyroxene host altered to ferro-hornblende, the lamellae altered, in this case, to carbonate. The dark blots in the lower part of the crystal are differently oriented ferro-hornblende fragments. This may indicate that the large enveloping ferro-hornblende crystal replaced several former pyroxene crystals. See section II.5.1.-2.
P.L. = 0.37 mm.

Figure 2: Exsolution lamellae in the ferro-hornblende part (B1016) of a larger grunerite/cummingtonite crystal (B2016). See section II.5.1.-2.
P.L. = 0.37 mm.

Figure 3: Orthopyroxene-ore symplectite domains surrounded by soft-coloured ferroan pargasite (par) in E 131. See section II.5.1.-3.
P.L. = 0.94 mm.

Figure 4: "Ladder structure" in amphibole. Clinopyroxene rims and rungs are altered to ferro-hornblende (R1269), former orthopyroxene lamellae (inverted pigeonite) are altered to ferro-hornblende + quartz near the rims of the crystal and to ferro-actinolite (R2269) in the central parts (dark coloured in the picture). See section II.5.2.
P.L. = 0.37 mm.

PLATE IV

Figure 1 : B 016

Figure 2 : B 016

Figure 3 : E 131

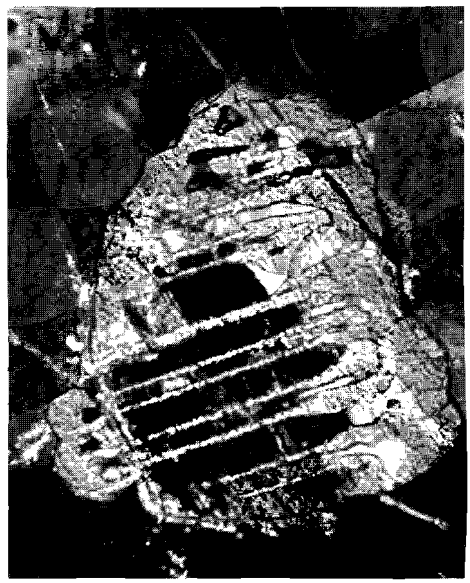

Figure 4 : R 269

Plate V :

Figure 1: Vermicular quartz in ferro-hornblende (R1269). See section II.5.2. P.L. = 0.94 mm.

Figure 2: Colourless exsolution lamellae in ferro-hornblende of the (quartz-) monzonitic phase of the lopolith. The lamellae are less than 1 micron thick. See section II.5.3.-1. P.L. = 0.17 mm.

Figure 3: Mortar structure in a mangerite near Bakka (F 419). The large mesoperthite crystals are quantitatively more important than the fine-grained matrix. See section II.5.3.-2. P.L. = 3.75 mm.

Figure 4: Mortar structure in a mangerite near Bakka (F 420). About 50 % of the rock is granulated. See section II.5.3.-2, and figure 3 of this plate. P.L. = 3.75 mm.

PLATE V

Figure 1 : R 269

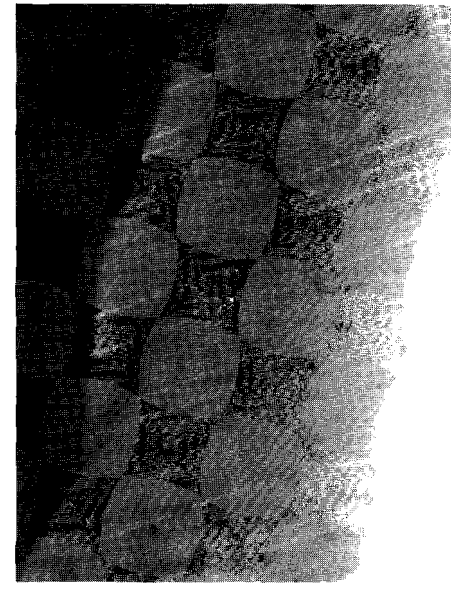

Figure 2 : R 98

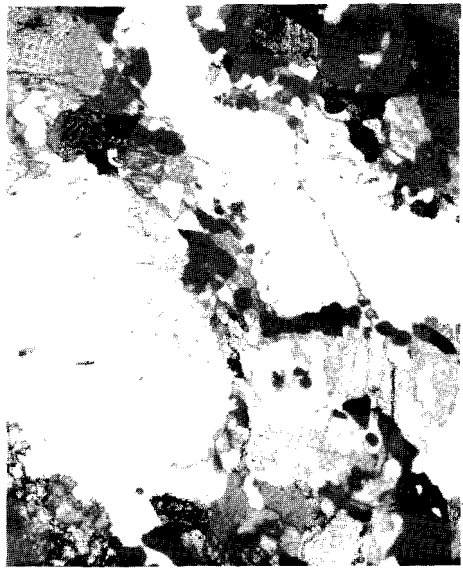

Figure 3 : F 419

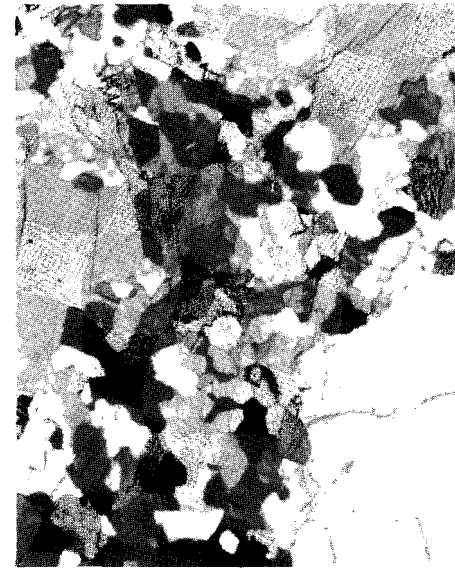

Figure 4 : F 420

Plate VI :

Figure 1: Completely granulated mangerite near Bakka (F 421). This rock type forms a dike-like zone of several meters wide and is surrounded by mangerites with a less intensive granulation (Plate V, figures 3 and 4). Orthopyroxene (opx) forms an extreme poikiloblast. See section II.5.3.-2. P.L. = 3.75 mm.

Figure 2: Ferro-hornblende rim (E1232 R) around a quartz + ferro-hornblende core (E1232 K) in a monzonitic xenolith in the Haaland-Helleren anorthosite. The ferro-hornblende in the core is lighter coloured than the rim. See section II.7.2. P.L. = 0.94 mm.

Figure 3: Amphibole aggregate in anorthosite. The outer rim consists of green ferro-hornblende (E3232) which gradually changes into light coloured actinolite (E2232) in the core. The aggregate is bent. Various orientations of the amphibole crystals can be seen. Ore inclusions delineate the curvature. See section II.7.2. P.L. = 3.75 mm.

Figure 4: Orthopyroxene core with complex amphibole rims. Compare with fig. II.14, section II.7.3.

1 : orthopyroxene; 2 : serpentine; 3 : cummingtonite/grunerite (L2143) with ore needle systems; 4 : magnesio-hornblende/actinolitic hornblende (L1143); 5 : ore needle zone. Egersund anorthosite. P.L. = 0.94 mm.

PLATE VI

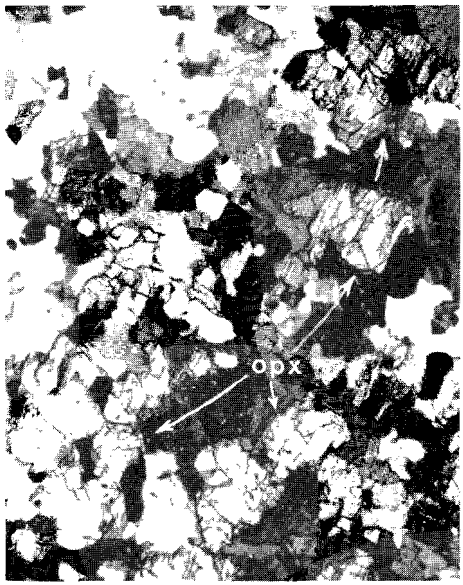

Figure 1 : F 421

Figure 2 : E 232 F

Figure 3 : E 232 N

Figure 4 : L 143

Plate VII :

Figure 1: Ore needles and lathes in amphibole (A 128). Section perpendicular to the c-axis. See Appendix, A 128. P.L. = 0.94 mm.

Figure 2: Ore needles and lathes in amphibole (A 128). Section perpendicular to n_y. The ore is aligned parallel to n_z and the c-axis. See Appendix, A 128. P.L. = 0.94 mm.

Figure 3: Exsolution lamellae in N 041, about parallel to (001). Crossed nicols. See Appendix, N 041. P.L. = 0.37 mm.

PLATE VII

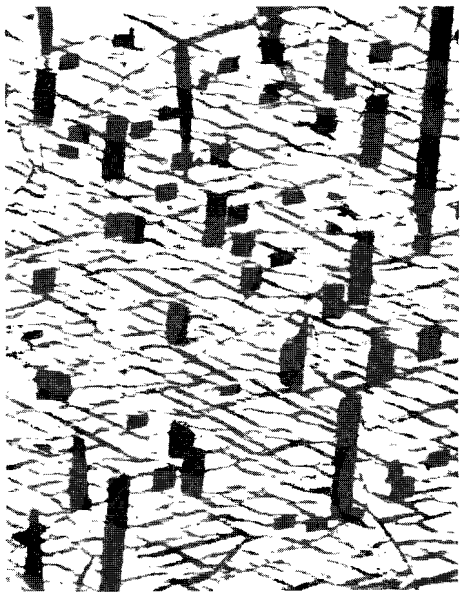

Figure 1 : A 128

Figure 2 : A 128

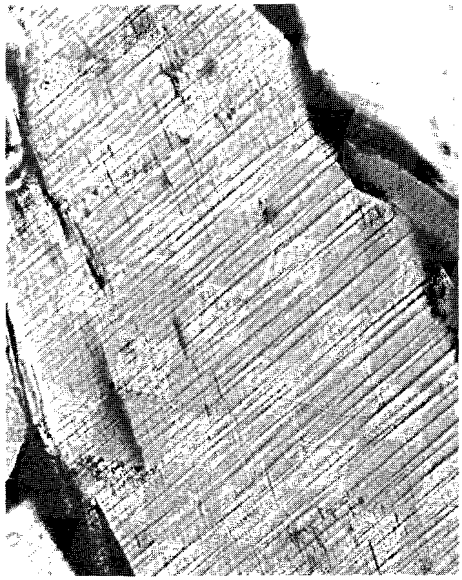

Figure 3 : N 04'

ERRATA

Apart from typing errors and linguistic failures, which, I feel, do not affect the understanding of the text, the following errors should be corrected:

p.8 : bottom line: variation for variance

p.26 : subscript of Fig.I.10., line 3 should read: Mg-rich amphibole; crosses: Fe-rich amphiboles from the igneous complexes

p.36 : line 2 from bottom: facies for formation

p.54 : lines 3 and 5: Hunnedal for Hunnendal

p.59 : subscript of Table II.4., last sentence: increase for decrease

p.87 : line 13: igneous for magmatitic

p.88 : line 8 from bottom: possibly for eventual

p.94 : subscript of Table III.1., bottom line: section $\perp$ a for section a

p.100 : line 7 from bottom: right-hand for right

p.122 : line 4 from bottom: combined water for crystalwater

p.159 : line 4: colours for axes

p.166 : line 7: (001) for (100)

p.221 : B 016, line 9: ∞ for 1.0

p.229 : line 8: $2V_z$ for $2V_x$